Interreg
Ελλάδα-Κύπρος
Ευρωπαϊκό Ταμείο Περιφερειακής Ανάπτυξης

ΕΥΡΩΠΑΪΚΗ ΕΝΩΣΗ

16th -18th June 2023
Limassol, Cyprus
hybrid event

www.anelixi.tuc.gr

ΑΝΕΛΙΞΗ

Τελικό Συνέδριο Πράξης ΑΝΕΛΙΞΗ
ANELIXI Final Conference

Πρόγραμμα Συνεργασίας Interreg V-A για αναβάθμιση ΕΕΛ
Συγχρηματοδοτείται από την Ευρωπαϊκή Ένωση (ΕΤΠΑ) και
από Εθνικούς Πόρους της Ελλάδας και της Κύπρου

Συντονιστής | Coordinator

ΠΟΛΥΤΕΧΝΕΙΟ ΚΡΗΤΗΣ
TECHNICAL UNIVERSITY OF CRETE

Εταίροι | Partners

Δ.Ε.Υ.Α.Π.

ΣΥΜΒΟΥΛΙΟ ΑΠΟΧΕΤΕΥΣΕΩΝ ΚΥΠΕΡΟΥΝΤΑΣ
Κυπριακή Δημοκρατία

Design of Environmental Processes Lab

ISBN 978-618-86417-1-6

2nd International Conference on Sustainable Chemical & Environmental Engineering

SUST ENG 2023

14th -18th June 2023
Limassol, Cyprus
hybrid event

www.susteng2023.tuc.gr

spirito
business & communication group

Design of Environmental Processes Lab

Technical University of Crete
School of Chemical and Environmental Engineering

Cyprus University of Technology

Proceedings of 2nd International Conference on Sustainable Chemical and Environmental Engineering

14-18 June 2023, Limassol, Cyprus

Publisher:

Design of Environmental Processes Laboratory
School of Chemical and Environmental Engineering, Technical University of Crete.

Editor-in-Chief:

Prof. Petros Gikas
Conference Chair, Head of the Design of Environmental Processes Laboratory, School of Chemicaland Environmental Engineering, Technical University of Crete.

Editors:

Dr. Michalis Koutinas
Associate Professor, Chemical Engineer, Department of Chemical Engineering, Cyprus University of Technology.

Dr. Ioannis Vyrides
Associate Professor, Chemical Engineer, Department of Chemical Engineering, Cyprus University of Technology.

Mr. Konstantinos Tsamoutsoglou
Environmental Engineer, Design of Environmental Processes Laboratory, School of Chemical and Environmental Engineering, Technical University of Crete.

Ms. Xanthi Evangelia Manaroli
Architect Engineer M.Sc., School of Chemical and Environmental Engineering, Technical Universityof Crete.

Ms. Anthoula Manali
Chemist M.Sc., Design of Environmental Processes Laboratory, School of Chemical andEnvironmental Engineering, Technical University of Crete.

Editorial Office:
Mr. Konstantinos Tsamoutsoglou
SUSTENG 2023 Conference Secretariat
Email: secretariat.susteng@tuc.gr
Telephone: +30 28210 06208
Website: www.susteng2023.tuc.gr

ANELIXI project & SUSTENG 2023 Conferences – Review

On behalf of the Organizing Committee, I am pleased to announce that the Final Conference of the ANELIXI Project "Upgrade of WWTPs for the management of increased demands and the reduction of the operational cost", in the frame of Interreg V-A Greece-Cyprus 2014-2020 between 16th to 18th June 2023 and the 2nd International Conference on Sustainable Chemical and Environmental Engineering (SUSTENG 2023), between 14th to 18th June 2023, both events held in Limassol, Cyprus, in either event with physical or virtual presence, have been successfully completed.

The conferences included 12 sessions, while 6 keynote lectures were also given. During the conference, 89 abstracts were presented, out of which 61 were oral presentations, while the remaining 28 were posters. With respect to the geographical origin of the presentations, 37 came from Greece, while the remaining 52 were from abroad, with the presence of 23 countries.

The purpose of the ANELIXI final conference is to describe and present the outcomes of ANELIXI project, an innovative wastewater treatment process. Additionally, hot issues on water and wastewater management and reuse will also be discussed with water specialists in an open forum.
The main objectives of the ANELIXI project are:
- Increase the capacity of existing WWTPs
- Low construction and operation cost compared to alternative technologies
- Reduction of energy cost of existing WWTPs by approximately 35%
- Production oaf biosolids with solids content over 35%

SUSTENG 2023 aims to encourage the exchange of knowledge between academicians, scientists and engineers on hot issues and current developments in chemical and environmental engineering through sustainable perspective. The participants will have the opportunity to present their recent research findings on an extended spectrum of conference topics and be informed about new challenges, future trends, and technological innovations on sustainable processes following the principles of circular economy.

The ANELIXI project of the Cooperation Program INTERREG V-A Greece - Cyprus 2014-2020 is co-financed by the European Regional Development Fund (ERDF) and national resources of Greece and Cyprus.

The SUSTENG 2023 is organized by the "Design of Environmental Processes Laboratory", of the School of Chemical and Environmental Engineering, Technical University of Crete, the Cyprus University of Technology and the Company Spirito Group.

May I thank our sponsors (KAOUSSIS, MOTOR OIL, PLASTIKA KRITIS, and Sewerage Board of Limassol-Amathus (SBLA)) for their valuable contribution to the SUSTENG 2023 conference.

The abstracts/full papers presented at SUSTENG 23 and ANELIXI project have been included in the present Conference Proceedings Book.

The conference Chair
Petros Gikas
Professor
Head of the "Design of Environmental Processes Lab"
School of Chemical and Environmental Engineering
Technical University of Crete

TOPICS

1. Industrial Waste Management
2. Air Emissions/ CO_2 Separation
3. Policies, Regulatory and Social Acceptance
4. Adsorption Processes
5. Solid Waste Management/ Biosolids Management and Valorization
6. Water Resources Management
7. Wastewater Treatment & Bioremediation (part I &part II)
8. Biochemical and Biomedical Engineering & Biotechnology
9. Waste to Energy/Hydrogen Production
10. Nanomaterials
11. Environmental Economics/ Industrial Economics
12. Agricultural Engineering/ Agricultural & Livestock Waste

SPECIAL ISSUES

SUST ENG 2023

Selected abstracts may be submitted to the four following Special Issues of Scientific Journals:

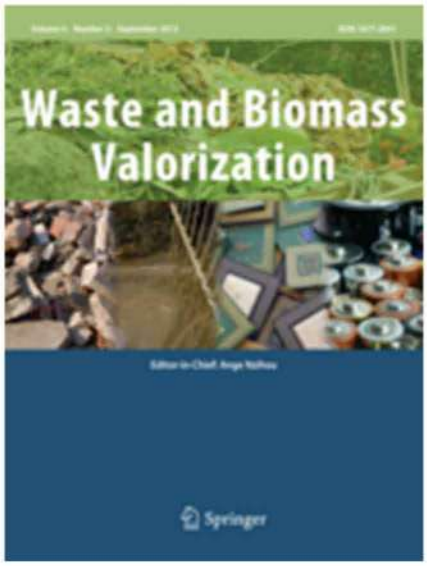

Resource Recovery from Wastewater and Biosolids
Waste and Biomass Valorization (Springer)

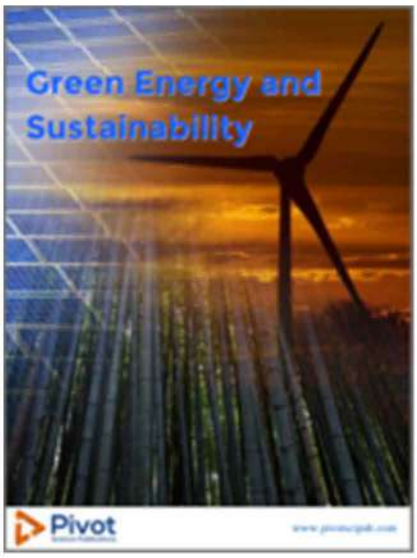

Selected Papers from the 2nd International Conference on Sustainable Chemical and Environmental Engineering
Green Energy and Sustainability (Pivot)

Solid Waste and Wastewater Management in Light of Circular Economy
Journal of Environmental Management (Elsevier)

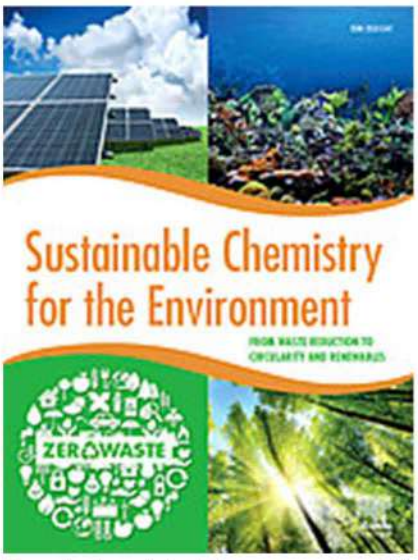

Sustainable Energy for the Environment
Sustainable Chemistry for the Environment (Elsevier, Open Access)

TABLE OF CONTENTS

ABSTRACTS

SUST ENG 2023

INDUSTRIAL WASTE MANAGEMENT

Interreg
Ελλάδα-Κύπρος
Ευρωπαϊκό Ταμείο Περιφερειακής Ανάπτυξης
ΕΥΡΩΠΑΪΚΗ ΕΝΩΣΗ
ΑΝΕΛΙΞΗ

Artificial Neural Network for the quantification of cobalt recovered from Li-ion batteries

I.I. Pérez Juárez[1]*, B.M. González Contreras[2], M.A. Munive Rojas[2], J.A. Guevara-García[2] and E. Bonilla Huerta[3]

[1]Postgrado Facultad de Ciencias Básicas, Ingeniería y Tecnología. Universidad Autónoma de Tlaxcala, Campus Apizaco, P.O. Box 140, 90300. Tlaxcala. México.

[2]Fac. de Ciencias Básicas, Ingeniería y Tecnología. Universidad Autónoma de Tlaxcala, Campus Apizaco, P.O. Box 140, 90300. Tlaxcala. México.

[3]Tecnológico Nacional de México/ Apizaco. Av. Instituto Tecnológico No. 418, San Andrés Ahuashuatepec, Tlaxcala, México. C.P. 90491.

Corresponding author email: 20224175@garzas.uatx.mx

keywords: *Artificial Neural Network; cobalt; Li-ion batteries; UV-visible spectroscopy.*

Introduction

Ultraviolet–visible (UV-Vis) spectrophotometry have several advantages such as online analysis, simultaneous multi-parametric measurements, easily operated and inexpensive sample pretreatment, between others, making this analytical technique cheaper and faster than many others (Ríos-Reina & Azcarate, 2022). Our research group has been working in the development of technologies for the recovery of metals from used batteries (Guevara-García & Montiel-Corona, 2012) and recently in ion-Li devices (Degante *et al*., 2022), where content of Li, Co, Mn, Ni, and Al of the initial cathodic material in leaching solutions of organic acids were recovered and analyzed by ICP, while the identification of the oxidation state of Co in the leachates was performed by UV-Vis.

The objective of this work is to develop the analytical and computational bases for the construction of an Artificial Neural Network for the quantification of cobalt recovered from Li-ion batteries based on the UV-Vis spectrophotometry.

Materials and methods

Preparation of standard solutions of cobalt extracted by organic acids. A mother solution was prepared using reactive-grade $Co(NO_3)_2$ salt (Baker, 99.8%) at 1M solution, 6% with respect to H_2O_2 and 1.5 M with respect lactic acid. Successive solutions of Co^{2+} known concentrations were prepared by taking the respective volume of the mother solution and diluting to 10 mL with bi-distilled water. Each prepared solution was subjected to the extraction procedure and measure with a UV-Vis spectrophotometer.

Modeling of Cobalt Removal Using UV-Vis-ANN. A Backpropagation (BP) architecture is proposed in this article, configured in such a way that the training is performed without using additional resources such as a GPU, only CPU. The minimum topology suggested to predict the level of Co (II) concentrations (mol/L) from the data set of absorbance levels is: 21x5x5x1. This means that 21 absorbance levels are taken as input to the neural network and a single hidden layer block of size 5x5 is defined, finally an output layer of 5x1 is defined.

The function defined for each neuron in the BP model is the exponential function. The assignment of weights is randomized with a normal distribution. The number of epochs defined to achieve learning is 700.

This basic neural network model is proposed instead of sophisticated models that consume a high quantity of computational resources and are frequent options in the scientific community such due to the multiple virtues (ref). One of the better are convolutional neural networks (CNN).

Results and discussion

The series of UV-Vis spectra obtained with this procedure reproduce successfully the characteristics of original leaching experiments as can be seen in Figure 1(Left), while the procedure BP reproduce successfully the concentration of the set of standard spectra with a R2 maximum of 0.9978 for a MSE BP21X3X3X1 topology (Table 1).

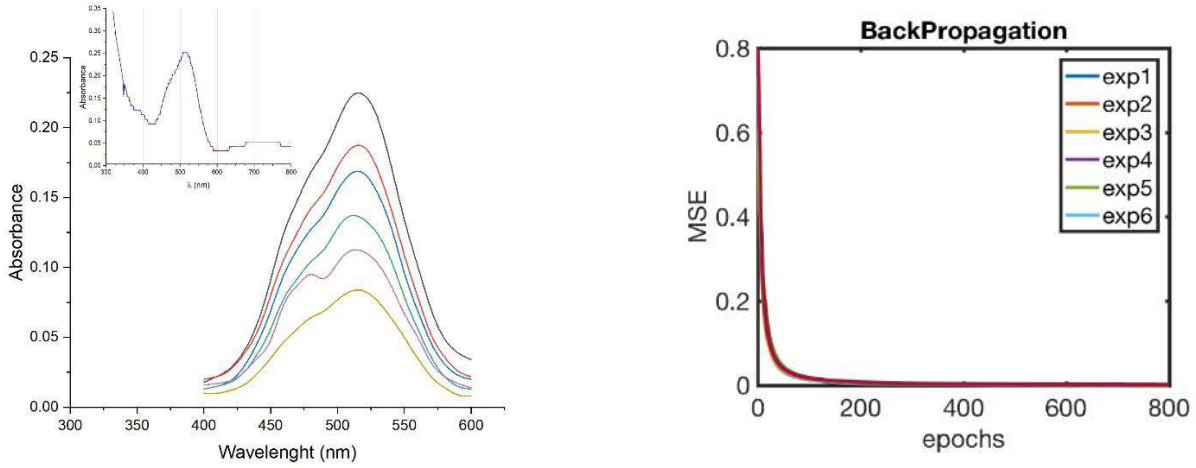

Figure 1. *(Left) A reduced number of UV-Vis spectra obtained with the standard procedure of this work, inset: UV-Vis spectrum of a typical solution after the extraction of Co2+ with lactic acid from chatodic material of ion-Li battery, taken from Degante et al., 2022. (b) (Right) Mean Squared Error (MSE) for Backpropagation with topology: 21x3x3x1 and 800 epochs.*

Table 1. *Experimental results using BP with two topologies and without pre-processing technique*

Co (II) concentrations (mol/L)	MSE BP21X5X5X1 Prediction	MSE BP21X3X3X1 Prediction
Experiment 1	0.9964	0.9977
Experiment 2	0.9977	0.9962
Experiment 3	0.9979	0.9978
Experiment 4	0.9971	0.9973
Experiment 5	0.9974	0.9970
Experiment 6	0.9977	0.9964
Experiment 7	0.9961	0.9959

Elapsed time 11.666960 seconds for first topology, 11.642327 seconds for second topology.

Conclusions

Up to our knowledge there has been no report concerning the application of UV-Vis-ANN to the quantification of valuable metals from residues, i.e., urban minery, which is a remarkable area of both economic and environmental benefits. While, a well-configured neural model can generalize concentration obtaining with higher performance rates than dense models such as convolutional networks.

References

Ríos-Reina, R., & Azcarate, S. M. 2022. How Chemometrics Revives the UV-Vis Spectroscopy Applications as an Analytical Sensor for Spectral print (Nontargeted) Analysis. *Chemosensors*, 11(1), 8.

Guevara-García, J. A., & Montiel-Corona, V. 2012. Used battery collection in central Mexico: Metal content, legislative/management situation and statistical analysis. *J. Environ. Manage.*, 95, S154-S157.

Degante, J. P., Escobar, S. R., Quintero, L. J., Rojas, M. M., & Guevara-García, J. A. 2022. Novel economical method for recovering valuable metals from used Li-ion batteries. Proceeding of 1st International Conference on Sustainable Chemical and Environmental Engineering. SUSTENG 2022, 31 Aug-04 Sep, Rethymno, Crete, Greece. Page 265. ISBN: 978-618-86417-0-9.

A citrus processing wastewater-based biorefinery approach for production of high-added value commodities

P. Karanicola[1,2], M. Patsalou[1], P. Christou[2], G. Panagiotou[2] and M. Koutinas[1]

[1]Department of Chemical Engineering, Cyprus University of Technology, Limassol, Cyprus
[2]KEAN Soft Drinks Ltd, Limassol, Agios Athanasios, Cyprus
Corresponding author email: michail.koutinas@cut.ac.cy

keywords: *biorefinery; citrus processing waste; polyphenols; bacterial cellulose.*

Introduction

The global production of citrus fruits is increasing over the years, accounting for 143 million t in 2019 (FAO, 2021). The worldwide industrial processing of citrus fruit is disposing half of its mass as citrus peel waste (CPW) generating 23 x 10^6 t annually, mainly consisting of peels, pulp seeds and segment membranes. Traditional management practices include first generation recycling methods, such as animal feed, composting, disposal in landfills and anaerobic digestion (Tsang *et al* 2019). However, the valuable composition of CPW renders it as a promising raw material for valorization through biorefinery-based treatment. Moreover, significant amounts of wastewater are disposed constituting up to 17 m^3 per t of processed fruit, which burdens citrus processing industries (CPIs). Citrus processing wastewater (CPWW) which includes water for factory cleaning, cooling water, juice concentration and water produced by essential oil extraction, is mainly characterized by large variability of organic loads and other soluble or insoluble compounds, such as sugars, bioactive compounds, essential oils and organic acids (Zema *et al* 2019). Thus, CPWW consists a valuable feedstock, which can be further treated in order to isolate or produce high-added value commodities.

Bacterial Cellulose (BC), which consists a fermentation product, constitutes a biopolymer of significant industrial importance due to numerous unique properties including high crystallinity, high degree of polymerisation, biodegradability, high purity, enhanced mechanical strength and large water holding capacity. These properties increase the industrial interest in various sectors such as food, medical and electronic industries (Hussain *et al* 2019). Previous studies have demonstrated BC manufacture using orange, grapefruit and lemon peels and pulp producing 0.68 g L^{-1}, 6.7 g L^{-1} and 5.2 g L^{-1} respectively (Karanicola *et al* 2021, Cao *et al* 2018, Andritsou *et al* 2018). Furthermore, essential oils as well as bioactive compounds such as polyphenols and carotenoids can be isolated from CPWW as high-added value commodities. Polyphenols consist mainly phenolic acids and flavonoids exhibiting important antioxidant, antiviral, anticarcinogenic, neuroprotective and antimicrobial properties, which could be used in food, pharmaceutical and cosmetic industries (Gomez-Mejia *et al* 2019). Moreover, the carotenoid content could contribute to health as protection from cancer and heart disease providing an important source of vitamin A (Ndayidhimiye and Chun, 2017).

Previous studies have mainly focused on the reduction of the chemical oxygen demand (COD) of CPWW using different treatment methods as anaerobic digestion for methane production (Rosas-Mendoza *et al* 2018) as well as dark fermentation for bio-hydrogen generation (Rosas-Mendoza *et al* 2020). However, given that CPWW constitutes a valuable feedstock for valorization, the present work aims to develop an innovative biorefinery strategy exploiting green technologies for isolation of essential oils as well as bioactive compounds (polyphenols, carotenoids) and production of BC via citrus processing waste valorization.

Materials and methods

CPWW was initially characterized through standard analytical methods. The physicochemical characteristics assessed included total sugars (TS), total phenolic content (TPC), COD, total solids and free amino nitrogen (FAN). Essential oils quantification was performed using GC-FID following extraction using hexane.

The phenolic content entailed in the liquid fraction of CPW has recovered using nonionic resins and biochar as adsorption materials, which are capable of adsorbing polar and non-polar polyphenolic

compounds, in batch experiments. The desorption capacity of each material was assessed using packed columns at different flowrates of ethanol.

The liquid fraction remaining following essential oils and bioactive compounds isolation was employed in BC fermentations using *Komagataeibacter sucrofermentans* DSM 15973.

Results and discussion

A biorefinery approach was used for isolation of high-added value commodities (bioactive compounds and essential oils) and production of bacterial cellulose using CPWW emitted from the industrial process. CPWW constituted 104 g L^{-1} COD, 57.3 g L^{-1} TS, 1.3 g L^{-1} TPC (gallic acid equivalents), 98.3 mg L^{-1} FAN, 357 mg L^{-1} d-limonene and 5.5% of total solids which are rich in bioactive compounds and fibre content.

The present work mainly focused on isolation of polyphenols from the aqueous stream through adsorption evaluating different types of resins, effluent volumes and polyphenols desorption. Specifically, polyphenols adsorption reached 75% using a non-polar resin, while 94% of polyphenols desorption was achieved at an ethanol flowrate of 0.1 L h^{-1}. The remaining sugar-rich liquid was employed in *Komagataeibacter sucrofermentans* fermentations yielding up to 0.26 g_{BC} g_{TS}^{-1}.

Conclusions

An innovative biorefinery strategy was developed for bioactive compounds recovery and BC production exploiting the waste streams emitted from CPIs.

Acknowledgements: The work is part of the project BioTECPro (ENTERPRISES/0521/0185) funded by the Cyprus Research & Innovation Foundation.

References

Andritsou V., De Melo E.M., Tsouko E., Ladakis D., Maragkoudaki S., Koutinas A.A., Matharu. A.S., 2018. Synthesis and characterization of bacterial cellulose from citrus-based sustainable resources. *ACS Omega* 3 (8):10365–73.

Cao Y., Lu S., Yang Y.,2018. Production of bacterial cellulose from byproduct of citrus juice processing (citrus pulp) by *Gluconacetobacter Hansenii*. *Cellulose* 25(12):6977–88.

FAO, 2021. https://www.fao.org/3/cb6492en/cb6492en.pdf.

Gomez-Mejia E., Rosales-Concardo N., Leon-Gonzalez M.E., Madrid Y., 2019. Citrus peel waste as a source of vlue-added compounds: Extraction and quantification of bioactive polyphenols. *Food Chemistry* 295:289–299.

Hussain Z., Sajjad W., Khan T., Wahid F., 2019. Production of bacterial cellulose from industrial wastes: A review. *Cellulose* 26(5):2895–2911.

Karanicola P., Patsalou M., Stergiou P-Y., Kavalliertou A., Evripidou N., Christou P., Panagiotou G., Damianou C., Papamichael E.M., Koutinas M., 2021. Ultrasound-assisted dilute acid hydrolysis for production of essential oils, pectin and bacterial cellulose via a citrus processing waste biorefinery. *Bioresource Technology* 342:126010.

Ndayidhimiye J. and Chun BS, 2017. Optimization of carotenoids and antioxidant activity of oils obtained from a co-extraction of citrus (Yuzu ichandrin) by-products using supercritical carbon dioxide. *Biomass and Bioenergy* 106:1–7.

Rosas-Mendoza E.S., Mendez-Contreras J.M., Martinez-Sibaja A., Vallejo-Cantu N.A., Alvarado-Lassman A., 2018. Anaerobic digestion of citrus industry effluents using an anaerobic hydrid reactor. *Clean Tecnhologies and Environmental Policy* 20:1387–1397.

Rosas-Mendoza E.S., Mendez-Contreras J.M., Aguilar-Lasserre A.A., Vallejo-Cantu N.A., Alvarado-Lassman A., 2020. Evaluation of bioenergy potential from citrus effluents through anaerobic gigestion. *Journal of Cleaner Production* 254:120128

Tsang Y.F., Kumar V., Samadar P., Yang Y., Lee J., Ok Y.S., Song H., Kim K-H., Kwon E.E., Jeon Y.J., 2019. Production of bioplastic through food waste valorization. *Environment International* 127:625–644.

Zema D. A., Calabro P. S., Folino A., Tamburino V., Zappia G., Zimbone S. M., 2019. Wastewater Management in Citrus Processing Industries: An Overview of Advantages and Limits. *Water* 11:2481.

Molybdenum recovery in a sulphate-reducing bioreactor

D.A. Strongyli, P. Kousi, A. Hatzikioseyian and E. Remoundaki

School of Mining and Metallurgical Engineering, National Technical University of Athens, Zografos, Greece
Corresponding author email: pkousi@metal.ntua.gr

keywords: *sulphate-reduction; molybdate reduction; bioreactor; PV wastewater; molybdenum sulfide.*

Introduction

The biological treatment of acidic wastewater with a significant sulphate and metal content, utilising Sulphate-Reducing Bacteria (SRB) (Postgate, 1979), has been demonstrated in lab- and pilot-scale (Bijmans et al., 2011). This bioremediation process occurs anaerobically, via the oxidation of organic carbon sources (or H_2) and the reduction of sulphate (SO_4^{2-}) to sulphide (H_2S, HS^-) by SRB (Rabus et al., 2007). Sulphide and bicarbonate ions, which are formed during sulphate reduction and carbon source oxidation, buffer the solution pH around neutral to slightly alkaline values. Sulphate-reducing bioreactors are considered advantageous for metal sequestering from wastewater via bioprecipitation (Kumar et al., 2021) and/or other secondary mechanisms (Hockin and Gadd, 2007), such as reductive precipitation (Lovley, 1993). Molybdate, being a structural analog to sulphate, can be reduced by SRB into Mo(V) and finally into Mo(IV) which can precipitate as sulfide (Biswas et al., 2009; Chen et al., 1998; Tucker et al., 1998). Molybdenum sulfide has been evaluated as a catalyst for hydrogen production (Bhat and Nagaraja, 2019).

This work demonstrates the capacity of a bioreactor to treat solutions containing Mo(VI) at levels up to 200 mg/L for the recovery of molybdenum as MoS_2. Such solutions may originate from wastewater generated upon the hydrometallurgical treatment of waste electronic equipment such as thin-film photovoltaic panels for critical metals recovery (Theocharis et al., 2021).

Materials and methods

The packed-bed reactor was a PVC tube (length: 50 cm; I.D.: 9.5 cm) which was filled with porous, sintered-glass cylindrical pieces (length: 2.5-3.5 cm; diam.: 1 cm – Biohome Ultimate Marine®, Aqua Bio UK), resulting in a bed height of 40 cm and reactor effective volume of 1.7 L. The reactor was inoculated by transferring sufficient support material with already grown microbial biomass from a previously operated bioreactor with ethanol as carbon/electron source. The bacterial culture was dominated by *Desulfobacter postgatei* (Kousi et al., 2011); an acetate-utilizing species.

The reactor operated at constant room temperature (25°C) in fed-batch upflow mode; it was fed from a 2 L bottle via a peristaltic pump. The feeding solution was replaced (every 4 days) without emptying the reactor. The reactor was fed with synthetic solutions based on a modified Postgate's medium (DSMZ GmbH, *Desulfovibrio* medium no.63), where lactate was replaced with ethanol. The solution also contained divalent iron (100 mg/L, added as $FeSO_4.7H_2O$), molybdate (100-200 mg/L added as $Na_2MoO_4.2H_2O$) and sulphate (1,600 mg/L, added as Na_2SO_4 and $MgSO_4.7H_2O$). Ethanol was supplied at 20% surplus vs. the stoichiometrically required quantity for the reduction of sulphate (reactions (1)-(2)) and molybdate, considering ethanol assimilation for biomass growth and preservation. The pH of the solution was adjusted to 3.0-3.5 by adding HCl.

$$2CH_3CH_2OH + SO_4^{2-} \rightarrow 2CH_3COO^- + H_2S + 2H_2O \quad (1)$$

$$2CH_3COO^- + 2SO_4^{2-} \rightarrow 4HCO_3^- + 2HS^- \quad (2)$$

The bioreactor performance was monitored in terms of pH and sulphate content. Sulphate concentration was determined by turbidimetry at 450 nm after formation of $BaSO_4$ (Hach DR/6000, Method 8051) and molybdate molybdenum concentration was determined at 420 nm after reaction with mercaptoacetic acid (Hach DR/6000, Method 8036). Total molybdenum and iron concentrations were determined by inductively-coupled plasma optical emission spectroscopy (Leeman Labs, Inc).

Results and discussion

Figure 1 demonstrates the high potential of the bioreactor in terms of solution neutralization and sulphate reduction; the pH of the treated solution reached 8 whereas the final sulphate concentration was below 150 mg/L after 72 h. The residual Mo(VI) concentration was below 3 mg/L indicating complete reduction without any inhibition on the sulphate reducing activity. Total Mo concentration followed Mo(VI) profile (data not shown) indicating molybdenum precipitation as sulfide.

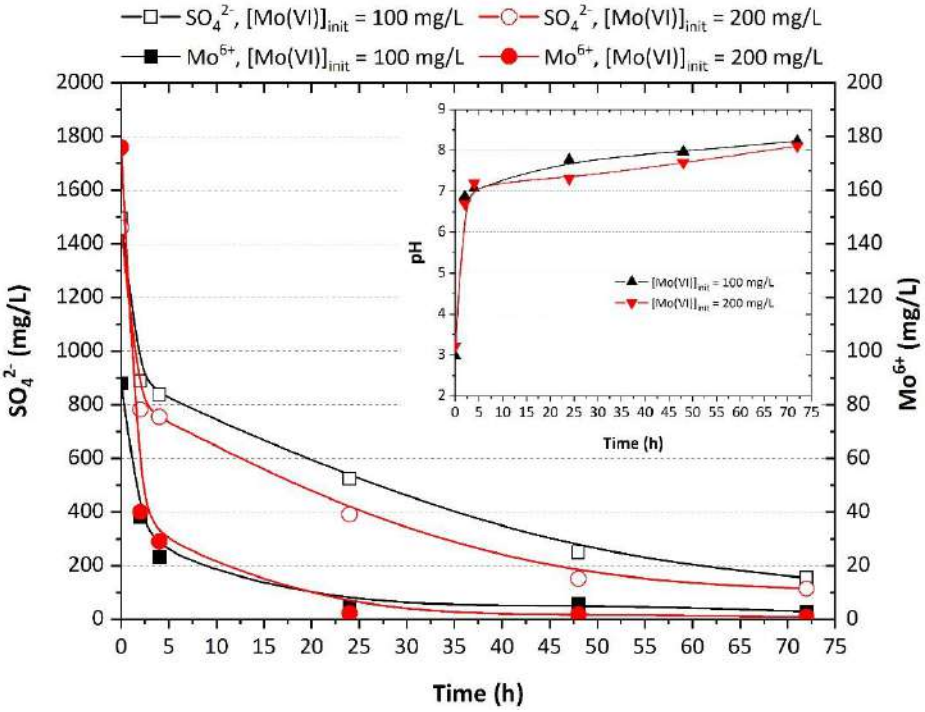

Figure 1. *Sulphate, molybdate molybdenum and (inset) pH profiles during a bioreactor run (data points are the mean values of duplicate experiments)*

References

Bhat, K.S., Nagaraja, H.S., 2019. Performance evaluation of molybdenum dichalcogenide (MoX_2; X= S, Se, Te) nanostructures for hydrogen evolution reaction. International Journal of Hydrogen Energy 44, 17878-17886.

Bijmans, M.F.M., Buisman, C.J.N., Meulepas, R.J.W., Lens, P.N.L., 2011. Sulfate reduction for inorganic waste and process water treatment, in: Murray, M.-Y. (Ed.), Comprehensive Biotechnology, 2nd ed. Academic Press, Burlington, pp. 435-446.

Biswas, K.C., Woodards, N.A., Xu, H., Barton, L.L., 2009. Reduction of molybdate by sulfate-reducing bacteria. BioMetals 22, 131-139.

Chen, G., Ford, T.E., Clayton, C.R., 1998. Interaction of sulfate-reducing bacteria with molybdenum dissolved from sputter-deposited molybdenum thin films and pure molybdenum powder. J. Colloid Interface Sci. 204, 237-246.

Hockin, S.L., Gadd, G.M., 2007. Bioremediation of metals and metalloids by precipitation and cellular binding, in: Barton, L.L., Hamilton, W.A. (Eds.), Sulphate-reducing bacteria: Environmental and engineered systems. Cambridge University Press, Cambridge, pp. 405-434.

Kousi, P., Remoundaki, E., Hatzikioseyian, A., Battaglia-Brunet, F., Joulian, C., Kousteni, V., Tsezos, M., 2011. Metal precipitation in an ethanol-fed, fixed-bed sulphate-reducing bioreactor. J. Hazard. Mater. 189, 677-684.

Kumar, M., Nandi, M., Pakshirajan, K., 2021. Recent advances in heavy metal recovery from wastewater by biogenic sulfide precipitation. J. Environ. Manage. 278, 111555.

Lovley, D.R., 1993. Dissimilatory metal reduction. Annu. Rev. Microbiol. 47, 263-290.

Postgate, J.R., 1979. The sulphate-reducing bacteria. Cambridge University Press, Cambridge Eng., New York.

Rabus, R., Hansen, T.A., Widdel, F., 2007. Dissimilatory sulfate- and sulfur-reducing prokaryotes, in: Dworkin, M., Falkow, S., Rosenberg, E., Schleifer, K.-H., Stackebrandt, E. (Eds.), The Prokaryotes: Ecophysiology and Biochemistry, 3rd ed. Springer, New York, pp. 659-768.

Theocharis, M., Tsakiridis, P.E., Kousi, P., Hatzikioseyian, A., Zarkadas, I., Remoundaki, E., Lyberatos, G., 2021. Hydrometallurgical Treatment for the Extraction and Separation of Indium and Gallium from End-of-Life CIGS Photovoltaic Panels. Materials Proceedings 5, 51.

Tucker, M.D., Barton, L.L., Thomson, B.M., 1998. Removal of U and Mo from water by immobilized *Desulfovibrio desulfuricans* in column reactors. Biotechnol. Bioeng. 60, 88-96.

Valorization of olive processing industry waste through biorefinery development for sustainable production of polyphenols, algal biomass, and lipids

A. Nicodemou[1], M. Kallis[1] and M. Koutinas[1]

[1]Department of Chemical Engineering, Cyprus University of Technology, Limassol, Cyprus
Corresponding author email: michail.koutinas@cut.ac.cy

keywords: *biorefinery; olive pomace; table olive processing wastewater; polyphenols; microalgae.*

Introduction

Olive industrial processing stages generate a large number of by-products, including pomace, stones and table olive wastewater (Rapa and Ciano, 2022). Olive pomace (OP) comprises a semi-solid residue obtained in large quantities following olive oil extraction, while table olive processing wastewater (TOPW) is generated by the processing of olives required to become edible, emitted in rapidly increasing volumes in recent years. In the current work, a biorefinery was developed employing *Isochrysis galbana* and *Scenedesmus obliquus* for the manufacture of polyphenols, lipids and algal biomass, using OP and TOPW. High biomass and lipid levels could be potentially formed during the cultivation of the aforementioned microalgal strains using OP and TOPW, given that the application of the specific microalgae strains under 1% glucose resulted in biomass productivity that reached 0.13 and 0.06 g L^{-1} d^{-1} for *S. obliquus* and *I. galbana* respectively (Nicodemou et al., 2022).

Materials and methods

OP was obtained by a two-phase system while TOPW was customly prepared using 1.5 kg of black olives and 3 kg of water or brine. Different operational parameters were investigated for the fractionation of OP into its main constituents, including the removal of residual oil, water extraction (WE), dilute acid (DA) pretreatment and enzyme hydrolysis (EH). Moreover, four different polymeric resins (XAD16N, XAD7HP, PAD900, XAD4) were evaluated for their capacity to recover the phenolic content of TOPW and OP extracts. Determination of cellulose, hemicellulose and lignin concentration was performed by employing a Fibre-Bag System. Reducing sugars and polyphenols were determined by DNS and Folin-Ciocalteu method, respectively. The growth of each microalgae culture was monitored by measuring the ash-free dry weight and optical density. Lipids were extracted from algae cells following Folch method.

Results and discussion

WE of defatted OP (100 °C, 15 min, 10% solids) resulted in the recovery of 9.4% reducing sugars and 1.1% polyphenols. Also, DA hydrolysis (1% w/v H_2SO_4, 135 °C, 60 min, 10% solids) achieved 92% hemicellulose removal, while EH (15 FPU Cellic® CTec 2 $g^{-1}_{substrate}$, 24 h) corresponded to 54% cellulose removal. Application of XAD16N and PAD900 exhibited the highest overall polyphenols recovery, that reached 79.5% and 58.0% for TOPW and OP extracts respectively. Cultivation of *S. obliquus* employing detoxified effluents resulted in 0.19 g L^{-1} d^{-1} and 61.4 mg L^{-1} d^{-1} biomass and lipid productivity, while *I. galbana* produced 0.032 g L^{-1} d^{-1} and 8.4 mg L^{-1} d^{-1}, respectively. Also, *I. galbana* performed high docosahexaenoic acid content, which reached 8.4-9.5 mg g^{-1} of ash-free dry weight.

Conclusions

The fermentation experiments attained significant results on biomass and lipids, without any optimization of the conditions. Future work will focus on enhancing the lipid content generated aiming to maximize process effectiveness.

Acknowledgements: This research did not receive any specific grant from funding agencies in the public, commercial, or not-for-profit sectors.

References

Nicodemou, A., Kallis, M., Agapiou, A., Markidou A. and Koutinas, M., 2022. The Effect of Trophic Modes on Biomass and Lipid Production of Five Microalgal Strains. *Water* 14. https://doi.org/10.3390/w14020240

Rapa, M. and Ciano, S., 2022. A Review on Life Cycle Assessment of the Olive Oil Production. *Sustainability* 14. https://doi.org/10.3390/su14020654

SUST ENG 2023

AIR EMISSIONS/ CO_2 SEPARATION

Effect of the polymer blend-based membranes composition on CO_2 separation efficiency

Mariana-Dana DAMACEANU[1], Irina BUTNARU[1], Catalin-Paul CONSTANTIN[1], and Aleksandra WOLIŃSKA-GRABCZYK[2]
[1]"Petru Poni" Institute of Macromolecular Chemistry, Electroactive Polymers and Plasmochemistry Laboratory, Iasi-Romania
[2]Centre of Polymer and Carbon Materials, Polish Academy of Sciences, Zabrze – Poland
Corresponding author email: damaceanu@icmpp.ro

keywords: *polyimide blends; miscibility; thermal stability; mechanical behavior; CO_2 separation.*

Introduction

The rapid developments in the polymer science have triggered the evolvement of the polymer membrane technology for CO_2 separation and capture due to some advantages, such as operational simplicity, energy efficiency, flexibility, and reduced cost [1]. The membrane-based carbon capture is currently applied for CO_2/N_2 separation from the flue gas, CO_2/H_2 separation in syngas processing, and CO_2/CH_4 separation in natural gas and biogas sweetening [2]. For efficient CO_2 capture, a membrane material needs to be placed on or above the Robeson Upper Bound, i.e., in the high permeability/moderate selectivity regime. The current membranes used in industry are based on conventional polymers like polysulfone, cellulose acetate, polyethylene oxide, etc. and did not surpass the cost efficiency of conventional CO_2 separation technologies. Therefore, new classes of advanced membrane materials are necessary to be developed, including mixed matrix and polymer blend membranes [3]. In this respect, membranes obtained from blends of aromatic polyimides, especially fluorinated polyimides are perspective due to their excellent balance of thermal, mechanical, chemical and electrical properties [4]. Here we report on our attempts to develop such membranes, with focus on their characteristics and performance in the separation of CO_2 and other gasses.

Materials and methods

The fluorinated polymers used in the present study were prepared by solution polycondensation reactions and structurally identified by spectral methods.

Membranes based on binary polymer blends with various contents of a fluorinated polyimide were synthesized by mixing polymer solutions in different ratios, followed by ultra-sonication, casting onto glass plates and gradual heating up to 160°C. The resulting dense membranes were stripped off the plates by immersion in boiling water, and then dried.

The blend membranes were characterized by different techniques, such as: differential scanning calorimetry (DSC), scanning electron microscopy (SEM), wide-angle X-ray diffraction (WAXD) and dynamo-mechanical analysis (DMA). The mechanical resistance was evaluated on the basis of the tensile tests, whilst the gas permeation measurements were performed by monitoring the increase of pressure in the downstream volume after a 6 bar pressure was applied to the membrane.

Results and discussion

In the pursuit to develop efficient polymer membranes for CO_2 separations, blending techniques was involved to obtain materials that synergistically combine the advantages of blend components. Thus, three blend membranes were obtained and morphologically investigated by SEM analysis. The cross-sectional images did not evidence any phase separation, indicating a good miscibility of the two components at the molecular level. The miscibility of the two different constituents of polymeric blends was also proved by DSC, XRD and DMA analyses. In the DSC curves, all polymers blends showed a single glass transition temperature (Tg), which is an important indicative of the blend components miscibility. Except from Tg, the blends did not exhibit other phase transitions (e.g., crystallization or melting), thus proving the amorphous nature of the samples. XRD studies revealed only one broad halo for all blend membranes whose center correspond to a single interchain spacing, being characteristic to an amorphous blend membrane based on a single entity.

The free-standing polymer blend membranes had thicknesses in the micrometer range and were flexible, tough, and maintained their integrity at repeated bending, as demonstrated by the investigated mechanical properties obtained during tensile tests. The highest value for the tensile strength was registered for the polymer blend with equal quantities of the two components, at the expense of a decreased elongation to break. In DMA analysis, the polymers showed two secondary transitions: γ - at low temperature, due to phenyl ring motions, that is influenced by moisture absorption content, aging history and morphology, and α - in the highest temperature domain, due to motions of very large segments of chains or coordinated movements of the entire polymer chains. The latter is associated with Tg and is in accordance with the results of other investigations, demonstrating the miscibility at the molecular level of the blend components.

For the gas permeation experiments, CO_2, O_2, N_2 and He of very high purity were passed through the membranes. For both neat fluorinated polyimide and blend membranes, gas permeability coefficients showed higher values for He, followed by CO_2, O_2, and N_2, which is the trend reported for many glassy polymers. For the studied membranes, the results of the gas transport measurements showed the variation in gas permeability with the ratio of the blends components. At the ratio 1:1 of the two components in the blend composition, a significant improvement was attained in gas permeability with respect to the reference polyimide, without any marked deterioration of membrane separation performance in terms of selectivity.

Conclusions

The investigation of a series of fluorinated polyimide blends revealed a strong structure-property correlation regarding the glass transition temperature, d-spacing, dynamo-mechanical analysis, mechanical behavior and gas permeation properties. All performed measurements highlighted better gas separation results for the blends compared to the reference polyimide in terms of permeability improvements along with a maintained selectivity. Thus, blending technique can be a promising approach for developing membranes for sustainable CO_2 separation with simultaneous high permeability and selectivity.

Acknowledgements: This work was supported by a grant of the Ministry of Research, Innovation and Digitization, CNCS/CCCDI – UEFISCDI, project PN-III-P2-2.1-PED-2021-1666, contract no. 718PED/2022, within PNCDI III.

References

Ramasubramanian, K., Zhao, Y. and Ho, W.S.W., 2013. CO_2 capture and H_2 purification: prospects for CO_2-selective membrane processes, *AIChE J.,* 59, 1033-1045.

Han, Y. and Winston Ho, W.S., 2021. Polymeric membranes for CO_2 separation and capture, *J. Membr. Sci.*, 628, 119244.

Tong, Z. and Sekizkardes, A.K., 2021. Recent Developments in High-Performance Membranes for CO_2 Separation, *Membranes* 11, 156.

Liaw, D. J., Wang, K. L., Huang, Y. C., Lee, K. R., Lai, J. Y. and Ha, C. S., 2012. Advanced polyimide materials: Syntheses, physical properties and applications, *Prog. Polym. Sci.*, 37, 907-974.

Reliable fugitive emissions measurements at a gas transmission network

N. Tsochatzidis and N. Katsis

Hellenic Gas Transmission System Operator (DESFA) SA, Greece
Corresponding author email: n.tsochatzidis@desfa.gr

keywords: *fugitives; methane emissions; gas network; greenhouse gases.*

Introduction

Natural gas is mainly composed by methane which is one of the most important contributors to climate change. Methane is responsible for around 30% of the rise in global temperatures since the industrial revolution (GMA, 2021). Gas Transmission networks are potential sources of methane emissions which are divided in three macro categories (Marcogaz, 2019):

- Fugitive emissions
- Vented emissions
- Emissions from incomplete combustion

Fugitive emissions (Figure 1) are the emissions to the atmosphere resulting from leaking piping components and equipment such as valves, flanges, pump seals etc. (OGMP, 2020). These emissions are not visible but can be measured with different measurement equipment. Although the emission of one single component might seem small, many of these leaking components result into significant emissions to the atmosphere. Companies and organizations should identify and eliminate these leaking components and the resulting emissions. Gas transmission operators, worldwide, are carrying out intensive programs on the quantification of the total methane emissions in their activities and are designing mitigation measures for methane emissions reduction. Leak detection and repair (LDAR) refers to the process of locating and repairing fugitive leaks. LDAR encompasses several techniques and equipment types (sniffers, IR cameras etc.). Ravikumar et al. (2020) reports that the total methane emissions reduced by 44% after one LDAR survey at natural gas facilities.

Materials and methods

A rigorous LDAR campaign is implemented at some of the main facilities of DESFA, the Hellenic gas transmission system operator and discussed in this study. The emission estimate is obtained by implementing the EN15446:2008 Standard. The activity consists of:

- inventory and classify the sources to configure the reference database
- register a methane emissions measurement for each source
- indicate sources with leakages to initiate corrective actions
- report the emissions in accordance with the Standard procedure

The inventory of sources of all the components of the gas facilities are grouped into the six main categories as per EN15446:2008 (Compressors, Pumps, Valves, Pressure Relief Valves, Connections such as flanges and fittings Open-Ended Line).
Monitoring the fugitive emissions is done using high-end Toxic Vapor Analyzers (TVA) (Figure 2) based on flame ionization or photo ionization technology. Flame Ionization Detectors (FID) measures organic compounds by utilizing a flame produced by the combustion of hydrogen and air in the measurement chamber. The TVA is calibrated with methane. The dynamic range of this device goes from 0 to 100,000 ppm of methane.

Results and discussion

A Leak Detection and Repair (LDAR) inspection is carried out on the main DESFA's gas transmission facilities and presented in this study. A very minimal percentage of components is identified with some leakages.

These leakages are repaired and reinspected to confirm the reduction of methane emissions at the inspected facilities. The LDAR inspection is going to be repeated regularly.

Figure 1. *Fugitive emissions*

Figure 2. *Methane emissions measurement using a TVA Analyser*

References

EN15446:2008 Fugitive and diffuse emissions of common concern to industry sectors - Measurement of fugitive emission of vapours generating from equipment and piping leaks. *CEN*, January 2008.

Global Methane Assessment. Benefits and Costs of Mitigating Methane Emissions, 2021. *United Nations Environment Programme*, ISBN: 978-92-807-3854-4.

Marcogaz, 2019. WG_ME-485, Assessment of methane emissions for gas Transmission and Distribution system operators.

OGMP, 2020. Mineral Methane Initiative OGMP2.0 Framework, 19 November 2020 https://www.eenews.net/assets/2020/11/23/document_ew_06.pdf.

Ravikumar, A.P., Roda-Stuart, D., Liu, R., Bradley, A., Bergerson, J., Nie, Y., Zhang, S., Bi, X. and Brandt, A.R, 2020. Repeated leak detection and repair surveys reduce methane emissions over scale of years, *Environ. Res. Lett.,* 15, 034029.

Monitoring of goat cheese whey wastewater VOCs by extraction techniques

S. Elia[1], M. Stylianou[2] and A. Agapiou[1*]

[1]Department of Chemistry, University of Cyprus, P.O. Box 20537, Nicosia, Cyprus
[2]Faculty of Pure and Applied Sciences, Open University of Cyprus, Latsia, Nicosia, Cyprus
Corresponding author email: agapiou.agapios@ucy.ac.cy

keywords: *Solid extraction; GC-MS; air pollution; odor.*

Introduction

A significant amount of wastewater is produced by the dairy industry, and this effluent exhibits strong odor characteristics as a result of its composition.

In the present study, the efficacy of the green micro-extraction techniques HiSorb and solid phase microextraction (SPME) was investigated for the analysis of volatile organic compounds (VOCs) from goat cheese whey effluents.

For this purpose, the experimental parameters of coating, extraction time, agitation speed, sample volume, extraction temperature, and salt addition were investigated for both extraction techniques.

Materials and methods

The triple-coated extraction tools of HiSorb with divinylbenzene/carbon wide range/polydimethylosiloxane (DVB/CWR/PDMS), as well as the SPME fiber with DVB/CAR/PDMS, were used to identify the goat cheese whey wastewater VOCs.

The analysis was performed using the thermal desorption-gas chromatography/mass spectrometry (TD-GC/MS) system for HiSorb, as well as the GC-MS for SPME, respectively.

Results and discussion

The DVB/CWR/PDMS HiSorb-coated probe resulted in a total of 34 VOCs, compared to 23 VOCs with the DVB/CAR/PDMS SPME fiber.

In addition, the reproducibility of the HiSorb was better, as the relative standard deviation (RSD) of the VOCs was 3.7%, compared to 7.1% for SPME.

Conclusions

In conclusion, the HiSorb technique can be successfully used for the analysis of VOCs in complicated matrices, such as cheese whey.

References

Elia, S., Stylianou, M., Agapiou, A., 2023. Combined EC/EO processes for treating goat cheese whey wastewater. *Sustainable Chemistry and Pharmacy* 32, 100963.

Elia, S., Stylianou, M., Agapiou, A., 2022. Aroma characterization of raw and electrochemically treated goat whey wastewater. *Sustainable Chemistry and Pharmacy* 27, 100640.

POLICIES, REGULATORY AND SOCIAL ACCEPTANCE

Evaluation of MULESL technology for wastewater reuse in light of Regulation (EU) 2020/741

V.G. Altieri[1], M. De Sanctis[1] and C. Di Iaconi[1]

[1]Water Research Institute, Italian National Research Council, Viale F. De Blasio 5, 70132, Bari, Italy
Corresponding author email: valerioguido.altieri@ba.irsa.cnr.it

keywords: *water reuse; reclaimed water; disinfection treatments; quality requirements.*

Introduction

About two thirds of the Earth surface is covered by water, but the vast majority (97.5%) is represented by saltwater. Since, of all the freshwater present on the planet, only 1% is not entrapped into glaciers or beneath the ground, we can easily understand how all the human needs can be met by a fraction (approximately 0,06%) of all the water resources on Earth [Ahuja, 2021].

Among all the human activities, agriculture is the most freshwater-demanding one. According to the Food and Agricultural Organization, the annual withdrawal of freshwater from natural water bodies is estimated at 4250 km^3, with the agricultural sector using more than 71% of the overall freshwater resources [Chen et al., 2021]. Water supply is such an important topic that water crisis has recently been considered as one of the top 10 long-term risks both in terms of probability and impact. Water shortage is a matter of resource availability as well as safety criteria, since the use of contaminated water poses health-related risks.

The emergency situation linked to the water shortage status could be addressed by resorting to "unconventional" water resources. Among the most promising and available ones, wastewater might represent a reliable, alternative supply. According some recent estimates, 380 km^3 (380 trillion L) of wastewater are produced globally every year, with predictions reporting a potential wastewater production on annual basis of 470 km^3 by 2030 [Qadir et al., 2020]. Given the large amount of freshwater employed in this sector, water reuse in agriculture has soon become one of the most employed alternative applications. Especially in regions characterized by water scarcity and arid or semi-arid climates, the use of reclaimed water has long-established itself as a feasible option.

The present study was focused on the application of MULESL technology (which leverages aerobic granular biomass) at full scale, to treat municipal wastewater, in order to meet the minimum quality requirements set out by the Regulation (EU) 2020/741, whose provisions will soon enter in force. The Regulation introduced minimum criteria for water reuse in agriculture, defining four different water quality classes (A-D).

Materials and methods

The experimental campaign was carried out at the municipal WWTP of Putignano, a city located in Puglia (Southern Italy). MULESL performances were evaluated either considering only the biological process or boosting it by means of a disinfection step performed with peracetic acid (PAA) under three different dosages (1, 2 and 3 mg/L) or by means of UV radiation (using four different UV doses: 48, 60, 80, and 120 mJ/cm^2).

Treatment efficiency was assessed by monitoring two chemical parameters included in the Regulation, namely biochemical oxygen demand, 5-day test (BOD_5) and total suspended solids (TSS). BOD_5 was determined by means of LCK555 Hach cuvette test, while TSS were determined through standard methods. The disinfection efficiency was assessed by investigating *Escherichia Coli*, which was included in the Regulation. *E. Coli* abundance was evaluated by using IDEXX Colilert-18 and Quanti-Trays/2000 according to the company instructions.

Results and discussion

Results showed that MULESL technology was able to meet the requirements set out by the Regulation (EU) 2020/741 for chemical parameters. Notably, the average BOD_5 content in the effluent of the biological process was 13.6 mg/L, while the TSS content was 33.2 mg/L. Disinfection did not affect TSS, so TSS content was assessed only in the biological process. Conversely, the treatment with PAA increased BOD_5 content in the final effluents (from 4 to 7 mg/L more, depending on the PAA concentration). Nevertheless, even after the chemical disinfection, BOD_5 concentration was lower than the level required by the Regulation. Thus, the two different schemes efficiently met either BOD_5 (25 mg/L) or TSS limit (35 mg/L) required for water quality classes from B to D. In these classes are included those food crops which, if eaten raw, would not have the edible part in direct contact with water.

In terms of *E. Coli*, the biological step ensured 2.3 log units removal (LUR), with an average concentration of $1.1 \cdot 10^5$ MPN/100 mL. Better performances were ensured through disinfection. PAA addition allowed a further reduction up to 3.2 LUR, while UV radiation improved $\log_{10}$ reduction up to 3.7 LUR. In particular, it was possible to be compliant with the upcoming legal limits for quality class B with regard to *E. Coli* average concentration (< 100 MPN/100 mL) by applying a radiation of 60 J/cm^2 or a PAA dosage of 3 mg/L. Even lower dosages might be employed to meet water quality class C, namely 48 mJ/cm^2 and 2 mg/L for UV and PAA, respectively. Results of the physical and chemical disinfection treatments are reported in Table 1.

Table 1. Mean concentrations and standard deviations of *E. Coli* after physical and chemical disinfection

			Physical disinfection by means of UV radiation			
	infl	**effl**	**48 mJ/cm²**	**60 mJ/cm²**	**80 mJ/cm²**	**120 mJ/cm²**
mean ± std dev	$(1.9\pm1.1)\cdot10^7$	$(1.1\pm0.9)\cdot10^5$	$(1.9\pm2.6)\cdot10^2$	$(1.0\pm2.0)\cdot10^2$	$(5.3\pm8.3)\cdot10^1$	$(3.4\pm6.3)\cdot10^1$
			Chemical disinfection by means of peracetic acid			
	infl	**effl**	**1 mg/L**	**2 mg/L**	**3 mg/L**	
mean ± std dev	$(1.9\pm1.1)\cdot10^7$	$(1.1\pm0.9)\cdot10^5$	$(5.0\pm5.4)\cdot10^4$	$(2.3\pm2.8)\cdot10^2$	$(6.2\pm5.0)\cdot10^1$	

Conclusions

In light of the upcoming entry into force of the Regulation (EU) 2020/741, laying down the minimum quality requirements for water reuse in agriculture, the treatment efficiency of the MULESL technology was assessed. The technology has proved capable to produce an effluent able to meet the limits set out by the Regulation for the classes B to D in terms of chemical parameters (namely, BOD_5 and TSS). Regarding the microbiological criteria, the enhancement of the biological treatment with a disinfection step (either chemical or physical treatment) allowed to meet quality requirements for classes B to D, even using lower dosages than those reported in literature.

Acknowledgements: This work was partially supported by the Italian National PON TARANTO Project (ARS01_00637).

References

Ahuja S, 2021. Handbook of Water Purity and Quality (Second Edition), Academic Press

Chen CY, Wang SW, Kim H, Pan SY, Fan C, Lin YJ, 2021. Non-conventional water reuse in agriculture: A circular water economy. Water Research 199, 117193

Qadir M, Drechsel P, Jiménez Cisneros B, Kim Y, Pramanik A, Mehta P, Olaniyan O, 2020. Global and regional potential of wastewater as a water, nutrient and energy source. Natural Resources Forum 44 (1), 40-51.

Social acceptance of sustainable bioenergy transition policies for public health

E. Lakioti[1], A. Itziou[2], I. Vasiliadou[3], V. Karayannis[3] and C. Tsanaktsidis[3]

[1]Department of Public and One Health, University of Thessaly, Karditsa, Greece
[2]Department of Midwifery, University of Western Macedonia, Ptolemaida, Greece
[3]Department of Chemical Engineering , University of Western Macedonia, Kozani, Greece
Corresponding author email: elakioti@uth.gr

keywords: *Social Acceptance; Public health; Sustainable Bioenergy; Policy; Decarbonization*

Introduction

The current study reviews and discusses cutting-edge research regarding social acceptance and support of bioenergy transition policies for public health.

Using renewable and clean biofuel energy efficient resources and processes could effectively eliminate any potential carbon emissions related to energy production and move closer to attaining a zero carbon footprint. In reality, the study of societal and environmental connections strives to promote active involvement for increasing public acceptance of developing technologies and enhancing human health and well-being, particularly in the wake of pandemics.

Social acceptance - Sustainable bioenergy transition - Public health policies

Studying social inputs in relation to important environmental and health issues is a common strategy that has garnered a lot of interest in this context. Particular attention is paid to the social perceptions, attitudes and awareness of increasingly prevalent renewable energy sources, with a recent focus on policies for sustainable bioenergy, including clean biofuel energy.

Decision-making in specifying realistic policy objectives and operational measures to find appropriate solutions for the transition from the traditional to bioenergy schemes will require encouragement of participation of multiple societal stakeholders, e.g. government, municipalities, industries, experts, and certainly public.

In particular, an understanding of important social factors that support the dissemination of expert information to society and influence and shape society's readiness for pertinent technical advancement is given. The need of social acceptance and preparedness is highlighted for policy making in order to hasten the adoption of novel pertinent processes for ensuring public health.

Concluding remarks

Suitable methods and thorough policies and plans should be created for the transition to a more extensive use of bioenergy in order to support the urgent need for decarbonization, in order to address climate change and minimize negative effects on public health.

The active involvement of society appears to be a key factor for establishing a high degree of confidence by placing the emphasis on the possible positive outcomes from sustainable policies for the environmental and human health and well-being.

References

Jaiswal, K.K., Chowdhury, C.R., Yadav, D. et al., 2022. Renewable and sustainable clean energy development and impact on social, economic, and environmental health. *Energy Nexus*, 7, 100–118.

Lakioti, E., Kokkinos, K., Samaras, P. and Karayannis, V., 2020. Exploring Environmental and Social determinants of Health using Explainable Artificial Intelligence, *Greenchem6 – 6th International Symposium on Green Chemistry, Sustainable Development and Circular Economy*, Thessaloniki, Greece

Mistur, E.M., 2017. Health and energy preferences: Rethinking the social acceptance of energy systems in the United States. *Energy Research and Social Science*, 34, 184–190.

Zafeiriou, E., Spinthiropoulos, K., Tsanaktsidis, C. et al., 2022. Energy and Mineral Resources Exploitation in the Delignitization Era: The Case of Greek Peripheries. *Energies*, 15(13), 4732.

Sustainable siting of offshore wind farms. Application in Crete (SusTainablE siting of offshore wind Parks. Application in Crete) Step – Ap

P. Gkeka Serpetsidaki[1] and T. Tsoutsos[2]

[1,2] Renewable and Sustainable Energy Systems Laboratory, School of Chemical and Environmental Engineering, Chania, Greece
Corresponding author email: theocharis.tsoutsos@chenveng.tuc.gr

keywords: *offshore wind farms; sustainable siting; islands; social acceptance.*

Abstract

The European Union (EU) has already set targets for climate neutrality with the main objective being the development of renewable energy sources (RES) for 2030 up to 40%. In this context, the development of offshore wind farms is now a political priority, as they can contribute the most to the achievement of the above goals and, in general, to the decarbonization of the planet. The European Parliament has already issued (2022) its strategy for increasing offshore wind farms, "A European strategy for offshore renewable energy (2021/2012(INI))", as well as our country according to ESEK (Government Gazette B΄4893/2019) has emphasized the importance of the development of offshore wind farms ("priority will be given, as well as marine wind farms with corresponding multiple combined benefits for the energy system, networks and the national economy (p. 283)". In this context, the PESPKA of Crete refers, on the one hand, to the need to protect marine fauna and flora from man-made activities, as well as to the existing plan for sustainable siting of onshore wind farms. It is based on the Special Study (Renewable and Sustainable Energy Systems Project, 2011), which evaluated necessary information for the siting of onshore wind turbines (areas of environmental interest and cultural heritage, residential activity areas, technical infrastructure networks and special uses and production activity zones or facilities), identified exclusion zones and optimal siting criteria, assessed available areas and calculated the (ground) bearing capacity of wind farm sites to minimize local environmental impacts. They are, however, subject to several limitations (social, environmental, Techno-economic, etc.) and are therefore a multifactorial "problem", which requires a holistic approach. At the same time, increasing land use conflicts, together with the increasing demand for green energy, combined with the untapped offshore wind potential, intensify the necessity to develop offshore wind farms. Therefore, their optimum placement based on marine spatial planning is a research field that needs to be further investigated, mainly for island environments due to:

- Their need for long distance energy security from the mainland
- Untapped offshore wind potential and land release needed.

In conclusion, the optimal location of offshore wind farms for Crete should be further investigated for sustainable development and energy independence. In the context of the research proposal, the following are envisaged:

1. Systematic study of existing databases.
2. Evaluation and ranking of the candidate areas, with criteria in addition to the legal and regulatory restrictions that apply in consultation with society and stakeholders, including the categories:

- Local governments (regional policymakers).
- Academic community (Academia)
- Municipalities
- Transmission and energy distribution

- Port Authorities
- Non-governmental organizations
- Energy Production- Energy producers' association
- Tourism - Tourist Associations

3. Field surveys in five (5) candidate areas that meet the criteria.
4. Emphasis on the study of the environment for the effective protection of marine species, with diving, for a more accurate assessment of the conditions prevailing in the area (type of seabed, relief, various types of measurements, etc.), as well as a more complete record of marine species, protected or not. Special emphasis will also be given to the review of the region's avifauna.
5. Consultation and dissemination of results.

Acknowledgements: This study entitled "Sustainable siting of offshore wind farms. Application in Crete (SusTainablE siting of offshore wind Parks. Application in Crete) Step – Ap" is supported by the Green Fund.

SUST ENG 2023

ADSORPTION PROCESSES

Studies on rare earth elements recovery on alginate sorbent modified with ion exchanger with phosphonic groups

D. Fila[1], Z. Hubicki[1] and D. Kołodyńska[1]

[1]Department of Inorganic Chemistry, Institute of Chemical Sciences, Faculty of Chemistry,
University of Maria Curie-Skłodowska, Lublin, Poland
Corresponding author email: dominika.fila@mail.umcs.pl

keywords: *alginate composite; rare earth elements; sorption; reusability.*

Introduction

Alginate is a natural and linear polysaccharide found in the cell walls of brown algae, mainly *Macrocystis* and *Laminaria*. It is composed in various proportions of β-D-mannuronic acid (M) and α-L-guluronic acid (G) residues linked by glycosidic 1-4 bonds. These residues are assembled as blocks for repeating G units (GG blocks) or M units (MM blocks) and for mixed M and G residues (MG blocks). Depending on the source from which it is obtained, alginate differs in the content of G and M residues, as well as in the length of the blocks. The sequence of the blocks determines the molecular structure of the alginate, which significantly affects its physical and mechanical properties. GG block segments exhibit a complex and rigid conformation, while MM block segments provide a linear and flexible conformation. Based on this, it was found that the highest stiffness would be observed for alginates containing GG blocks, and the lowest for alginates containing MG blocks [1]. Alginate, due to its specific properties and structure, is used in the food, paper, and textile industries, medicine and pharmaceuticals, cosmetics, biotechnology, and environmental protection as a metal biosorbent and a carrier for immobilizing microorganisms. Among the most important benefits of using alginate as a biosorbent are its low price, efficiency, selectivity, and lack of toxicity [2]. In addition, alginate sorbents have high sorption capacities even at low concentrations of metal ions in solution. Alginate sorbents obtained by appropriate processing are characterized by their reusability after regeneration. Metal sorption takes place throughout the structure of alginate granules, so they can be regarded as porous ion exchangers with high permeability and capacity. Alginate granules can be used in processes and apparatus solutions that are similar to ion exchangers. Due to its numerous advantages, alginate is still the subject of intensive research by various scientists around the world.

Alginate-based composites are considered highly efficient and environmentally friendly adsorbents. They have been extensively tested to remove industrial dyes, heavy metals, antibiotics, rare earth metals, and other contaminants from water and wastewater [2]. It has been proven that natural polymer-based composites have better adsorption capacities towards pollutants compared to the pure natural polymers [3]. Costa et al. [4] prepared a natural polymeric bioadsorbent (SAPVA) based on calcium alginate/sericin and poly(vinyl alcohol) (PVA) to recover the ytterbium from aqueous solution. The adsorbed amount of Yb(III) was found to be 0.142 mol/kg at equilibrium state. Another alginate-based composites such as alginate-biochar and alginate-clinoptilolite composites were synthetized by Fila et al. [5]. Satisfactory results were obtained for the lanthanum(III), cerium(III), praseodymium(III) and neodymium(III) sorption. So, this type of natural sorbents are recommended towards rare earth elements sorption.

In the paper, recovery of rare earth elements (REEs) such as lanthanum(III), neodymium(III), samarium(III), and holmium(III) from aqueous solutions through biosorption onto the green adsorbent are proposed.

Materials and methods

To modify the alginate (ALG), the ion exchanger Duolite ES63 (DES63), which contains phosphonic functional groups was added to its structure. As a crosslinker, calcium chloride anhydrous was used. The ALG@DES63 beads were obtained by dropping a mixture of alginate with Duolite ES63 into a calcium chloride solution using a peristaltic pump. Composite beads with two grain sizes were synthesized: before drying, their diameters were 2 and 4 mm, while after drying, they were 0.6 and 1.1 mm.

The adsorption performances of alginate@Duolite ES63 composite beads towards lanthanum(III), neodymium(III), samarium(III), and holmium(III) ions were evaluated via batch adsorption tests, which included a solution pH effect test, adsorption kinetics, and an adsorption isotherm.

Results and discussion

Alginate@Duolite ES63 composite beads exhibited excellent adsorption properties at pH 3–6, which achieved a complete removal of rare earth element ions (99–100%). Meanwhile, REEs adsorption at pH 2 showed a slower speed and lower removal (about 38–46%). Alginate sorbent has shown a very high affinity toward rare earth metal ions (La(III), Nd(III), Sm(III), and Ho(III) ions). The selectivity order can be expressed as: Ho(III) > Sm(III) > La(III) > Nd(III).

Figure 1. *General scheme of sorption procedure.*

The pseudo-second order kinetic model and the Langmuir isotherm model were the best models described the sorption process of La(III), Nd(III), Sm(III), and Ho(III) ions onto ALG@DES63, according to the kinetic and isotherm equilibrium investigations.

Conclusions

In the present work, the alginate modified with duolite ES63 proved to be excellent choice as metal ions adsorbents. Alginate modification was prepared successfully. In the case of REEs ions, ALG@DES63 was very promising adsorbents where the uptake reached 100% at pH= 5.

Acknowledgements: This study is supported by the National Science Centre in accordance with decision No. 2019/35/N/ST8/01390.

References

Hecht, H., Srebnik, S., 2016. Structural Characterization of sodium alginate and calcium alginate. *Biomacromolecules*, 17, 2160–2167.

Thakur, S., Sharma, B., Verma, A., Chaudhary, J., Tamulevicius, S., Thakur, V.K., 2018. Recent progress in sodium alginate based sustainable hydrogels for environmental applications. *J. Clean. Prod.*, 198, 143–159.

Kayan, G.Ö., Kayan, A., 2021. Composite of natural polymers and their adsorbent properties on the dyes and heavy metal Ions. *J. Polym. Environ.*, 29, 3477–3496.

Barcelos da Costa, T., Carlos da Silva, M.G., Adeodato Vieira, M.G., 2021. Development of a natural polymeric bioadsorbent based on sericin, alginate and poly(vinyl alcohol) for the recovery of ytterbium from aqueous solutions. *J. Clean. Prod.*, 279, 123555.

Fila, D., Hubicki, Z., Kołodyńska, D., 2022. Applicability of new sustainable and efficient alginate-based composites for critical raw materials recovery: General composites fabrication optimization and adsorption performance evaluation. Chem. Eng. J., 446, 137245–137267.

Hydrotalcite modified biochar as a sorbent to remove cerium ions from water media

J. Bąk[1] and D. Kołodyńska[1]

[1]Department of Inorganic Chemistry, Institute of Chemical Sciences, Faculty of Chemistry, Maria Curie-Skłodowska University, Lublin, Poland
Corresponding author email: justyna.bak@mail.umcs.pl

keywords: *cerium ions; hydrotalcite modification; LDHs-modified biochar; water media.*

Introduction

The use of rare earth elements (REE) in various industries is constantly increasing, which leads to an increase in demand and, consequently, to the depletion of their natural resources. It is therefore necessary to develop ecological solutions aimed at their effective recovery and reuse. The following methods are used to separate and pre-concentrate REE: co-precipitation, ion exchange and solvent extraction. However, due to secondary pollution, inefficiency and high operating costs, new and more effective methods are sought. Therefore, adsorption has been recognized as one of the best methods due to its non-toxicity, reusability, ease of use and abundance of adsorbents in nature.

Therefore, research is underway to search for sorbents that will effectively remove REE ions from aqueous solutions. The use of different types of biochars affects the transport of REE through the processes of sorption/desorption, surface precipitation and oxidation/reduction reactions, and enables their effective recovery from aqueous solutions. In addition, these sorbents are cheap because they are obtained from waste materials. Biochar materials have a homogeneous composition in relation to the raw material from which they are obtained. In addition, the decisive feature for their use in many technological aspects is the adsorption capacity and the possibility of modifying their surface. The adsorption capacity of biochars results from the presence of surface functional groups such as: hydroxyl, carboxyl and carbonyl, which enable their easy binding with various types of impurities.

Hydrotalcite was used as an example of a biochar modifier. Hydrotalcite is a mixed layered magnesium hydroxide aluminum with the summary formula: $Mg_6Al_2(OH)_{16}CO_3{\cdot}4H_2O$, a naturally occurring mineral. In hydrotalcite, divalent cations (Mg^{2+}) are substituted by o cations higher valence (Al^{3+}), which leads to the appearance of a positive charge on layers. This charge is compensated by the hydrated anions found in interlayer space. The name "hydrotalcite" is more and more often used to describe the synthetic group equivalents or compounds mimicking a characteristic structure so-called layer double hydroxides (LDH) of the general formula of $[M^{2+}_{1-x}M^{3+}_x(OH)_2]^{x+}(A^{n-})^{x/n}{\cdot}\,mH_2O$, where M^{2+} and M^{3+} are divalent and trivalent metal cations located on the sheets, x ($M^{3+}/M^{2+}+M^{3+}$) is molar fraction of trivalent metals, n is valence of anion in the interlayer space and m is number of hydrated water molecules. The condition for the formation of the correct hydrotalcite structure is the use of cations metals with similar ionic radii, e.g. Mg^{2+}, Ni^{2+}, Cu^{2+}, Zn^{2+}, Mn^{2+} and Fe^{3+}, Al^{3+}, Cr^{3+}. In addition, the appropriate proportions of di- and trivalent metals must be maintained, which is determined by the mole fraction x ranging from 0.2 to 0.33. One of the most commonly used methods of LDH synthesis is co-precipitation at constant pH. It consists in slowly adding the solution containing di- and trivalent metal salts to the reactor containing water (aqueous sodium carbonate solution is also often used). At the same time, an alkaline solution (usually NaOH) is also added to the reactor to maintain a constant pH. The pH range in which the synthesis takes place should be selected so that both metals precipitate in the form of hydroxides.

Materials and methods

The investigations on cerium(III) ions sorption efficiency from water media was carried out using the static method in 100 mL conical flasks by adding 0.04 g of sorbent and shaking with 20 mL of the solution at 293 K. Examining the impact of pH in the range of 2 to 6 was the first stage in identifying the process conditions.

The effect of the phase contact time, which ranged from 1 to 240 minutes, and the starting solution concentration, which ranged from 10 to 100 mg/L, were both determined in the following step.

The scheme of LDHs-modified biochar is presented below.

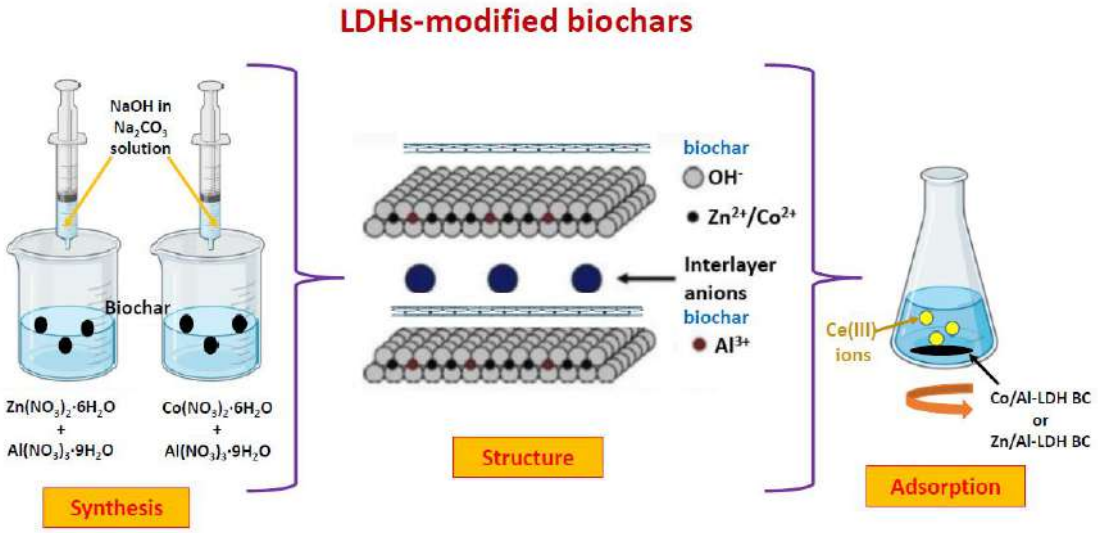

Results and discussion

Based on the preliminary studies, it was found that the highest q_e values were obtained for pH 5. Thus, this values was found for further research.

Conclusions

The obtained satisfactory amounts of adsorbed cerium(III) ions on the LDH-s modified biochars confirm that these sorbents can be used for water and wastewater treatment.

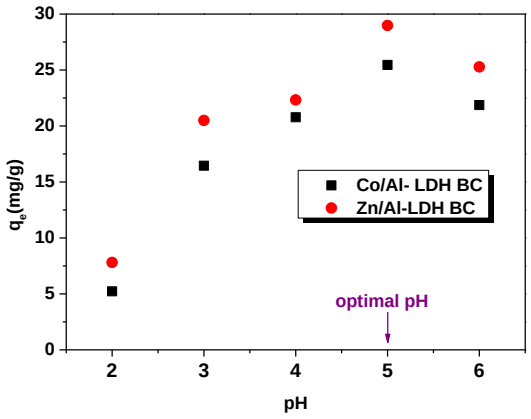

Figure 1. Impact of the equilibrium capacity on the initial pH for the Ce(III) ions sorption on Co/Al-LDH BC and Zn/Al-LDH BC.

References

Zhao, F., Repo, E., Meng, Y., Wang, X., Yin, D. and Sillanpää, M., 2016. An EDTA-β-cyclodextrin material for the adsorption of rare earth elements and its application in preconcentration of rare earth elements in seawater. *J. Colloid Interface Sci.,* 465, 215–224.

Fila, D., Hubicki, Z. and Kołodyńska, D., 2022. Applicability of new sustainable and efficient alginate-based composites for critical raw materials recovery: General composites fabrication optimization and adsorption performance evaluation. *Chem. Eng. J.,* 446, 137245–137267.

Chen, Y., Zhang, X., Chen, W., Yang, H. and Chen, H., 2017. The structure evolution of biochar from biomass pyrolysis and its correlation with gas pollutant adsorption performance, *Bioresour. Technol.,* 246, 101–109.

Kołodyńska, D., Krukowska, J. ad Thomas, P., 2017. Comparison of sorption and desorption studies of heavy metal ions from biochar and commercial active carbon. *Chem. Eng. J.,* 307, 353–363.

Liao, W., Zhang, X., Jingai, S., Yang, H., Zhang, S. and Chen H., 2022. Simultaneous removal of cadmium and lead by biochar modified with layered double hydroxide. *Fuel Process. Technol.,* 235, 107389–107399.

Wang, T., Li, C., Wang, C. and Wang, H., 2018. Biochar/MnAl-LDH composites for Cu(II) removal from aqueous solution. *Colloids Surf. A.,* 538, 443–450.

Column adsorption of polyphenols from olive mill wastewater by activated biochar

E. Karefylaki[1], C. Galanakis[2], A. Veksha[3], G. Lisak[3] and A. Giannis[1]

[1]School of Chemical and Environmental Engineering, Technical University of Crete, University Campus, Chania, Greece
[2]Research & Innovation Department, Galanakis Laboratories, Chania, Greece
[3]Residues and Resource Reclamation Centre (R3C), Nanyang Environment and Water Research Institute (NEWRI), Nanyang Technological University, Clean TechOne, Singapore
Corresponding author email: agiannis@tuc.gr

keywords: *total polyphenols; column adsorption; biochar; regeneration; adsorption kinetic models.*

Abstract

The purpose of this study was the fixed bed column adsorption of total polyphenols (TPh) for the purification of oil olive mill wastewater (OMW). The OMW was collected from a three-phase olive oil factory in Chania (Greece). The adsorbent material was prepared from palm-pruning leaves. The palm leaves were initially cut, dried, pyrolyzed (4 h at 600 °C) and activated with KOH at 800 °C for 4 h. Continuous mode adsorption experiments with upward flow were conducted at different OMW dilution rates (1/30, 1/50, 1/70) and flow rates (1 mL/min, 1.5 mL/min, 2 mL/min). Effluent samples from the column were collected at specified time intervals, and remaining TPh concentrations in the solution were measured by the Folin-Ciocalteu method. The best adsorption performance was observed for 1/70 dilution and 1 mL/min flow rate. The spent adsorbent was regenerated at 800 °C for 1 h. In total, four consecutive regeneration experiments were conducted. Based on the results, the second time regenerated biochar (third round experiment) was the most effective adsorbent material. Last, the adsorption kinetic models were applied to experimental data derived from the regeneration experiments to determine the characteristic parameters of the column. The kinetic models were Thomas, Yoon-Nelson and Adams-Bohart models. The experimental data fit well with Thomas and Yoon-Nelson models predicting good performance of the fixed bed column. Material characterization (BET, SEM-EDS, TGA) was also conducted for data interpretation. The BET analysis revealed that the first regenerated biochar had the highest specific surface area of 204 m^2/g, followed by the second regenerated biochar of 101 m^2/g with mesoporous structure. The SEM-EDS analysis revealed that SiO_2 microsphere composites were self-assembled on the surface of the regenerated biochar. Such formations increased the adsorption capacity of regenerated biochar. The TGA analysis confirmed the adsorption of several organic (polyphenols, carbonyls, alcohols, oily, etc.) and inorganic (K, Si, Mg oxides, etc.) compounds that are present in OMW.

SUST ENG 2023

SOLID WASTE MANAGEMENT/ BIOSOLIDS MANAGEMENT AND VALORIZATION

Decontamination of antibiotics from aqueous solution using citrus fruit waste biochar – silicate composite adsorbents

M. Gamble and C. Mangwandi

School of Chemistry and Chemical Engineering, Queen's University Belfast, Northern Ireland, UK
Corresponding author email: c.mangwandi@qub.ac.uk

keywords: *Biochar; Tetracycline; silicate; composite material; pyrolysis.*

Introduction

Maintaining water purity is an essential endeavour because it is fundamental for both humans and the natural world. In spite of this, water sources around the globe are increasingly becoming impure due to factors like huge population growth, industrial activities and increasing urbanization (Kumar et al. 2021). One source of water contamination are antibiotics entering water supplies. Antibiotics are not benign contaminants and have been associated with health issues like liver damage and ecological problems such as hindered algae growth. In addition to direct water pollution, the long-term presence of antibiotics within water supplies can cause the creation of antibiotic-resistant bacteria, which has been identified as one of the biggest threats to global health (Chu et al. 2020).

One example of an antibiotic water contaminant is tetracycline hydrochloride (TCH). It is a broad-spectrum antibiotic that is used to treat human disease and has been detected in rivers, lakes and groundwater. It enters these water supplies because of its widespread use and the fact that a large portion of it is not metabolized within the patient and is instead excreted into the environment (Xiang et al. 2022). As well as contributing to antibiotic-resistant bacteria, it has been observed to harm renal function and cause cancer. As a result, finding an environmentally-friendly and efficient method of develop a citrus fruit based low cost biochar adsorbent material for removal of TCH from aqueous solution. Silica will be incorporated into biochars to enhance the removal capacity of the adsorbent (Zhao et al. 2019).

Materials and methods

Production of Citrus Fruit Biochar (CFBC)

The pre-treated citrus fruit powder was pyrolyzed within a tubular furnace at 600°C in an atmosphere of nitrogen. During pyrolysis a heating rate of 10°C/min was adopted and a holding time of 15 minutes was utilised. After pyrolysis, the generated citrus fruit biochar (CFB) was naturally cooled to room temperature within the tubular furnace and the atmosphere of nitrogen inside it was maintained for this cooling period. Whenever the samples of citrus fruit biochar were obtained, they were washed three times with distilled water and then dried within an oven at 105°C.

Preparation of Silicate Citrus Biochars

SCBs of various biochar-to-silica ratios were produced through the physical mixing of predetermined volumes of sodium silicate solution and masses of citrus fruit biochar. Specifically, the SCBs were produced by mixing a predetermined mass of CFB, in grams, with a pre-established volume of SS, in milliliters, with a pestle and mortar. After physical mixing, the created SCBs were passed through a 1.4mm sieve so that their particle size distribution would be uniform. At the end of this portion of experimental work, SCBs with biochar-to-silica ratios of 2:1, 1:1, 1:2 and 1:3 were produced.

Analysis of the batch adsorptions

In order to be able to assess the TCH concentrations in solution after adsorption, the suspensions of TCH and adsorbent were initially allowed to settle for 20 minutes (except during the kinetic study). Subsequent to the settling period, the supernatant of the suspension was extracted and the TCH concentration, with the effects of leaching present, was measured using an ultraviolet-visible spectrometer (Aligent Technologies, Cary 60 UV-Vis) set to a wavelength of 357nm. After the absorbance measurement, the effect of leaching and TCH degradation was accounted for and the true TCH concentration adsorbed by the adsorbent was obtained.

The equilibrium adsorption capacity (Qe, mg/g) of the biochars used was calculated using equation (1) shown below:,

$$Q_e = \frac{(C_o - C_e)(V)}{m} \quad \textbf{(1)}$$

Where C_o symbolises the initial concentration of TCH in solution, C_e represents the equilibrium concentration of TCH after 3hrs of shaking, V is the volume of the TCH-biochar suspension and m is the mass of adsorbent used.

Results and discussion

Comparison of the performance of the different samples is shown Figure 1. The bar chart shows that the average Q_e of the citrus fruit biochar is 7.63 mg/g. Even though this Q_e has been naturally lowered because the adsorption is endothermic and the temperature used for its measurement is smaller than what would typically be used in literature, the magnitude of Q_e is still comparable in effectiveness to other pure biochars for TCH adsorption (Hoslett et al. 2021). Figure 1 shows that compositing pure biochar with any quantity of silica dramatically increases its adsorptive capacity. For instance, even the worst-performing SCB, with a biochar-to-silica ratio of 1:2, reported a 48% increase in adsorptive capacity compared to pure biochar. This relationship is expected and may have been caused by the pore-expanding effect of silica, which allowed the adsorption sites of the biochar to become more available to TCH (Zho et al. 2019).

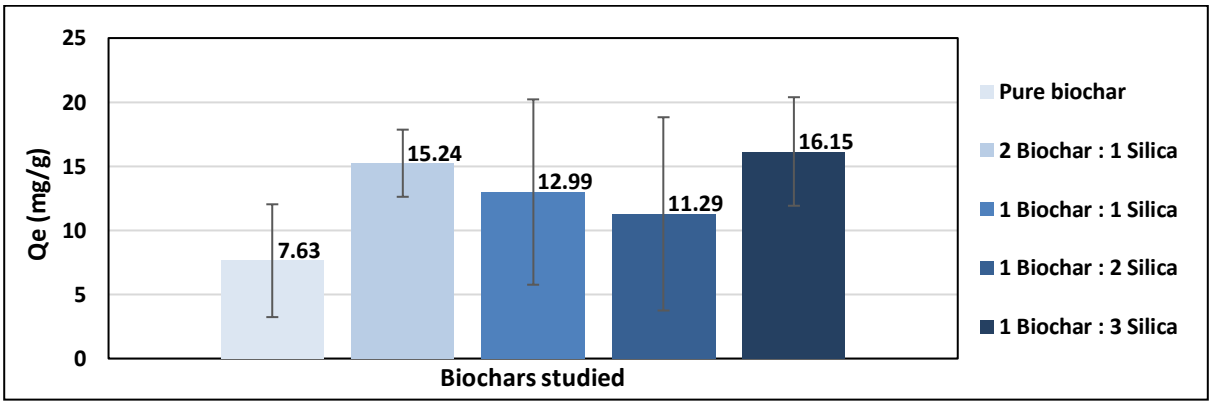

Figure 1. *Average adsorptive capacity of pure biochar and the various SCBs created*

Results indicated that while the CFB was a satisfactory adsorbent, compositing it with silica greatly improved its adsorption capacity (7.63mg/g for CFB and 16.15mg/g for the SCB with a biochar-to-silica ratio of 1:3) and this was anticipated to be somewhat due to the reported pore-expanding effect of silica. Furthermore, it was also found that the best SCB produced was the one which was composited with the most silica, which in this research was 1:3 SCB. After characterisations were completed, it was noted that the 1:3 SCB was the most thermally stable. Additionally, it was found to have a larger H/C ratio and O/C ratio than the CFB, indicating it was less aromatic and more polar. This was attributed to hydration that occurs to the CFB after it is mixed with the sodium silicate solution to form an SCB.

Conclusions

A composite material consisting of biochar produced from citrus fruit skin and silica was successfully produced. The material shows great potential for use as an adsorbent for removal of antibiotics from aqueous solution. The optimum mixing ratio of biochar to silica was found to be 1: 3.

References

Chu L., D. Chen, J. Wang, Z. Yang, Q. Yang and Y. Shen, "Degradation of antibiotics and inactivation of antibiotic resistance genes (ARGs) in Cephalosporin C fermentation residues using ionizing radiation, ozonation and thermal treatment," *Journal of Hazardous Materials,* vol. 382, pp. 1-9, 2020.

Kumar P. S., R. Gayathri and B. S. Rathi, "A review on adsorptive separation of toxic metals from aquatic system using biochar produced from agro-waste," *Chemosphere,* vol. 131483, no. 285, pp. 1-26, 2021.

Hoslett J., H. Ghazal, E. Katsou and H. Jouhara, "The removal of tetracycline from water using biochar produced from agricultural discarded material," *Science of the Total Environment,* vol. 751, pp. 1-10, 2021.

Xiang W., X. Zhang, J. Luo, Y. Li, T. Guo and B. Gao, "Performance of lignin impregnated biochar on tetracycline hydrochloride adsorption: Governing factors and mechanisms," *Environmental Research,* vol. 215, pp. 1-8, 2022.

Zhao Z., T. Nie and W. Zhou, "Enhanced biochar stabilities and adsorption properties for tetracycline by synthesizing silica-composited biochar," Environmental Pollution, vol. 254, pp. 1-9, 2019.

Pretreatment of cotton stalk residues for biogas production

A. Makri[1], P. Melidis[1] and S. Ntougias[1]

[1] Laboratory of Wastewater Management and Treatment Technologies, Department of Environmental Engineering, Democritus University of Thrace, Xanthi, Greece
Corresponding author email: pmelidis@env.duth.gr

Keywords: *cotton stalks; anaerobic digestion; biological pretreatment; BMP; CSTR.*

Introduction

Lignocellulosic biomass from agricultural activities is estimated to be 10 billion tons per year (Nguyen et al., 2019). The remaining organic residues in agricultural fields can be converted into biogas, during the biological process of anaerobic digestion. Through this process, we can manage these wastes and produce bioenergy from a renewable source. However, the complex lignocellulosic structure is a limited step for their exploitation. Current methods for the breakdown of the structure, like chemical and physical processes, are inefficient, because of their limited effectiveness, energy-intensive and high cost (Nguyen et al., 2019). Biological treatment with specific microbial communities from ruminant animals can be used to enhance cellulose degradation efficiency.

Greece is the main producer of cotton in the EU. Cotton stalk contains a high concentration of lignocellulose, crude fiber, nitrogen and phosphorus, making it a suitable feedstock for biofuel production. Cotton stalks are usually left in the field after harvesting, causing a waste management problem, and delaying the subsequent plantation (Afif et al., 2019). Burning of leftovers in the field is an approach that has been used, but this is of environmental concern (Kaur et al., 2012). Anaerobic digestion of cotton stalks as lignocellulosic biomass without pretreatment usually results in low biogas yield (Isci, 2007), although pretreatment with lignocellulolytic microorganisms could enhance the degradation of the cotton stalk (Ferial et al., 2010).

The current study attempts to develop a biological pretreatment method for effective management of cotton stalks through anaerobic digestion, using rumen microbiota to enhance the bioconversion of lignocellulosic biomass and increase biogas production. This was achieved through the use of BMP tests and subsequently of a continuous stirred tank reactor (CSTR) to estimate the cumulative biogas production and biogas yield under mesophilic conditions, investigating the effectiveness of rumen microbial community to bioconvert cotton stalk under various quantities of rumen fluid.

Materials and methods

Cotton residues were collected from fields in the vicinity of the city of Xanthi, were then air-dried and cut into pieces of less than 3-mm diameter. The dry weight was assessed by placing the residues at 105 ^{o}C until reaching a constant weight, whereas the volatile solids (VS) were determined after heating the dried residues at 550 ^{o}C (APHA,2006). The cotton stalk biomass used in the downstream experiments contained 92.6% total solids (TS), 83.3% VS (as % of TS) and ash content of 9.3% (as % of TS).

BMP experiments were conducted in triplicate, according to Angelidaki et al. (2009), by using 0.25 L bottles with a working volume of 0.15 L, which were placed in a water bath at 37.5 ^{o}C for 28 days. A BMP setup containing only inoculum was served as the control.

The anaerobic digestion of cotton stalk residues was also examined in a laboratory-scale CSTR of a working volume of 2 L, which was initially inoculated with anaerobic sludge from a full-scale anaerobic digestion plant. Feeding of the CSTR with cotton stalk and rumen fluid (1.5% v/v) was performed on a daily basis. A CSTR fed only with the inoculum was served as the control.

Results and discussion

The capability of rumen microbiota of improving the hydrolysis of cotton's lignocellulosic biomass and subsequently enhancing biogas production was assessed through the employment of both BMP tests and CSTR.

During BMP tests, the degradation of cotton stalks without pretreatment was limited, as expected, due to their high lignin and cellulose content. By applying the rumen inoculum at various concentrations, the biogas yield of anaerobic digestion process was increased by increasing rumen concentration. In particular, rumen fluid at dose applications of 16%, 33% and 50% resulted in improved biogas production by at least 99% during shifting from one concentration to the next greater one. The cumulative biogas production was shifted from 551 to 758 mL BG by increasing the inoculum of rumen microbiota from 16% to 50%, whereas the cumulative biogas production was in average 3.8 mL BG in the blank (cotton stalk without pretreatment with rumen fluid).

Moreover, the digestion of cotton stalks in the laboratory-scale CSTR in the presence of rumen microbiota showed the same effectiveness as in BMP tests. The hydrolysis stage, which is the limited step during this process, was clearly improved with the addition of rumen fluid. At organic loading rate of 1 g VS L^{-1}, the biogas production from the anaerobic digestion of cotton stalks was enhanced by the addition of rumen fluid, i.e. from 0.24 to 0.75 L/g VS added.

Conclusions

Pretreatment of lignocellulosic biomass by rumen fluid can be considered a promising way for the anaerobic digestion of agricultural residues, including cotton stalk, in order to improve biogas production. In this study, anaerobic digestion of cotton stalk residues treated by various concentrations of rumen fluid resulted in higher biomethane production compared to the digestion of cotton stalk without inoculation with rumen microbiota. Thus, the use of rumen fluid could be an alternative method for valorizing lignocellulosic biomass in a sustainable way.

References

APHA, Standard Methods for the Examination of Water and Wastewater, 21st ed., American Public Health Association, Washington, DC, USA, 2006

Angelidaki, I., Alves, M., Bolzonella, D., Borzacconi, L., Campos, J. L., Guwy, A. J., … van Lier, J. B. (2009). Defining the biomethane potential (BMP) of solid organic wastes and energy crops: a proposed protocol for batch assays. Water Science and Technology, 59(5), 927–934

Al Afif, R., Wendland, M., Amon, T., & Pfeifer, C. (2020). Supercritical carbon dioxide enhanced pre-treatment of cotton stalks for methane production. Energy, 194, 116903.

Atelge, M. R., Atabani, A. E., Banu, J. R., Krisa, D., Kaya, M., Eskicioglu, C., … Duman, F. (2020). A critical review of pretreatment technologies to enhance anaerobic digestion and energy recovery. Fuel, 270, 117494.

Bhatt, A. H., & Tao, L. (2020). Economic Perspectives of Biogas Production via Anaerobic Digestion. Bioengineering, 7(3), 74.

Ferial M. Rashad, Walid D. Saleh, Mohamed A. Moselhy (2010). Bioconversion of rice straw and certain agro-industrial wastes to amendments for organic farming systems: 1. Composting, quality, stability and maturity indices. Bioresource Technology, 101: 5952–5960.

Isci, A., & Demirer, G. N. (2007). Biogas production potential from cotton wastes. Renewable Energy, 32(5), 750–757.

Kaur, U., Oberoi, H. S., Bhargav, V. K., Sharma-Shivappa, R., & Dhaliwal, S. S. (2012). Ethanol production from alkali- and ozone-treated cotton stalks using thermotolerant Pichia kudriavzevii HOP-1. Industrial Crops and Products, 37(1), 219–226.

Li, J.X., Bian, K., Xu, B., 2007. Properties and applications of cotton straw in agriculture. Henan Agric. Sci. 1, 46–49 (Chinese).

Nguyen, L. N., Nguyen, A. Q., Hasan Johir, M. A., Guo, W., Ngo, H. H., Chaves, A. V., & Nghiem, L. D. (2019). Application of rumen and anaerobic sludge microbes for bio harvesting from lignocellulosic biomass. Chemosphere.

Yuan, X., Ma, L., Wen, B., Zhou, D., Kuang, M., Yang, W., & Cui, Z. (2016). Enhancing anaerobic digestion of cotton stalk by pretreatment with a microbial consortium (MC1). Bioresource Technology, 207, 293–301.

Usefulness of waste from the cultivation of tobacco for energy production

M. Pituła[1], A. Kowalczyk-Juśko[2], P. Pochwatka[2] and J. Dach[3]

[1]Polish Biomethane Association, Warsaw, Poland
[2]Department of Environmental Engineering and Geodesy, University of Life Sciences in Lublin, Lublin, Poland
[3]Department of Biosystems Engineering, Poznań University of Life Sciences, Poznań, Poland
Corresponding author email: jacek.dach@up.poznan.pl

keywords: *tobacco stems; combustion; boilers fouling; anaerobic digestion; solid waste.*

Introduction

Cultivation of some agricultural crops involves the formation of a large biological mass, which is not useful from a technological point of view. An example of such a plant is tobacco (*Nicotiana tabacum* L.). For many plants, crop residues can be utilized on farms, as is the case with, for example, cereal straw, which is used as bedding in animal production. The excess of such a by-product can also be plowed, enriching the soil with organic matter. In the case of tobacco, the management of plant residues is more complicated. Tobacco is affected by many diseases, which are often transmitted through plant debris left in the field. Therefore, their plowing is associated with the risk of exacerbating diseases. Incineration of such waste is prohibited in Europe, as it is dangerous for the environment and people. This study aims to evaluate the possibility of using tobacco plant residues as a raw material for energy production through combustion and anaerobic digestion.

Materials and methods

The research was carried out in 2022 on a farm located in south-eastern Poland. The object of the research were the remains of Virginia-type tobacco plants, collected after the leaves were harvested in the third decade of September. The biomass consisted mainly of stems (85-90%), while the remains of leaves, remaining on the tops of the stems, accounted for 10-15% of the mass. Biomass was harvested manually from the field, randomly selecting 3 plots of 10 m^2 each. The stems were weighed, then half of the mass was crushed using a knife chopper and samples were taken to assess physical parameters. The stem chaff was ensiled in a glass jar for 6 weeks. The obtained silage was analyzed for biogas efficiency in accordance with the DIN 38 414 standard. The second half of the obtained biomass was dried in natural conditions, and then subjected to the analysis of energy parameters according to the methods appropriate for each feature. To evaluate the impact of tobacco biomass combustion on heating devices, ash melting points were determined (according to CEN/TS 15370-1:2007), and the chemical composition of the ash was analyzed.

Results and discussion

Since Poland's accession to the EU, the area of tobacco cultivation has decreased, and raw tobacco production has become less profitable. As a result, the area dedicated to tobacco cultivation has declined from over 20,000 ha in 2003 to less than 10,000 ha in 2021, making it a less significant plant in the overall sowing structure. However, for farms that specialize in tobacco cultivation, it can still be a major source of income. After the leaves are harvested, there are stalks left in the field with leaf remnants on the tops. In own studies, it was estimated that the amount of biomass residues was 10.3-15.7 t/ha. The tobacco stalks are quite moist: in working condition, the water content was close to 50% (Table 1). As a solid fuel, the stems require additional drying, which requires energy or being placed in an airy, roofed room. The unfavorable feature found in the tests was the high ash content (7.31%). This may be due to the fact that tobacco stalks are covered with sticky secretory trichomes to which impurities, such as soil particles, easily stick. Dry stems are characterized by the higher and lower heating value typical for other types of biomass (18.1 and 16.9 MJ/kg, respectively).

Tobacco stalks are considered as a raw material for the production of briquettes (Peševski et al. 2010). Unfortunately, burning tobacco stalks can be detrimental to heating boilers. Very low ash fusing temperatures (650-740°C) and its chemical composition result in a high risk of creating sticky slag, depositing on heat exchangers, reducing the efficiency of the boiler and its rapid wear.

Table 1. *Tobacco stems parameters important from the energetic point of view*

Parameter	Symbol	Status*	Unit	Value	Extended uncertainty u
Total moisture	M_{ar}	r	%	48.1	1.2
Ash	A_d	d	%	7.31	0.26
Volatile solids	V_d	d	%	73.1	3.4
Higher heating value	HHV	d	J/g	18130	650
		r	J/g	9420	450
Lower heating value	LHV	d	J/g	16910	660
		r	J/g	7670	410
Carbon	C	d	%	45.83	1.32
Hydrogen	H	d	%	5.95	0.27
Nitrogen	N	d	%	1.11	0.07
Total sulfur	S	d	%	0.17	0.01
Chlorine	Cl	d	%	0.474	0.08

* - r - as received; d – dry

The results of biogas yield tests from silage made from shredded tobacco stalks indicate that it is not a particularly good raw material. The silage was characterized by an unfavorable physical structure due to the high lignification of the stems and problems with their proper fragmentation, which then translated into biogas yield. To improve biogas efficiency, it may be worth considering ensilaging the tobacco stems with other agricultural and waste materials. Since the end of the tobacco harvest in Poland coincides with the period when farms also produce other by-products, such as sugar beet leaves, which are easily ensiled. Improving the quality of silage can have a positive impact on biogas efficiency, despite the relatively high ash content, which is a negative feature both in the case of combustion and anaerobic digestion.

Conclusions

Tobacco cultivation is associated with the formation of a large amount of waste biomass in the form of stems with leftover leaves. Leaving them in the field and plowing is associated with the spread of pests and diseases. These stems are a potential energy biomass. The parameters of dry stem biomass indicate that it is an energy resource that requires additional drying, contains a lot of ash and can negatively affect the condition of power boilers. The yield of biogas from ensiled stalks is not high, which is largely due to the low quality of the silage. Technologies for improving the raw material for energy use should be considered, especially on farms that grow tobacco on large areas.

References

Peševski, M.D., Iliev, B.M., Živković, D.L., Jakimovska Popovska, V.T., Srbinoska, M.A., Filiposki, B.K., 2010. Possibilities for utilisation of tobacco stems for production of energetic briquettes. *Journal of Agricultural Sciences*, 55, 1, 45–54.

Biodegradation of phenolic compounds from grape pomace of Vitis vinifera Asyrtiko by Chlamydomonas reinhardtii

M. Belenioti[1], E. Mathioudaki[1], E.Spyridaki[2], D. Ghanotakis[1] and N. Chaniotakis[1]

[1]Department of Chemistry, University of Crete, Heraklion, Greece
[2]Agrochemicals of Crete, Industrial area of Heraklion, Heraklion, Greece
Corresponding author email: eirini.mathiou@gmail.com

keywords: *grape pomace; Chlamydomonas reinhardii; Vitis vinifera; Bioidegradation; soil improver*.

Introduction

Grape pomace from Vitis vinifera Asssyrtiko is an important sub-product of the Greek wine industry. However, its accumulation is a serious problem with a negative environmental impact. Grape pomace is rich in bioactive compounds and its utilization for alternative uses, such as a fertilizer, is an interesting area of research. On the other hand, its high concentration of phenolic compounds inhibits germination processes. Therefore, there is a need to decrease the high phenolic level in grape pomace before it can be used as a fertilizer. The main objective of our study is the fast reduction of polyphenols in grape pomace, and more specifically catechin and epicatechin in Vitis vinifera Assyrtiko. For this purpose, Chlamydomonas reinhardii was used for polyphenol biodegradation in grape pomace extract. It is shown that the bioremediation proceeds very fast, while the final product has a high potential to be used as a soil conditioner.

Materials and methods

Grape pomace from *Vitis vinifera Assyrtiko* was collected directly from a basket press available at 'Diamantakis winery' and the fresh material was collected during the harvest of 2020 (in September) and was stored at -20°C until use.The extraction of polyphenolic compounds was carried out by using deionized water as a solvent. *Chlamydomonas reinhardii* was cultivated in 100ml grape pomace extract and three replicates were analyzed. The determination of catechin and epicatechin (by HPLC), as well as the determination of total polyphenolic compounds (Folin -Ciocaltue assay) after biodegradation were measured in different time points (0, 8, 24, 48, 72, 96, 120 and 144 hours), while the total minerals determination (sodium (Na), potassium (K), calcium (Ca), magnesium (Mg), copper (Cu), manganese (Mn), iron (Fe), and zinc (Zn) were measured by Atomic Absorption Spectroscopy) took place after the end of cultivation and the removal of the biomass. For the statistical analysis of experiments results, the reported mean and standard deviation (SD) were calculated using software IBM SPSS Statistics 24 was used.

Results and discussion

The results of this study identify that after 6 days of cultivation, *C. reinhardtii* was able to reduce the total polyphenolic amount by 43%, while catechin and epicatechin were decreased by 100% (Figue 1). In addition, it is shown that the final aqueous product is rich in minerals, such as sodium, phosphorus and potassium.

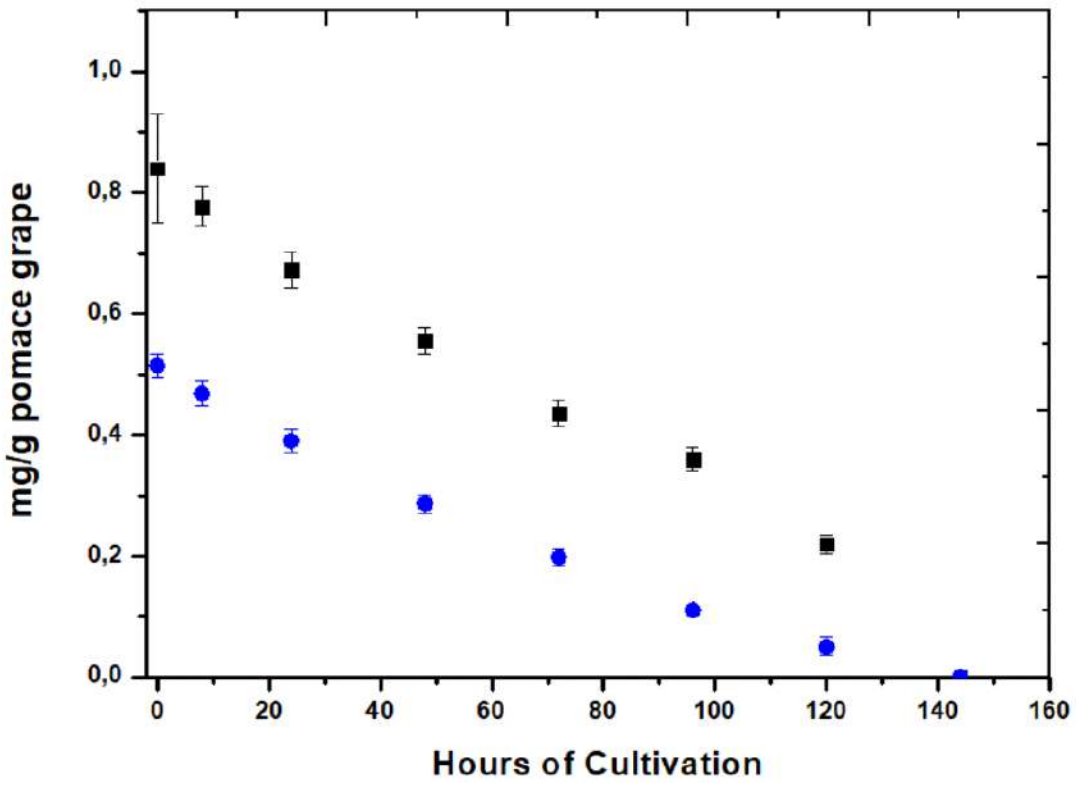

Figure 1. Catechin (■) and epicatechin (●) of pomace grape *V. vinifera Assyrtiko* extract at different cultivation time points.

Conclusions

Through this work we were able to develop a method that allows for the efficient decrease of polyphenols in grape pomace. C. reinhardtii biodegrades a sufficient amount of polyphenols in grape pomace with a high rate, while the product obtained 6 days after cultivation contains high concentrations of minerals and low levels of polyphenols. These results suggest that there is a great potential in using the Vitis vinifera Asssyrtiko biodegraded product as a soil conditioner. © 2023 Society of Chemical Industry (SCI).

Acknowledgements: This research has been co-financed by the European Regional Development Fund of the European Union and Greek national funds through the Operational Program Competitiveness, Entrepreneurships and Innovation, under the call RESEARCH- CREATE- INNOVATE (project code: T2EDK-00523).

European Union
European Regional Development Fund
HELLENIC REPUBLIC
MINISTRY OF DEVELOPMENT AND INVESTMENTS
SPECIAL SECRETARIAT FOR ERDF & CF PROGRAMMES
MANAGING AUTHORITY OF EPAnEK
EPAnEK 2014-2020
OPERATIONAL PROGRAMME
COMPETITIVENESS
ENTREPRENEURSHIP
INNOVATION
ΕΣΠΑ 2014-2020
Partnership Agreement 2014 - 2020
Co-financed by Greece and the European Union

The authors would like to acknowledge the PhD candidate Napoleon Stratigakis for his excellent assistance.

Valorization of spent coffee grounds for removal of chromium from wastewater

R. Campbell and C. Mangwandi*

School of Chemistry and Chemical Engineering, Queen's University Belfast, Northern Ireland, UK

Corresponding author email: c.mangwandi@qub.ac.uk

keywords: *Chromium; Spent coffee grounds; Chemical Activation; Pyrolysis; Adsorption; Porous adsorbent.*

Introduction

Heavy metal exposure has been on the increase due to modern industrialization. Contamination of water by toxic metals is an environmental concern and hundreds of millions of people are being affected around the world. Chromium is one of the most toxic heavy metals. Though naturally found in rocks, plants, and volcanic dust, several industrial activities such as chrome plating, leather tanning, metal fabrication and textile dyeing have been sources of chromium in drinking water. The most common forms of chromium are trivalent chromium (Cr^{3+}) and hexavalent chromium (Cr^{6+}) with hexavalent chromium being more toxic as it is a known carcinogen and a reproductive toxicant for males and females. Persons who have consumed chromium in drinking water over the years have faced several health problems such as kidney problems, liver damage and allergic dermatitis (Chakraborty et al., 2022).

The goals of this study were to produce a porous adsorbent material from spent coffee grounds by activating it with potassium hydroxide (KOH) at different mass ratios, pyrolysis temperatures and activation durations to find the optimum adsorbent for chromium removal. From this material produced, the capacity of the adsorbent to remove Cr^{6+} from wastewater was found and evaluated in different adsorption conditions such as temperature and dosage.

Materials and methods

Based on the chemical activation method in literature, dried spent coffee grounds (SCG) and potassium hydroxide (KOH) are weighed in two mass ratios – 1:1 and 2:1 (KOH g: SCG g). Potassium hydroxide is the activating agent used and its role is to increase the porosity of the coffee grounds (Yang et al., 2017). The mixture is then placed in a blender along with 20 grams of distilled water to increase the particle size (granulation). The mixture is weighed in crucibles and placed in the tubular furnace with nitrogen gas flow connections set up. Nitrogen gas flowed through the system for a minimum of 5 minutes and then the furnace is switched on and the temperature set to 400°C and 600°C. The mixture is heated for a constant heating rate of 5°C per min and the pyrolysis duration varied for 1 and 2 hours. After pyrolysis, the material is cooled down with N_2 gas still flowing for 1 hour and then the gas flow ceased. The sample is collected from the furnace and the weight recorded. The activated coffee grounds are then washed with distilled water in a packed column until a neutral pH is reached. The adsorbent is then placed in the oven to be dried for ~12 hours at 105°C. Once completely dried, the final product is weighed and stored in a sealed, labelled vial. Overall, eight adsorbent samples are made by varying pyrolysis temperature, pyrolysis duration and mass ratio of potassium hydroxide to spent coffee grounds.

Each of the 8 samples made were contacted with chromium (VI) solution with concentrations ranging from 5.2 – 52 ppm over a 3-hour period. The residual concentration of the solution was determined using UV–Visible spectrophotometry. The chromium concentration in solid phases was calculated from the equation:

$$Qe = \frac{(C_i - C_e)\,V}{m}$$

Where Ci and C_e are the liquid-phase concentrations of chromium initially and at equilibrium respectfully and both measured in mg/L. Volume of solution (L) and m is the mass of dry adsorbent used for the experiment in grams.

Results and discussion

Figure 1 shows the removal % of Cr^{6+} for each sample made. The highest removal was obtained with the adsorbent produced with a duration of thermal activation of 2 hours, pyrolysis temperature of 400 °C and with a mass ratio of 1:1 (KOH: SCG). Furthermore, this adsorbent sample has the highest Q_{max} value of 207 mg/g as shown in Table 1. The worst percentage removal over the 3-hour duration of the adsorption experiment was 75% for AC4R under the conditions of 600°C for 2 hours with 2:1 mass ratio. According to the Q_{max} values in Table 1, for the 1-hour pyrolysis samples, as the pyrolysis temperature and the impregnation ratio increase, greater removal of Cr^{6+} is seen. However, for the 2-hour pyrolysis samples, there is an opposite effect where, as the activation temperature and ratio increase, the removal performance decreases. There is a strong correlation between removal % and surface area as shown in the Table 1, where the worst adsorbent sample (AC4R) has the lowest surface area of 1.07 m^2/g and the best adsorbent sample (AC1R) has one of the highest surface areas of 11.26 m^2/g.

Table 1. *Adsorbent samples produced under varying process conditions*

Sample	Pyrolysis Temp (°C)	Mass Ratio	Pyrolysis Duration (hrs)	Q_{max} (mg/g)	Surface Area (m^2/g)
AC1	400	1:1	1	57.94	1.07
AC2	600	1:1	1	75.08	1.97
AC3	400	2:1	1	114.10	5.80
AC4	600	2:1	1	145.00	827.91
AC1R	400	1:1	2	207.21	11.26
AC2R	600	1:1	2	194.71	2.55
AC3R	400	2:1	2	125.99	2.98
AC4R	600	2:1	2	98.03	1.07

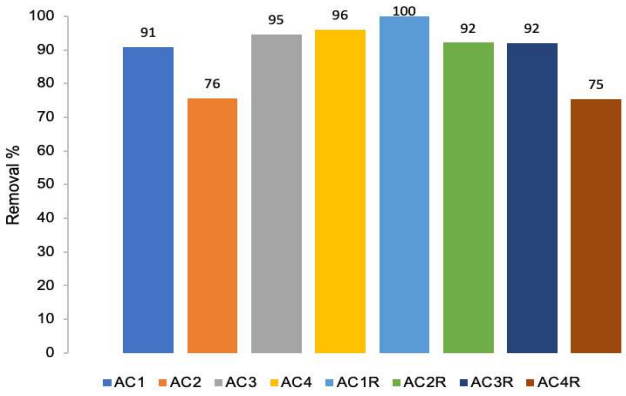

Figure 1. Cr^{6+}Removal % for each sample produced

Conclusions

According to Figure 1, the worst percentage removal over the 3-hour duration of the adsorption experiment was 75% for AC4R under the conditions of 600°C, 2 hours and 2:1 mass ratio. The optimum adsorbent was 1:1 ratio, 400°C for pyrolysis temperature and the time of pyrolysis was 2 hours. The detailed adsorption study showed that the best coffee ground adsorbent had a Cr^{6+} removal capacity (207 mg/g) which is competitively high when compared to other adsorbent materials reported in literature. The new adsorbent developed in this work show great potential for heavy metal removal. Future studies will focus on optimizing adsorption conditions through kinetic, thermodynamic and dosage studies.

References

Chakraborty, R., Renu, K., Eladl, M.A., El-Sherbiny, M., Elsherbini, D.M.A., Mirza, A.K., Vellingiri, B., Iyer, M., Dey, A. and Valsala Gopalakrishnan, A. (2022). Mechanism of chromium-induced toxicity in lungs, liver, and kidney and their ameliorative agents. Biomedicine & Pharmacotherapy, [online] 151, p.113119. doi:https://doi.org/10.1016/j.biopha.2022.113119.

Yang, H.M., Zhang, D.H., Chen, Y., Ran, M.J. and Gu, J.C. (2017). Study on the application of KOH to produce activated carbon to realize the utilization of distiller's grains. IOP Conference Series: Earth and Environmental Science, 69, p.012051. doi:https://doi.org/10.1088/1755-1315/69/1/012051.

Challenges with Strategic Planning for Disaster Waste Management in Developing Countries

M. Massoud[1] and L. Al Tawil[1]

[1]Department of Environmental Health/Faculty of Health Sciences, American University of Beirut, Beirut, Lebanon
Corresponding author email: mm35@aub.edu.lb

keywords: *waste; disaster; management, challenges.*

Introduction

Disasters around the world generate large amounts of debris requiring urgent management strategies. Given the potential effects of disaster wastes on public health and the environment, both developed and developing countries must overcome a number of challenges at the technical, administrative, institutional, and financial levels in order to be able to create effective disaster waste management plans. Lebanon is a developing country plagued by multiple problems, including infrastructure and financial deficits and political intrusion that hamper its ability to manage disaster waste.

Materials and methods

This study focuses on the August 4, 2020, explosion at the Beirut port, which produced more than 800,000 tons of catastrophe trash. Accordingly, in-depth interviews were conducted with various stakeholders involved in disaster management. The executed disaster waste management strategies were evaluated and the implementation challenges and enabling factors were identified. The study concludes by proposing a disaster waste management roadmap that includes emergency, risk mitigation, and implementation plans that can improve decision-making and expedite the recovery process.

Results and discussion

Apparently, the lack of a disaster waste management plan in Lebanon has led to inadequate waste management, resulting in significant public health and environmental impacts. Major challenges include lack of infrastructure and technology, lack of a legal framework to define the institutional basis of disaster waste management, and lack of human and financial resources. Management of large volumes of disaster waste requires a coherent action plan that addresses technical, managerial, administrative, legal, institutional and financial issues that may challenge national disaster waste management capacity.

Conclusions

The development of an action plan could speed up the recovery process and enhance coordination among stakeholders, with the aim of minimizing the costs levied on the government.

SUST ENG 2023

WATER RESOURCES MANAGEMENT

Smart Irrigation recommendation system using Machine Learning

K. Dolaptsis[1], X. E. Pantazi[1], G. Tziotzios[1], D. Stavridou[1], A. Morellos[1], C. Paraskevas[1], S. Arslan[2], Y. Tekin[3] and A. Mouazen[4]

[1]School of Agriculture, Aristotle University of Thessaloniki, Thessaloniki, Greece
[2] Department of Biosystems Engineering, Bursa Uludağ University, Bursa, Turkey
[3] Vocational School of Technical Sciences, Bursa Uludağ University, Bursa, Turkey
[4]Department of Environment, Ghent University, Ghent, Belgium
Corresponding author email: kdolapts@agro.auth.gr

***keywords**: irrigation need; water management; machine learning; remote sensing; soil data; weather data.*

Introduction

Inefficient water management practices in agriculture lead to substantial water wastage. Traditional irrigation scheduling solutions appear ineffective since they frequently fail to take into account site-specific, spatially varying factors and weather conditions occuring in the irrigated area, thereby increasing the risk of runoff, which most of the time results in water waste and water resource contamination (Bhoi et al., 2021). To address this issue, novel methods that can precisely estimate the amount of water required for future irrigation should be investigated. Predictive modelling for precise irrigation can lead to the adoption of improved water management strategies in order to conserve scarce water resources in irrigated areas while ensuring optimal crop growth and yield productivity (Kelly et al., 2021). Machine Learning (ML) models are capable of performing this task successfully with minimum human intervention.

The current study proposes a ML-trained variable rate irrigation recommendation system which takes in consideration a collection of data acquired from three distinct sources including soil sensors, weather station and satellite imaging. Three different machine learning models have been employed namely, Quadratic – Support Vector Machine (Quadratic-SVM), MLP neural network and Random Forest (RF), to data collected in a maize field in Bursa, Turkey. By integrating these data sources, the prediction accuracy of the forecasting models regarding irrigation need is enhanced, providing a valuable tool for farmers to make effective management decisions regarding irrigation scheduling.

Materials and methods

Soil sensors in nine different locations throughout the investigated field located in Bursa, Turkey were used to collect soil data measurements every half an hour from May to October of 2022. The soil measurements included soil electrical conductivity, soil temperature and soil moisture content. Weather data were collected per hour by a weather station in the region of Bursa, including mean air temperature, solar radiation, vapour pressure, relative humidity and wind speed. Additionally, satellite images were acquired from Sentinel-2 in order to extract the vegetation index LAI and the crop coefficient K_c.

The whole dataset (except ground truth), was pre-processed and fused before being fed to the models. Standardization procedure was used for preprocessing, transforming the features of the dataset so that they have a mean of 0 and a standard deviation of 1. Feature level fusion was used due to the combination of the features extracted from multiple sources. From a total number of samples equal to 3208, 2567 were used for training and 641 for testing. Then, the dataset was subjected to various regression algorithms including Quadratic-Support Vector Machines (quadratic-SVM), Random Forest (RF) and the neural network MultiLayer Perceptron (MLP) so as to create models that were capable of predicting the recommended irrigation need at a specific time. The above mentioned models, are well known machine learning algorithms, capable of learning patterns and relationships between the input variables and the output variable, which can help in accurately predicting the amount of water required by crops.

Results and discussion

The models were evaluated, using standard evaluation metrics that are commonly used in regression problems, such as the coefficient of determination (R^2) and the root mean squared error (RMSE). The models' performance for the prediction of the irrigation need in the study are shown in Table 1.

Table 1. *Performance of ML models for the prediction of irrigation need in maize field.*

	Q-SVM		MLP		RF	
	Training	**Test**	**Training**	**Test**	**Training**	**Test**
R^2	90%	81%	99%	87%	99%	70%
RMSE	6.373	7.6467	2.7023	6.0983	2.4088	9.1284

The results of the analysis suggest that the MLP model performed the best, with an R^2 value of 87% on the testing data, indicating that the model was able to explain a high proportion of the variance in the irrigation need data based on the soil, weather, and satellite data. The Q-SVM model also performed well, with an R^2 value of 81%, suggesting that it is a suitable method for predicting irrigation need using this type of data. The RF model demonstrated moderate performance, with an R^2 value of 70%, indicating that it may not be the most appropriate method for this particular application. Overall, these results indicate that MLP and quadratic-SVM models are the most promising for predicting irrigation need using soil, weather, and satellite data. Further research will explore the use of these models in different contexts and with different types of data to assess their generalization capability. Figure 1, demonstrates the distribution of the predicted irrigation need for two specific dates. As it can be seen the IN values are classified in five management zones. The greater the intensity of a zone's colour, the greater its watering requirements.

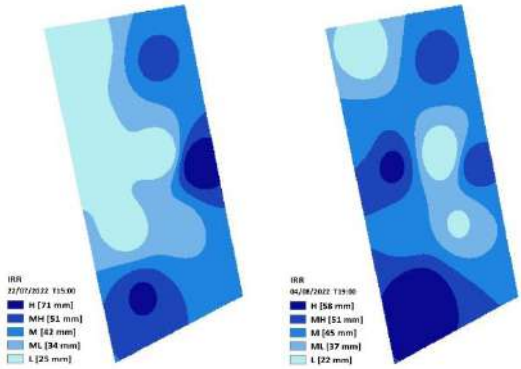

Figure 1. *IN per MZ on 22/07/22 at 15:00(left)-IN per MZ on 04/08/22 at 19:00(right)*

Conclusions

The current approach utilizes proximal, weather and remote sensing data as inputs to ML models so as to predict successfully the predicted variable irrigation need in a maize field. Among the three utilized predictive models (Quadratic-SVM, MLP and RF), the MLP model demonstrated the best performance (R^2=87%) in predicting irrigation need using soil, weather, and satellite data, ascertaining the effectiveness of the proposed method into providing better water management strategies for conserving precious water resources in irrigated areas. The employed ML models have also the potential to be further applied to provide irrigation recommendations for other crops, as well as to additional decision-making processes in agriculture including fertilization and pest-control.

Acknowledgements: This research has been cofinanced by the European Regional Development Fund (ERDF) and Greek national funds through the Partnership Agreement for the Development Framework 2014-2020 (Action: ERANETS - 2021A).

References

Kelly, T. D., Foster, T., Schultz, D. M., & Mieno, T. (2021). The effect of soil-moisture uncertainty on irrigation water use and farm profits. Advances in Water Resources, 154, 103982.

Bhoi, A., Nayak, R. P., Bhoi, S. K., Sethi, S., Panda, S. K., Sahoo, K. S., & Nayyar, A. (2021). IoT-IIRS: Internet of Things based intelligent-irrigation recommendation system using machine learning approach for efficient water usage. *PeerJ Computer Science*, *7*, e578.

HRES: The solution to cover water and energy needs in a Greek arid island

S. Skroufouta, A. Lemonis and E. Baltas

Department of Water Resources and Environmental Engineering, School of Civil Engineering, Technical University of Athens, Athens, Greece
Corresponding author email: sofiaskroufouta@chi.civil.ntua.gr

keywords: *Renewable Energy; Hydroelectricity; Stochastic time-series; Wind Power; Water management.*

Introduction

Due to population growth, the depletion of fossil fuels and their adverse effects on the environment, renewable energy sources (RES) are essential and their demand is increasing globally. Today, sustainability seems to be the approach to prevent the depletion of current natural resources in order to maintain an ecological balance that does not jeopardize the quality of life for future generations (Ferreira et al., 2019; Jäger-Waldau, 2007). The technology of hybrid renewable energy systems (HRES) coupled with a desalination plant is a step closer to this direction (Kershman, 2003; Al-Karaghouli, Kazmerski, 2013), enabling the storage of energy from wind, photovoltaic, or hydroelectric projects as well as intelligent energy management, depending on the variation of demand that must be met (. In this research, an investigation and simulation of such a system is carried out, aiming to meet the water and energy needs of the island of Leros. The under-study HRES comprises of a wind park (4.2 MW), a hydroelectric supply station (5 m^3/s), two desalination plants (2,000 m^3/day) and two reservoirs. Given that the operation of the HRES is simulated for 40 years, like the estimated long-term system's lifespan, the use of stochastic methods is essential.

Materials and methods

Leros is an arid island, with an area of 54 km^2 in area and a coastline of 71 km. The average monthly temperatures vary from 11.04 ° to 26.24 °C. The average monthly maximum temperature of 29.65 °C is recorded in August, while the average monthly minimum temperature of 7.35 °C is recorded in February. Regarding the lowest and maximum temperatures, respectively, they occur in February when the mercury hits 0 °C and in July when it reaches 36.80 °C.

Concerning the data processing, the historical timeseries are shorter than the required 40 years project's lifespan; therefore, synthetic timeseries are produced, including the necessary uncertainty of the natural processes as well. The rainfall and temperature synthetic timeseries are produced using two linear models, assuming that the white noise of these timeseries is Gaussian. These models are the AR(1), the Auto-Regressive model of 1st order, and the ARMA(1,1), the Auto-Regressive Moving Average model of 1st order as well (Mimikou er al., 2016). For the production of synthetic timeseries of wind speed, the applied model (Negra et al., 2007)) differs, due to the high seasonality of the wind for each month separately; where coupled with the power curve of the chosen wind turbines, the generated wind energy is estimated.

The drinking water needs are estimated based on the following three consumptions: i) for the permanent population and tourists, the typical consumption amounts to 150/l/day/capita, ii) for the summer residents, 200/l/capita, and iii) the potential yearly increase of the population is also included. The Blaney-Criddle method estimates the irrigation needs to calculate the evaporation, using the synthetic rainfall and temperature timeseries (Hargreaves, Samani, 1982). Lastly, the energy needs are estimated based on the available energy needs of a neighboring island, with comparable agriculture and economic activity (Sarris et al., 2019).

esults and discussion

The under-study HRES consists of a 4.2 MW wind park, two desalination plants with a combined capacity of 2,000 m3/d, a desalinated water reservoir of 785,000 m^3, a 2 MW pumping station, a 5 m^3/s hydroelectric supply station, and a seawater reservoir with a capacity of 780,000 m^3 at 170 m above sea level. The

simulation takes place in an hourly step and prioritizes meeting the desalination plant's energy requirements before addressing energy demand. The desalination plant uses the remaining 70% of the wind park's power, which is supplied straight to the grid and used to produce drinking water. Pumped-Storage Hydroelectricity (PSH), which has the shape of a reversible HP and is suitable and "renewable" in addition to being a low-cost method of storing electricity for the Greek islands, is used to store any excess energy after producing the necessary drinking and irrigation water.

Concerning the drinking and irrigation water needs, the HRES manages to fulfill its goal and achieve a reliability of 99%, since it prioritizes the coverage of the energy demand of the desalination plant and therefore the water needs of the study area. This incredible reliability is explained by the immense capacity of the desalinated water reservoir, along with the generation of the energy required for the desalination plant's operation. The energy needs are covered by a ratio of 73.9%, thereby proving that the configuration of the HRES is very effective. Of this 73.9%, 51.7% is the energy produced by the HHP station, 22.9% from the wind park solely, while the supplementary percentage is covered by the national network of PPC (Public Power Corporation). Although the nationwide network of PPC and wind farms contribute more electricity on average each month than hydropower does, there are some months when PPC is primarily responsible for meeting demand. The highest yearly output is 35000 MWh, whereas the greatest annual demand is 46000 MWh. The overall annual energy production is consistently above 28000 MWh.

Conclusions

Many arid islands, like Leros, experience a water shortage that threatens, not only the survival of the islanders, but also the growth of their agriculture, herds of animals, and eventually their economies. This issue arises because of the islands' small drainage basins, and it is more severe in the summer because of the large number of visitors, as well as the increased requirement for irrigation water. Due to the desalination process' compatibility with renewable energies, the incorporation of such a plant with a HRES seems to be the solution to water and energy scarcity. Based on this research, the HRES attains a reliability of 99%, concerning the coverage of drinking, as well as irrigation needs. Additionally, in terms of energy, the reliability of the system amounts to 74%, reducing significantly the island's dependence on the national network of PPC.

Acknowledgements: This study is not funded by any institution or project.

References

Ferreira, A., Pinheiro, M. D., de Brito, J. and Mateus, R., Decarbonizing strategies of the retail sector following the Paris Agreement. Energy Policy, 2019, 135.

Jäger-Waldau, A., Photovoltaics and renewable energies in Europe. Renewable and Sustainable Energy Reviews, 11 (7), 2007, pp. 1414-1437

Kershman, S. A., Rheinländerb, J. and Gabler, H., Seawater reverse osmosis powered from renewable energy sources hybrid wind/photovoltaic/grid power supply for small-scale desalination in Libya. Desalination, 153 (1-3), 2003, pp. 17-23.

Al-Karaghouli, A., Kazmerski, L. L., Energy consumption and water production cost of conventional and renewable-energypowered desalination processes, Renewable and Sustainable Energy Reviews, 24, 2013, pp. 343-356.

Mimikou M. A., Baltas E. A., and Tsihrintzis V. A., Hydrology and Water Resource Systems Analysis, CRC Press-Taylor & Francis Group, Boca Raton, FL, USA ISBN: 978-1-4665-8130-2, 2016.

Negra, N. B., Birgitte, B. J., Sorensen, P., Model of a Synthetic Wind Speed Time Series Generator, 2007

Hargreaves, G. H. and Samani, Z. A., Estimating potential evapotranspiration. Journal of Irrigation and Drainage Engineering, 108, 1982, pp. 223-230.

Sarris, D., Bertsiou, M. M. and Baltas, E., Evaluation of a Hybrid Renewable Energy System (HRES) in Patmos Island International Journal of Renewable Energy Sources, 4, 2019, pp. 40-47.

Environmental, Health and Safety Challenges of 300MW Floating Solar Plant

M. Karim and R. Rimsa

University of Waterloo, Health Science, Waterloo, Ontario, Canada
Corresponding author email: masud@eng-consult.com

Abstract

An Environmental Impact Assessment (EIA) was conducted for a 300MW Floating Photovoltaic (FPV) plant based on the World Bank's new Environmental and Social Framework (ESF). The World Bank is financing first FPV Project in Pakistan as part of its commitment in renewable energy development. The Project is planning to install a FPV plant to operate at the Tarbela Reservoir and Ghazi Barotha Forebays, as a hybrid scheme with the already established hydro power facilities. Key components of this installation will be high-density polyethylene floats, PV panels, underwater transmission cable to floating or shoreline inverters and transformers, and overhead transmission line to existing or new substation. This project is the first of its kind in Pakistan and one of the very few in Asia. The success of this project will allow for the possibility for other renewable energy projects in the region funded by the World Bank and a crucial step of the climate change initiative in South Asia.

The main environmental challenges identified include pollution of surface water due to the cleaning of accumulated bird droppings on the floating panels; aquatic habitat degradation as a result of altered quantity of bird droppings causing changes to water quality; changes to thermal structure and evaporation as a result of decreased sunlight access; direct impacts of shading on fish and aquatic algae; impacts on migratory birds and their habitats; and anchoring and cabling of the floats impacting fish movements. Some of the mitigation measures suggested include making design modifications to make the physical structure as compact and efficient as possible in order to leave more water surface for the migratory birds; performing fish population surveys to better understand the impacts; and improving the habitat quality of the nearby waterbodies to offset negative impacts on the wildlife. The main project-specific Occupational Health and Safety (OHS) challenges were risk of falling in water or drowning during installation of panels over water. The preventive measures suggested are to assemble panels and connecting the arrays on land and minimize the operation over water; minimize manual works overwater and use mechanical equipment instead; and using passive safety systems such as fencing and safety nets if workers must work above water.

Assessing the value of seasonal forecasts for improved reservoir operations in a water-stressed Mediterranean basin: A case study in the Faneromeni reservoir, Crete

A. Tsilimigkras[1], N. Crippa[2], M. Grillakis[1], G. Yang[3], M. Giuliani[4] and A. Koutroulis[1]

[1]School of Chemical and Environmental Engineering, Technical University of Chania, Crete, Greece
[2]Department of Mechanical Engineering, Politecnico di Milano, Milan, Italy
[3]College of Hydrology and Water Resources, Hohai University, Nanjing, China
[4]Department of Electronics, Information and Bioengineering, Politecnico di Milano, Milan, Italy
Corresponding author email: akoutroulis@tuc.gr

keywords: *water resources; reservoir operation; seasonal forecast; drought management.*

Introduction

The Mediterranean region is increasingly experiencing water scarcity due to the seasonal demand for water, the interannual climate variability, and the impacts of climate change on hydroclimatic patterns (Koutroulis et al., 2011, 2016).

The water resources in this region are often exploited in an unsustainable way, and traditional management practices are insufficient to cope with the progressive and substantial drying. Reservoirs are vital to compensate for the different precipitation time distribution and shift water from wet to dry seasons. Still, their operation must be flexible and anticipatory to support the sustainable use and preservation of water resources. In recent years, seasonal forecasting has progressed, providing an opportunity to improve drought risk management in advance (Grillakis et al., 2018; Yang et al., 2021).

This work evaluates the potential benefits of incorporating seasonal forecasts into the operation of the Faneromeni irrigation dam on Crete Island, Greece (Figure 1). We developed downscaled seasonal forecasts of reservoir inflow, which informed the design of flexible rules to cope with the variability of hydrologic conditions and include forecast information for conditioning operational decisions. Our goal was to determine the value of these seasonal forecasts in informing reservoir operations and improving system performance. We investigated alternatives to the current operation, which is based on the available storage at the beginning of the irrigation season, using the Evolutionary Multi Objectives Direct Policy Search method (Giuliani et al., 2016).

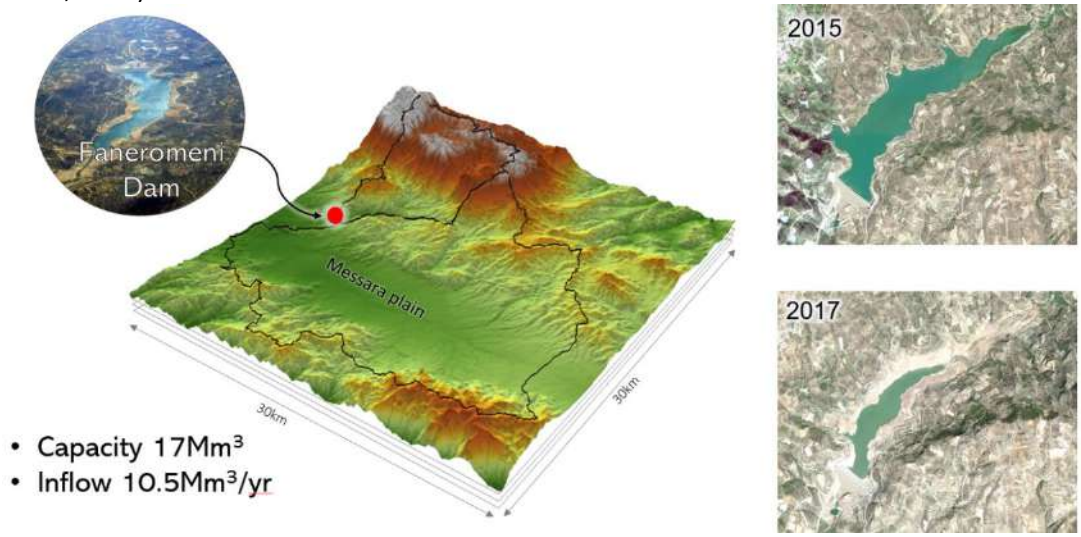

Figure 1. *Study site location. The Faneromeni dam supports the increased irrigation water demand of the Messara valley. During the 2016-2017 drought, ineffective water management policies led to the dam being drained and little water being stored in the basin.*

Materials a nd methods

We study streamflow forecasts with a seven-month lead time to inform reservoir operation policies.

We first developed a reservoir model to support the design of improved operating strategies, comprehending the primary water-related dynamics and various objectives of the parties involved. Then, we designed Pareto-optimal operating policies that allowed exploration of the tradeoffs across the considered objectives and informed the operating policies with forecast information. We compared the results of forecast-informed policies to a "no forecast-informed" scenario, which served as a benchmark to quantify the added value of the forecast information. Our analysis considered the interannual variability of inflow, which is challenging to predict accurately, and the region's different water management objectives. Finally, we evaluated the performance of the proposed operating policies under historical climate conditions, considering both the forecast skill and the value of the forecasts in informing operational decisions.

Results and discussion

Our results indicate that introducing flexible rules, even not based on forecasts, can significantly boost system performance.

The traditional management practice of releasing a volume equal to a pre-agreed demand during the irrigation season does not perform well under extreme inflow variability and summer droughts. We found that perfect seasonal forecasts lead to a significant improvement in the system's performance, as they provide a useful instrument in reservoir operation. However, the skill of the real forecast product limits how well real forecast-informed policies can perform. This could be since we used the median of the ensemble, which loses the inflow variability and misses wet years when there is room to expand the water supply. Therefore, carefully selecting the best forecast member is necessary to enhance the system's functionality.
The tradeoffs between the considered objectives reveal that there is no single solution that optimally satisfies all objectives simultaneously. Instead, there are several tradeoff solutions that balance the competing demands in the region. Forecast-informed policies help to identify these tradeoffs, allowing the design of more flexible and anticipatory strategies for sustainable water exploitation. Our findings are expected to improve the management of water resources, and the framework we developed can be used at other study sites with similar problems.

Conclusions

The study assessed the value of seasonal forecasts in improving the operational policies of the Faneromeni reservoir in a water-scarce Mediterranean basin.

The reservoir supplies water to two competing irrigation districts and is critical for the local economy. Results showed that incorporating seasonal forecasts improved system performance but selecting the best forecast member to optimize performance is challenging due to interannual inflow variability. The study is expected to enhance the sustainable management of water resources in the region and other water-stressed regions with similar challenges.

Acknowledgements: This work was implemented in the framework of the research project "Sustainable Reservoir Management in water-stressed Mediterranean areas" (www.streamflows.eu). The project benefits from the support of the Prince Albert II foundation (http://www.fpa2.org).

References

Giuliani, M., Castelletti, A., Pianosi, F., Mason, E., & Reed, P. M. (2016). Curses, Tradeoffs, and Scalable Management: Advancing Evolutionary Multiobjective Direct Policy Search to Improve Water Reservoir Operations. *Journal of Water Resources Planning and Management*, *142*(2). https://doi.org/10.1061/(ASCE)WR.1943-5452.0000570

Grillakis, M., Koutroulis, A., & Tsanis, I. (2018). Improving Seasonal Forecasts for Basin Scale Hydrological Applications. *Water 2018, Vol. 10, Page 1593*, *10*(11), 1593. https://doi.org/10.3390/W10111593

Koutroulis, A. G., Grillakis, M. G., Daliakopoulos, I. N., Tsanis, I. K., & Jacob, D. (2016). Cross sectoral impacts on water availability at +2 °C and +3 °C for east Mediterranean island states: The case of Crete. *Journal of Hydrology*, *532*, 16–28. https://doi.org/10.1016/J.JHYDROL.2015.11.015

Koutroulis, A. G., Vrohidou, A. E. K., & Tsanis, I. K. (2011). Spatiotemporal Characteristics of Meteorological Drought for the Island of Crete. *Journal of Hydrometeorology*, *12*(2), 206–226. https://doi.org/10.1175/2010JHM1252.1

Yang, G., Guo, S., Liu, P., & Block, P. (2021). Sensitivity of Forecast Value in Multiobjective Reservoir Operation to Forecast Lead Time and Reservoir Characteristics. Journal of Water Resources Planning and Management, 147(6). https://doi.org/10.1061/(ASCE)WR.1943-5452.0001384

SUST ENG 2023

WASTEWATER TREATMENT & BIOREMEDIATION (PART I &PART II)

Fate of benzotriazoles in biochemical methane potential (BMP) tests

E. Gkalipidou, D. Kalantzis, L. Koutsellis, G. Gatidou*, M. Fountoulakis and A. Stasinakis

Water and Air Quality Laboratory, Department of Environment, University of the Aegean,
Mytilene, Lesvos, Greece
Corresponding author email: ggatid@env.aegean.gr

Keywords: *anaerobic digestion; fate; BTRs; thermal pretreatment; conductive material; voltage.*

Introduction

Benzotriazoles (BTRs) are partially removed during conventional wastewater treatment (Stasinakis et al., 2013) while they are often accumulated in sewage sludge (Zhang et al., 2022). These substances are manufactured chemicals that are widely used in numerous applications and they are considered as environmental contaminants of emerging concern (Menger et al., 2022). According to the literature, various pretreatment strategies, including chemical, physical, or thermal ones, have been studied in order to improve the effectiveness of conventional anaerobic digestion (AD) process. Among the different pretreatment processes, thermal hydrolysis it is preferred because it is simple and yet cost-effective (Bonu et al., 2023). Thermal hydrolysis is favored above other pretreatment methods due to its simplicity and affordability (Bonu et al., 2023). Activated carbon (granular or powdered) is also utilized to improve removal efficiencies (Wanninayake, 2021), while application of voltage and addition of conductive materials are also tested during the last years in order to improve the performance of AD. The main goals of the present study was to investigate the fate of several micropollutants belonging to BTRs (1H-BTR, 5TTR, CBTR, and XTR) group during sludge AD as well as the impact of voltage, thermal pretreatment, graphite and granulated active carbon (GAC) on their removal.

Materials and methods

Batch experiments were performed in duplicates using glass serum bottles of 120 mL total volume (80 mL working volume) as reactors. Anaerobic sludge was used as inoculum and a mixture (30:70) of primary and secondary sludge was used as substrate. The target compounds were spiked at a concentration of 50 μg L^{-1} into the substrate (1:1 substrate: inoculum). Thermal pretreatment was performed on the substrate under different conditions, GAC or graphite was added at concentration of 10 gL^{-1}, while the applied voltage was 0.8 V. Serum bottles were sealed with butyl rubber stoppers and aluminium crimps and purged with nitrogen gas for approximately 1 minute to maintain anaerobic conditions and were placed in a water bath (37 ℃). The experiments were performed for a total period of up to three (3) months. Gas measurements were taken daily up to eight days and periodically thereafter during the end of each experimental cycle. The determination of methane content was achieved using GC-TCD. COD, TS, VS and target micropollutants were determined at t=0 and in the end of each experimental cycle. BTRs analysis was based on the method reported by Mazioti *et al.* (2013).

Results and discussion

The operation of all reactors was stable during the experimental period, the pH values in the reactors after the end of the experiments ranged between 7.0-7.5. Both COD removal and methane production was enhanced by the presence of GAC and voltage application in the reactors. Specifically, the maximum biogas yield increased from 707 ± 9 ml gVS^{-1} in the reactors containing untreated substrate to 804 ml gVS^{-1} in the reactors containing thermally pre-treated substrate for 1h and GAC. Interestingly, the application of longer thermal pretreatment times (3 hours) seems to inhibit methanogenesis. However, the addition of GAC can help overcome this inhibition. The ability of anaerobic sludge to biodegrade target BTRs seem not to be significantly affected by the application of voltage or/and the addition of graphite. However, the use of GAC

together with pretreated sludge, shown significant removal of this class of compounds. Among the different pretreatment conditions best results were obtained after heating the substrate for 1h.

Conclusions

According to the results of the present study, application of thermal pretreatment in combination with GAC can significantly increase the biodegradation of BTRs improving the performance of sludge AD process and methanogenesis.

Acknowledgements: This project has received funding from the European Union's Horizon 2020 research and innovation programme under grant agreement No 101036756, ZeroPM (https://zeropm.eu/).

References

Asimakopoulos, A.G., Ajibola, A., Kannan, K., Thomaidis, N.S., 2013. Occurrence and removal efficiencies of benzotriazoles and benzothiazoles in a wastewater treatment plant in Greece. *Science of the Total Environment* 452–453, 163–171.

Bonu, R., Anand, N., Palani, S.G., 2023. Impact of thermal pre-treatment on anaerobic co-digestion of sewage sludge and landfill leachate. Mater Today Proc 72, 99–103.

Gago-Ferrero, P., Borova, V., Dasenaki, M.E., Thomaidis, N.S., 2015. Simultaneous determination of 148 pharmaceuticals and illicit drugs in sewage sludge based on ultrasound-assisted extraction and liquid chromatography-tandem mass spectrometry. *Analytical and Bioanalytical Chemistry* 407, 4287–97.

Mazioti, A.A., Stasinakis, A.S., Gatidou, G., Thomaidis, N.S., Andersen, H.R. 2015. Sorption and biodegradation of selected benzotriazoles and hydroxybenzothiazole in activated sludge and estimation of their fate during wastewater treatment. *Chemosphere 131, pp. 117-123.*

Menger, R.F., Funk, E., Henry, C.S., Borch, T., 2021. Sensors for detecting per- and polyfluoroalkyl substances (PFAS): A critical review of development challenges, current sensors, and commercialization obstacles. *Chemical Engineering Journal* 417, 129133.

Stasinakis A.S., Thomaidis N.S., Arvaniti O.S., Asimakopoulos A.G., Samaras V.G., Ajibola A., Mamais D., Lekkas T.D. (2013) Contribution of primary and secondary treatment on the removal of benzothiazoles, benzotriazoles, endocrine disruptors, pharmaceuticals and perfluorinated compounds in a sewage treatment plant. *Science of the Total Environment* 463-464, 1067-1075.

Wanninayake, D.M., 2021. Comparison of currently available PFAS remediation technologies in water: A review. J Environ Manage 283, 111977.

Zhang, W., Jiang, T., Liang, Y., 2022. Stabilization of per- and polyfluoroalkyl substances (PFAS) in sewage sludge using different sorbents. *Journal of Hazardous Materials Advances* 6, 100089.

Sustainable municipal wastewater treatment through novel pilot-scale aerated Vertical Flow Constructed Wetlands

P. Regkouzas[1*], I. Asimakoulas[1], K. Paragioudakis[1], E. E. Koukouraki[1] and A. Stefanakis[1]

[1]School of Chemical and Environmental Engineering, Technical University of Crete, Chania, Greece
Corresponding author email: astefanakis@tuc.gr
*Presenting author**

keywords: *constructed wetlands; nature-based solutions; ecological engineering; wastewater treatment; aerated constructed wetlands.*

Introduction

Over the last years, the need for alternative, nature-based and environmentally friendly technologies for wastewater treatment increased significantly, especially concerning low-income countries, where conventional wastewater treatment technologies may be harder to be adopted due to financial and technical difficulties [Gholipour & Stefanakis, 2021]. Constructed Wetlands (CWs) represent an effective, sustainable and cost-efficient wastewater treatment technology, characterized by its low operational and maintenance costs along with the absence of toxic chemicals usage to achieve effective treatment [Gomes et al., 2018]. Vertical Flow CWs (VFCWs) are widely applied in several countries, due to their lower surface area demand, combined with the promotion of their aerobic nature that leads to more efficient organic matter (OM) oxidation and nitrification rates [Al-Wahaibi et al., 2021]. Towards higher treatment efficiency and pollutant removal, aerated VFCWs have shown favorable experimental results in previous studies, leading to higher nitrogen and OM removal, due to the supplementary oxygen supply in the CW bed that promotes aerobic conditions [Stefanakis, 2021; Xu et al., 2023].

The goal of this study was to investigate the efficiency of pilot-scale aerated VFCWs on municipal wastewater treatment. In this context, three different aerated VFCWs were implemented, two containing recycled plastic HDPE and one containing gravel as filling mediums, while wetland vegetation was comprised of common reeds (*Phragmites australis*), collected locally in the Chania region. The units have been operational for more than 9 months and are still monitored on a regular basis regarding their pollutant removal efficiency.

Materials and methods

Three different units of aerated VFCWs were developed in the premises of Technical University of Crete; one containing recycled HDPE plastic with no vegetation (control treatment) (C), one containing recycled HDPE plastic with P. *australis* vegetation (P) and one containing gravel with P. *australis* vegetation (G). The units were continuously aerated by adopting a fixed 6 L/h supply rate. About 12L of primary municipal wastewater was added in each unit every 2 days and the leachate effluent volume was also recorded, to consider the climatic conditions and the actual evapotranspiration rates. The primary effluent was collected every time from the wastewater treatment plant of Chania. Influent and effluent samples were taken on a weekly basis and respective physicochemical analyses were conducted in order to determine the removal of several parameters, such as BOD5, COD, TOC, Total N, Total P, NH_4-N and PO_4-P. Other parameters, such as pH, Electrical Conductivity (EC) and Total Suspended Solids (TSS) were also monitored.

Results and discussion

During the first 9 months of operation, the pilot units showed high removal rates of the investigated parameters. These results are presented in Table 1. High removal rates were measured for BOD5 and COD (>90% and >85% accordingly) in the planted units, with the P unit showing the highest removal rate (94.9%). The same was also found for nitrogen where an almost complete ammonia removal was found in the P unit and a slightly lower removal in the G unit. Total P was removed in lower rates (44-48%) in the planted units G and P and a lower removal was found in the control unit. TOC was also sufficiently removed (43-55%) in all units. Generally, the results indicate that the planted unit containing the recycled HDPE was the most

effective in the pollutant removal, followed closely by the planted unit G but at lower removal rate. Similar high removals are also elsewhere reported [Stefanakis, 2019]. The unplanted unit C had in general the lowest performance indicating the important role of plants' presence in the system performance.

Table 1. *Influent values and removal rates of the tested parameters*

Parameter	Inlet (mg/L)	VFCW unit		
		Removal (%)		
		C	P	G
BOD5	311.1	66.3 ± 17.3	94.9 ± 3.3	86.8 ± 6.0
COD	383.6	66.3 ±14.5	92.1 ± 2.9	85.4 ± 6.2
TOC	45.9	54.2 ± 21.8	60.9 ± 18.4	44.4 ± 31.1
Total N	60.1	24.8 ± 16.4	85.0 ± 12.1	69.6 ± 22.4
NH_4-N	36.9	52.4 ± 21.0	97.3 ± 2.3	85.2 ± 15.9
Total P	7.2	27.4 ± 13.4	55.6 ± 28.5	45.6 ± 22.3
PO_4-P	5.5	23.5 ± 12.4	57.5 ± 23.1	44.7 ± 23.4

Conclusions

The first results of this work showed that aerated VFCWs could represent a sustainable, nature-based, cost-efficient and effective technology for wastewater treatment, providing a high treatment efficiency. The use of novel media can further enhance the performance of these systems which is something that needs further investigation.

Acknowledgements: This research was funded by internal funds of the Technical University of Crete.

References

Al-Wahaibi, B. M., Jafary, T., Al-Mamun, A., Baawain, M. S., Aghbashlo, M., Tabatabaei, M., & Stefanakis, A. I. (2021). Operational modifications of a full-scale experimental vertical flow constructed wetland with effluent recirculation to optimize total nitrogen removal. *Journal of Cleaner Production*, *296*, 126558. https://doi.org/10.1016/j.jclepro.2021.126558.

Gholipour, A., & Stefanakis, A. I. (2021). A full-scale anaerobic baffled reactor and hybrid constructed wetland for university dormitory wastewater treatment and reuse in an arid and warm climate. *Ecological Engineering*, *170*, 106360. https://doi.org/10.1016/j.ecoleng.2021.106360.

Gomes, A. C., Silva, L., Albuquerque, A., Simões, R., & Stefanakis, A. I. (2018). Investigation of lab-scale horizontal subsurface flow constructed wetlands treating industrial cork boiling wastewater. *Chemosphere*, *207*, 430-439. https://doi.org/10.1016/j.chemosphere.2018.05.123.

Stefanakis, A. I. (2019). The role of constructed wetlands as green infrastructure for sustainable urban water management. *Sustainability*, *11*(24), 6981. https://doi.org/10.3390/su11246981.

Stefanakis, A. I. (2021). A Two-Stage Constructed Wetland Design Integrating Artificial Aeration and Sludge Mineralization for Municipal Wastewater Treatment. *Environmental Pollution and Remediation*, 195-211. https://doi.org/10.1007/978-981-15-5499-5_7.

Xu, W., Yang, B., Wang, H., Wang, S., Jiao, K., Zhang, C., Li, F., & Wang, H. (2023). Improving the removal efficiency of nitrogen and organics in vertical-flow constructed wetlands: The correlation of substrate, aeration and microbial activity. *Environmental Science and Pollution Research*, *30*(8), 21683-21693. https://doi.org/10.1007/s11356-022-23746-7.

Removal of chromium from aqueous solution using CeO_2@starch nanocomposite material and olive stone in a continuous system.

O. Jaiyeola and C. Mangwandi[1]

[1]School of Chemistry and Chemical Engineering, Queen's University Belfast, Belfast, United Kingdom
Corresponding author email: c.mangwandi@qub.ac.uk

keywords: *Chromium; Starch; adsorption; Starch cerium oxide.*

Introduction

Industrial wastewater is commonly contaminated with heavy metals, which can harm aquatic organisms and pose health risks to humans through the food chain. One of the heavy metals of concern is chromium, which is found in industries such as electroplating, tanning, and paint manufacturing. Chromium can exist in two forms in aqueous solutions: hexavalent chromium (Cr(VI)) and trivalent chromium (Cr(III)). Cr(VI) is much more toxic than Cr(III) and prolonged exposure to it can lead to a range of health issues such as abdominal pains, vomiting, gastrointestinal diseases, and genetic mutations(Mona et al., 2011).. Therefore, it is crucial to remove hexavalent chromium from wastewater before it is released into natural water bodies.

Several methods can be used to remove heavy metals from wastewater, including precipitation, ionic exchange, electrochemical reduction, membrane filtration, and adsorption. Among these, adsorption is one of the most economical and widely used due to its simple design and low operational costs. Various biomass-based materials such as teawaste, date pit, fruit peelings and starch have been used for the adsorption of Cr(VI). A fixed bed column was packed with starch with a secondary column packed with olive stone. The wastewater was passed through the column. The effect of various parameters such as bed height, flow rate, initial concentration of chromium was investigated.

Materials and methods

A dispersed solution of starch was prepared by mixing 3.0g of starch in 100ml of deionised water. 3.0 grams of citric acid (the crosslinking agent) and 1.5g of the sodium hypophosphite monohydrate catalyst ($NaH_2PO_2{\cdot}H_2O$) was dissolved in the starch solution for cross-linking (M. Naushad et al.2016). The resulting starch suspension was continuously stirred at 60°C for 2 hours, then left to cool to room temperature.

To prepare the hydrous cerium oxide, 0.02 moles of sodium hydroxide powder was dissolved in 100 mL of ethanol (absolute) to prepare 0.2 M sodium hydroxide/ethanol solution. 0.005 moles of $Ce(NO_3)_3{\cdot}6H2O$ powder was dissolved in 100 mL of ethanol (absolute) to prepare 0.05 M $Ce(NO_3)_3$/ethanol solution. The sodium hydroxide/ethanol solution was then added into the $Ce(NO_3)_3$/ethanol solution at ambient temperature under vigorous stirring.

After the two solutions were mixed, the colour of the precipitates was white in just 20 minutes after continuous stirring. Precipitate was collected by centrifugation, rinsed with deionised water and ethanol (absolute) three to four times and then dried in an oven at 60°C for 12 hours to obtain Starch/CeO_2 adsorbent. Finally, the dried product was crushed using a mortar and pestle into fine particles of uniform size and shape(Ronghui Li et al.2012). The Cr(VI) concentration in solid phases was calculated from the equation:

$$Qe = \frac{(C_i - C_e)\,V}{m}$$

where C_i and C_e are the liquid-phase concentrations of chromium initially and at equilibrium respectfully and both measured in mg/L. Volume of solution (L) and m is the mass of dry adsorbent used for the experiment in grams. A colour reagent was synthesized using methods reported by (Albadarin et al. 2013) by adding 0.25g of 1,5-diphenylcarbohydrazide to 50mL methanol, 14mL sulfuric acid and 500mL deionised water. To determine Cr(VI) concentration after treatment using the nanocomposites 6mL of the solution was added to 2mL of the colour reagent for each sample. The second column employed crushed olive stones with particle

sizes ranging from 0-500um. The olive stones were not subjected to any pre-treatment prior to absorption experiments. To eliminate any adhering dirt, the olive stone was washed within the column for four hours with de-ionized water before each experiment.

Results and discussion

The study aimed to determine the rate constant, K_t, and maximum absorption capacity, q_o, for Cr(VI) absorption onto CeO_2/starch nanocomposite and olive stone under varying system conditions. The R^2 values ranged from 0.91 to 0.99, demonstrating a good fit to the data for all conditions studied. As the inlet concentration increased, the Kt value decreased while the q_o values increased. A similar trend was observed in the bed depth experiment, indicating an increase in availability of active sites for Cr(VI)/Cr(III) to bind to as the nanocomposite bed depth increased. The study confirmed that the Thomas model is suitable for describing Cr(VI) absorption onto the nanocomposite and olive stone with varied system conditions.

Table 1. *Thomas Model Constants and Parameters of Starch/CeO_2 at pH 2 with varied initial concentrations.*

Parameter	K_t (mL/min.mg)	$q_{o\ (mg/g)}$	R_2
Initial Concentration (ppm)			
20	1.15	20	0.91
40	0.42	30	0.96
60	0.34	40	0.98
80	0.166	35	0.98

Table 2*. Thomas Model Constants and Parameters of Starch/CeO_2 at pH 2 with varied flowrates.*

Initial Flow Rate (mL/min)	K_t (mL/min.mg)	$q_{o\ (mg/g)}$	R_2
5.5	1.175	20	0.82
7	0.998	40	0.83
8.5	2.146	16	0.95
10	2.33	10	0.99

Table 3. *Thomas Model Constants and Statistical Parameters, Nanocomposite at pH 2 with varied bed depth.*

Bed Depth CeO2/Starch (cm)	K_t (mL/min.mg)	$q_{o\ (mg/g)}$	R_2
1 (0.3473g)	0.924	130	0.91
1.5 (0.6461g)	0.29	100	0.96
2 (0.8617g)	0.27	100	0.98
2.25 (1.077g)	0.322	100	0.93

Conclusions

In conclusion, the use of starch and olive stone as adsorbents for the removal of chromium from wastewater in a continuous flow fixed-bed column was investigated. The results showed that starch is an effective adsorbent for the removal of chromium. The maximum adsorption capacity for removing chromium (VI) and chromium (III) of olive stone was found to be 3.1 mg/g and 5.19 mg/s respectively. The optimal conditions for chromium removal were found to be a bed height of 2.25 cm, a flow rate of 5.5 mL/min, at a pH of 2. This would suggest that to achieve the highest removal of Cr(VI) and Cr(III), the bed depth should be as high as possible, and the flow rate should be as low as reasonably practicable enabling the system to handle varying concentration levels of industrial wastewater containing chromium.

References

M. Naushad, T. Ahamad, G. Sharma, A. a. H. Al-Muhtaseb, A. B. Albadarin, M. M. Alam, Z. A. Alothman, S. M. Alshehri and A. A. Ghfar, *Chemical Engineering Journal*, 2016, 300, 306-316.

Ronghui Li, Qi Li, Shian Gao, Jian Ku Shanga (2012) 'Exceptional arsenic adsorption performance of hydrous cerium oxide nanoparticles: Part A. Adsorption capacity and mechanism', Chemical Engineering Journal, 246(1), pp. 127-135

Albadarin, C. Mangwandi, G. M. Walker, S. J. Allen, M. N. M. Ahmad and M. Khraisheh, *Journal of Environmental Management*, 2013, 114, 190-201.

S. Mona, A. Kaushik, C.P. KaushikBiosorption of chromium(VI) by spent cyanobacterial biomass from a hydrogen fermentor using Box-Behnken model. International Biodeterioration & Biodegradation, 65 (2011), pp. 656-663.

Primary Filtration Systems for upgrade of overloaded municipal Wastewater Treatment Plants in the Mediterranean Countries

K. Tsamoutsoglou[1], I. Maniaki[1] and P. Gikas[1]

[1]Design of Environmental Processes Laboratory, School of Chemical and Environmental Engineering, Technical University of Crete, Chania, Greece
Corresponding author email: pgikas@tuc.gr

keywords: *wastewater treatment plant; primary filtration; energy savings; capacity increase.*

Abstract

Numerous Wastewater Treatment Plants (WWTP) are prioritising the reduction of energy use by employing low-cost wastewater technologies. Advanced Primary Filtration (APF) systems are emerging technologies in wastewater treatment, providing substantial benefits to existing and new WWTPs. These systems are currently being installed at the activated sludge WWTPs of Kyperounda, Limassol (Cyprus) and Marpissa, Paros (Greece), with respective hydraulic capacities of 1,800 and 2,500 m^3/d. The wastewater process includes microsieves, in series, followed by Continuous Backwash Upflow Media Filters (CBUMFs) and lamella clarifier. Microsieves offer several advantages for activated sludge wastewater treatment plants. The wastewater treated with microsieves has comparable or better characteristics, compared to primary sedimentation (Koliopoulos & Gikas, 2013). It is noted that simultaneously with the removal of solids, particulate BOD_5 is also removed. Also, microsieves have shown significant potential for removal of cellulose from raw wastewater (Gupta et. al, 2018). Microsieves are regarded as a compact industrial system, wherein the spatial footprint necessary for the installation of a microsieve is at least 20 times smaller in comparison to primary sedimentation (Franchi et al, 2012). In the first step of the APF system, the wastewater is fed into microsieves. Following microsieves, the combined system includes CBUMFs and a lamella clarifier for further removal of suspended solids and settling of reject water from CBUMFs, respectively. Due to the decreased organic load in the aeration tank, the retrofitted WWTPs anticipated a 30-35% decrease in total energy consumption and a 40% increase in capacity.

Acknowledgements: This study is co-financed by the European Regional Development Fund (ERDF) and national resources of Greece and Cyprus, through the of the Cooperation Program INTERREG V-A Greece - Cyprus 2014-2020: “Upgrade of WWTPs for the management of increased demands and the reduction of the operational cost" (ANELIXI).

References

Franchi, A., Stedman, K. & Gikas, P., 2012. *Enhanced primary solids removal from municipal wastewater by two steps filtration executive summary.*

Koliopoulos, G., and Gikas, P., 2013. Fine mesh sieving of raw municipal wastewater for TSS and COD removal, *13th International Conference on Environmental Science and Technology*.

Gupta, M., Ho, D., Santoro, D., Torfs, E., Doucet, J., Vanrolleghem, P. A., & Nakhla, G. 2018. Experimental assessment and validation of quantification methods for cellulose content in municipal wastewater and sludge. *Environmental Science and Pollution Research*, 25, 16743-16753.

The rehabilitation of the main sewer collector of Limassol - An innovative approach

Y. Tsouloftas, M.Vrionides and G. Panayiotou*

Sewerage Board of Limassol - Amathus (SBLA)
Corresponding author email: Gregoris@sbla.com.cy

Abstract

During the early 90s, Phase A of the sewerage system of Limassol city was constructed. A big part of the works comprised the construction of the main sewer collector ~~on~~ along the coastal front of the city. This pipe is made of asbestos/cement with a lifetime of around 25-30 years, according to the manufacturer, meaning that the end of the pipe's lifetime was estimated to be somewhere between 2025-2030. According to this situation, the Sewerage Board of Limassol - Amathus (SBLA) had to choose between two solutions: digging the whole coastal front of the city and replace the pipe or find another solution. This is when the personnel and the Consultants of SBLA came up with the innovative and out-of-the-box solution to reline the pipe internally by using special material without any digging using CIP (Cure-In-Place) Pipe Lining trenchless method. The contract for these works concerned the relining of 8.5km of gravity pipe and had a budget of 8 million euros. The contractor was CYBARCO CONTRACTING Ltd and the specialised subcontractor was BLEJKAN (POLAND) and QuakeGUARD (CYPRUS) while the Contract period was 24 months. By applying this method SBLA succeeded to extend the lifetime of the main Collector pipe by 50 years and eliminated the danger of pipe collapsing due to erosion causing an environmental catastrophe, with no excavations at all and with the minimum possible inconvenience for the citizens of Limassol.

SUST ENG 2023

BIOCHEMICAL AND BIOMEDICAL ENGINEERING & BIOTECHNOLOGY

Development of biochar-based biocatalysts for fermentative bioethanol overproduction via whole-cell immobilisation under multiple environmental stresses

M. Kyriakou[1], M. Christodoulou[1], A. Ioannou[2], V. Fotopoulos[2] and M. Koutinas[1]

[1]Department of Chemical Engineering, Cyprus University of Technology, Limassol, Cyprus
[2]Department of Agricultural Sciences, Biotechnology & Food Science, Cyprus University of Technology, Limassol, Cyprus
Corresponding author email: michail.koutinas@cut.ac.cy

keywords: *Saccharomyces cerevisiae; bioethanol; biochar; environmental stress; gene transcription.*

Introduction

Although *Saccharomyces cerevisiae* is the industrial workhorse of bioethanol production, the strain encounters a plethora of stress conditions during fermentation including high temperature, nitrogen limitation, osmotic stress from substrate sugars and ethanol inhibition (Elbakush and Güven, 2021). However, biochar-based biocatalysts (BBB) have been proposed to enhance the production of renewable energy from biowaste, mitigating the environmental effects from food waste disposal while improving the sustainability of energy systems (Kyriakou et al., 2020). This study aimed to test the efficiency of BBB in ethanol production under inhibitory bioprocess conditions. The significance and novelty of the study included the use of the proposed technology against heat, ethanol, osmotic and oxidative stress aiming to understand the transcriptional patterns of genes involved in the molecular mechanisms controlling the metabolic responses of the yeast in supported and suspended cells.

Materials and methods

Biochar was obtained via conventional pyrolysis of pistachio shells (*Pistachia vera*) at 500 °C and it was used for the preparation of the biocatalyst via immobilization of *S. cerevisiae* as previously described (Kyriakou et al., 2020). The biocatalyst prepared was employed in bioethanol production experiments at the elevated temperature of 39 °C, while q-PCR analysis was conducted to determine mRNA expression from genes *HSF1* and *TPS1* known to impose instrumental effect in coping with heat shock stress. The expression levels of *HSP104* and *HSP12* were additionally investigated upon exposure of yeast cells to high bioethanol contents, while the intracellular proline level was determined to assess the protective effect of the biomolecule against various stresses, including heat-shock and elevated bioethanol concentration.

Results and discussion

Bioethanol fermentations of both freely suspended and supported cells of *S. cerevisiae* were conducted at 30 °C and 39 °C. Supported cells reached final concentration of 41 g L^{-1}, while the suspended culture yielded 34 g L^{-1}. Faster kinetics were obtained using BBB producing 30.9 g L^{-1} of bioethanol following 4 h of incubation as opposed to free cells that formed only 8 g L^{-1} (Figure 1). The mRNA expression levels monitored confirmed the stress protective role of BBB against heat stress, given that relative expression of *HSF1* was significantly higher in suspended cells as opposed to BBB at 39 °C, demonstrating that the heat-shock response pathway was not triggered following attachment of the yeast on the biomaterial. Moreover, the BBB system could efficiently sustain fermentations conducted under 90 g L^{-1} initial bioethanol content, which resulted in complete failure of conventional fermentations.

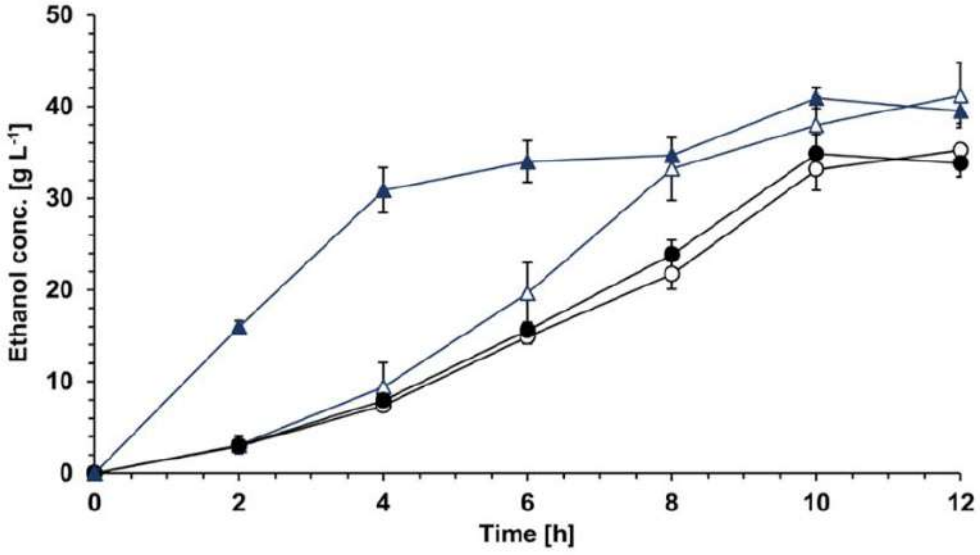

Figure 1. *Bioethanol production achieved at 30 and 39 °C using immobilised and freely suspended cells of S. cerevisiae. Symbols represent: (i) —△— immobilised cells at 30 °C; (ii) —▲— immobilised cells at 39 °C; (iii) —○— freely suspended cells at 30 °C; (iv) —●— freely suspended cells at 39 °C.*

Conclusions

The current work demonstrates that biochar-based biocatalysts can protect cells from heat shock stress and elevated bioethanol contents improving the performance of the fermentation process. This work will also include fermentations of *S. cerevisiae* under osmotic and ethanol stress.

References

Elbakush AE., Güven D. 2021. Evaluation of ethanol tolerance in relation to intracellular storage compounds of *Saccharomyces cerevisiae* using FT-IR spectroscopy. Process Biochem, 101, 266-273.

Kyriakou M., Patsalou M., Xiaris N., Tsevis A., Koutsokeras L., Constantinides G., Koutinas M. 2020. Enhancing bioproduction and thermotolerance in *Saccharomyces cerevisiae* via cell immobilization on biochar: Application in a citrus peel waste biorefinery. Renew Energy, 155, 53–64.

Can biodiesel become a determinant Bioeconomy factor towards sustainability: Mixture physicochemical composition and Input-Output (I-O) indicators of biodiesel sector

M.E. Kyriklidis[1], C. Kyriklidis[2], V. Vasileiadis[2], E. Loizou[3] and C. Tsanaktsidis[2]

[1]*Department of Regional Development and Cross Border Studies, University of Western Macedonia, Kila, Kozani, Greece*
[2]*Department of Chemical Engineering, University of Western Macedonia, Kila, Kozani, Greece*
[3]*Department of Regional Development and Cross Border Studies, University of Western Macedonia, Kila, Kozani, Greece*
Corresponding author email: er.kiriklidis@gmail.com

keywords: *Sustainability; Biodiesel mixtures; Input-Output (I-O) Multipliers; Bioeconomy; Physicochemical composition.*

Introduction

Energy markets became overburdened in 2021 because of a variety of factors, including the rapid economic revival after the pandemic. The above situation intensified into an absolute global energy crisis following Russia's invasion of Ukraine in February 2022. At the same time, price of natural gas reached record highs, and as a result so did electricity in many markets, while Oil prices hit their highest level since 2008. Therefore, energy prices led to very high inflation, forcing factories to reduce production or even shut down, slowing economic growth to the point that some countries are heading towards severe recession and pushing in general, many people into poverty.

Energy deployment owns an important role by introducing dynamic strategies, in order to achieve the long-term purpose of sustainability. The challenge of climate change and a potential increase in the energy demand, following the expected society development rebound after COVID-19 and war in Ukraine, could ideally lead central decision-making policies to produce technological, economic, social, environmental viable solutions.

According to the EU, Bioeconomy involves the above decision-making policies, so as to produce renewable biological resources and convert them and their waste streams into value-added products, such as food, feed, organic-based products and bioenergy. The goal of Bioeconomy, through sustainable production and the rational use of biological resources (including waste), is to produce more from less. By 2030, the EU aims to increase the share of renewable energy in transport to at least 14%, including a minimum share of 3.5% of advanced biofuels. EU countries are required to set out an obligation on fuel suppliers that ensures the achievement of this target.

Materials and methods

The purpose of this paper is to point out the beneficial effects of using biodiesel or mixtures of biodiesel, both as in the physicochemical composition of the mixture, and also as an indicator employed to reveal the potential of biodiesel to induce knock-on effects in the national economy of Greece. In order to analyze the composition of the mixture, extensive experimentation (about 3500) has been executed in the Laboratory of Chemical Engineering Department in the University of Western Macedonia under normal conditions (as it is defined by government protocols), providing significant information about the two mixture ingredients (diesel and biodiesel). Moreover, in order to assess the significance of biodiesel at national level, in terms of output, employment and income creation, an Input-Output (I-O) model and I-O multipliers were used.

Results and discussion

In this context, a series of new mixtures of diesel and biodiesel were implemented in the laboratory, both at different temperatures and at different percentages of element participation in the final mixtures. Important data were obtained both from the changes in temperature and the percentages of the elements, concerning

their effects on the physicochemical properties of the new fuels. Beyond that, interesting results emerged regarding the potential of biodiesel in the national economy. Particularly, in terms of output, employment, income multiplier, biodiesel is ranked high among the 74 sectors of the national economy, indicating that through any final demand change (e.g. external fund inflows), there will be high positive effects, displaying the importance of the sector.

Cultivation of *Clorella sorokiniana* in a flat-plate gas-lift photobioreactor and harvesting with the use of *Pleurotus ostreatus* fungal pellets

S. Schiza, A.S. Stasinakis and M.S. Fountoulakis

Department of Environment, University of the Aegean, Mytilene, Greece
Corresponding author email: fountoulakis@env.aegean.gr

keywords: *microalgae; anaerobic digestate; fungi; bio-flocculation; wastewater.*

Introduction

Cultivating microalgae in wastewater is a promising and sustainable solution for producing high-value products and biofuels. Specifically, microalgae require substantial amounts of nutrients and minerals, which can be readily supplied by nutrient-rich wastewaters. This approach not only allows for the treatment of wastewater but also reduces or even eliminates the need for additional chemicals during microalgae cultivation.

However, the harvesting of micro-algal biomass remains a significant challenge for the practical application of this technology. Typically, the cost of harvesting is accounts for around 20-30% of the total cost (Gouveia et al., 2016). Several methods have been tested for algal biomass harvesting, including centrifugation, coagulation, flocculation, filtration, flotation, and others (Singh and Patidar, 2018). Among them, coagulation and flocculation are the most cost-effective and convenient processes since they allow for the rapid treatment of large volumes of microalgal cultures. However, the use of chemicals during the process, renders the harvested biomass unsuitable for use in food or feed production. To address this issue, co-cultivation of fungi with microalgae has emerged as a promising strategy for efficient harvesting of microalgae (Leng et al., 2021). Fungi-based flocculation of microalgae is a green method that does not require chemicals and expands the possible utilization of harvested biomass in several applications.

The objective of this study was to examine a) the cultivation of *Clorella sorokiniana* in a flat-plate gas-lift photobioreactor using the effluent of an anaerobic digester treating agro-industrial wastewater as a medium and b) the harvesting of produced biomass by fungi-based bio-flocculation. For bio-flocculation, the edible mushroom *Pleurotus ostreatus* was used.

Materials and methods

The cultivation of *C. sorokiniana* was carried out using an automated flat-plate gas-lift photobioreactor system (Labfors 5, Infors HT, Switzerland) that was pH and temperature-controlled. The experiments were conducted at a temperature of 30°C, with the pH set at 7. A constant photon flux density of 200 µmol/m2/s was maintained using an LED-panel equipped with 260 warm white LEDs with a dark/light cycle of 8:16 h. The medium used for the experiments was tap water diluted liquid digestate (5%) from a pilot-scale digester treating agro-industrial wastewater (manure, olive mill wastewater and dairy wastewater).

The mycelia of *P. ostreatus* were grown in 0.5 L conical flasks containing a glucose-based medium on a rotary shaker for 5-7 days at 25°C and three different pH values of 4.5, 5.5, and 6.5. For the harvesting experiments, the produced fungal pellets were collected and added to the *C. sorokiniana* suspension in 500-mL conical flasks, which were placed on a rotary shaker at 100 rpm.

Results and discussion

Figure 1 illustrates the growth of *C. sorokiniana*. The saturation of oxygen decreased from 90-92% to 85-87% during dark periods, which coincided with a decrease in microalgal growth. However, a nearly linear increase in algal biomass was observed during the light periods, indicating that no nutrient deficiency occurred.

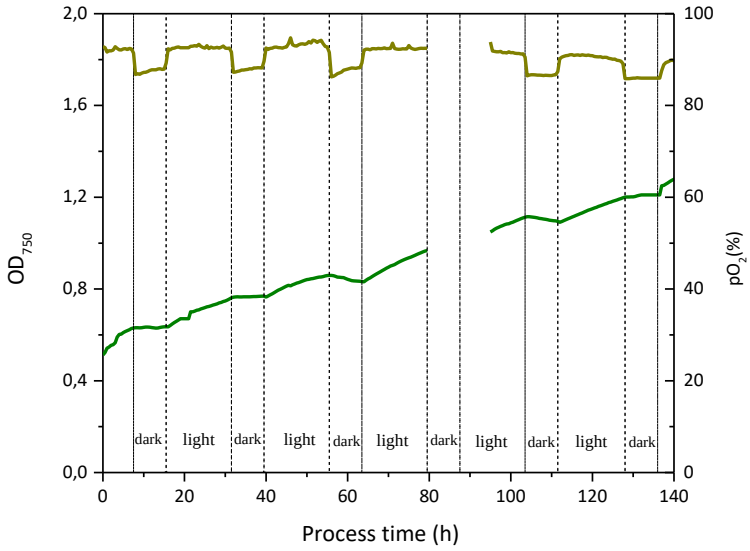

Figure 1. *Growth of C. sorokiniana and oxygen saturation in the flat-plate gas-lift photo-bioreactor using diluted liquid digestate as substrate. Batch process was conducted at 30 °C and a constant photon flux density of 200 µmol/m²/s.*

Harvesting efficiency of *C. sorokiniana* ranging from 30% to 70% was observed with the use of fungal pellets (Figure 2). The pH value, size of pellets, and ratio of fungal to microalgal biomass seems to influence harvesting efficiency.

Figure 2. *Harvested micro-algal biomass on the surface of P. ostreatus pellets*

Conclusions

The use of edible fungus *P. ostreatus* for producing fungal pellets and utilizing them for the bio-flocculation of microalgae *C. Sorokiniana* is a promising method for producing harvested biomass that could be utilized as feed or food.

References

Gouveia, L., Graça, S., Sousa, C., Ambrosano, L., Ribeiro, B., Botrel, E.P., Neto, P.C., Ferreira, A.F., Silva, C.M., 2016. Microalgae biomass production using wastewater: Treatment and costs: Scale-up considerations. Algal Res. 16, 167–176.

Leng, L., Li, W., Chen, Jie, Leng, S., Chen, Jiefeng, Wei, L., Peng, H., Li, J., Zhou, W., Huang, H., 2021. Co-culture of fungi-microalgae consortium for wastewater treatment: A review. Bioresour. Technol.

Rossi, S., Visigalli, S., Castillo Cascino, F., Mantovani, M., Mezzanotte, V., Parati, K., Canziani, R., Turolla, A., Ficara, E., 2021. Metal-based flocculation to harvest microalgae: a look beyond separation efficiency. *Sci. Total Environ.* 799

Singh, G., Patidar, S.K., 2018. Microalgae harvesting techniques: A review. J. Environ. Manage. 217, 499–508.

Optimization of microalgae bio-products under industrial flue gas exposure

G. Makaroglou[1], D. Mitrogiannis[1] and P. Gikas[1]

[1]School of Chemical and Environmental Engineering, Technical University of Crete, Kounoupidiana, Greece
Corresponding author email: gmakaroglou@tuc.gr

keywords: *Stichococcus sp.; photo-bioreactors; flue gas; CO_2 fixation; high added value products.*

Introduction

Microalgae are a promising source of products with added value and can be an alternative source of fuels. Microalgae require water, light, and CO_2. An ideal option could be flue gas sequestration for the production of microalgae biomass (Ullmann and Grimm, 2021). Therefore, one can profit from microalgae and at the same time, use them as a phycoremediation strategy that helps to reduce the environmental impact of this effluent (Katiyar et al., 2021; Ullmann and Grimm, 2021). Hence, large-scale cultivation of microalgae is one of the green, clean and sustainable development directions to achieve carbon neutrality (Li et al. 2023). The scope of the present study is carbon fixation contained in flue gas, emitted from industrial sources, using microalgae cultures as a sustainable solution. Prior to that, microalgae cultivation was optimized on smaller scale.

Materials and methods

For the small-scale experiments, two *Stichococcus* sp. microalgae strains were cultivated; the wild-type and a mutant, which exhibits greater biomass and lower total chlorophyll productivity, compared to the wild strain. Microalgae were cultivated in beaker vessels with 150 mL of Bold's Basal Medium. Different levels of illumination type (constant/flashing), $NaNO_3$ concentration (0.25/0.75 g L^{-1}) and nitrogen starvation (0/3 days) were examined as growth parameters. Illumination was provided by led strip lights (4,500 K) and the illuminance intensity was set to 5,100 lux. Microalgae were aerated with synthetic flue gas, containing 5% v/v CO_2 and the salinity level was 35 g L^{-1}. Furthermore, microalgae were grown attached on sandblasted glasses, placed at the bottom of the containers (Makaroglou et al., 2021). After 25 days of cultivation, biomass, lipids, proteins, carbohydrates, and pigments production were measured.

After the completion of small-scale experiments, microalgae cultivation was scaled-up in photobioreactor scale. Large scale experiments took place in Lavrio power plant station, one of Greece's Public Power Corporation power plants. Two identical closed type photobioreactors were utilized for microalgae cultivation, in which the cells were grown attached on sandblasting glass for 26 days. The culture volume of each photo-bioreactor was 15 L and microalgae were fed with real-time natural gas flue gas at a rate of 0.6 L per minute. Cultures were illuminated by LED lamps with ON-OFF frequency of 0 and 1,000 Hz. Photobioreactors were placed inside a shed to provide protection and the temperature was controlled by an A/C unit (25 ± 1 °C). $NaNO_3$ concentration was adjusted to 0.75 g L^{-1}. And nitrogen starvation was implemented 3 days prior to harvesting. At the end of cultivation period, the extracted biomass was converted into high added value products: carbohydrates, proteins, pigments, and lipids).

Results and discussion

Biomass production reached up to 40.70 g m^{-2} (Fig. 1A) and up to 45.71 g m^{-2} (Fig. 1B) for the wild-type and mutant strain, respectively, under constant light conditions and 0.75 g L^{-1} $NaNO_3$ concentration. As for bio-products production, when nitrogen-rich conditions were applied, there was an increase in the content of proteins, carbohydrates, lipids, total chlorophyll and β-carotene. These increases are translated as, up to 103%/88%, 142%/162%, 121%/122 %, 500%/487% and 408%/220%, for the wild/mutant strain, respectively. The maximum total bio-product content was 33.95 (Fig. 2A) and 34.98 g m^{-2} (Fig. 2B) for the wild and mutant strain, respectively. Three-day nitrogen starvation applied prior to biomass harvesting, increased lipids production by up to 63%/71%, for the wild/mutant strain (Fig. 2A, 2B).

With respect to large-scale experiments, *Stichococcus* was able to adapt to industrial flue gas and provided sufficient biomass, noting 50.5 g m^{-2} in the case of constant lighting and 47.9 g m^{-2} in the case of flashing lighting. Total bio-products were 79% and 80% of the dry biomass, respectively, with the carbohydrates concentration exceeding that of the remaining bioproducts measured (49% of dry biomass).

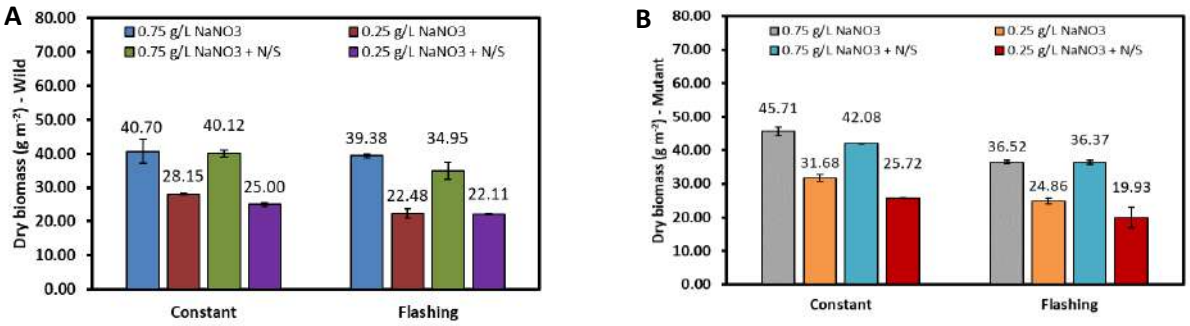

Figure 1. *Biomass production of Wild (A) and Mutant (B) Stichococcus sp. strain in lab scale.*

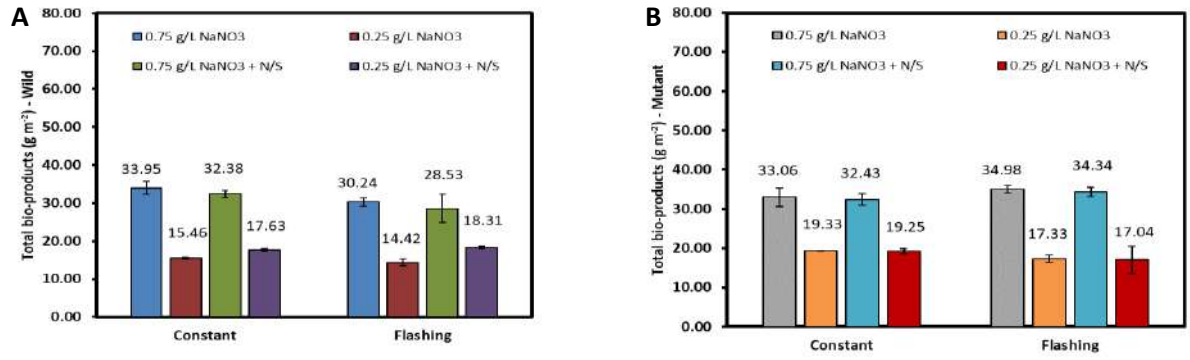

Figure 2. *Bio-products production of Wild (A) and Mutant (B) Stichococcus sp. strain in lab scale.*

Conclusions

In the present study, the production of biomass from the microalgae *Stichococcus* sp. strain, growing on small and large scale photobioreactors was investigated. Two strains of *Stichococcus* sp. were tested under different growth conditions and CO_2 addition to investigate their response in the biomass and bioproducts production. Results showed that $NaNO_3$ concentration plays a key role in biomass and bioproducts production, while the rest parameters have a minor influence. Furthermore, *Stichococcus* sp. was successfully grown under industrial natural gas flue gas, producing sufficient amounts of biomass and bioproducts. Therefore, it could be an efficient way to reduce CO_2 concentration from flue gases before they are released into the atmosphere, while the produced biomass could be harvested and processed for the production of high added value products.

Acknowledgements: This research was co-financed by Greece and the European Union (European Social Fund-ESF) through the Operational Programme «Human Resources Development, Education and Lifelong Learning» in the context of the Act "Enhancing Human Resources Research Potential by undertaking a Doctoral Research" Sub-action 2: IKY Scholarship Programme for PhD candidates in the Greek Universities».

References

Katiyar, R., Banerjee, S. and Arora, A., 2021. Recent advances in the integrated biorefinery concept for the valorization of algal biomass through sustainable routes. *Biofuels Bioprod. Biorefin*., 15, 879-898.

Li, P., Huang, Y., Xia, A., Zhu, X., Zhu, X. and Liao Q., 2023. Bio-decarbonization by microalgae: a comprehensive analysis of CO_2 transport in photo-bioreactor. *DeCarbon*, 2, 100016.

Makaroglou, G., Marakas, H., Fodelianakis, S., Axaopoulou, V. A., Koumi, I., Kalogerakis, N. and Gikas, P., 2021. Optimization of biomass production from *Stichococcous* sp. biofilms coupled to wastewater treatment. *Biochem. Eng. J.*, 169, 107964.

Ullmann, J. and Grimm, D., 2021. Algae and their potential for a future bioeconomy, landless food production, and the socio-economic impact of an algae industry. *Org. Agric.*, 11, 261–267.

CO_2 utilization in a system of anaerobic granular sludge and magnesium ribbon for acetic acid production

C.G. Samanides and I. Vyrides

Department of Chemical Engineering, Cyprus University of Technology, Limassol, Cyprus
Corresponding author email: ioannis.vyrides@cut.ac.cy
Presenting author email: samanides.kavtech@outlook.com

keywords: *Anaerobic granular sludge; CO_2 utilization; Homoacetogens; Magnesium ribbon; Methanogen inhibition; Volatile fatty acids.*

Introduction

Substantial research interest has been focused over the past decades on human activities that affect negatively the climate system, specifically focusing on carbon dioxide (CO_2) emissions. It is estimated that human activities contribute to releasing of 25 to 35 gigatons of CO_2 into the environment annually (Ruiz-Valencia et al., 2019). European Union (EU) concerned about the noticeable effect on the climate due to CO_2, promoted the "European Green Deal", so all the member states committed to cutting emissions by at least 55% by 2030, compared to 1990 levels, and becoming climate-neutral by 2050 (European Commission, 2022). As a main strategy to achieve this target a lot of technological processes are proposed for the utilization of CO_2 known as Carbon Capture and Storage, Carbon Capture and Utilization, and Bioenergy with Carbon Capture and Storage (Hepburn et al., 2019). However, these methods are high energy intensive.

In the present research, it is proposed a new sustainable process for CO_2 utilization. The conversion of the CO_2 was carried out in a system of anaerobic granular sludge and magnesium ribbon, *in situ*, for the bioconversion to acetic acid. The H_2 that generated from the oxidation of Mg^0 can be utilized along with CO_2 by homoacetogens, for the production of acetic acid according to Eq. (1) (Samanides et al., 2020):

(1) $4\,H_2 + 2CO_2 \rightarrow CH3COO^- + H^+ + 2\,H_2O$ ($\Delta G^0 = -95$ kJ mol^{-1})

However, in a mixed anaerobic system, hydrogenotrophic methanogens thermodynamically favored utilizing H_2 in comparison with homoacetogens and methanogenesis can be carried out according to Eq. (2) (Li et al., 2020):

(2) $4H_2 + CO_2 \rightarrow CH_4 + 2\,H_2O$ ($\Delta G^0 = -131$ kJ mol^{-1})

Apart from this, acetoclastic methanogens can utilize the produced by homoacetogen acetate to CH_4 according to Eq. (3) (Samanides et al., 2020):

(3) $CH3COO^- + H^+ \rightarrow CH_4 + CO_2$ ($\Delta G^0 = -75{\cdot}7$ kJ mol^{-1})

The aim of this study is to examine a new proof of concept; the utilization of CO_2 (as the only carbon source) to acetic acid in a system consisting of Mg ribbon and anaerobic granular sludge (AnGrSL) performed by applying several strategies to suppress methanogenesis and enhance homoacetogenesis.

Materials and methods

As inoculum, AnGrSL was used, which that gathered from a mesophilic up-flow anaerobic sludge blanket reactor (UASB). All batch laboratory-scale experiments were conducted in triplicates in screw cap serum bottles of 250 ml (working volume of 120 ml). To each serum bottle, AnGrSL and Mg^0 (≥ 99.5%, Sigma Aldrich, CAS Number: 7439–95–4) was used at a concentration of 8% w/v and 0.4% w/v respectively. A carbonate-buffered mineral medium (as described by Schink) was used. Several strategies to suppress methanogenesis and enhance homoacetogenesis were independently investigated, such as (a) short exposure of AnGrSL to heat before the exposure to Mg^0, (b) addition of 4 mM of 2-bromoethanesulfonate (BES), and (c) exposure of AnGrSL to high salinity (50; 70; 90 g L^{-1} NaCl). The concentrations of CO_2, H_2 and CH_4 were analyzed *via* gas chromatography and the products of the fermentation that consisted of short-chain volatile fatty acids (SVFAs) with a number of carbon atoms from 1 to 5 were measured through HPLC.

Results and discussion

As reflected in Fig. 1, the system that generates the maximum accumulation of acetic acid (2023 mg L^{-1}) at cycle 7 was the system where AnGrSL was thermally pre-treated at 95 °C for 30 min before the inoculation as a strategy for minimizing the depletion of H_2 and acetic acid by methanogens. Next-generation sequencing shows that *Methanolinea* which is a typical hydrogenotrophic methanogen was the most dominant phylum in systems.

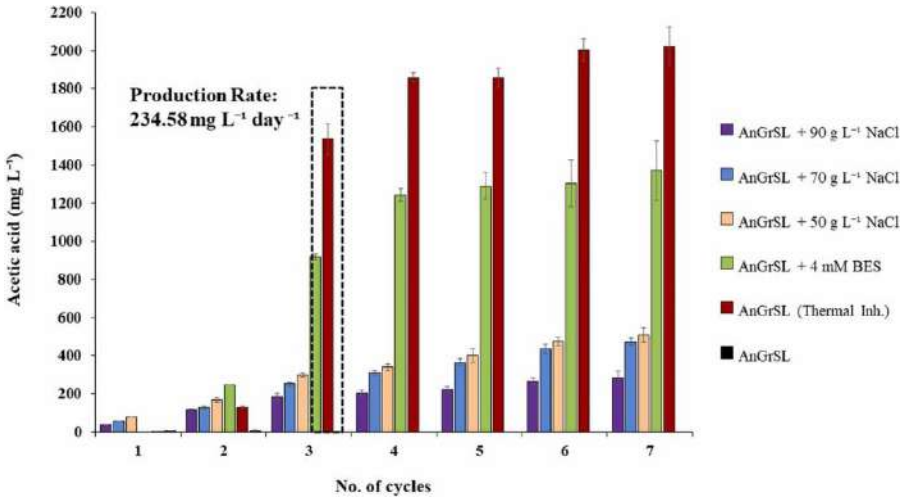

Figure 1. Acetic acid accumulation of all systems at cycles 1–7.

Conclusions

This study demonstrated a new and efficient approach to produce acetic acid by homoacetogens using magnesium ribbon *in situ* (H_2 producer) and CO_2 as the only carbon source in a system with AnGrSL. The use of Mg^0 *in situ* enhanced the availability of H_2 as an electron donor for CO_2 utilization by homoacetogens for the synthesis of VFAs under ambient conditions. For the selective acetate production by homoacetogen-enriched sludge was achieved by the inhibition of methanogenesis by applying different strategies such as the use of different concentrations of NaCl (50; 70; 90 g L^{-1}), the use of a specific inhibitor (4 mM BES) and heat-shock pre-treatment. Among the three methanogenesis inhibition methods, the use of heat as pre-treatment was the most effective procedure producing 2023 mg L^{-1} of acetic acid at the end of the experiment (Cycle 7 – day 32) with a maximum production rate of 235 mg L^{-1} day^{-1} at the 3rd cycle (Day 14). Follow the system where BES inhibitor was used producing 1369 mg L^{-1} (Cycle 7 – day 32) with a maximum production rate of 111 mg L^{-1} day^{-1} at the 3rd cycle (Day 14).

References

E. Commission, Delivering the European Green Deal, (2022). https://ec.europa.eu/info/strategy/priorities-2019–2024/european-green-deal/delivering-european-green-deal_en

Hepburn, C. et al. (2019). The technological and economic prospects for CO_2 utilization and removal. *Nature*, 575, pp. 87-97.

Li, Z. et al., (2020). Comparative microbiome analysis reveals the ecological relationships between rumen methanogens, acetogens, and their hosts. *Front. Microbiol.,* 11.

Samanides, C. G. et al. (2020). Methanogenesis inhibition in anaerobic granular sludge for the generation of volatile fatty acids from CO_2 and zero valent iron. *Front. Energy Res*., 8.

Schink, B. (1994). Diversity, ecology, and isolation of acetogenic bacteria. Drake H. L. (Ed.), Acetogenesis, Springer, Boston, pp. 197-235.

Optimal Biodiesel Mixtures: Cost and Density Evaluation Function Application by Genetic Algorithm

V. Vasileiadis[1], M.E. Kyriklidis[2], C. Kyriklidis [1], E.Terzopoulou [1] and C. Tsanaktsidis[1]

[1]*Department of Chemical Engineering, University of Western Macedonia, Kila, Kozani, Greece,*
[2]*Department of Regional Development and Cross Border Studies, University of Western Macedonia, Kila, Kozani, Greece*
Corresponding author email: vvasiliadis@uowm.gr

keywords: *Optimal Biodiesel Mixtures; Optimization Problems; Genetic Algorithms; Evolutionary Computation.*

Abstract

Diesel as a fuel, is high sulfur content and its consumption produces emission of sulfur oxides in large amounts. Its desulphurization consumes time and requires significant investments. As a result, Diesel emissions in combination with the high cost, converge to the searching of alternative fuels. Biodiesel as an alternative solution, has become more attractive because it is produced from renewable and environmentally friendly materials.

In this work, an adjusted genetic algorithm that investigates initially the ingredients percentages in the fuel mixtures to optimally create their combinations as Biodiesel fuel, is improved. Intelligent techniques, nature inspired intelligence, machine learning and evolutionary computation approaches provide high quality near-optimal results, to complicated optimization problems. Thus, operational research (OR) application bases on their implementation and evolution. This new decision-making tool is available for the Laboratory researchers and advances optimal fuels. The genetic algorithm, in short time after solution evaluation, proposes the optimal mixture for experimentation in Laboratory, between 750*106 alternative mixtures per experiment set. The profit of the proposed approach contributes to mixture production process while the new Biodiesel becomes more attractive than the competitive fuels.

The approach effectiveness concerns:

(a) the problem innovative modelling, with specific function evaluation modelling improvements

(b) and the way genetic algorithm is defined and tuned.

For the new Biodiesel production, extensive experimentation (about 3500) has been executed in the Laboratory of Chemical Engineering Department in the University of Western Macedonia, providing significant information about the two mixture ingredients (diesel and biodiesel). Biodiesel as second ingredient is produced from 50% animal fat sources and 50% vegetable sources. The evaluation of the new Biodiesel was implemented from a fitness function which estimates the fuel cost and density. Except cost, density as a physicochemical characteristic of fuels determines the suitability of a new fuel for general use and sale. Detailed experiments produced highly accurate Biodiesel mixtures, proposing an optimal fuel solution per set. Fuel Mixture in Set 1 is produced from 75.031% diesel and 24.969% biodiesel with mixture cost: 1.6975 €/l and mixture density: 0.8355 g/ml. In Set 2, the Fuel Mixture consists of 75.016% diesel and 24.984% biodiesel with mixture cost: 1.6977 €/l and mixture density: 0.8366 g/ml. The new Biodiesel fuels cost less 17.82% (Set 1) and 17.80% (Set 2) than the diesel cost (2.0000 €/l), provide competitive fuel prices, have lower sulfur content and their consumption reduces the pollutant emissions.

Impact of organic and biodynamic vineyard management on microorganism community, chemical and sensory properties of Cabernet Sauvignon wines in Ningxia, China

Y. Sun[1], F. Zhang[1], F. Y. Guo[1] and J. Zhang[2]

[1]School of Food and Wine, Ningxia University, Yinchuan, China
[2] Chinese Research Academy of Environmental Sciences, Beijing, China
Corresponding author email: jingzhang.ecp@hotmail.com

keywords: *biodynamic; organic agriculture; wine; flavor; microorganisms community.*

Abstract

In recent years, there is growing demands for healthy products. Consequently, there has been a change from conventional practices of vineyard management and winemaking to more environmentally sustainable approaches such as organic and biodynamic farming. A better understanding of the microbial dynamics and their effect on the final wine is of great importance to help winemakers produce the wine with consistent, high quality and its safety. This study focus on the characterization of microbiota, chemical and sensory properties of Cabernet Sauvignon wines in Ningxia, China under the three vineyard management systems. High-throughput sequencing technique and culture-dependent approaches were combined for microbiota identification. There were significant differences in the diversity of bacteria and fungi during spontaneously fermented wines under different vineyard management systems. For bacteria, *Lactobacillus* and *Massilia* were the most dominant genera in the samples from the organic samples, while *Sphingomonas*, unidentified *mitochondria*, *Pantoea* and *Tatumella* were the most abundant genera in the samples from the biodynamic cultivation. As for fungi, *Gibberella* and *Fusarium* were the most dominant genera in the samples from the organic cultivation group, while *Kodamaea* and *Hanseniaspora* were the most abundant genera in the samples from the biodynamic samples. A total of 40 volatile aroma compounds were identified during spontaneous fermentation of Cabernet Sauvignon wines including 13 esters, 20 alcohols, 4 acids and 3 other compounds. The wines produced under different vineyard management systems could be easily classified by principal component analysis. The higher content of higher alcohols was found in the biodynamic wines. The overall content of aroma substances in the organic wines were relatively low. The conventional wines for organic planting control has the characteristics of high ester content and low alcohol content. The results of this study suggest a possible correlation between the succession of the microbial dynamics and the chemical wine profiles. In summary, the results of this study will help find out the distinctive indigenous yeast species for further exploitation of local yeast resources and provide theoretical basis for the production of organic and biodynamic wines.

SUST ENG 2023

WASTE TO ENERGY/HYDROGEN PRODUCTION

The impact of a biogas plant on the energetic and economic situation of a dairy farm

J. Dach[1], P. Pochwatka[2], A. Kowalczyk-Juśko[2] and A. Mazur[2]

[1]Department of Biosystems Engineering, Poznań University of Life Sciences, Poznań, Poland
[2]Department of Environmental Engineering and Geodesy, University of Life Sciences in Lublin, Lublin, Poland
Corresponding author email: jacek.dach@up.poznan.pl

keywords: *anaerobic digestion; methane production; biogas plant; dairy farm; milk production.*

Introduction

Although Poland is not the largest milk producer, it is one of the leading milk producers in the European Union. However, in recent years, due to strong competition and drastic increases in feed prices, the profitability of milk production has significantly decreased. The situation may become even worse for milk producers if agricultural greenhouse gas (GHG) emission charges are introduced. It is important to note that cattle breeding is one of the main sources of GHG emissions in agriculture, including emissions from cows and urgent emissions of methane and nitrous oxide from stored manure, especially manure (Pochwatka et al. 2020). Unlike Western European countries, Poland produces significantly more solid manure than liquid manure, which can be a significant source of CH_4 and N_2O emissions when stored in piles. The formation of these emissions is related to an increase in temperature inside the manure pile within the first 24 hours, which leads to increased microbial activity and consumption of all the available oxygen, resulting in anaerobic conditions and decomposition of organic matter in manure, leading to the emission of carbon dioxide and energy in the form of methane. The introduction of mandatory payments for GHG emissions in agriculture, similar to those in the energy sector and heavy industry, will create a significant financial burden for cattle breeders (Mazurkiewicz et al. 2022). However, modern manure management technologies, such as biogas plants that convert manure into energy, can transform this issue into a significant energetic and economic asset for dairy farms. The objective of this study is to determine the energy and economic benefits for dairy farms that invest in a biogas plant supplied by cow manure.

Materials and methods

To analyze the benefits of investing in biogas, a dairy cow farm in the Wielkopolska region was considered, which annually produces 16,000 Mg of manure and 4,000 Mg of slurry. Biogas production efficiency tests were carried out in the Ecotechnologies Laboratory at the Poznań University of Life Sciences – the largest Polish biogas laboratory.

Figure. 1. *Biogas plan (499 kW of electric power) in the Przybroda experimental farm with dairy production related to Poznań University of Life Sciences*

The energy efficiency of a biogas plant supplied with such substrates was calculated using the methodology described by Cieślik et al. (2016) and Pochwatka et al. (2020). The operating costs of a 499 kW capacity biogas plant were obtained from actual data from an experimental farm in Przybroda, owned by the Poznań University of Life Sciences.

Investment costs were acquired from Dynamic Biogas, a leading Polish biogas company based in Poznań. The guaranteed price for selling electricity produced by biogas plants with a capacity of up to 500 kW is 219.8 EUR/MWh.

Results and discussion

The test results indicate that the available quantity of manure and slurry can produce 1.042 million m^3 of methane. This amount of CH_4, with an electrical efficiency of 40% (and thermal efficiency of 45%) from the cogeneration unit, can generate 4,158 MWh of electricity. Considering that the biogas plant consumes 8% of the electricity generated and 15% of the heat throughout the year, the available electricity is 3,825 MWh and heat 14,313 GJ. The revenue from the sale of electricity is 841 kEUR, and heat 102 kEUR (the heat price is 7.17 EUR/GJ). The operating costs of the biogas plant (including technical and technological service, personnel, insurance, depreciation) amount to 96.2 kEUR. Therefore, the profit after tax (18%) will be 695 kEUR and the payback period will be only 4.24 years (at the investment price of 2.95 EUR million).

Conclusions

The analysis of the energy efficiency and economic operation of the biogas plant at the dairy cow farm demonstrates that such an investment is highly advantageous for the farm, generating a profit of almost 0.7 million EUR annually. This results in a rate of return (ROCE) of nearly 24% and a payback period of just over 4 years. The above analysis does not include the costs of fees for GHG (methane and nitrous oxide) emissions from stored manure piles - which would further enhance the investment's profitability.

Acknowledgements: *This study was created in the framework of 2018 Joint Call FACCE ERA-GAS, SusAn and ICT-AGRI2 on "Novel technologies, solutions and systems to reduce greenhouse gas emissions in animal production systems" of the project "Decision support system for sustainable and GHG optimized milk production in key European areas" No. ICT-AGRI-3 ID 39288, Acronym MilKey, realized at Poznań University of Life Sciences. The work was created in the framework of the National Center for Research and Development project "Mitigating emissions from livestock systems", Acronym: MELS; FACCE ERA-GAS, SusAn and ICT-AGRI2.*

References

Cieślik M.; J. Dach; A. Lewicki; A. Smurzyńska; D. Janczak; J. Pawlicka-Kaczorowska; P. Boniecki; P. Cyplik; W. Czekała and K. Jóźwiakowski. 2016. "Methane fermentation of the maize straw silage under meso- and thermophilic conditions, Energy, 115 (2), 1495–1502.

Mazurkiewicz, J. 2022. Energy and Economic Balance between Manure Stored and Used as a Substrate for Biogas Production. *Energies*, 15, 413.

Pochwatka, P., Kowalczyk-Juśko, A., Sołowiej, P., Wawrzyniak, A., Dach, J., 2020. Biogas Plant Exploitation in a Middle-Sized Dairy Farm in Poland: Energetic and Economic Aspects. *Energies*, 13, 6058.

Spent coffee grounds and orange peel residues based biorefinery development towards biolubricants production and biodiesel properties estimation

E. Stylianou[1], K. Zygouraki[1], M. Carmona-Cabello[2], N. Giannakis[1], M.P. Dorado[2] and A. Koutinas[1]

[1]Department of Food Science and Human Nutrition, Agricultural University of Athens, Athens, Greece
[2]Department of Physical Chemistry and Applied Thermodynamics, EPS, Edificio Leonardo da Vinci, Campus de Rabanales, Universidad de Córdoba, Córdoba, Spain
Corresponding author email: elea.stylianou@outlook.com

keywords: *spent coffee grounds; orange peel residues; biorefinery; biolubricants; biodiesel.*

Introduction

The transition from the current fossil-based economy into the bio-economy era necessitates the utilisation of crude renewable resources as sustainable feedstocks for the production of bio-based chemicals, polymers and materials. The sustainable production of such bio-based products requires the development of innovative biorefinery concepts.

Coffee and fruit juices are two of the most popular beverages worldwide (Fereidoon and Cesarettin, 2016). Processing 1 kg soluble coffee generates 2 kg wet spent coffee grounds (SCGs) as biowaste (Battista et al., 2020). In 2020, the total consumption of fruit juice in Europe was estimated at 1.24 billion litres with citrus juice being the predominant one. Besides the orange juice production industry that generates 50-60% of the total mass of citrus fruit as peel waste (Pacheco et al., 2019), significant quantities of orange peel residues (OPR) are also generated by catering services selling orange juice. Many catering services produce both SCGs and OPR. The combined utilisation of SCGs and OPR generated by catering services as renewable feedstocks in novel biorefinery concepts could lead to the production of biofuels and value-added co-products.

The present study focuses on the development of a holistic biorefinery using SCGs and OPR from catering services for the production of microbial oil and value-added co-products. The proposed process involves extraction of coffee oil and antioxidant-rich extract from SCGs and extraction of free sugars and pectin extract from OPR, followed by hydrolysis of glucan and hemicellulose to obtain fermentable sugars. The microbial oil obtained was converted into fatty acid methyl esters (FAMEs) and the biodiesel properties were estimated. Finally, microbial oil production using OPR-SCGs derived hydrolysate was carried out in a 30 L bioreactor using *Lipomyces starkeyi* ATCC 70296. Bioprocess development using microbial oil as raw material for the production of bio-based lubricants in a lipase-catalysed solvent-free system was performed.

Materials and methods

The SCGs and OPR were obtained from local catering companies. After collection, the residues were air dried at 40°C to achieve a moisture content less than 10%. Compositional analysis of raw materials was initially performed, including oil (Soxhlet extraction with hexane), protein (Total Kjeldahl Nitrogen), Total Phenolic Content (TPC) (Folin-Ciocalteu colorimetric method), ash and moisture. Additionally, an extractive-free sample was subjected to analysis of structural carbohydrates and lignin, applying 72% (w/w) H_2SO_4.

A consolidated biorefinery was developed for the extraction of oil and phenolic compounds. Coffee oil was initially extracted from SCGs focused on the extraction of the oil fraction with solvents with different environmental impact, such as ethyl acetate and hexane. Following that, the extraction of phenolic compounds was performed by ultrasound-assisted extraction with 70% (v/v) aqueous ethanol solution at different solid-to-solvent ratios. OPR were treated for free sugars aqueous extraction and acid treatment for pectin extraction. Crude hydrolysate of a ratio of OPR-SCGs of 1:4 (w/w) residual solids were prepared with a consortium of commercial enzymes. The hydrolysate and the free sugars were used as fermentation feedstock for microbial oil production using *Lipomyces starkeyi* ATCC 70296.

The biodiesel properties were calculated based on the FAMEs profiles of microbial oil. The extracted microbial oil was enzymatically hydrolysed and the FAMEs were esterified enzymatically in a solvent-free

system with trimethylolpropane (TMP) and neopentyl glycol (NPG). Different esterification conditions were evaluated (i.e. substrate to molar ratio, enzyme concentration and temperature).

Results and discussion

SCGs contain lipids (12.2%), hemicellulose (28.9%), lignin (28.1%), glucan (10.6%), protein (14.8%) and phenolics (0.9%), while OPR contain free sugars (31.3%), protein (6.5%), glucan (25.3%), hemicellulose (5.3), lignin (5.4%), phenolics (1.0%), oil (2.1%) and pectin (17.6%). The SCGs were treated with hexane for 97.8% lipid recovery, while 96.9% lipid recovery was achieved with ethyl acetate. Aqueous ethanol was used for phenolics extraction. Free sugars were aqueous extracted from OPR. More than 90% of the total free sugars were obtained in the first extraction. The individual sugars were sucrose (28.9%), glucose (37.6%) and fructose (33.5%).

The SCGs and OPR solids remaining after extraction of all value-added components were subjected to enzymatic hydrolysis to obtain a sugar-rich hydrolysate for microbial oil production. The OPR-SCGs hydrolysate contained 29.1 g/L total sugars, of which 15.1 g/L was glucose, corresponding to a glucan hydrolysis yield of 71.7%.

A scale-up of the bioprocess was efficiently demonstrated in a 30 L semi-pilot bioreactor using OPR-SCGs hydrolysate with free sugars as feeding solution. Microbial oil production reached 52 g/L with a productivity of 0.32 g/(L·h) and yield of 0.20 g/g. Biomass production reached 91.7 g/L, corresponding to an intracellular lipid accumulation of 56.7%. The concentration of free amino nitrogen decreased from 302 mg/L to 12.1 mg/L after 46.5 h when lipid accumulation was triggered. Fatty acid methyl esters (FAMEs) were analysed at the early and the late growth stage of the culture. The microbial lipids produced by *Lipomyces starkeyi* ATCC 70296 mainly contained oleic acid ($^{\Delta 9}$C18:1) followed by palmitic acid (C16:0), linoleic acid ($^{\Delta 9,12}$C18:2) and stearic acid (C18:0).

The biodiesel properties (e.g., cetane number, low calorific value, Cold filter plugging point) were calculated based on the FAMEs profiles of microbial oil obtained, showed that they generally conformed with the limits set by European standards. The microbial oil of *Lipomyces starkeyi* ATCC 70296, derived via fermentation was used as a raw material together with NPG and TMP for polyol esters production. The production of biolubricants was monitored during enzymatic reaction by recording the reduction of the acidity caused by the esterification of free fatty acids. The highest conversion yield was achieved in the case of NPG-esters (81%) than TMP esters after 24 h.

Conclusions

This study has shown that fractionation of various value-added fractions and bioconversion of SCGs and OPR from the catering services sector will provide additional revenue for the biotechnological production of microbial oil. The process has been successfully implemented on a larger scale, suggesting that OPR-SCGs hydrolysate can be efficiently used for microbial oil production and subsequent biolubricant production. The microbial oil could be efficiently used for biodiesel production.

Acknowledgements: This work was supported by the project "Production of sustainable biofuels and value added products from municipal organic solid wastes of catering services - Brew2Bio" (MIS5071807) which is implemented under the Action "Research - Create - Innovate", funded by the Operational Programme "Competitiveness, Entrepreneurship and Innovation" (NSRF 2014-2020) and co-financed by Greece and the European Union (European Regional Development Fund).

References

Battista, F., Barampouti, E.M., Mai, S., Bolzonella, D., Malamis, D., Moustakas, K., Loizidou, M., 2020. Added-value molecules recovery and biofuels production from spent coffee grounds. Renew. Sustain. Energy Rev. 131, 110007. https://doi.org/10.1016/J.RSER.2020.110007

Fereidoon, S., Cesarettin, A., 2016. Handbook of Functional Beverages and Human Health, Handbook of Functional Beverages and Human Health. https://doi.org/10.1201/b19490

Pacheco, M.T., Moreno, F.J., Villamiel, M., 2019. Chemical and physicochemical characterization of orange by-products derived from industry. J. Sci. Food Agric. 99, 868–876. https://doi.org/10.1002/jsfa.9257 .

Hydrogen gas generation by anaerobic oxidation of metallic iron Fe^0 or scrap iron under low-temperature carbonates conditions and the role of citric acid

D. Constantinou[1] and I. Vyrides[1]

[1]Department of Chemical Engineering, Cyprus University of Technology, Limassol, Cyprus
Corresponding author email: ioannis.vyrides@cut.ac.cy

keywords: *hydrogen gas; scrap iron; siderite; weak acids; CO_2 utilization.*

Introduction

Hydrogen (H_2) exhibits remarkable potential as an environmentally friendly fuel source, mainly due to its high energy density (140 MJ/kg), and its characteristic of produce zero carbon emissions during combustion. Nearly 96% of H_2 is produced from non-renewable sources (e.g. coal, natural gas, etc.) and the remaining 4% by water electrolysis (Yukesh Kannah et al., 2021). Meanwhile, researchers have studied the oxidation of metallic iron or zero-valent iron (Fe^0) in the presence of carbon dioxide for the purpose of hydrogen generation, mainly at high temperatures (Jin et al., 2011; Michiels et al., 2015). The current work points out a new perspective on CO_2 sequestration and H_2 gas generation in an anaerobic system of either zero-valent iron (Fe^0) or scrap iron along with $NaHCO_3$ and citric acid in low temperature (33 °C). Carbonate ions create a passivation layer on the outer surface of Fe^0, called siderite ($FeCO_3$), that entrapped Fe^0 and hindered H_2 production. By comparing citric, oxalic, and ascorbic acids for their ability to remove the siderite layer, citric acid was found to be the most effective (Constantinou et al., 2023).

Materials and methods

Batch laboratory experiments were carried out to investigate the reaction rate of the system at various concentrations of Fe^0 (10 μm) and bicarbonate solution (as CO_2 source). Moreover, the process of anaerobic corrosion of Fe^0 was examined at several temperatures in the range of T = 4- 50 °C. Weak acids (citric, oxalic, and ascorbic acid) in two different concentrations 0.5 and 1 M have been assessed for their ability to dissolve the passivation layer. Scrap iron and Fe^0 were added separately to $NaHCO_3$ and citric acid (3:1 and 2:1) solution for H_2 generation. The experiment was conducted for seven consecutive cycles.

The gas phase constituents were identified and quantified over time by gas chromatography method. Fe^{2+} and Fe^{3+} were measured based on ferrozine method. XRD analysis was performed to identify the passive layer.

Results and discussion

The reaction rate of the system was 0.75 order with respect to Fe^0, 0.65 order with respect to HCO_3^- and 1.4 order overall. The activation energy was calculated to be 45.4 kJ/mol at the temperature range of 4 – 50 °C. Micro-size Fe^0 (5–40 g/L) at bicarbonate conditions is oxidized at mild anaerobic conditions, generating hydrogen gas with a production rate in the range of 0.09–0.55 $g(H_2)/kg(Fe^0)\cdot h$. Fe^0 in the presence of $NaHCO_3$/citric acid (3:1) solution, releases up to 95.2 vol% and 68.5 vol% H_2 at the end of the 5th and 6th cycles, respectively, whereas Fe^0 with only $NaHCO_3$ produces 48.9 vol% and 25.4 vol% H_2. In a system of scrap iron, along with $NaHCO_3$/citric acid (2:1) solution, it was found that by replacing the media solution with a new media ($NaHCO_3$/citric acid) after the end of each cycle resulted in higher than 85 vol% H_2 after one day of exposure and higher than 94 vol% H_2 at the end of each cycle (Figure 1).

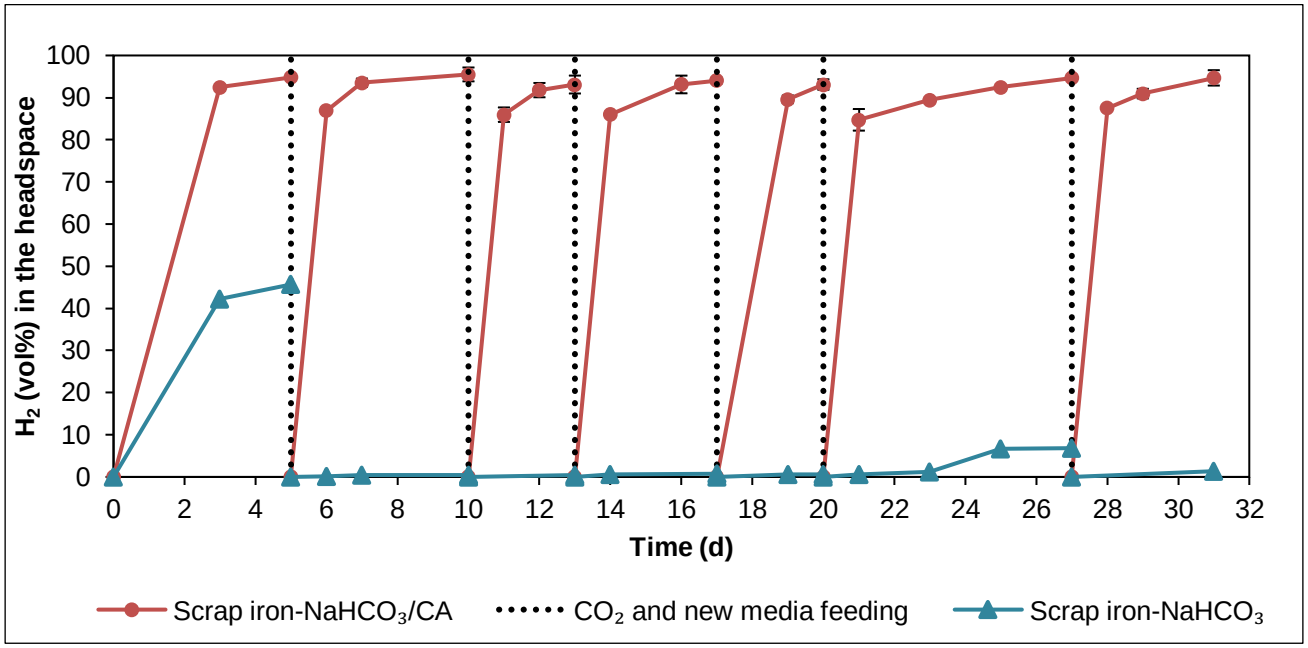

Figure 1. *H_2 (vol%) in the headspace over time.*

Conclusions

Hydrogen gas can be produced through a redox reaction between zero-valent iron and $NaHCO_3$. The presence of citric acid prevents the formation of the passivation layer and improves hydrogen generation. Further research will focus on the redox reaction between Fe^0 or scrap iron and organic waste materials for H_2 production.

Acknowledgements: This study is supported by the Research Promotion Foundation (RPF) (Cyprus) under the project CONCEPT-HYDRO/0421/0014 "IroNGaSweetening".

References

Yukesh Kannah, R., Kavitha, S., Preethi, Parthiba Karthikeyan, O., Kumar, G., Dai-Viet, N. Vo. and Rajesh Banu, J., 2021. Techno-economic assessment of various hydrogen production methods – A review. *Bioresource Technology,* 319, 124175.

Fangming, J., Ying, G., Jin, Y., Zhang, Y., Cao, J., Wei, Z. and Smith, Richard L., 2011. High-yield reduction of carbon dioxide into formic acid by zero-valent metal/metal oxide redox cycles. *Energy Environ. Sci., 4, 881-884.*

Michiels, K., Spooren, J. and Meynen, V., 2015. Production of hydrogen gas from water by the oxidation of metallic iron under mild hydrothermal conditions, assisted by *in situ* formed carbonate ions. *Fuel.,* 160, 205-216.

Constantinou, D., Samanides, G. C., Koutsokeras, L., Constantinides, G. and Vyrides, I., 2023. Hydrogen generation by soluble CO2 reaction with zero-valent iron or scrap iron and the role of weak acids for controlling FeCO3 formation. *Sustain. Energy Technol. Assess.,* 56, 103061.

In situ hydrogen peroxide (H_2O_2) production in carbonaceous electrodes with different interfacial properties

P. Petsi[1,2], K. Plakas[1], Z. Frontistis[2] and A. Karabelas[1]

[1] Chemical Process and Energy Resources Institute, Centre for Research and Technology-Hellas, Thessaloniki, Greece
[2]Department of Chemical Engineering, University of Western Macedonia, Kozani, Greece
Corresponding author email: petsi@certh.gr

keywords: *Gas Diffusion Electrode; Activated Carbon Fiber; flow by electrochemical reactor; contact angle; pore size.*

Introduction

H_2O_2 is a very important and common chemical, which is widely used in daily life and industry (Dong et al., 2020). Until nowadays, approximately 95% of total H_2O_2 industrial production is based on the Anthraquinone Oxidation (AO) process. This process has many disadvantages concerning the costs of operation (use of noble metals), transport and storage, whereas special handling is needed for highly concentrated H_2O_2 solutions (Campos-Martin et al., 2006). The in situ electrogeneration of H_2O_2 is an alternative solution, where the H_2O_2 is produced at the cathode according to the $2e^-$ pathway Oxygen Reduction Reaction ($2e^-$ ORR) (Reaction 1) (Bard al., 1974):

$$O_2 + 2e^- + 2H^+ \rightarrow H_2O_2 \qquad \text{(Reaction 1)}$$

The cathode material is very important and it should be an inexpensive material with high electrical conductivity, high selectivity to the $2e^-$ ORR and high stability. The carbonaceous materials are considered as the optimum candidate for the electogeneration of H_2O_2. A variety of carbonaceous materials has been studied in literature; Reticulated Vitreous Carbons (RVC), Graphite, Gas Diffusion Electrodes (GDE), etc. The scope of this work is to investigate the H_2O_2 electrogeneration performance of three carbonaceous electrodes with different interfacial properties. Firstly an optimization regarding the operational conditions is conducted and afterwards their performance is tested in saturated with O_2 electrolyte solution and in continuous air flow conditions.

Materials and methods

Experiments were conducted with the aid of a flow by electrochemical cell (see fig. 1b) with 0.001 m^2 cathode surface, supplied by ElectroCell A/S (Denmark). Three different cathode materials were used, Activated Carbon Fiber (ACF) purchased from SO-EN CO., Ltd (Japan), Non Activated Carbon Fiber supplied by MAST Carbon International, Ltd (UK) and a GDE supplied by Gaskatel GmbH (Germany). The H_2O_2 was determined by using KI and measuring the absorption at the 305 nm with the use of UV-Vis spectrophotometer. The specific surface area and the pore sizes were obtained through Brunauer–Emmett–Teller (BET) method and the N_2 adsorption isotherms, respectively and the hydrophobicity was determined with the aid of a contact angle goniometer.

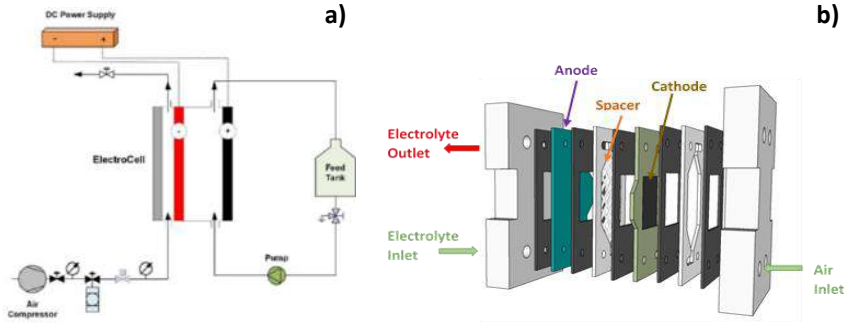

Figure 1. *a) Flow chart of the experimental set up b) schematic illustration of the electrochemical reactor.*

Results and discussion

Figure 2 shows the H_2O_2 concentrations obtained by experiments with initially saturated with O_2 electrolyte solutions (Figure 2a) and experiments with continuous air supply (Figure 2b) under the near optimum operating conditions (current density, inlet velocity and pH) for each electrode. The non ACF electrode showed the optimum H_2O_2 (appx. 4 mg/L) production compare to the other two electrodes for saturated with O_2 electrolyte. According to contact angle analysis, the hydrophilicity sequence from the more hydrophilic electrode is Non ACF>GDE>ACF. When the electrode is hydrophilic the dissolved O_2 of the electrolyte can penetrate the body of the electrode and as a result it can reach more active sites (Sheng et al., 2011). In the second case, where air is continuously applied at the back side of the electrode, the electrodes showed totally different behavior. By comparing the Non ACF and ACF performances the latter exhibited higher H_2O_2 productivity. According to SEM and pore size analyses both electrodes had similar structure however, the latter is more hydrophobic. In this case hydrophobicity promoted the diffusion of the gaseous O_2 molecules within the body of the electrode. The higher H_2O_2 electrogeneration was observed in the case of the GDE (appx. 45 mg/L), which has mediate hydrophobicity but also belongs to mesoporous materials (2-30nm), hence its properties enhance the Three Phase Boundary (TPB) phenomenon.

Table 1. *Electrodes characterization results*

Cathode electrode	*Bet surface (m^2/g)*	*Pore size (nm)*	*Contact Angle (°)*
Activated Carbon Fibre (ACF)	1129	1.62	119.20
Non Activated Carbon Fibre (Non ACF)	763	1.64	96.65
Gas Diffusion Electrode-Ni	11	31.56	100.30

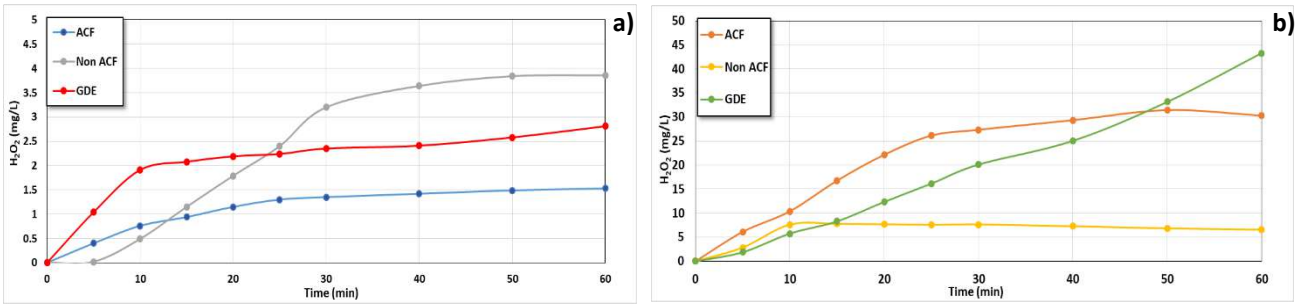

Figure 2. *H_2O_2 electrogeneration of the ACF, Non ACF and GDE electrodes with a) initially saturated with O_2 electrolyte and b) continuous air supply.*

Conclusions

The general conclusion is that the continuous air supply improves the H_2O_2 electrogeneration in all cases, however the interfacial properties play a crucial role in the performance of the electrodes. The higher H_2O_2 concentration measured was appx. 45 mg/L and was achieved by the GDE under continuous air supply and after 60 min of operation. According to the characterization of the electrodes hydrophilic/hydrophobic character of the electrode is an important parameter, nevertheless other characteristics like the pore size and the specific surface area should be considered.

References

Dong K., Lei Y., Zhao H., Liang J., Ding P., Liu Q., Xu Z., Lu S., Li Q., Sun X., 2020. Noble-metal-free electrocatalysts toward H_2O_2 production. J. Mater. Chem. A 8, 23123–23141.

Campos-Martin J. M., Blanco-Brieva G., Fierro J. L., 2006. Hydrogen peroxide synthesis: an outlook beyond the anthraquinone process. Angewandte Chemie International Edition. 45(42), 6962-6984.

Bard, A. J., and Ketelaar, J. A. A., 1974. Encyclopedia of Electrochemistry of the Elements. Journal of the Electrochemical Society, 121(6), 212C.

Sheng, Y., Song, S., Wang, X., Song, L., Wang, C., Sun, H., & Niu, X., 2011. Electrogeneration of hydrogen peroxide on a novel highly effective acetylene black-PTFE cathode with PTFE film. Electrochimica Acta, 56(24), 8651-8656.

Biosolids gasification: state-of-the-art and industrial-scale application at the WWTP of Rethymno

A. Manali, A. Pothoulaki, K. Tsamoutsoglou and P. Gikas

Design of Environmental Processes Laboratory, School of Chemical and Environmental Engineering, Technical University of Crete, Chania, Greece
Corresponding author email: pgikas@tuc.gr

keywords: *biosolids; gasification; energy production; wastewater treatment.*

State-of-the-art

Thermal and electric energy can be produced from biosolids through thermochemical processes, which transform them into valuable products and recover a significant amount of their internal energy. One of the most efficient thermochemical biosolids treatment technologies is gasification, which turns solid carbonaceous materials into a combustible gas (syngas) (Sansaniwal et al., 2017). Gasification process does not require large amounts of fuel, while in parallel produces small amounts of hazardous by-products. The biomass is partially burned due to insufficient air/fuel ratios for stoichiometric combustion, producing CO, H_2, H_2O, CH_4, N_2, O_2, and higher hydrocarbons. Gasification offers numerous advantages that make it a viable biosolids treatment method, such as high-efficiency energy recovery, energetic self-sufficiency, and zero-waste material-producing energy (Gao et al., 2020).

Gasification can be classified into different categories based on its agent (air, steam, and oxygen) and enthalpy (endothermic or exothermic). Numerous factors (temperature, feedstock type, equivalence ratio - ER, etc.) affect the process, as well as the nature and volume of the end-gases. Typically, the process's temperature ranges from 750°C to 1100°C. To reduce the moisture content, the feedstock -in this case, biosolids- requires drying beforehand. Regarding the ER, an increase of it accelerates the oxidation reaction and enhances the production of the produced syngas (Khan et al., 2021).

Syngas mainly consists of H_2 and CO, but it also contains small amounts of CO_2, N_2, water vapor, and various light hydrocarbons. The impurities in the feedstock and the method used to produce the syngas have a significant impact on the quantities of its contaminants, which can vary greatly. Cleaning of syngas before use is necessary as it contains undesirable by-products -i.e., tar, particulate matter, and inorganic substances (alkali metals, nitrogen, sulfur, and chlorine compounds)- and falls short of ideal syngas characteristics (high purity, high calorific value, low tar content, and absence of potentially harmful elements). According to the gas temperature at the cleanup equipment's exit, the syngas cleaning methods are divided into three categories: cold, hot, and warm. The most established method for cleaning syngas is the cold route, which uses water/liquid absorption through a variety of scrubbing equipment, and success to remove almost all syngas impurities. The hot route is a new strategy with improved total energy efficiency, as there is no need to cool or reheat the gas. Finally, warm cleaning technologies work in temperatures between cold and hot, giving the chance to avoid both of their downsides (Woolcock and Brown, 2013).

Application of microsieved biosolids gasification at the WWTP of Rethymno

The Design of Environmental Processes Laboratory, School of Chemical and Environmental Engineering, Technical University of Crete is currently coordinating the "LIFE B2E4sustainable-WWTP" project, in the framework of which an innovative industrial-scale (capacity of 5,000m^3/d of incoming wastewater) biosolids management pilot plant has been installed at the WWTP of Rethymno, Crete, Greece. Initially, pre-treated wastewater passes through a microsieve (for the removal of biosolids upstream of the aeration tank) and through a dryer (for moisture removal). Then, the biosolids are gasified producing syngas, which is combusted in a cogeneration engine producing thermal and electric energy.

The gasification system consists of the following components: (i) the feeding system, which connects the dryer to the gasifier and provides dried and microsieved biosolids (having 10-15% moisture, which is the ideal proportion for this specific gasification process), (ii) a storage tank followed by a briquetting machine

(required for the proper operation of a downdraft gasifier, which needs the production of a porous bed), and (iii) a downdraft gasifier fitted with an air supply ejector. The gasifier is made up of drying-pyrolysis-combustion-reduction zones and an ash pit (for removing ash without interfering with the gasification process). After the gasification system, the syngas treatment apparatus follows, consisting of a cyclone (for the removal of solid particles and tar), a straight tube heat exchanger (for syngas cooling), a granular biomass filter (for the removal of solid particles and tar) along with a combustion flare (for the combustion of excess/unsuitable syngas) and a scrubber (for the removal of sulfur, chlorine, ammonia, and tar). Also, the system is equipped with a syngas analyzer and a flowmeter to record the composition and flow rate for the treated syngas. Finally, there is a co-generation engine for syngas combustion and energy production (Figure 1).

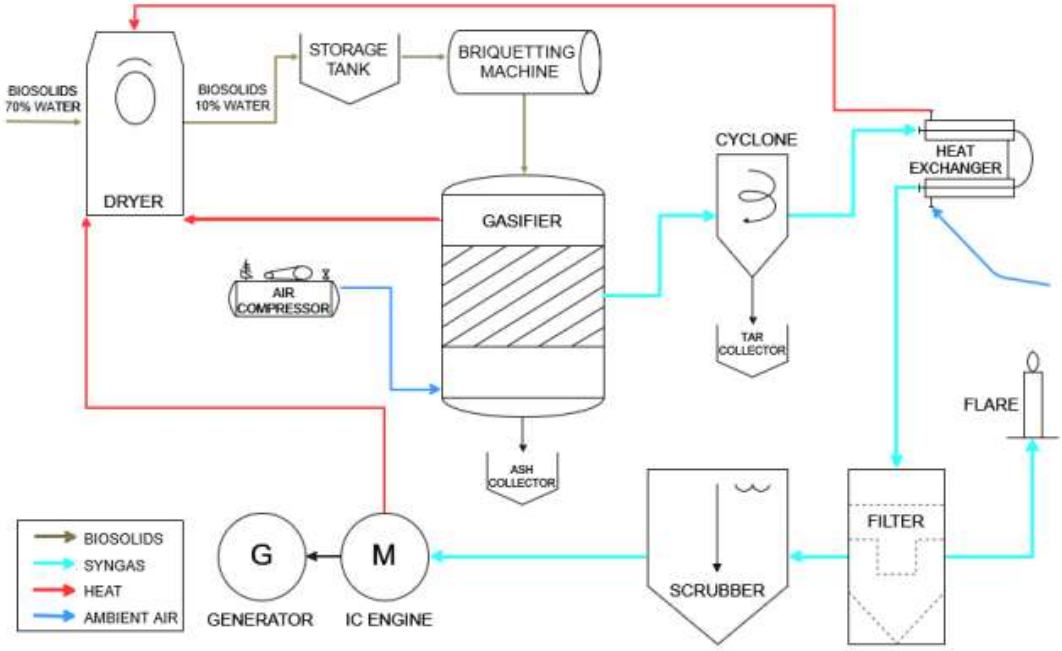

Figure 1. *Process flow diagram for the energy-producing drying and gasification of microsieved biosolids.*

Expected results - Conclusions

Microsieved biosolids with a 70 % moisture content are produced at a rate of 38.3 kg/h. For the drying of the biosolids (from a moisture level of 70 % to 10 %), about 20 kWh are required. The gasification-energy generation system is anticipated to provide the dryer with significantly more energy (about 34 kWh), but the dryer's estimated actual energy requirements are expected to be in the same ballpark as the thermal power source.

Acknowledgements: This study is supported by the Green Fund and the LIFE project (EC): "New concept for energy self-sustainable wastewater treatment process and biosolids management (LIFE B2E4sustainable-WWTP)", LIFE16 ENV/GR/000298.

References

Gao, N., Kamran, K., Quan, C., Williams, P.T., 2020. Thermochemical conversion of sewage sludge: A critical review. Prog Energy Combust Sci.

Khan, M.A., Naqvi, S.R., Taqvi, S.A.A., Shahbaz, M., Ali, I., Mehran, M.T., Khoja, A.H., Juchelková, D., 2021. Air gasification of high-ash sewage sludge for hydrogen production: Experimental, sensitivity and predictive analysis. Int J Hydrogen Energy.

Sansaniwal, S.K., Rosen, M.A., Tyagi, S.K., 2017. Global challenges in the sustainable development of biomass gasification: An overview. Renewable and Sustainable Energy Reviews 80, 23–43.

Woolcock, P.J., Brown, R.C., 2013. A review of cleaning technologies for biomass-derived syngas. Biomass Bioenergy 52, 54–84.

SUST ENG 2023

NANOMATERIALS

Solution Processed Perovskite Nanocrystal Photovoltaics

F. Galatopoulos [1*], P. Papagiorgis [2], A. Ioakeimids [1], C. Christodoulou [1], A. Chrusou [1], E. Charalambous[2], A. Manoli[2], C. Bernasconi[3], M.I. Bodnarchuk[4], M. V. Kovalenko[3,4], G. Itskos[2] and S.A. Choulis[1*]

[1] Molecular Electronics and Photonics Research Unit, Department of Mechanical Engineering and Materials Science and Engineering, Cyprus University of Technology, Limassol, Cyprus.
[2] Department of Physics, Experimental Condensed Matter Physics Laboratory, University of Cyprus, Nicosia, Cyprus.
[3] Institute of Inorganic Chemistry, Department of Chemistry and Applied Biosciences, ETH Zürich, Zürich, Switzerland
[4] Laboratory for Thin Films and Photovoltaics, Empa – Swiss Federal Laboratories for Materials Science and Technology, Dübendorf, Switzerland.
* Corresponding Authors: fedros.galatopoulos@cut.ac.cy, stelios.choulis@cut.ac.cy

keywords: photovoltaics; nanocrystals perovskite solar cells; processing; solar cell characterization.

Introduction

In recent years, perovskite nanocrystals (PNCs) have attracted research interest for various optoelectronic applications that include light emitting diodes (LEDs) and solar cells [1]. Several inherent material properties are desirable for both applications such as high photoluminescence quantum yield (PLQY), strong light absorption as well as the minimization of radiative recombination losses [2], importantly, PNCs show relatively high defect tolerance and tunability of the band gap by controlling the size and composition of the nanocrystals [3]. The presentation will discuss the processing conditions and device performance of PNC SCs.

Materials and methods

Device fabrication: The TiO_2 films were coated in prepatterned ITO substrates using spin coating at 3000 rpm for 20s in ambient atmosphere. The substrates were then annealed at 115 °C for 30 minutes on a hotplate followed by 450 °C for another 30 minutes. The substrates were then transferred inside a GB in order to coat the $FAPBI_3$ films. The $FAPBI_3$ films were coated using spin coating at 1000 rpm for 60s followed by a drying step at 4000 rpm for 20s. A ligand washing (LW) procedure was followed and after that a Spiro-MeOTAD film was coated in the GB using spin coating at 4000 rpm for 30s. Finally, thermal evaporation of MoO_3 and Al was used to achieve a thickness of 15 nm and 200 nm respectively. (0.1 A/s for MoO_3 and 2 A/s for Al).

Results and discussion

Full devices based on the structure ITO/TiO_2/$FAPbI_3$/spiro-MeOTAD/MoO_3/Al were characterized in order to optimize the PV performance and identify the main limitations for such devices. The significance of the LW step is displayed in Figure 1.a). By utilizing a pristine active layer in the device structure, we see barely functional PV devices. Thus, we introduced a range of LW procedures to optimize the removal of oleic acid and improve the charge transport in the device. The optimized LW process improved the J_{SC} from 2.70 to 5.45 mA/cm^2 while the V_{OC} drop was marginal, resulting in an improvement to PCE from 0.83 to 1.93 %.

Table 1. PV parameters of PNC SCs utilizing different LW conditions

Treatment type	V_{OC} (V)	J_{SC} (mA/cm^2)	FF (%)	PCE (%)
10s LW	0.90	2.70	34.2	0.83
20s LW	0.60	3.33	44.7	0.89
10s Dual process LW	0.88	5.45	40.4	1.93

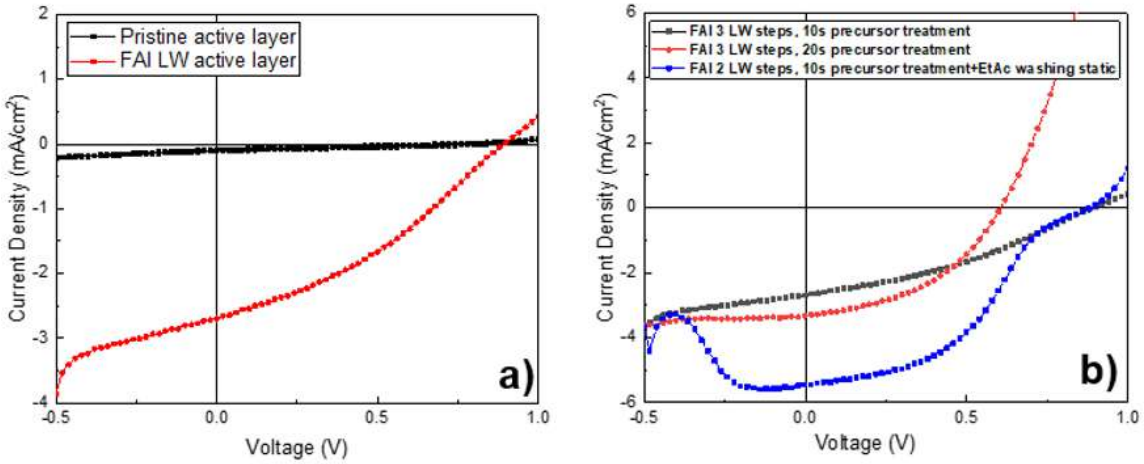

Figure 1. Illuminated J/V characteristics of: a) pristine and FAI LW active layer, b) FAI LW active layer in various precursor treatments

Conclusions

We have shown that a ligand washing (LW) step is essential in order to obtain optimum PV performance. The oleic acid ligands need to be removed due to their insulating nature. By optimizing the LW procedure we will present solution processed perovskite nanocrystal photovoltaics with a PCE of 1.93 %

Acknowledgements: This work was financially supported by the Research and Innovation Foundation of Cyprus under the "NEW STRATEGIC INFRASTRUCTURE UNITS-YOUNG SCIENTISTS" Programme (Grant Agreement No. "INFRASTRUCTURES/1216/0004", Acronym "NANOSONICS")

References

Yuan, J. *et al.* Metal Halide Perovskites in Quantum Dot Solar Cells: Progress and Prospects. *Joule* **4**, 1160–1185 (2020).

Protesescu, L. *et al.* Nanocrystals of Cesium Lead Halide Perovskites (CsPbX 3, X = Cl, Br, and I): Novel Optoelectronic Materials Showing Bright Emission with Wide Color Gamut. *Nano Lett.* **15**, 3692–3696 (2015).

Song, J. *et al.* Quantum Dot Light-Emitting Diodes Based on Inorganic Perovskite Cesium Lead Halides (CsPbX 3). *Adv. Mater.* **27**, 7162–7167 (2015).

Metal nanoparticles as pesticide alternatives

A. Malandrakis[1]*, N. Kavroulakis[2] and C. Chrysikopoulos[3,1]

[1]School of Environmental Engineering, Technical University of Crete, Chania, Greece
[2]Hellenic Agricultural Organization "Demeter", Institute for Olive Tree, Subtropical Plants and Viticulture, Agrokipio-Souda, Chania, Greece
[3]Department of Civil Infrastructure and Environmental Engineering, Khalifa University of Science and Technology, Abu Dhabi, UAE
Corresponding author email: amalandrakis@tuc.gr

Abstract
Pesticides have provided the means for sustainable food production for decades, being the driving force of the so-called "Green Revolution" together with the use of new varieties and fertilizers. This resulted in a significant increase in yield and quality of crops but came with a price: high environmental footprints, toxic effects to non-target organisms, and the emergence of pesticide resistance. High environmental risks by the misuse of pesticides highlight the need for the development of more eco-friendly pesticide alternatives that could alleviate the drawbacks of synthetic chemicals and be effective against sensitive and resistant pests. Nanotechnology could be the answer for such a challenge by providing novel agents for controlling pests. Metal nanoparticles (MNPs), due to their unique physico-chemical properties can control a number of pests and counter pesticide resistance. In this study, we aimed to investigate the: (a) the effectiveness of various metal NPs against plant pathogens, (b) the potential synergy between pesticides and MNPS and (c) the effect of MNPs on beneficial symbiotic microorganisms.

High Mechanical Strength Carbon Nanofibers Fabrication: A Comparative Study of Biomass Electrospun Nanofibers and CVD Synthesized Nanofibers Over Nickel Decorated RANR

F. Dziike[1], T. D. Ntuli[2] and O. A. Olagunju[1]

[1]Technology Transfer and Innovation Directorate, Open House, Steve Biko Campus Durban University of Technology, Durban, South Africa
[2]DST-NRF Centre of Excellence in Strong Materials and Materials Physics Research Institute, School of Chemistry, University of the Witwatersrand, Johannesburg, South Africa
Corresponding author email: FaraiD1@dut.ac.za

keywords: *Nano fibres; electro spinning; nanoparticles; nanofibrous; electro spraying.*

Introduction

Fabrication of carbon nano fibres using waste biomass electro spinning technique was contrasted to the catalytic vapour deposition method over nickel decorated radially aligned nanoparticles. Preparation of the supported catalyst was successfully done by loading Ni nanoparticles onto radially aligned nanoparticles (RANR) support using the deposition-precipitation using urea (DPU) method. The biomass electro spinning technique is non-catalytic and has simple material preparation for use in the technical mechanism. The effectiveness of the Ni/RANR as a catalyst is due to the success of DPU method of catalyst preparation that proliferates formation of Ni particles of homogeneous particle size distribution on the RANR nano rods and hence a close interaction with the RANR support. The efficacy of biomass electro spinning gives provision for internal access of the set-up parameters such as solvent and the method of fibre collection that consequentially improves the intrinsic control of the construction mechanism of the final nanofibrous architecture. It was observed that some of the twisted CNFs were formed by the crossing of two primary coils which grew in the same direction from a diamond-like or polyhedral-shaped Ni particle

Materials and methods

Preparation procedure for the Ni catalysts supported on RANR was via a hydrothermal method carried out at 200 °C. $Ni(NO_3)_2{\cdot}6H_2O$ and $TiCl_4$ were precursor materials and (DPU) was used to load the Ni metal onto RANR. The DPU method was used to make Ni/TiO_2 as described in previous studies.

Twisted CNFs were prepared in a horizontal quartz tube reactor in which 0.5 g of the Ni/RANR catalyst was placed in a quartz boat positioned at the centre of the furnace

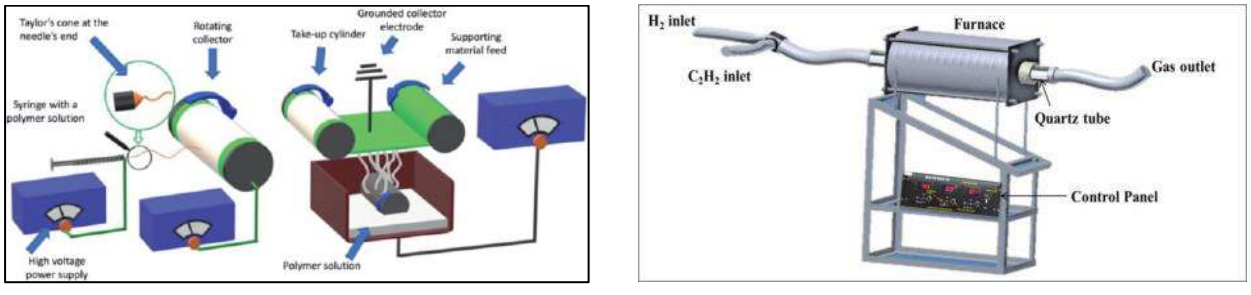

Fig. 1. Schematic drawing of the Electrospinning and CVD set-up for the preparation of CNMs.

A needleless mechanism performs the electrospinning of the polymer solution from the surface of a revolving roller. The roller is partially immersed in a tank containing material to be electrospun, as shown in Figure 1. On the roller's surface, a layer of consistently new material is generated by a rotating roller

Results and discussion

The fibrous nanostructures in Fig. 3 were prepared through manipulation of many experimental parameters of a multifluid electrospinning process. This is an innovative shift from the traditional single-fluid blending electrospinning process. However, there were difficulties in using multifluid processes. This include compatibility concerns of set up parameters including fluids, rate of stock feed and average proportions, interfacial tensions, and electrospinning sustainability influencing the shape of the CNMs formed.

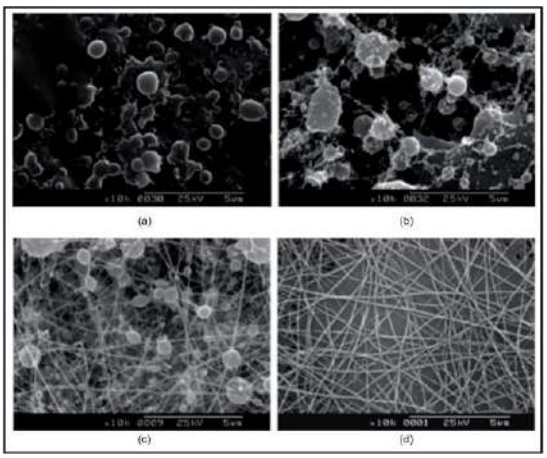

Fig. 3. SEM micrographs of electrospun SF nanofibers with concentration of (a) 3%, (b) 6%, (c) 9%, and (d) 12%

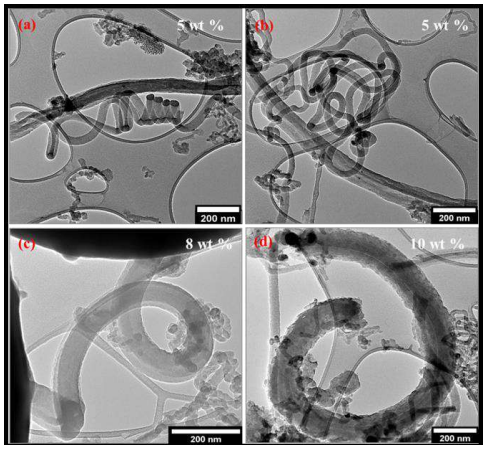

Fig. 4 TEM micrographs of CNFs synthesised at 600 °C, 1 h, 75 mL min^{-1} (a) and (b), 5 wt. % Ni/RANR (c) 8 wt. % Ni/RANR (d) 10 wt. % Ni/RANR

The thickness of the fibres is proportional to the diameter of the Ni nanoparticle over which it grows (Fig. 4). However, varying wt. % loading did not affect the particle size distribution on the support but particle density as proved by narrow particle size ranges across the entire wt. % loading.

Conclusions

The growth of fibres is consistent over a set of conditions required to achieve uniform coverage. Time variation has a direct effect on the degree of graphitisation in the CNFs prepared by CVD synthesis method and hence the mechanical strength of the synthesized CNFs. It can be concluded that the longer the time in the CVD production, the more graphitic are the CNFs. However, in electrospinning, The molecular flow in the spinning process, as well as the molecular direction in nanofibers, can be tailored to advance the electronic, and physico-chemical properties of nanofibrous materials.

Acknowledgements: This study is supported by the NRF, the University of Witwatersrand and the DST-NRF Centre of Excellence in Strong Materials for financial support. The funding was provided by the Durban University of Technology NRF grant hosted in the DUT Research and Postgraduate Support Directorate.

References

Su, D. S., Perathoner, S. & Centi, G. Nanocarbons for the Development of Advanced Catalysts. (2016).

Lu, M., Lau, K. T., Xu, J. C. & Li, H. L. Coiled carbon nanotubes growth and DSC study in epoxy-based composites. Colloids Surfaces A Physicochem. Eng. Asp. 257–258, 339–343 (2005).

Du, Jin Hong, SU Ge, BAI Shuo, S. C. and C. H. Solid catalytic growth mechanism of micro-coiled fibres. Sci. China 44, 5–10 (2001).

Mini-review NEA, Liu M, Cai N, Chan V, Yu F. Development and applications of mofs derivative onedimensional development and applications of mofs derivative one-dimensional nanofibers via electrospinning: A minireview. Nanomaterials. 2019;9:1-21. DOI: 10.3390/nano9091306

Dias JR, Granja PL, Bártolo PJ. Advances in electrospun skin substitutes. Progress in Materials Science. 2016;84:314-334

Sasmazel H, Ozkan O. Advances in electrospinning of nanofibers and their biomedical applications. Current Tissue Engineering. 2013;2:91-108. DOI: 10.2174/22115420113029990007

Fabrication of Ceramic Composite Films for Solid Oxide Electrochemical Cells(SOEC) by Solution Spray Pyrolysis(SSP)

C. Ziazias[1], C. Matsouka[2], C. Tsanaktsidis[1] and N.E. Kiratzis[3]

[1] Department of Chemical Engineering /School of Engineering, University of Western Macedonia, ZEP, Kozani, Greece
[2] Chemical Process and Energy Resources Institute-CPERI / Centre for Research and Technology Hellas-CERTH, Thermi, Thessaloniki, Greece
[3] Department of Mineral Resources Engineering /School of Engineering, University of Western Macedonia, Kila, Kozani, Greece
Corresponding author email: nkiratzis@uowm.gr

keywords: *Solid Oxide Electrochemical Cell; Spray Pyrolysis; Ceramic Films; Ceramic Composites; Electrodes.*

Introduction

Low electrodic polarization resistances in Solid Oxide Cells (SOC) operating either as Fuel (SOFC) or Electrolyzer Cells i.e. SOEC) are always desirable in order to assure high performance and low degradation rates. This is also important in the case of operation of a reversible solid oxide cell (RSOC) (i.e. the same device operating either in a Fuel Cell or Electrolyzer mode).

With respect to the oxygen or air electrode based on a typical $Zr_{0.84}Y_{0.16}O_{1.92}$ (YSZ16) electrolyte, composites of $La_{0.75}Sr_{0.25}MnO_3$ (LSM)-YSZ are ubiquitously used due to the thermodynamic stability of LSM. Alternatively, Sr substituted $LaFeO_{3-\delta}$ (LSF) constitutes an interesting material for a cathodic electrode in a SOFC due to its mixed conductivity mode (i.e. electronic and ionic) and good electrocatalytic activity for oxygen reduction. In the case of LSF, interfaces with the electrolyte $Ce_{0.9}Gd_{0.1}O_{1.95}$ (CGO10) instead of direct contact with YSZ due to the accompanying reactions with YSZ at high sintering temperatures.

The technique of solution spray pyrolysis (SSP) offers an attractive method of producing thin films of electrodes and electrolytes due to its simplicity, low cost and potential for industrial large scale application. In the present communication, we focus on the cathodic interface by fabricating composites of LSM-$Zr_{0.92}Y_{0.08}O_{1.96}$(YSZ8) on dense YSZ (i.e. $Zr_{0.84}Y_{0.16}O_{1.92}$) substrates by SSP. Alternatively, films of composites of $La_{1-x}Sr_xFeO_{3-\delta}$–CGO10 on dense $La_{1-x}Sr_xFeO_{3-\delta}$ (LSF) (x=0.3 or 0.5) substrates were fabricated and compared.

Materials and methods

The experimental setup consists of a syringe pump, to provide the solution at the desired flow rate control during spraying, an air compressor (vol.50L) with a manometer and a flow controller for adjusting the air flow rate. Solution and air were mixed in a spray nozzle that produced a spray consisting of 10-100 μm diameter droplets. Aqueous solutions of the precursor salts were prepared using distilled water at total ion concentrations of either 0.025M or 0.1M. Characterization was performed by XRD and SEM in addition to TGA of the precursor salts and obtained post deposition films.

Results and discussion

Experimental results are summarized in Table 1.

Table 1. *Experimental results*

Sample#	Film(Total Precursor Ion Concentrations, M)	Substrate	Sintering scheme*	T_{dep}	Characterization
1	YSZ(0.1)/LSM(0.025)	YSZ16	A2	339±28/219±16	-
2	YSZ(0.025)/LSM(0.025)	YSZ16	A2	141±13/220±28	XRD,SEM-EDS
3	YSZ(0.025)/LSM(0.025)	YSZ16	B2	142±3/98±38	-
4	YSZ(0.1)/LSM(0.025)	YSZ16	B2	168±13/208±23	XRD,SEM-EDS

5	LSF30(0.025)/CGO10(0.1)	LSF30	A1	229±6/195±8	XRD,SEM-EDS
6	CGO10(0.025)	LSF50	A2	232±9	XRD,SEM-EDS

Key: A=Whole composite sintered (700°C/4hr), B=Intermediate sintering of first deposited layer followed by additional sintering of the composite (1, 2 denote single or double layered film)

Typical XRD results showed that the peaks resolved of LSM and CGO10 films correspond to angles depicted for polycrystalline film reference data with no extra phases formed at this sintering temperature. This shows that 700°C is an adequate sintering temperature to form the desired phases while being relatively low to prevent formation of detrimental additional phases.

SEM pictures of the YSZ/LSM composites fabricated with different sintering profiles showed that smooth films are produced with minimal cracks when one sintering step is applied to the as deposited YSZ/LSM composite layer. Large values of temperature standard deviation could also have played a role to the more extensive cracking observed in these films. SEMs of the LSF30/CGO10 composite coated on an LSF30 substrate following a one sintering step (i.e. 700°C/4h) showed a better quality film in terms of fully coating the substrate and thickness uniformity (Fig 1). Here, a better temperature control was achieved. Interestingly, in the case of the film of sample #6 of Table 1, no film of CGO10 was detected after spraying for 100 min on the LSF50 dense substrate as verified by EDS. This could be due to the high deposition temperature (i.e. 232°C) which could promote the appearance of the Leidenfrost effect resulting in partial or lack of coating on the substrate surface.

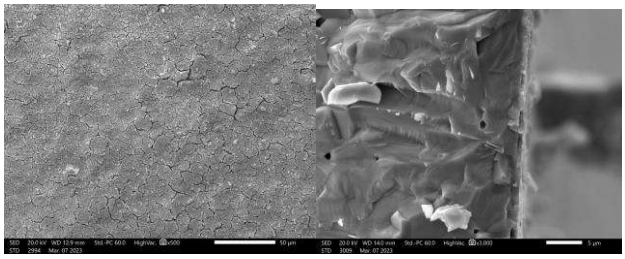

Figure 1. *Surface (left) and cross section SEM of LSF30/CGO10 film on a LSF30 substrate (for deposition conditions see Table 1, sample#5).*

Conclusions

For the YSZ/LSM composite films it was concluded that one sintering step of both sequentially deposited films is preferable to applying two separate sintering steps for each film in terms of thickness uniformity and extent of cracking. For the LSF/CGO10 film, it was found that a good interface is formed with the LSF substrate at a deposition temperature of the CGO10 film of about 195°C though to avoid surface cracks a lower concentration than 0.1 M should be used. On this particular substrate, it was found that lower concentration of either CGO10 or LSF30 of the order of 0.025 M do not result in coating at temperatures of or above 230°C most probably due to the appearance of the Leidenfrost effect that cause droplets to levitate above the substrate surface and subsequently to be removed by the air stream. Finally the thermal characteristics of the precursor salts and deposited mixed oxide films as revealed by TGA showed that a temperature of 700°C is adequate for decomposition of all salts except that of $Sr(NO_3)_2$ which requires a temperature of 800°C for complete decomposition.

Acknowledgements: We acknowledge the University of Western Macedonia for partially supporting financially this research through the postgraduate program (MSc) in Energy Investments and Environment.

References

M.B. Mogensen M. Chen, H.L. Frandsen, C. Graves, J.B. Hansen, K.V. Hansen, A. Hauch, T. Jacobsen, S.H. Jensen, T.L. Skafte and X. Sun, 2019. Reversible solid-oxide cells for clean and sustainable energy. *Clean Energy*, 3 (No. 3), 175–201.

C. Matsouka, V. Zaspalis , L. Nalbandian, 2018. Perovskites as oxygen carriers in chemical looping reforming process–Preparation of dense perovskite membranes and ionic conductivity measurement. *Materials Today: Proceedings*, 5, 27543–27552.

N. E. Kiratzis, A. Barbatsis, N. Kosmarikos, A. Bisbas, C Matsouka and L. Nalbandian, 2022. Fabrication of Fluorite and Perovskite Functional Films by Solution Spray Pyrolysis. Nano Hybrids and Composites, 34, 47–52.

SUST ENG 2023

ENVIRONMENTAL ECONOMICS/ INDUSTRIAL ECONOMICS TOPICS

Sustainable blue economy and ecosystem services in transitional water bodies: Case study of a lagoon and a river delta in Northern Greece

A. Pournara[1] and F. Sakellariadou[2]

[1]Department of Maritime Studies, University of Piraeus, Athens, Greece
Corresponding author email: anthpour@gmail.com

keywords: *Sustainable blue economy; transitional waters; ecosystem, services; lagoon; delta.*

Abstract

Recently, the importance of the marine environment has started to be widely known and accepted, showing its great potential for blue growth. Blue Economy includes all the economic activities related to oceans, seas and coastal areas. The last decade, the emerging need to protect and strive for the sustainable development of the marine and coastal environments led to the need for transition to a Sustainable Blue Economy. According to the United Nations, it is supposed that the ocean-based economy's worth is about 3 trillion dollars per year. To remain sustainable, the growth obtained from the blue economy activities, should protect and preserve the natural resources of the ocean ecosystem. The blue economy, as a continuously expanding field of growth with a significant pace of development, provides people with a series of benefits in multiple levels. The concept of sustainable blue economy has been interpreted in multiple different ways according to the preferences of each stakeholder. except of the oceans, seas and coastal areas, the sustainable blue economy concept also includes transitional waters. According to the WFD 2000/60, transitional waters are bodies of surface water in the vicinity of river mouths which are partly saline in character as a result of their proximity to coastal waters, but which are substantially influenced by freshwater flow. Transitional water bodies and especially lagoons and deltas, provide to the environment and the society a series of important ecosystem services. Pressures from human activities, as well as climate change threaten the availability and the quality of the ecosystem services provided by the estuarine and lagoon ecosystems. Under this scheme, a sustainable blue economy framework should be implemented for the protection of the vulnerable estuarine and lagoon ecosystems. Case study of this paper are the lagoons of Keramoti and Nestos delta, located in Northern Greece, in the Region of Eastern Macedonia and Thrace. These transitional water bodies accept a series of important pressures from human activities, while the ecosystem services of the lagoon and estuarine ecosystems are at risk, facing the impacts of the human pressures.

Acknowledgements: This study was financially supported by the Research Centre of the University of Piraeus, Greece.

The role of standards for the transition to a Sustainable Blue Economy

A. Pournara[1]

[1]Department of Maritime Studies, University of Piraeus, Athens, Greece
Corresponding author email: anthpour@gmail.com

keywords: *Standards; Sustainable Blue Economy; Ocean governance; SDGs.*

Introduction

The last decade globalization leads to a great shift on the way people, markets and finally the ecosystems interact with each other. On the same time, marine and coastal ecosystems are facing multiple challenges, deriving from the impacts of anthropogenic pressures, such as marine pollution from land-based activities and the degradation of the coastal zone. Under this scheme, a higher economic and social value should be attributed to the marine and coastal ecosystems, with the acceptance of sustainability initiatives and standards. Simultaneously, focus should be given to the interrelation between ocean health and sustainability, as environmental pressures can be a driver for the development of new standards. The emerging sectors of Blue Economy include the extraction of marine living and non-living resources, tourism, marine traffic, shipbuilding and repair, marine renewable energy and many more, while new activities are continuously arising. Since around 70% of the earth is covered by oceans, the importance for a sustainable blue economy is even more crucial in economic, social and environmental level. Only in the European Union the blue economy has a turnover of € 667.2 billion, while almost 4.5 million people work in blue economy sectors.

A useful tool for the transition to a sustainable blue economy is the adoption of standards, for the investigation of the ecological, economic and social dimensions of blue economy. This study underlines the importance of the enforcement of definite standards for the blue economy and their specification per sector of blue economy activities, according to the structure and the environmental footprint. Among others, the enactment of standards has a significant influence on an economic level, as voluntary standards affect market prices and tendences. In contrary to general and obligatory guidelines, voluntary standards present specific pathways and alternatives, showing the way to sustainability and a sustainable blue economy. Voluntary standards cover the existing gap between the theoretical legislative view of sustainability and the true state of the market and the blue economy activities. In other words, voluntary standards can be the key to the transition to a sustainable blue economy, providing an integrated approach incorporating numerous criteria and adopting positive practices, although there are multiple constraints for the enforcement of standards in all blue economy sectors.

Ulterior motive is the creation of standards with a broader impact, covering the whole sphere of ocean governance and blue economy activities. On the other hand, the adoption of a global agenda of voluntary standards could potentially be a systematic challenge and create contradictions in administrative, social and economic level. It should be noted that voluntary standards can regulate the performance of sustainable blue economy activities in all sectors, harmonized with the need for achievement of the SDGs by 2030. More specifically, voluntary standards can be a tool for monitoring the progress of the achievement of the SDGs and a sustainable blue economy, under the prism of SDG 14. At the same time, more focus should be given to the adoption of standards in the social pillar, because of the existing inequities, the absence of corresponding mentality and the gap in gender equality issues (SDGs 5 and 10).

As for the economic pillar of sustainability, the creation of economic voluntary standards defining the exploitation of marine living resources, will be an important step to the achievement of sustainable blue economy and the SDGs that regulate the balance between economic growth, social prosperity, and environmental protection.

Acknowledgements: This study was financially supported by the Research Centre of the University of Piraeus, Greece.

Techno-economic learning in biorefinery research – A meta-level perspective of three exemplary cases

P. Krassnitzer, J. Wenger and T. Stern

Institute for Systems Sciences, Innovation and Sustainability Research, University of Graz, Graz, Austria
Corresponding author email: paul.krassnitzer@uni-graz.at

Abstract
The production of liquid fuels and chemicals from biomass is an essential part in establishing a bioeconomy. Numerous techno-economic studies have been published on different processing pathways for biomass. To examine the progress made in this field, meta-analyses for three exemplary biobased products were conducted. Using recently published techno-economic studies, the (average) unit production cost of biodiesel, cellulosic ethanol and the extraction cost of kraft lignin were investigated. Findings in this study are based on the understanding of the two phenomena of economies of scale and the learning effect. Economies of scales can be observed for each case with the production of cellulosic ethanol showing the largest and kraft lignin extraction the smallest cost advantages. The investigation of potential learning effects present in the data leads to unexpected results: In two out of three cases, it was observed that the calculated average unit production cost increases over time. These results contradict the expected influence of learning effects on calculated unit production costs since these didn't decrease over time for a specific technology. Upon closer investigation of processing pathways and feedstocks, a diversification over the last three decades in research becomes observable. This leads to the conclusion that the (economic) optimization of a technology is not as much prioritized in the research community as the exploration of new processing pathways and novel feedstocks.

2nd International Conference on
Sustainable Chemical and
Environmental Engineering
14th – 18th June 2023, Limassol, Cyprus

Cost-benefit analyses for agricultural soils health: a literature review

S. Rozakis[1] and E. Androulidaki[2]

[1]School of Chemical and Environmental Engineering, Technical University of Crete, Chania, Greece
Corresponding author email: srozakis@.tuc.gr

keywords: *cost-benefit; agricultural soil; eco-system services; cost-effectiveness; SNA.*

Introduction

Soil improvement practices represent a long time research topic in agricultural literature. Because of the multiple functions of soils their evaluation is performed by means of cost-benefit analysis (CBA). The key elements for cost-benefit analysis of a project include:

- Identifying possible alternatives to attain the target, including maintaining the status quo.
- Determining the scope of the analysis (key stakeholders and associated costs and benefits.
- Systematically assessing the benefits and costs of various alternatives in monetary terms.
- Measuring external benefits and costs, including environmental benefits and costs, using methods appropriate for them and the degree of uncertainty in available data.
- Consider all life span of activities, meaning future values of benefits and costs are included in present values.
- Applying fixed criteria or objectives to reach a decision (mostly net present value and benefit-cost ratio).

As the reader can observe this is a particularly demanding analysis not easy to implement in all cases. For this reason it is implemented in two steps firstly calculating financial costs and benefits then include social ones. When limited to the calculation of costs Cost-effectiveness analysis is a technique that relates the costs of a program to its key outcomes not necessarily monetary values. Cost benefit analysis takes that process one step further, attempting to compare costs with the dollar value of all (or most) of a program's many benefits. The purpose of this literature review is to detail the mode of application of CBA in the literature regarding agricultural soils.

Materials and methods

Cost-benefit analysis literature is studied with a focus on ecosystem services in relation to healthy soils. For this purpose we searched the Scopus database of scientific publications. A query including the terms “cost-benefit”, soil*, ecosystem*, service* (asterisk means that search is extended to all versions of the term) drilled from article keywords is performed. A total number of 82 publications are detected starting from year 2001. We organized these papers using Social Network Analysis to reveal co-occurrence in the keywords so that to group them in clusters. Then a systematic review followed in order to understand relation to the theory and classify publications according to the extent of CBA exercise.

Results and discussion

The fair number of publications revealed different approaches to the implementation of CBA mostly determined from the specific question and case study. Applications include mere financial cost-benefit analysis, cost-effectiveness analyses and in few cases partial or fully fledged cost-benefit analysis. These latter necessitate not only theoretical knowledge of the subject which should not be granted as given and also important resources including long-term experiments which is a daunting task. Time dimension is not directly related to the degree of CBA application.

Acknowledgements: This study is supported by the Horizon 2020 and the PRIMA program (EC): “RESilient to Climate CHange Extremes MeDiterranean AgricUltural Systems: LEveraging the Power of Soil Health and Associated Microbiota”, RESCHEDULE.

SUST ENG 2023

AGRICULTURAL ENGINEERING/ AGRICULTURAL & LIVESTOCK WASTE

Machine Learning based Prediction of Fusarium Head Blight spatial distribution in wheat fields

A. Morellos[1], X.E. Pantazi[1], C. Tsitsopoulos[1], K. Dolaptsis[1], G. Tziotzios[1], D. Stavridou[1], C. Paraskevas[1], O.E. Apolo-Apolo[2], M.B. Almoujahed[2], R. Whetton[2], Z. Kriauciuniene[3], M. Kazlauskas[3], E. Šarauskis[3] and A. Mouazen[2]

[1]School of Agriculture, Aristotle University of Thessaloniki, Thessaloniki, Greece
[2]Department of Environment, Ghent University, Ghent, Belgium
[3]Faculty of Engineering, Agriculture Academy, Vytautas Magnus University, Kaunas, Lithuania
Corresponding author email: amorello@agro.auth.gr

keywords: *crop protection; FHB; machine learning; artificial intelligence; precision agriculture.*

Introduction

Fusarium Head Blight (FHB), belongs to one of the main and most damaging fungal diseases of wheat (*Triticum aestivum*) in worldwide level, with significant negative impact on the grain yield, grain quality and harvest as well as on safety of the produced food with mycotoxin contamination (McMullen et al., 2012). The accurate and timely prediction of FHB occurrence can assist farmers to adopt effective management strategies for the efficient reduction of the fungicide application and associated costs in wheat production (Paul et al., 2016). Common applied techniques for the FHB monitoring are regarded time-consuming, laborious and subjective, since they require visual inspection and destructive testing procedures, that make the accuracy of disease recognition questionable for large-scale management. This study demonstrates a novel approach to FHB prediction, based on machine learning and features acquired by proximal and remote sensing data. Two different machine learning models have been employed namely, Least Squares – Support Vector Machines (LS-SVM) and Gaussian Process Regression (GPR) to ground and satellite data collected from wheat fields in Belgium and Lithuania. By integrating these data sources, the predictive accuracy of FHB forecasting models has reached an R^2 value higher than 0.8 in the selected fields, providing a valuable tool for farmers to make timely and effective management decisions.

Materials and methods

Crop data were collected in August of 2022, using a manual moving platform in the field trial plot of CRA-W in Gembloux in Belgium (51°01’53.9’’N 2°34’16’’E) and in in Naujamiesčio sen. in Lithuania (55°40’17.5’’N 24°08’49.2’’E). Regarding the FHB field assessment, observed FHB spatial distribution was evaluated in the whole field area per square meter. The infection is defined as a percentage of infected wheat ears in an area of 1 m^2. The data that there used for the models training were ground data such as relative humidity, electrical conductivity, elevation, soil temperature, K content and pH, as well as satellite-derived indices, including the Normalized Difference Vegetation Index (NDVI), Leaf Area Index (LAI), and Chlorophyll content. The acquired data were subjected to essential preprocessing, prior their import to the machine learning algorithms. Firstly, the most important data for every field, were selected using the mutual information method. Secondly, the selected variables have been preprocessed using Min-Max Scaler, which normalizes the data in the range of [0, 1], in order to scale the data and reduce the effect of outliers. For the machine learning (ML), two methods were employed namely Least-Squares support vector machines (LS-SVM), which uses a nonlinear kernel function to map the input data to a higher dimensional space and Gaussian Process Regression (GPR), which is a non-parametric Bayesian approach to regression that models the target function as a Gaussian process. The models were evaluated, using standard evaluation metrics, commonly used in regression problems; the coefficient of determination (R^2) and the root mean squared error (RMSE).

Results and discussion

Based on the mutual information method, the data that were selected for the training of the models that were developed for the Belgian field were NDVI, LAI, Chlorophyll content and field elevation, while for the Lithuanian field the respective selected variables were field elevation, soil temperature, relative humidity

and K content. The selection of only ground and no satellite data in the case of the Litnuanian field, in comparison to the Belgian field, was most likely because of the cloud coverage in the day of the measurements distortion that were produced by cloud coverage.

The applied models' performances for the prediction of the FHB distribution in the study areas are demonstrated in Table 1.

Table 1. *Performance of ML models for the prediction of FHB in wheat fields in the study areas.*

	Belgium		Lithuania	
	LS-SVM	**GPR**	**LS-SVM**	**GPR**
R^2	0.85	0.92	0.73	0.83
RMSE	0.627	0.45	0.700	0.43

The results show that both models have a satisfactory and comparable performance in the prediction of the FHB in the selected fields, as it is also validated by the values of R^2. The GPR model, though, has outperformed the LS-SVM in the FHB prediction. This may have happened due to the fact that GPR provides a probabilistic output in the form of predictive mean and variance, which quantifies the uncertainty associated with the predictions. This information could have led to more accurate and reliable predictions compared to LS-SVM, which provides point estimates without directly quantifying uncertainty.

The performance of the models is also depicted in the Figure 1, where the distribution of the predicted FHB is compared with the actual values in the field. The FHB values are classified in 5 classes, according to the values of the FHB percentage in the field. As it is apparent, the general pattern of the predicted values follows very well the respective actual pattern of the disease spread. There are only a few spots that have been misclassified. In the case of the Belgian field most of these spots belong mainly to the central-western axis of the field and very small areas in the most south parts of the field, while for the Lithuanian field most of the misclassified spots belong to the central and the northern-east part of the field.

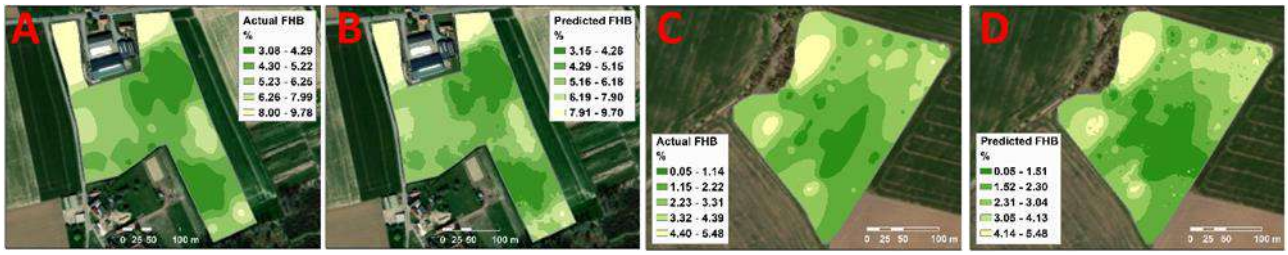

Figure 1. *Actual (A, C) vs predicted FHB (B, D) FHB distribution in the Belgium (A, B) and Lithuanian (C, D) field.*

Conclusions

The problem addressed in this study is the accurate and timely prediction of Fusarium Head Blight (FHB) distribution in wheat fields by demonstrating a novel approach to the disease's prediction using ML and features acquired by proximal and remote sensing data. It was concluded that using proximal and remote sensing data as inputs to machine learning techniques have led to a successfully predicted FHB distribution in the wheat fields that were tested. Additionally, GPR has outperformed LS-SVM in both fields, scoring an R^2 of 0.92 and 0.83 for the Belgian and Lithuanian fields respectively, in contrast with the respective scores for LS-SVM. All these lead to the conclusion that an effective and sustainable solution towards the reduction of fungicide application, during preventive site-specific spraying is possible through the management zones that can be generated, using the findings of this study.

Acknowledgements: This research has been co-financed by the European Regional Development Fund (ERDF) and Greek national funds through the Partnership Agreement for the Development Framework 2014-2020 (Action: ERANETS - 2021A).

References

McMullen, M., Bergstrom, G., De Wolf, E., Dill-Macky, R., Hershman, D., Shaner, G., & Van Sanford, D. (2012). A unified effort to fight an enemy of wheat and barley: Fusarium head blight. *Plant Disease*, 96(12), 1712-1728.

Paul, P. A., El-Allaf, S. M., Lipps, P. E., & Madden, L. V. (2016). Rain splash dispersal of Gibberella zeae within wheat canopies in Ohio. Phytopathology, 94(12), 1342-1349.

Valorisation of agricultural waste towards enhanced biopolymer via cathodic electrofermentation

O. Vittou, M. Sarafidou, O. Psaki, C. Pateraki and A. Koutinas

Department of Food Science and Human Nutrition, Agricultural University of Athens, Athens, Greece
Corresponding author email: olga.and.vittou@gmail.com

keywords: *agricultural waste; sugar beet pulp (SBP); biopolymers; electrofermentation.*

Introduction

Sugar beet is a commercially important root crop that accounts for nearly 20% of the world's sugar production. Sugar beet pulp (SBP), a co-product of the sugar processing industry, is the main stream accounting for 3-5% (w/w) of sugar beet after the diffusion process. It has been estimated that the processing of 1 t of sugar beet produces 160 kg of sugar, 500 kg of wet pulp and 38 kg of molasses (Ladakis et al., 2020). Current uses and management practices for SBP are limited to use as animal feed and to a lesser extent, as an energy feedstock. On this basis, research is focused on the valorization of SBP to obtain a variety of value-added products such as pectin, free sugars and bioactive compounds for the production of platform chemicals, biofuels and biopolymers (Alexandri et al., 2019).

Polyhydroxyalkanoates (PHAs) are natural, bio-based and biodegradable polymers that are synthesized intracellularly by various microorganisms as carbon and energy reserves. The most well-known member of the PHAs family is poly-3-hydroxybutyrate (PHB) with similar properties to polypropylene (Wang et al., 2013). One of many reasons that impede the industrial production of PHB is the high production cost, leading to the exploration of alternative approaches to reduce this cost (Pagliano et al., 2017).

Within this concept, SBP valorisarion was carried out in a biorefinery framework by extracting such bioactive molecules as pectin and free sugars, while the residual solids were used for the production of sugar-rich hydrolysate for PHB production. Additionally, a comparative study of the implementation of electrical power in fermentation systems for the production of bio-based polymers as an alternative source of reductive energy in microbial factories was performed. The direct interaction of an electrode can be utilized in bioelectrochemical system (BES) to electrochemically support microorganisms with an aim to regulate their intracellular redox balance. An oxidation process occurs at the anodic BES, while at a cathodic BES a reduction process occurs (Srikanth et al., 2012). BES involve the interaction of electrons or water electrolysis products with microbial cells in a metabolic level. Cathodic electrofermentations (EF) create a reductive environment that can partially replace the enzymatically produced reductive energy (Pateraki et al., 2023).

Materials and methods

The compositional analysis of SBP was initially carried out. A biorefinery concept using SBP was developed leading to the production of pectin-rich extract and free sugars. Pectin-rich extract was first extracted from SBP a solid to liquid ratio of 1:20 (w/v) at 80°C for 3 h of extraction time using sulfuric acid, followed by aqueous extraction of free sugars. The SBP residual solids obtained after free sugars and pectin extraction were subjected to enzymatic hydrolysis of glucan and hemicellulose.

Fed-batch bioreactor fermentations were performed in a 2 L bioreactor with an initial working volume of 1 L using SBP hydrolysate as fermentation raw material for PHB production using the strain *Paraburkholderia sacchari*. Regarding the impact of electrical power on PHB production, fed-batch fermentations were carried out using a synthetic medium with commercial carbon sources in a ratio similar to that contained in the SBP hydrolysate. The electrodes (Figure 1) were placed inside the bioreactor supplying 0.57 A. Electricity was supplied at different stages during fermentation (e.g. after lag phase, growth phase) for different durations in order to evaluate its effect on bacterial growth and PHAs production.

Results and discussion

SBP pellets are characterized by a high content of carbohydrates, of which glucan (27.9%) and hemicellulose (24.9%) account for about 50%. The lignin content in SBP pellets is relatively low at 2.3%. In addition, SBP pellets are characterized by high pectin content equal to 19.1%. The protein, lipid, and aqueous-extracted free sugar contents of the SBP pellets used in this study were 9.1%, 0.9%, and 10.9%, respectively. Free sugars consisted mainly of sucrose (9.0%), while glucose and fructose were detected in lower concentrations. Extraction of phenolic compounds with aqueous ethanol revealed a total phenolic content of 2.1 mgGAE/g_{SBP}.

A consolidated biorefinery was developed for the extraction of free sugars and pectin-rich extract via acid hydrolysis with sulfuric acid. Free sugars extraction precedes pectin extraction, gave pectin recovery yield of 90.2% and a GA content of 67%. The experimental results show that the inclusion of a step before pectin extraction increases the content of GA in the obtained pectin-rich extract, making it more suitable for further applications. SBP residual solids obtained after the extraction of all aforementioned components were used for the production of a sugar and nutrient-rich hydrolysate. The SBP hydrolysate containing mainly glucose (67%), arabinose (14.2%), and mannose (14.4%) was evaluated as a carbon source for PHB production.

Fed-batch fermentation resulted in the production of 120 g/L total dry weight with PHB content of 70% (w/w). The PHB concentration was 48.5 g/L with a yield and productivity of 0.16 g/g and 1.26 g/L/h. In a similar manner, fed-batch bioreactor fermentation of *P. sacchari* was performed evaluating the impact of the BES in bacterial growth and PHB production. The overall fermentation efficiency was improved in comparison to the control case.

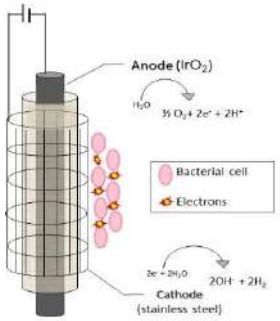

Figure 1. Schematic representation of electrode set up inside the bioreactor

Conclusions

Extraction of various value-added fractions could facilitate biorefinery feasibility for the complete valorisation of SBP. Higher fermentation efficiency was achieved when the electrode was integrated inside the bioreactor as compared to the control fermentations.

References

Alexandri, M., Schneider, R., Papapostolou, H., Ladakis, D., Koutinas, A., & Venus, J. (2019). Restructuring the Conventional Sugar Beet Industry into a Novel Biorefinery: Fractionation and Bioconversion of Sugar Beet Pulp into Succinic Acid and Value-Added Coproducts. ACS Sustainable Chemistry and Engineering, 7(7), 6569–6579.

Ladakis, D., Papapostolou, H., Vlysidis, A., & Koutinas, A. (2020). Inventory of food processing side streams in European Union and prospects for biorefinery development. In Food industry wastes (pp. 181–199). Academic Press.

Pagliano, G., Ventorino, V., Panico, A., & Pepe, O. (2017). Integrated systems for biopolymers and bioenergy production from organic waste and by-products: A review of microbial processes. In *Biotechnology for Biofuels*.

Pateraki, C., Magdalinou, E., Skliros, D., Flemetakis, E., Rabaey, K., & Koutinas, A. (2023). Transcriptional regulation in key metabolic pathways of Actinobacillus succinogenes in the presence of electricity. *Bioelectrochemistry*, *151*.

Srikanth, S., Venkateswar Reddy, M., & Venkata Mohan, S. (2012). Microaerophilic microenvironment at biocathode enhances electrogenesis with simultaneous synthesis of polyhydroxyalkanoates (PHA) in bioelectrochemical system (BES). *Bioresource Technology*, *125*, 291–299.

Wang, Y., Chen, R., Cai, J. Y., Liu, Z., Zheng, Y., Wang, H., Li, Q., & He, N. (2013). Biosynthesis and Thermal Properties of PHBV Produced from Levulinic Acid by Ralstonia eutropha. *PLOS ONE*, *8*(4), e60318.

Modeling of methane production with the application of artificial intelligence techniques

P. Pochwatka[1], A. Kowalczyk-Juśko[1], A. Mazur[1] and J. Dach[2]

[1]Department of Environmental Engineering and Geodesy, University of Life Sciences in Lublin, Lublin, Poland
[2]Department of Biosystems Engineering, Poznań University of Life Sciences, Poznań, Poland
Corresponding author email: patrycja.pochwatka@up.lublin.pl

keywords: *methane production; biogas plant; artificial neural networks; sensitivity analysis; anaerobic digestion.*

Introduction

The production of biomethane, used for cogeneration (i.e. electricity and heat production) and as an eco-friendly gas fuel, has gained increasing importance in Poland in recent years. More and more companies are seeking alternative energy sources to reduce operating costs or decrease the carbon footprint of their products. Energy sources such as photovoltaics or wind farms are uncontrolled and weather-dependent, making energy production based solely on them without energy storage impossible. Biogas plants are a much better alternative because the produced biogas can be stored and used at the convenience of the company. Recently, many companies have commissioned certified laboratories to conduct biogas productivity analyses to determine the methane efficiency of their substrates. The duration of these analyses is substrate-dependent and can range from several to several dozen days. Additionally, the cost of preparing the laboratory report is associated with the performance of these analyses. As a result, alternative methods are increasingly being sought to expedite the process and enable the calculation of methane yield from the substrate based on the available knowledge base.

The use of artificial intelligence techniques becoming increasingly prevalent across various scientific fields and aspects of everyday life. Techniques employed in such modeling include artificial neural networks (ANN), fuzzy logic, and Bayesian networks (Chen et al. 2023). ANN have found particular applications in modeling the methane production process and optimizing process parameters (Kowalczyk-Juśko et al. 2020). Based on available data from the methane production process and independent variables, such as HRT, conductivity, pH, dry matter, dry organic matter, and substrate type, artificial neural networks can help predict dependent variables, most commonly methane yield. The study aimed to determine the feasibility of using artificial neural networks to predict substrate methane yield (Pochwatka et al. 2022). Furthermore, this study aims to rank the individual physicochemical characteristics of the substrate based on their impact on methane yield, using sensitivity analysis.

Materials and methods

To achieve the study's objective, a knowledge base was developed using previously conducted anaerobic digestion studies at the Ecotechnologies Laboratory of Poznań University of Life Sciences and tests of own prepared substrates that underwent fermentation studies in the same laboratory. The study considered substrate characteristics such as dry matter (D.M.), dry organic matter (O.D.M.), pH, conductivity, Hydraulic Retention Time (HRT), type of substrate, and methane efficiency [m^3/Mg of fresh matter] as the dependent variable. The database was then subjected to neural modeling using Statistica 13.3 software, and the study utilized MLP (Multilayer perceptron) and RBF (Radial basis function) neural networks for modeling.

Various network structures were analyzed during the study. In the first step, the Automatic Network Designer function was used to aid in the model creation process. The second step involved learning the models created using the User Network Designer function. An example of the network structure is shown in Figure 1.

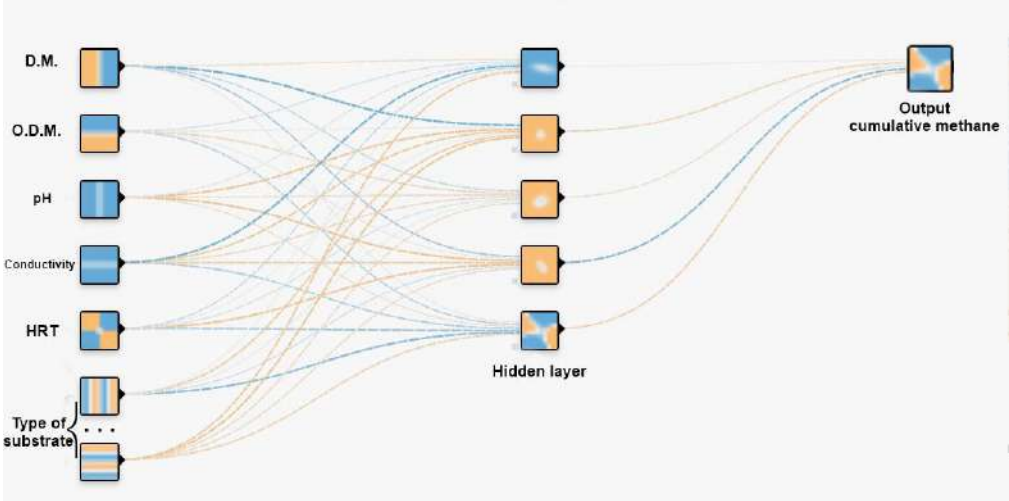

Figure 1. *Structure of the tested artificial neural network*

Following the selection of the optimal neural network, a sensitivity analysis was conducted to determine the rank of the significance of the analyzed parameters.

Results and discussion

The study found that the MLP neural networks had the best performance on the created database containing data on various substrates such as maize silage, sorghum silage, oat, pea, sunflower, grasses, and reeds. Specifically, the MLP-26-6-1 network exhibited the best performance with a learning quality of 99.9%, test quality of 99.5%, and validation quality of 99.4%. This network utilized Tanh activation and linear functions for the output. According to the sensitivity analysis, the type of substrate was found to be the most significant parameter affecting methane yield, followed by HRT, dry matter (D.M.), conductivity, pH, and organic dry matter (O.D.M.).

Conclusions

Based on the research conducted, it can be concluded that artificial neural networks are a useful tool for predicting the methane yield of substrates. With a well-developed knowledge base, it is possible to extrapolate results based on substrate parameters. Additionally, sensitivity analysis provides insight into the most important parameters for the anaerobic digestion process. This information can be used to approximate the amount of substrate needed to supply a biogas plant with a given electrical power or biomethane yield per unit of time, without the need for a lengthy and expensive methane efficiency analysis process.

Acknowledgements: *This study was created in the framework of the Young Scientists project "Application of artificial intelligence techniques in modeling the biogas production process" TKD/MN-2/IŚGiE/21 realized at University of Life Sciences in Lublin, Poland.*

References

Chen, J.W., Chan, Y.J., Arumugasamy, S.K. and Yazdi, S.K., 2023. Process modelling and optimisation of methane yield from palm oil mill effluent using response surface methodology and artificial neural network, *J. Water Process. Eng.*, 52, 103493.

Kowalczyk-Juśko, A., Pochwatka, P., Zaborowicz, M., Czekała, W., Mazurkiewicz, J., Mazur, A., Janczak, D., Marczuk, A. and Dach, J., 2020. Energy value estimation of silages for substrate in biogas plants using an artificial neural network. *Energy*, 202, 117729.

Pochwatka, P., Kowalczyk-Juśko, A., Mazur, A., Nowak, M. and Dach, J., 2022. The use of sensitivity analysis in ANN to determine the significance of the parameters of the anaerobic digestion process, *Proceedings of the 1st International Conference on Sustainable Chemical and Environmental Engineering*, 288-289. ISBN: 978-618-86417-0-9.

Treatment and technology of rural domestic wastewater in China

J. Zhang*, S. Lu, Y. Jiang and H. Zhang

State Key Laboratory of Environmental Criteria and Risk Assessment, State Environmental Protection Key Laboratory for Lake Pollution Control, National Engineering Laboratory for Lake Pollution Control and Ecological Restoration, Chinese Research Academy of Environmental Sciences, Beijing, , PR China
Corresponding author email: jingzhang.ecp@hotmail.com

keywords: *rural domestic wastewater; bibliometric analysis; technology; constructed wetland.*

Introduction

Survey showed that globally, about 2.68×10^9 rural residents do not have access to clean drinking water, and the discharge of untreated wastewater is one of the most important reasons (Huang et al., 2022). As China is a rapid urbanization country, the issue of rural domestic wastewater treatment is an urgent problem that needs to be addressed in China today. In 2021, about 35 billion m^3 wastewater was discharged into rural areas in China, while the treatment percentage is still low. Thus, the government takes the environmental protection seriously, and on January 19, 2022, four ministries and the China's Rural Revitalization Bureau jointly issued the Action Plan for the Agricultural and Rural Pollution Control (2021-2025), which states that "By 2025, the overall utilization rate of livestock and poultry manure will reach more than 80%, and the rural domestic wastewater treatment will reach 40%".

In this study, first, the most outstanding issue in the field of rural domestic wastewater in China's was addressed by bibliometric analysis. Second, the state art of constructed wetland (CW), the most frequent keywords in the rural domestic wastewater filed, was studied by international literature search. Finally, CW was compared to other common technologies to address the advantage and disadvantages.

Materials and methods

The "rural domestic wastewater" was used as the keywords to set up the database via a search of China National Knowledge Infrastructure (CNKI). A number of 3910 Chinese articles in the periods from 1996 to 2023 were addressed by the April 30, 2023. A bibliometric analysis of literature was performed used software of CiteSpace (Chen, 2004).

Results and discussion

Bibliometric analysis of rural domestic wastewater. The analysis of 3190 articles extracted from CNKI database shows that the number of articles on this topic has gradually increased since 2004 and exceeded 300 in 2019. Among them, 80.59% were distributed in the discipline of "environmental science and resource utilization", 79 on the topic of "human habitat", 33 on "rural revitalization", and the rest on "governance measures". Among them, the most frequently used treatment is "constructed wetland", which was the subject of 196 articles (Figure 1).

Characteristics of rural domestic wastewater. Rural domestic wastewater can be divided into two categories: gray water and black water. Black water includes urine wastewater, fecal water or manure, while gray water includes kitchen, bathing water and floor drainage wastewater. In general, black water contains more contaminants than grey water (Table 1). The amount of grey water produced is related to working and resting conditions of people, and is higher during the midday and evening (Li et al., 2021). The pollutant content of the water body is affected by regional, seasonal and economic development. In some regions, there are seasonal differences in effluent, with more water used in summer leading to a higher pollutant in summer than in spring.

Rural domestic wastewater treatment technology. Rural domestic wastewater treatment can be divided into two modes: decentralized and centralized treatment. Both modes have their own advantages and disadvantages, and commonly used treatment technologies include septic tank, A/O, A^2/O, MBR,

anaerobic/anoxic biofilm, biofilm/activated sludge, CW and hybrid treatment (Guo et al., 2014), among which CW technology is widely used due to its low price and ecological functions.

The state art of the constructed wetlands. CWs have been developed since 1903, when they were first established in England, and the first CW to begin operation in China was in 1990. Including free water surface flow, subsurface flow, floating and hybrid CWs. The main current challenges about CW are clogging, low temperature, and the adaptable design (Wu et al., 2023). After all, the contribution of CW to carbon neutrality should be clarified.

Table 1. *Physicochemical characteristics of grey and black water*

Type of water	Amount L/(person·d)	Biological Oxygen Demand (BOD_5, mg/L)	Chemical Oxygen Demand (COD, mg/L)	Ammoniacal-nitrogen (NH_3-N, mg/L)	Total nitrogen (TN, mg/L)	Total phosphorous (TP, mg/L)
Grey water	20～225	33～296	76～1461	1.58～47	7.14～54	0.3～5.2
Black water	10～175	93.3～410	200～1500	3.1～770	12.4～800	1.1～29.9

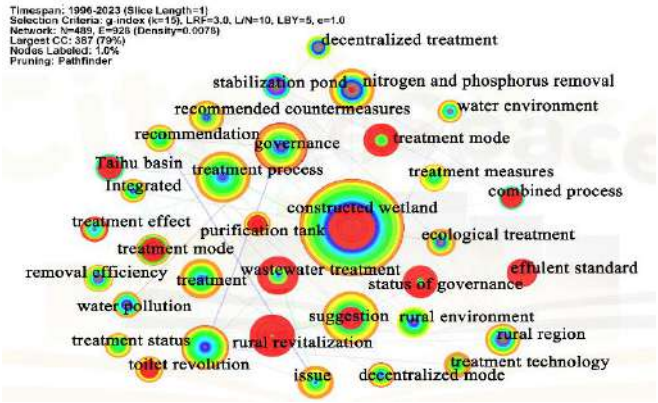

Figure 1. *The keywords co-occurrence analysis on the research of* rural domestic wastewater.

Conclusions

CW is one of the most popular ecological technologies in rural domestic wastewater treatment and has been used in more than 50 countries. However, it currently faces several major problems, namely low temperature, clogging, and initial construction design, which limit its promotion. It needs further research by technicians and proper planning during construction to improve its practicality as well as service life.

Acknowledgements: This work is supported by the Fundamental Research Funds for the Central Public-interest Scientific Institution (2022YSKY-50), the National Natural Science Foundation of China (Grant No. 42207154).

References

Chen, C. 2004. Searching for intellectual turning points: Progressive Knowledge Domain Visualization. Proc. Nat. Acad. Sci., 101(Suppl.), 5303-5310.

Guo, X., Liu, Z., Chen, M., et al., 2014. Decentralized wastewater treatment technologies and management in Chinese villages. Front Environ Sci Eng, 8, pp.929-936.

Huang, Y., Wu, L., Li, P., et al., 2022. What's the cost-effective pattern for rural domestic wastewater treatment?. J. Environ Manage., 303, p.114226.

Li Y., He Z.Q., Xia X.F., et al., 2021. Research progress of greywater treatment technology at home and abroad. J. Environ. Sci. Eng. Technol., 11(5): 935-941 (In Chinese).

Wu, H., Wang, R., Yan, P. et al., 2023. Constructed wetlands for pollution control. Nat Rev Earth Environ 4, 218–234.

SUST ENG 2023

POSTERS

Biogas upgrading with membrane gas separation; Construction and operation of a pilot-scale polyimide membrane system

P. Gkotsis[1], C. Koutsiantzi[2], T. Deligiannis[3], A. Zouboulis[1], M. Mitrakas[2] and E. Kikkinides[2]

[1]Department of Chemistry, Aristotle University of Thessaloniki, Thessaloniki, Greece
[2]Department of Chemical Engineering, Aristotle University of Thessaloniki, Thessaloniki, Greece
[3]Water Business Unit, Thessaloniki WWTP (EELTH), AKTOR SA, Thessaloniki, Greece
Corresponding author email: kikki@auth.gr

keywords: *biogas upgrading; membrane technologies; gas permeation; polyimide membranes; pilot-scale units.*

Introduction

The increase of CH_4 content in biogas by effectively separating the other gases has become a necessity, especially if considered as an industrial renewable energy source (Ahmed et al., 2021; Kougias et al., 2018; Seong et al., 2020). The separation involves two main steps: i) biogas cleaning/purification, which is an energy-demanding process, and refers to the removal of minor unwanted components of biogas and ii) biogas upgrading, which aims to increase the low calorific value of the biogas, and refers to the removal of CO_2. After the separation, the final product, which is called biomethane, consists of CH_4 (95-99%) and CO_2 (1-5%) and no trace of H_2S (Adnan et al., 2019). The present work is part of a research study (BiogasUp) which aims at the holistic exploration of an innovative system for simultaneous biogas upgrading, using inorganic membranes and biogas enhancement through recycling and utilization of waste CO_2 as catalyst for sludge pretreatment.

Materials and methods

After the initial production of biogas from the full-scale digesters of Thessaloniki's Wastewater Treatment Plant (TWWTP), biogas is channelled into an upgrading system which includes a two-stage membrane unit (Figure 1).

Figure 1. Two-stage membrane separation unit for biogas upgrading.

Results and discussion

The two-stage pilot-scale membrane unit was successfully designed and constructed, and the preliminary results have shown significant potential for the production of high purity biomethane (>95%). The achieved results can be considered as a starting point which can lead to the designing, construction and operation of the appropriate multi-stage set-ups, or to the evaluation and comparison of the separation performance of different membrane materials (polymeric or ceramic) or configurations (hollow fibre or tubular).

Conclusions

The present work focuses on the design, construction and operation of a two-stage biogas upgrading pilot-scale unit. Biogas upgrading is based on a polyimide membrane module which is fed with pre-treated sludge substrate from the facility of sewage treatment of Thessaloniki. BiogasUp aims at developing and optimizing a renewable energy technology, focusing on the production of high-value second-generation biofuels (biomethane), opening new horizons to the use of biogas beyond its conventional combustion. The results of the project will be a common benchmark for all members of the supply chain of biogas production sector and municipal wastewater treatment.

Acknowledgements: This study has been co-financed by the European Union and Greek national funds through the Operational Program Competitiveness, Entrepreneurship and Innovation, under the call RESEARCH – CREATE – INNOVATE (project code: T2EDK-01293).

References

Adnan, A.I., Ong, M.Y., Nomanbhay, S., Chew, K.W., Show, P.L., 2019. Technologies for biogas upgrading to biomethane: a review, *Bioengineeging*, 6(4), 92.

Ahmed, S.F., Mofijur, M., Tarannum, K., Chowdhury, A.T., Rafa, N., Nuzhat, S., Kumar, P.S., Vo, D.V.N., Lichtfouse, E., Mahlia, T.M.I., 2021. Biogas upgrading, economy and utilization: a review, *Environ. Chem. Lett.*, 19, 4137-4164.

Kougias, P.G., Angelidaki, I., 2018. Biogas and its opportunities – a review, *Front. Environ. Sci. Eng.*, 12, 14.

Seong, M.S., Kong, C.I., Park, B.R., Lee, Y., Na, B.K., Kim, J.H., 2020. Optimization of pilot-scale 3-stage membrane process using asymmetric polysulfone hollow fiber membranes for production of high-purity CH_4 and CO_2 from crude biogas, *Chem. Eng. J.*, 384, 123342.

Digestate from agriculture biogas plants as a potential source of tetracycline antimicrobials and antibiotic resistance genes

E. Korzeniewska[1], I. Wolak[1], M. Harnisz[1], Magdalena Męcik[1], K. Stando[2] and S. Bajkacz[2,3]

[1]Department of Water Protection Engineering and Environmental Microbiology, Faculty of Geoengineering, University of Warmia and Mazury, Olsztyn, Poland
[2]Silesian University of Technology, Faculty of Chemistry, Department of Inorganic Chemistry, Analytical Chemistry and Electrochemistry, Gliwice, Poland
[3]Silesian University of Technology, Centre for Biotechnology, Gliwice, Poland
Corresponding author email: ewa.korzeniewska@uwm.edu.pl

keywords: *antibiotic resistance determinants; mobile genetic elements; antibiotics; digestate; solid waste.*

Introduction

Due to growing levels of waste generation around the world and a higher demand for alternative and environmentally friendly energy, anaerobic digestion (AD) is becoming an increasingly popular method of stabilizing various types of organic matter substrates. Therefore, the popularity of installations such as biogas plants (BPs) is on the rise in Europe and in the world. Most BPs use manure, sewage sludge and agriculture waste as substrates for AD. These substrates are processed into nutrient-rich digestate finally used mainly as agricultural fertilizer around the world. Digestate is a rich source of nutrients that promote plant growth, but simultaneously it also contains antibiotics, antibiotic-resistant bacteria (ARB) and, antibiotic resistance genes (ARGs). Therefore, there is a high risk that these micropollutants can be transmitted to the soil when digestate is used as organic fertilizer. For this reason, the concentrations and spread of antibiotics and ARGs in digestate produced by agricultural BPs should be monitored to prevent or limit the transmission of ARB and ARGs in the environment, and to minimize selection pressure on environmental microorganisms.

Tetracyclines' broad action spectrum and low-cost favors its wide use in humans and animals. Therefore, in this preliminary study, digestate samples from agricultural BPs stocked with various substrates, including sewage sludge, animal manure, and green waste, were analyzed for the presence of tetracycline group of antibiotics: tetracycline (TC), oxytetracycline (OXY), doxycycline (DOX), chlortetracycline (CHLOR). Digestate samples were also examined for the presence of tetracycline resistance genes such as *tet*A, *tet*M as well as class 1 and 2 integrase genes (*int*I1 and *int*I2) whose reflected the presence of mobile genetic elements (MGEs).

Materials and methods

Three fully operational agricultural BPs operating under mesophilic conditions were selected for the study and labeled as BP1 (sewage sludge), BP2 (cattle manure and maize silage), and BP3 (maize silage, slaughterhouse waste, potato pulp and confectionery press cake). Digestates were sampled in winter and spring seasons which differ in the availability of various substrates, weather conditions (such as temperature) and antibiotic consumption. Digestate samples were collected directly from the outlets of full-scale bioreactors.

The analytical procedure for identifying antibiotics was based on the methods that had been used in our previous research. Genomic DNA (gDNA) from digestate samples was isolated in triplicate, according to the instructions provided by the manufacturer of the Fast DNA Spin Kit for Soil® (MP Biomedicals™). The abundance of *tet*A, *tet*M genes encoding resistance to tetracyclines and the prevalence of class 1 and 2 integrase genes (*intI*1 and *intI*2) were determined in digestate samples. ARGs and intgrase genes were quantified in the quantitative Polymerase Chain Reaction (qPCR) in the LightCycler® system (Roche Diagnostics) according procedure published in our previous papers.

Non-parametric Spearman's correlation analysis and Kruskal–Wallis test (Statistica v. 13.3) was performed to indicate the effect of antibiotic concentration on the ARGs and integrase genes studied. The results were regarded as statistically significant at $p<0.05$.

Results and discussion

Tetracyclines, as a family of broad-spectrum antibiotics, are the most widely used antibiotics in the livestock industry owing to cost-effectiveness and favorable antimicrobial activity. However, antibiotics are generally not completely metabolized because of poor absorption in animal guts, and a portion of parent compounds are excreted via manure or urine in either their original state or as active/non-active metabolites. The analyzed digestate samples contained TC and DOX antibiotics from the tetracycline class. Chlortetracycline and oxytetracycline have not been detected in analysed samples. Tetracycline was identified in samples BP1, in both liquid and solid fractions of the examined matrix. However, TC concentrations differed significantly (Kruskal-Wallis, ANOVA, $p<0.05$) between liquid and solid fractions and it was determined at 464.8 and 1164.4 ng/g in the solid fraction and 275.6 and 368.7 ng/L in the liquid fraction in samples collected in winter and in spring, respectively. Significant differences in DOX concentrations were observed between digestate samples, depending on their substrate composition (Kruskal-Wallis, ANOVA, $p<0.05$). Doxycycline was identified in solid and liquid fractions of the samples collected from two out of the three analyzed BPs (samples BP1 and BP2). In the solid fractions of samples DOX concentration ranged from 218.1 ng/g to even 1282.5 ng/g and in the liquid fractions of samples its concentration was determined in the range of 620.4 ng/L to 1555.9 ng/L.

ARGs as well as integrase genes in substrates processed during anaerobic digestion in agricultural BPs can reach the digestate which is used as fertilizer. Digestates obtained from plant-based substrates were characterized by high concentrations of ARGs ranging from 1.10×10^4 to 2.22×10^6 copies/g_D and from 1.64×10^5 to 2.25×10^6 copies/g_D for *tem*A and *tem*M, respectively. The abundance of class 1 and 2 integrase genes ranged from 2.78×10^5 to 8.76×10^6 copies/g_D and from 1.11×10^5 to 5.84×10^7 copies/g_D for *int*I1 and *int*I2, respectively. The results of this study indicate that tetracycline class drugs are not fully removed in the AD process, and that repeated soil fertilization with digestate containing tetracyclines can lead to their accumulation in soil and can directly affect the soil microbiome and resistome.

Conclusions

Studies confirmed that digestate samples were highly contaminated with various tetracycline antibiotics whose concentrations were influenced by the composition of the substrates processed by the examined BPs. Unlike sewage sludge and cattle manure digestates, the plant-based digestates did not contain drugs, but were characterized by high concentrations of many ARGs and integrase genes. High concentrations of integrase genes suggest that MGEs can participate in the transmission of AR in digestate. The results of this study indicate that the use of digestate as organic fertilizer may increases the risk of soil contamination with antibiotics and ARGs.

Acknowledgements: This research was funded by National Science Center (Poland), grant 2020/37/N/NZ9/00431.

References

Sun H., Schnürer A., Müller B., Mößnang B., Lebuhn M., Makarewicz O., 2022. Uncovering antimicrobial resistance in three agricultural biogas plants using plant-based substrates. Sci. Total Environ., 829, 154556.

Buta M., Korzeniewska E., Harnisz M., Hubeny J., Zieliński W., Rolbiecki D., Bajkacz S., Felis E., Kokoszka K., 2021. Microbial and chemical pollutants on the manure-crops pathway in the perspective of "One Health" holistic approach. Sci. Total Environ., 785, 147411.

Bajkacz S., Felis, E., Kycia-Słocka E., Harnisz M. Korzeniewska E., 2020. Development of a new SLE-SPE-HPLC-MS/MS method for the determination of selected antibiotics and their transformation products in anthropogenically altered solid environmental matrices. Sci. Total Environ., 726, 138071.

Kokoszka K., Zieliński W., Korzeniewska E., Felis E., Harnisz M., Bajkacz S., 2022. Suspect screening of antimicrobial agents transformation products in environmental samples development of LC-QTrap method running in pseudo MRM transitions. Sci. Total Environ., 808, 152114.

Variations of Organic Characteristics for Influent and Effluent of BAC Filter in AOC Bioassay Using SFS with Integrated Areas

Shang-Cyuan Chen[1], Wen –Liang Lai [2,*], Tang-Yao Hong[3]
[1,2.3] Graduate Institute of Environmental Management, Tajen University, Pingtung 907, Taiwan
Corresponding author email: lai@tajen.edu.tw;laisiff@gmail.com

keywords: *AOC bioassay; protein-like fluorescence; microbial humus-like fluorescence; fulvic-like fluorescence; humus-like fluorescence.*

Introduction

Recently, spectroscopic techniques, including ultraviolet–visible (UV–VIS), synchronous fluorescence spectra (SFS), and three-dimensional fluorescence excitation-emission matrices (FEEMs), have been widely used to understand the complexation between DOM and organic contaminants due to their sensitive, non-destructive and rapid analysis techniques. Regarding SFS spectra, the protein-like fluorescence (PLF) peak, microbial humus-like substance, fulvic-like fluorescence (FLF) substance, and humus-like fluorescence (HLF) substance were, respectively, in the wavelength regions of 260–314 nm (Hur et al., 2011), 314-355 nm (Yu et al., 2013), 355–420 nm (Yu et al., 2011), and 420–500 nm (Kalbitz et al., 1999).

In this research, the integrated area in the SFS diagram was applied to compare the variation of organic fluorescent classification for a BAC filter located at CCL water treatment in Southern –Taiwan. as an AOC assay. All data collected, further possible surrogate parameter was also evaluated to replace the tedious, time-consumed, labor-intensive AOC bioassay (Liu et al., 2013).

Materials and methods

The AOC measurement procedures in this investigation were described in the report of Van der Kooij and Veenendaal(KOOIJI, 1995). Both *P. fluorescens* strain P17 (ATCC 49642) and *Spirillum* species, a strain NOX (ATCC 4964,3), was selected in the biometric experiments. In this study, water samples were taken from influent and effluent of the biological activated carbon (BAC) filter. SFS was operated by a fluorescence spectrophotometer (F-4500, Hitachi, Japan) with a xenon lamp as the excitation source. SFS is a technique wherein a simultaneous scan of the excitation and emission spectra is done at a constant difference of 50 nm ($\Delta\lambda=E_{em}-E_{ex}$). Integrated areas in the synchronous fluorescent spectrum were calculated by fluorescent intensity by the increment of excitation wavelength with 1 nm.

Results and discussion

P17 strains.

Regarding the variations of organic characteristics using integrated areas in the SFS diagram, those values on the seventh day and initial day in the AOC-P17 assay applied to influent and effluent from the BAC filter are shown in Figure 1. Figure 1 A reveals that the integrated area on the seventh day is more significant than on the initial day, especially in PLF and MHLF substances. The integrated area of HLF keeps constant while the AOC-17 assay was compared at two-stage incubation. However, a significant increase occurs in PLF substances, and a minor decrease happens in MHLF and FLF substances.

NOX strains.

As for the AOC-NOX strain inoculated into the influent, as shown in Figure2, the integrated areas of PLF and MHLF substance on the seventh day is more significant than on the initial day, but the rising rate is less than that of AOC-P17 bioassay. About the AOC-NOX strain inoculated into the effluent, only the PLF substance shows an increasing amount than other substances; however, its value is still far less than that of AOC-P17 performance on the effluent.

Conclusions

Several findings were summarized as the following. In similar conditions, the integrated area of the SFS diagram of water samples from the BAC filter and the variations of the AOC-P17 assay on the seventh day relative to the initial day is more significant than those of the AOC-NOX assay. Whatever the variation of the four classifications, PLF substances in both AOC assays reveal the same rising trend, indicating that a possible surrogate procedure could be adapted in AOC measurement.

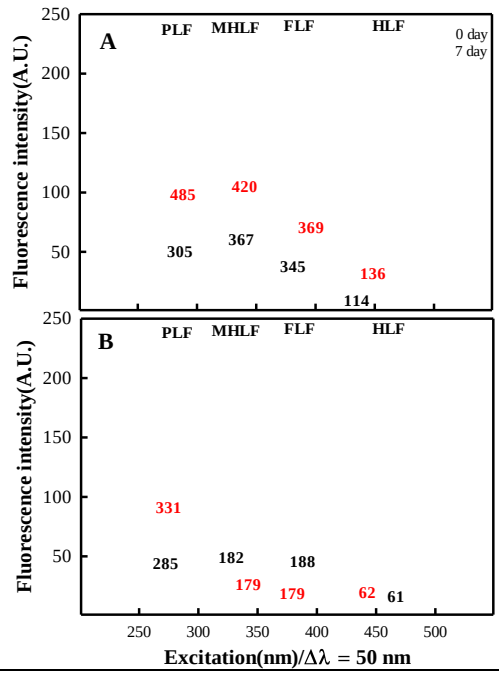

Figure 1. *Variations of organic characteristics using integrated areas from SFS diagram(A)influent (B)effluent of BAC filter in AOC- p17 bioassay. (Bule numeral representing the integrated area at 7th dad; Red numeral representing the integrated area at initial day)*

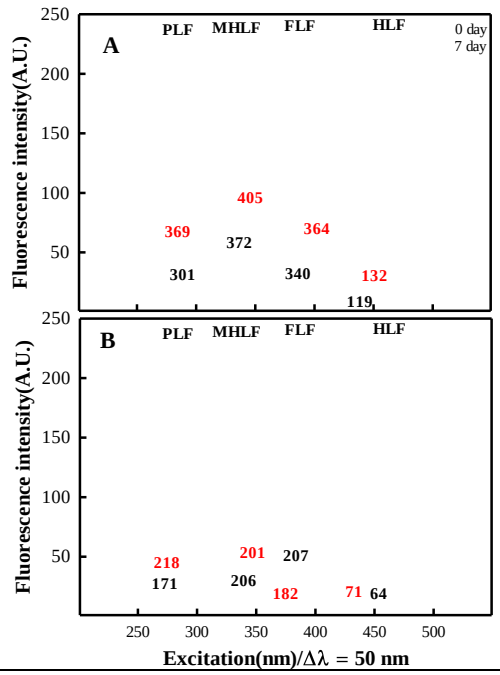

Figure 2. *Variations of organic characteristics using integrated areas from SFS diagram (A)influent (B)effluent of BAC filter in AOC- NOX bioassay. (Bule numeral representing the integrated area at 7th dad; Red numeral representing the integrated area at initial day)*

Acknowledgments

Authors appreciate the financial support from NSC in Taiwan to complete this research (MOST 106-2221-E-127-001; MOST 107-2221-E-127-001-MY2; MOST 110-2221-E-127 -001 -MY2) as well as the assistant, Jing-Wen Cao, and Dr. Ho, Hsiao-Jung who make a strenuous effort, data arrangement, and drawing in the research.

References

Hur, J., Jung, K.Y., Jung, Y.M. (2011) Characterization of spectral responses of humic substances upon UV irradiation using two-dimensional correlation spectroscopy. Water research 45, 2965-2974.

Kalbitz, K., Geyer, W., Geyer, S. (1999) Spectroscopic properties of dissolved humic substances—a reflection of land use history in a fen area. Biogeochemistry 47, 219-238.

KOOIJI, D. (1995) Determination of the concentration of easily assimilable organic carbon (AOC) in drinking water growth measurements using pure bacterial cultures. Kiwa AOC manual.

Liu, G., Van der Mark, E., Verberk, J., Van Dijk, J. (2013) Flow cytometry total cell counts: a field study assessing microbiological water quality and growth in unchlorinated drinking water distribution systems. BioMed Research International 2013.

Yu, H., Song, Y., Tu, X., Du, E., Liu, R., Peng, J. (2013) Assessing removal efficiency of dissolved organic matter in wastewater treatment using fluorescence excitation emission matrices with parallel factor analysis and second derivative synchronous fluorescence. Bioresource technology 144, 595-601.

Yu, H., Xi, B., Ma, W., Li, D., He, X. (2011) Fluorescence Spectroscopic Properties of Dissolved Fulvic Acids from Salined Flavo-aquic Soils around Wuliangsuhai in Hetao Irrigation District, China. Soil Science Society of America Journal 75, 1385-1393.

The energetic potential of surgical masks: a possible approach as solid recovered fuels

S. Pinho[1]

[1]*LEPABE,* Laboratory for Process Engineering, Environment, Biotechnology and Energy, Faculty of Engineering, University of Porto

Corresponding author email: scpinho@fe.up.pt

keywords: *Surgical mask; energetic potencial; incineration.*

Introduction

Until the arising of the novel coronavirus (SARS-CoV-2), the surgical mask was essentially used to protect healthcare professionals from preventing the risk of infections. These wastes generated within healthcare facilities are treated as medical waste. Autoclaving and incineration are the main processes used for treating medical waste. Since the appearance of SARS-CoV-2, the use of face masks has been recommended by the World Health Organization (WHO) and different countries governments to the population to prevent the risk of coronavirus transmission. This recommendation has a phenomenal demand for surgical masks.

The surgical mask to single-use is used by millions of persons worldwide, it is estimated that will be required 129 billion face masks per month by the world population (Prata et al, 2020), causing a colossal increase in the number of masks discarded in unsorted waste, being more worrying when their discarded in the environment. As a result of indiscriminately disposed of the surgical mask into the environment, a new source of microplastics has been emerging. Mask reuse is an option to increase your usage time; therefore, some attention has been turned to decontaminating face masks.

Some researchers have studied decontamination by ultraviolet germicidal irradiation, chemical disinfection, microwaves, and heat-based methods. However, there is limited evidence on the safety or efficacy of decontamination and reuse of surgical masks (Zorko et al. 2020).

In this context, the utilization of wastes, such as surgical masks, that can be used to recover energy and reduce the disposal of landfills could be an option to consider. In the last years, the use of alternative fuel (such as refuse derived fuel, tire derived fuel, sewage sludge, and municipal solid wastes) has shown to be ecologically and economically profitable (Chatziaras and Psomopoulos, 2016). However, current laws only recognize nonhazardous wastes as potential solid recovered fuels (SRF), which does not include the hazardous medical wastes. Nevertheless, in the current pandemic context, the surgical mask used by the population has been managed as urban solid waste.

The objective of this study was to evaluate the energetic potential of using surgical mask wastes as SRF, analyzing the parameters set as mandatory by European standards.

Materials and methods

Surgical masks used in this work consist of three layers; an inner layer made of polyester (PE) and pressed polypropylene (PP), a middle layer constituted by PP and an outer layer made of PP and tapes made of polyurethane.

The gross calorific value was performed at a temperature 25 °C in a bomb calorimeter model Parr 1672 according to EN 15400:2011. The chlorine was carried out according to CEN/TS 15408:2011 and total carbon was determined according to EN 13137 (2001). The ash content and moisture content were determined according to CEN/TS 15403:2011 and CEN/TS 15414-1: 2011, respectively. For metal quantification, the samples were subjected to chemical attack with aqua regia, according to the ISO 11466:1995 standard. The metals were determined in the solutions by Atomic Absorption Spectrometry (AAS). Elemental analysis was carried out on a Vario MICRO cube analyzer from Elemental GmbH in CHNS mode.

Results and discussion

Table 1 shows the mandatory specification parameter values analyzed on the surgical mask. As expected, due to this polymeric composition, the total carbon content was very high as well as the calorific value, and the content of mercury and chlorine was low.

The ISO 21640:2021 standard uses a classification system for SRF based on three parameters: an economic parameter (net calorific value), a technical parameter (chlorine content), and an environmental parameter (mercury content). Each parameter is divided into five classes (described in table 2 of the standard), and the class code consists of a combination of the three classifications.

The net calorific value of the mask is greater than 25 MJ/kg; therefore, is in class 1, the chlorine content was <0.05 %, corresponding to class 1. The median mercury content was 0.0082 mg/MJ, and the 80th percentile value was 0.0092 mg/MJ, thus corresponding to class 1. Therefore, the surgical mask with the characteristics described has the following classification code: PCI 1; Cl 1; Hg 1.

***Table 1**. Mandatory specification parameters*

Parameter	Value
Total carbon, %	84.54 ± 0.72
Hydrogen, %	12.82 ± 0.55
Ash content, %	5.40 ± 0.05
Moisture content, %	0.66 ± 0.02
Gross calorific value, MJ/kg	43.64 ± 0.003
Net calorific value, MJ/kg	40.85 ± 0.003
Chlorine, %	<0.05
Mercury [mg/MJ] Median 80th percentile	0,0082 0.0092
∑ Heavy metals (mg/kg)	24.56

Conclusions

Although it is lower than diesel and fuel oil, the calorific value of the masks is above coal, so it can say that the capacity of these residues can be used as an alternative fuel. This capacity is also ensured by its classification according to ISO 21640:2021 since, in terms of economic, technical, and environmental parameters, they are class 1, which is the best value provided for in the standard.

References

Chatziaras, N, Psomopoulos, C. S., 2016. Use of waste derived fuels in cement industry: a review. *Management of Environmental Quality: An International Journal*, 27, 178–193

EN 15400:2011. Solid recovered fuels - Determination of calorific value.

EN 13137:2001. Characterisation of waste – Determination of total organic carbon (TOC) in wastes, sludges and sediments.

EN 15403:2011**.** Solid recovered fuels - Determination of ash content.

EN 15414-1: 2011. Solid recovered fuels - Determination of moisture content using the oven dry method - Part 3: Moisture in general analysis sample.

ISO 11466:1995. Soil quality—Extration of trace elements soluble in aqua regia.

ISO 21640:2021. Solid recovered fuels — Specifications and classes.

Prata, JS., Silva, AL., Walker, TR., et al., 2020. COVID-19 pandemic repercussions on the use and management of plastics. *Envirnomental Science & Technology*, 54, 7760 – 7765.

Zorko, DJ., Gertsman, S., O´Hearn, K., et al, 2020. Decontamination interventions for the reuse of surgical mask personal protective equipment: a systematic review. *Journal of Hospital Infection*, 106, 283-294

A nanopore long-read sequencing points out a modification of hospital wastewater microbiome after chlorine disinfection

D. Rolbiecki [1], Ł. Paukszto[2], K. Krawczyk[2], E. Korzeniewska[1] J. Sawicki[2] and M. Harnisz[1*]

[1]Department of Water Protection Engineering and Environmental Microbiology, University of Warmia and Mazury in Olsztyn, Poland
[2]Department of Botany and Nature Protection, University of Warmia and Mazury in Olsztyn, Poland
Corresponding author email: monika.harnisz@uwm.edu.pl

keywords: *chlorination; disinfection; hospital; wastewater; microbiome.*

Introduction

Hospital wastewater (HWW), discharged from operating rooms, laboratories, and infectious wards contains pathogenic microorganisms, toxic organic pollutants, and pharmaceutical compounds such as antimicrobials and psychiatric drugs. The presence of numerous pathogenic bacteria in HWW highlights the potential threat to public health posed by HWW discharge to municipal sewer systems followed by wastewater treatment plants and receiving water. To reduce that risk, HWW is often treated in local disinfection stations. Chlorine-based wastewater disinfection is widely used around the world.

The aim of this study was to analyze changes in the HWW microbiome caused by the process of chemical disinfection based on chlorine compounds. The nanopore method was used to sequence the metagenome DNA of HWW samples collected before and after the disinfection process in four research seasons. The long reads obtained enabled the direct identification of the host taxa of ARGs.

Materials and methods

The research object and the sampling procedure were previously described in detail in the preliminary studies (Rolbiecki et al. 2022). In short, the study was conducted in a hospital that treats patients with respiratory diseases in north-eastern Poland. Wastewater is disinfected by an automated electrolytic sodium hypochlorite (NaClO) generation system. Samples of wastewater before disinfection and samples of disinfected wastewater were analyzed. The samples were collected in four seasons: spring (20 April 2021), summer (24 August 2021), fall (16 November 2021), and winter (3 February 2022).

Extracted and purified eDNA samples was sequenced using ONT long-read technology, which enable strain level characterization of microbiomes.

Results and discussion

Depending on the sample, 172,532 - 865,879 reads were analyzed, of which 37.28 to 94.86% of reads were successfully taxonomically classified. The vast majority of them (94.65-97.94%) were classified to *Bacteria* domain, and the others to *Eukaryota* (1.68-4.24%), Viruses (0.12-1.02%) and *Archaea* (0.01-0.09%) domains, respectively. A total of 37 types, 74 classes, 167 orders, 387 families and 1,442 genera were detected in hospital wastewater samples. In the samples of hospital wastewater, the dominance of 4 phyla was observed: *Proteobacteria, Bacteroidetes, Cyanobacteria* and *Firmicutes*, whose representatives represented 97.87% and 99.28% of the entire bacterial population in the wastewater before and after disinfection, respectively. In the HWW samples, bacteria from the Proteobacteria group dominated at both sites. This cluster increased its frequency in disinfected wastewater samples (on average by 5.64%, from 53.27 to 59.91%). An increase was also observed for *Cyanobacteria* (by 15.66%, from 0.06% to 15.72%) (Fig. 1). Representatives of *Bacteroidetes* and *Firmicutes* clusters decreased their share in the bacterial population in the samples after disinfection (*Bacteroides* decrease by 17.30%, from 31.86 to 14.56%; *Firmicutes* decrease by 2.60%, from 12.68 to 10.08%). However, no significant differences were observed in the total composition of bacterial populations at the assigned sites at the cluster level (adonis R2=0.2, p=0.24).

Discriminant analysis indicated the class *Clostrida* with the order *Eubacteriales* as the most strongly associated with the sewage before disinfection, and the family *Enterobacteriaceae* as the most closely associated with the site of disinfected sewage. The analysis of the frequency of pathogens from ESKAPE group showed differences in the frequency of specific species: *Acinetobacter baumannii, Klebsiella pneumoniae, Enterococcus faecium, Pseudomonas aeruginosa, Staphylococcus aureus* and *Enterobacter* genus in wastewater samples before and after disinfection. The disinfection process resulted in a statistically insignificant decrease in the frequency of *Enterococcus faecium, Staphylococcus aureus and Acinetobacter baumannii*. However, disinfection resulted in a significant increase in the incidence of bacteria belonging to the *Enterobacteriaceae* family: *Klebsiella pneumoniae* species and *Enterobacter* genus.

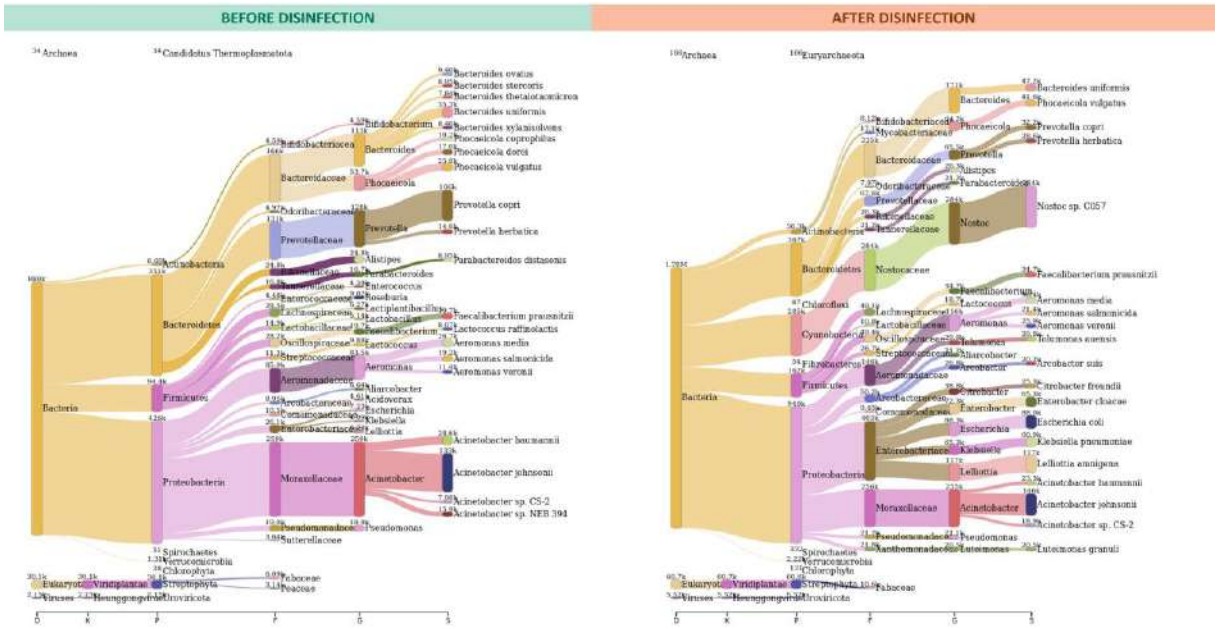

Figure 1. Sankey diagrams showing the distribution of the reading pool between taxa in wastewater samples before disinfection (left side) and after disinfection (right side). The distribution of reads is shown for all taxa (including Archaea, Eukaryota, Viruses domains). The number of readings characteristic for that taxon is shown next to the taxon name. Distribution is shown at different taxonomic levels (X-axis) including domain (D), kingdom (K), phylum (P), family (F), genus (G) and strain (S). Minimum abundance cutoff 0.5% was applied.

Conclusions

The research provides new insights into the changes in the population of bacteria present in HWW. The results suggest that disinfection with chlorine compounds significantly modifies the bacterial community mainly by the increase of *Enterobacteriaceae* frequency in HWW after disinfection. Consequently, despite the use chlorine-based disinfection, HWW may pose a risk to the environment and public health.

Acknowledgements: This research was funded by grants from the National Science Center (Poland) No. 2021/41/N/NZ9/03292.

References

Rolbiecki D., Korzeniewska E., Czatzkowska M., Harnisz M., 2022. The impact of chlorine disinfection of hospital wastewater on clonal similarity and ESBL-production in selected bacteria of the family *Enterobacteriaceae*. Int. J. Environ Res. Public Health, 19, 13868. https://doi.org/10.3390/ijerph192113868

2nd International Conference on
Sustainable Chemical and
Environmental Engineering
14th – 18th June 2023, Limassol, Cyprus

Experimental and Mathematical study on CO_2 separation performance of biogas using commercial polyimide hollow membrane in a 2-stage process

C. Koutsiantzi[*,1], P. Gkotsis[2], A. Zouboulis[2], M. Mitrakas[1] and E. Kikkinides[1]

[1]Department of Chemical Engineering, Aristotle University of Thessaloniki
[2]Department of Chemistry, Aristotle University of Thessaloniki
* Corresponding author email: vkoutsiantzi@gmail.com

keywords: *Biogas Upgrade; Membranes; Gas Separation; CO_2 removal; 2 stage Separation; Mathematical Modeling.*

Introduction

Biogas is considered a renewable energy source, which is expected to play an important role in the future of meeting energy needs worldwide (Nguyen et al., 2020). The production of biogas is achieved by the decomposition of organic matter, in the absence of oxygen. Specifically, biogas is the product of the anaerobic digestion of microorganisms in a closed system, such as in an anaerobic digester (or bioreactor). Methane (CH_4) and carbon dioxide (CO_2) are the main components of biogas, while traces of moisture and hydrogen sulfide (H_2S) are also contained. After biogas upgrading, the process which leads to the production of biomethane, it can be used as a fuel. The capture and use of the CO_2, which is separated in the permeate stream either directly or after treatment (cleaning) is a promising approach, which in the context of a circular economy reuses an environmentally harmful gas by converting it into a useful product for future applications (Khosroabadi et al., 2021). Previous studies and tests on membrane biogas upgrading have shown that the production of high purity biomethane (>95%) is feasible for 1-stage processes, but the capture of a CO_2-rich permeate stream (>95%) is not easily achieved employing 1-stage processes (Koutsiantzi et al., 2022).

Materials and methods

The gas feed is a binary mixture of CH4/CO2 in various concentrations simulating that of biogas, and the goal is to recover high purity of CH4 (>95%) at the retentate stream of the 1st stage, and then use an identical 2nd stage for further treatment of the permeate stream to recover high purity CO2 (>95%). At the laboratory unit, the mass flow of the inlet gas mixture, was controlled by a mass controller between 1000-3000 mL/min and the feed pressure was controlled by a back pressure regulator (BPR) in a range between 2-10 bars. The gas streams were analyzed directly, applying a specific gas analyzer for the CH4 and CO2 content. The examined membrane is the polyimide hollow fiber UBE UMS-B2 module. The biogas upgrade membrane assembly in continuous flow is designed to operate under the optimal defined separation conditions.

A cross-flow mathematical model is employed to describe the process (Geankoplis, 2003). The model has been validated against experimental data, in 1-stage configurations and accordingly it is employed to simulate the 2-stage membrane separation process.

Results and discussion

It is seen that for the 2-stage separation process of 60%/40% CH4/CO2 mixture, at a feed pressure of 5 bar, a high purity CH4 of 95% is achieved in the retentate stream, while an enhanced CO2 purity between 75-90% is achieved in the permeate stream. The latter is fed to the 2nd membrane module, reaching a CO2 purity above 95% in the permeate stream of the 2nd stage. Hence an overall CO2 purity above 95% with overall CO2 recoveries around 90% can be obtained with the proposed 2-stage membrane separation process, as can be seen in Fig. 1.

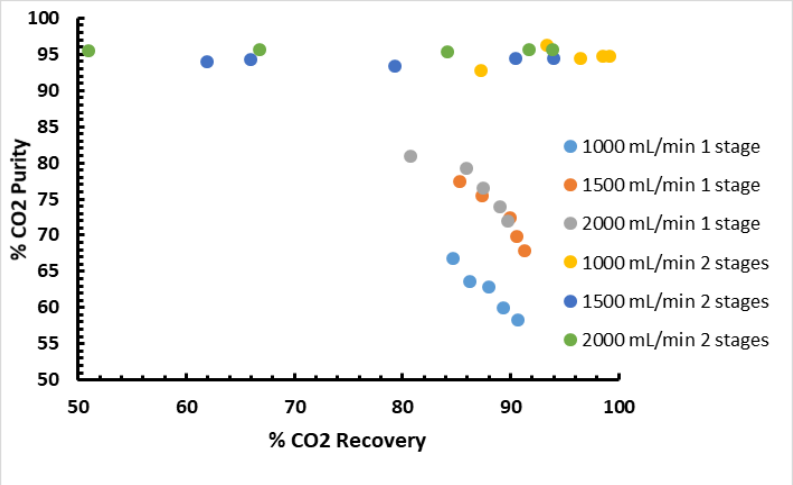

Figure 1 Comparison of CO_2 recovery and purity in permeate stream for 1- and 2-stage processes. (65/35% CH4/CO2, P=5-9 bar for the 1st stage, and P= 2 bar for the 2nd stage (first exit))

Acknowledgements: This research has been co-financed by the European Union and Greek national funds through the Operational Program Competitiveness, Entrepreneurship, and Innovation, under the call RESEARCH-CREATE-INNOVATE (project code: T2EDK-01293).

References

Geankoplis, Christie. J. (2003). *Transport Processes and Separation Process Principles: (includes Unit Operations)* (4th ed.). Prentice Hall Professional Technical Reference.

Khosroabadi, F., Aslani, A., Bekhrad, K., & Zolfaghari, Z. (2021). Analysis of Carbon Dioxide Capturing Technologies and their technology developments. *Cleaner Engineering and Technology*, *5*, 100279. https://doi.org/https://doi.org/10.1016/j.clet.2021.100279

Koutsiantzi, C., Mitrakas, M., Zouboulis, A., Kellartzis, I., Stavropoulos, G., & Kikkinides, E. S. (2022). Evaluation of polymeric membranes' performance during laboratory-scale experiments, regarding the CO2 separation from CH4. *Chemosphere*, *299*, 134224. https://doi.org/https://doi.org/10.1016/j.chemosphere.2022.134224

Nguyen, L. N., Kumar, J., Vu, M. T., Mohammed, J. A. H., Pathak, N., Commault, A. S., Sutherland, D., Zdarta, J., Tyagi, V. K., & Nghiem, L. D. (2020). Biomethane production from anaerobic co-digestion at wastewater treatment plants: A critical review on development and innovations in biogas upgrading techniques. *Science of The Total Environment*, 142753. https://doi.org/https://doi.org/10.1016/j.scitotenv.2020.142753

Analysis of the Impact of Renewable Energy Promotion Policy on Taiwan's Electricity Mix

S. K. Ning[1] and J. S. Huang[2]

[1] Professor, Department of Civil and Environmental Engineering, National University of Kaohsiung, Taiwan.
[2] Graduate Student, Department of Civil and Environmental Engineering, National University of Kaohsiung, Taiwan
Corresponding author email: ning@nuk.edu.tw

keywords: *electricity mix; feed-in tariff; renewable energy; mathematical programming model.*

Introduction

In order to maintain economic development while taking into account environmental protection, countries around the world are actively developing renewable energy to replace the use of fossil energy, and have formulated a series of renewable energy systems to accelerate its growth. Taiwan is a resource-poor country, and most of its energy is imported. In recent years, many development plans and large-scale industrial expansions have been proposed, which have increased the demand for energy. How to supply more energy that is environmentally friendly and has high stability is the most important issue at present. In this regard, the government has formulated many systems such as Renewable Portfolio Standards (RPS), Feed-in Tariff (FIT), and Renewable energy certificate, REC) are promoted to encourage the development of renewable energy in recent years, hoping to accelerate the increase in the proportion of renewable energy There are many studies on the use of mathematical programming models to assist energy allocation. Factors considered include energy technology, energy costs, economic impacts, environmental impacts, and national policies. The techniques used include linear programming models (Iniyan and Sumathy, 2003), game theory (Florentino and Sartori, 2003), life cycle assessment (Ning and Wu, 2019) and index system (Granovskii et al., 2006), etc. This study uses the technology of optimization model analysis, considering the energy cost, energy supply and demand, technology conversion and environmental impact to evaluate the Impact of renewable energy FIT program on Taiwan's electricity mix.

Materials and methods

A mathematical programming model with the considerations of energy cost changes, energy demand growth, energy development potential and technology conversion period was established to realize the influence of renewable energy promotion strategies on the electricity mix with the goal of minimizing energy supply costs and/or environmental impact. Through the analysis of four scenarios, try to establish the most suitable power configuration in Taiwan. Table 1 shows the planning objectives and constraints set for each scenario. The settings of parameters as list in Table 2.

Table 1. *The settings of various scenarios*

scenario	Objective	Constraint
1	Minimize energy supply costs	energy demand growth energy cost changes energy development potential technology conversion period
2	Minimize energy supply costs*	
3	Minimize greenhouse gas emissions	
4	Minimize greenhouse gas emissions*	
Remark	* included renewable energy promotion program	

Table 2. *The settings of parameters*

Type of power	coal	oil	nature gas	solar	wind	hydro	Geo-thermal	Incine-ration	bio-gas	nuclear
Unit cost in 2020 (NT$/Kwh)	1.32	5.26	1.91	6.521	2.916	2.842	5.227	2.233	3.953	1.95
Cost annual growth rate (%)	0.52	0.63	1.2	-2.19	1.79	0.11	-1.18	0.11	-0.62	1
Carbon emission factor	800	650	400	58	5	5	45	1340	18	5

(g-CO_2/Kwh)										

Results and discussion

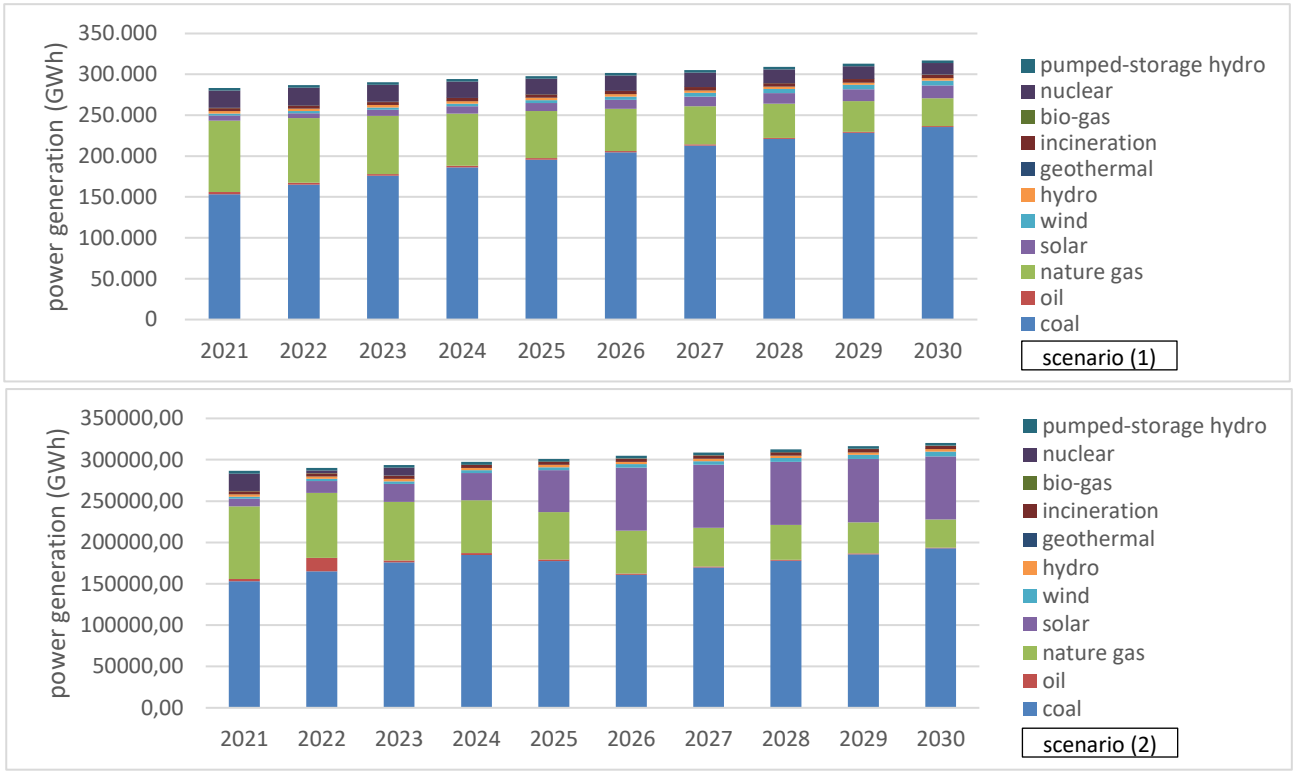

Figure 1. *The electricity mix for scenario (1) and (2)*

Conclusions

1. The promotion of the renewable energy system has had obvious effects on the development of renewable energy. However, during the planning period, both solar and wind power generation have reached the upper limit of the energy generation potential of this energy.
2. When the energy cost is considered in the planning objective, the main source of electricity is still the low-cost coal-fired power generation, and it is used as the main energy type of base load electricity. When considering greenhouse gas emissions, the main source of electricity will be natural gas power generation, followed by renewable energy, but this will obviously increase the cost of power generation.
3. Solar power generation has excellent performance in terms of cost and greenhouse gas reduction, but it has high water resource consumption. On the contrary, wind power generation has low water resource consumption, but is limited by terrain and environment. Therefore, more thoughtful consideration should be given to the selection of renewable energy types.

Acknowledgements: The authors would like to thank the National Science Council in Taiwan for supporting this study (MOST 108-2221-E-390 -014 -MY3).

References

Florentino, H. d. O. and Sartori, M. M. P., 2003. Game theory in sugarcane crop residue and available energy optimization, *Biomass & Bioenergy* 25, 29–34.

Granovskii, M., Dincer, I. and Rosen, M. A., 2006. Economic and environmental comparison of conventional, hybrid, electric and hydrogen fuel cell vehicles. *Journal of Power Sources* 159, 1186–1193.

Iniyan, S. and Sumathy, K., 2003. The application of a Delphi technique in the linear programming optimization of future renewable energy options for India. *Biomass & Bioenergy* 24, 39–50.

Ning, S. K. and Wu, C. 2019. Integrating life cycle assessment and optimization model to evaluate the environmental impact of Taiwan's power structure, 5th International Conference on Environmental Science and Technology, 9-13 Oct, Sarajevo, Bosnia and Herzegovina.

Screen-printing interdigitated microelectrodes for dielectrophoretic alignment MWCNT-based flexible gas sensors

I. Turcan[1], T. A. Filip[1] and M. A. Olariu[1]

[1] Department of Electrical Measurements and Materials, Faculty of Electrical Engineering, Technical University of Iasi, Iasi, Romania
Corresponding author email: ina.turcan@yahoo.com

keywords: *screen-printed interdigitated microelectrodes; carbon nanotube; dielectrophoresis.*

Introduction

Nano- or microparticles as carbon nanotubes (single- or multi-walled), nanorods, nanowires or onion-like carbon have been extensively employed as sensing elements for developing various impedimetric or chemoresistive sensors. The basic working principle in developing these sensors assumes immobilization of sensing element(s) at the level of interdigitated microelectrodes (µIDEs) using dielectrophoretic (DEP) force. Manipulation of carbon nanotubes (CNTs) with DEP is widely used in microfluidic systems and the fabrication of electronic devices such as transistors and sensors. The electrode's geometry is the main component in DEP systems due to its role in shaping the electric field gradients, thus controlling the density and location where CNTs might trap. Moreover, electrodes provided with wide gaps (spacing) are desirable in CNT based sensor applications in order to increase the detection area of the sensing material. The screen-printing technique is a common technique for fabrication of electrodes of optimal pattern geometries on various substrates with the advantages of fast processing, low fabrication cost, and high throughput, all of which make it suitable for DEP electrode fabrication.

Within the herein paper, we are reporting the functionality of DEP for electromanipulation of multi-walled carbon nanotube (MWCNTs) with the help of screen-printed silver based µIDEs. In order to ensure optimal generation of DEP forces, the effect of the printed µIDEs geometry (line and castellated) on the induced electric field have been priory numerically simulated in COMSOL Multiphysics while afterwards, the convenient architecture was selected and used within the stage of manufacturing the µIDEs. The density and location of the deposited MWCNTs are easily controlled by varying the AC signal parameters. The role of the signal amplitude, frequency and time was investigated experimentally.

Materials and methods

The dielectrophoretic alignment of MWCNTs has a simple setup consisting of three main components, which are the screen-printed electrodes, MWCNTs medium, and an AC signal source.

The flat screen-printing experiments were performed with the help of a precision hand-guided screen-printer by employing a 325 stainless steel screen-mask with a 10 µm EOM (Emulsion on mask) and a diamond shape squeegee. Conductive silver Ag-510 ink (Kayaku Advanced Materials, USA) was screen-printed on the polyester based substrates commercially available under the name of ST506. The screen-printing process variables were the following: snap-off distance 2 mm and curing temperature 110^{o}C.

The commercially available MWCNT powder (NanoLab Inc.), with a length of 5–20 µm and a diameter of 30±15 nm, was dispersed by sonication in low conductivity (6.5 mS/m) surfactant based water solution.

For the DEP experiments, a Keysight 33521A Function/Arbitrary Waveform Generator was employed to generate a sinusoidal AC electric field. The electrodes were connected to the generator by using a Micrux drop-cell connector. The MWCNTs distribution at microelectrode level was monitored and recorded using Dino-Lite Edge Digital Microscope AF4915ZTL.

Results and discussion

Numerical simulations indicated that for interdigitated line electrodes, the electrical field intensity increases to the maximum value at the edges of microelectrodes and drops to the minimum value in the center between two neighboring electrodes (figure 1a). For castellated electrodes, the strongest and

weakest electric fields are located at the electrode tips and intermediate region between electrode tips, respectively (figure 1 b). Given the same simulation conditions, i.e., the applied voltage was 5 V and gap between neighboring electrodes was 150 µm, the value of the electric field is maintained constant at a value around 1.7 *10^4 V/m for interdigitated line electrodes and 2.2*10^4 V/m for castellated electrodes (at the electrode tips), indicating that castellated electrodes can generate larger DEP forces compared with interdigitated line electrodes.

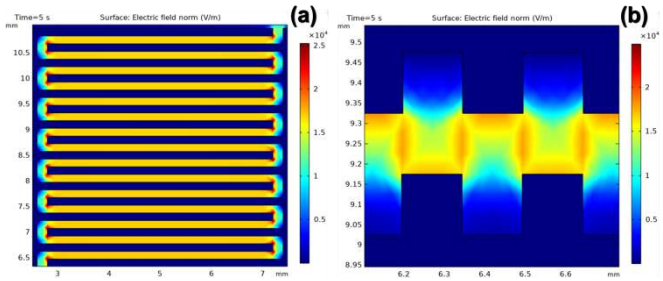

Figure 1. *Simulated electric field distributions for various electrode configurations: linear (a) and castellated (b).*

The DEP trapping of MWCNTs to the castellated microelectrode was performed with ac voltage of different frequencies and amplitudes for 5 minutes in order to analyze the particle's motion under non-uniform electric. Voltage amplitude of 15 V was enough to polarize MWCNTs and align them between the microelectrode edges to form connections of 150 µm in a few minutes. Signals with low frequencies (<10^5 Hz) resulted in medium drag velocity dominated the MWCNTs motion, while high frequencies (>10^5 Hz) resulted in positive DEP derived the MWCNTs to the deposition location.

Conclusions

In this work, MWCNTs with controllable bridging were successfully deposited across screen-printed silver based µIDEs using dielectrophoretic (DEP) force. For the first time, the isolation of MWCNTs across castellated microelectrodes separated by a distance of 150 µm is demonstrated to form an aligned network. The role of the AC signal amplitude, frequency, and duration was investigated experimentally. We found that the alignment was improved as the frequency increases (>10^5 Hz). The results of this study could serve as a basis in integrating MWCNT-based flexible gas sensors for environmental monitoring.

Acknowledgements: This study is supported by a grant of the Romanian Ministry of Research, Innovation and Digitization, CNCS - UEFISCDI, project number PN-III-P1-1.1-TE-2021-0751, within PNCDI III.

References

M.T. Rabbani, M. Sonker, A. Ros, 2020. Carbon nanotube dielectrophoresis: Theory and applications. *Electrophoresis*, 41, 1893–1914.

A. Abdulhameed, M.N. Mohtar, M.N. Hamidon, I. Mansor, I.A. Halin, 2021. The role of the AC signal on the dielectrophoretic assembly of carbon nanotubes across indium tin oxide electrodes. *Microelectron. Eng.*, 247, 111597.

A. Abdulhameed, I.A. Halin, M.N. Mohtar, M.N. Hamidon, 2022. The role of the electrode geometry on the dielectrophoretic assembly of multi-walled carbon nanotube bundles from aqueous solution. *J. Electrostat.,* 116, 103694.

Valorization of citrus processing industry waste for production of essential oils, pectin and bacterial cellulose

P. Karanicola[1,2], M. Patsalou[1], A. Nicodemou[1,2], N. Evripidou[3], P. Christou[2], G. Panagiotou[2], C. Damianou[3] and M. Koutinas[1]

[1]Department of Chemical Engineering, Cyprus University of Technology, 30 Archbishop Kyprianou Str., Limassol, Cyprus
[2]KEAN Soft Drinks, Ltd, Promachon Eleftherias, Agios Athanasios, Limassol, Cyprus
[3]Department of Electrical Engineering, Computer Engineering and Informatics, Cyprus University of Technology, 30 Archbishop Kyprianou Str., Limassol, Cyprus
Corresponding author: michail.koutinas@cut.ac.cy

keywords: *Citrus processing waste; Ultrasound-assisted dilute acid hydrolysis; Bacterial cellulose; Essential oils; Pectin.*

Introduction

Citrus processing industry (CPI) for juice and concentrate, generates substantial amounts of by-products given that only 50% of the fruit's mass is used during the production process. The worldwide production of citrus fruits accounts for 143 x 106 t per year resulting in industrial generation of citrus peel waste (CPW) which exceeds 24 x 106 t and mainly consists of peels, pulp, seeds and segments membranes (Patsalou et al., 2020). Bacterial cellulose (BC) constitutes a biopolymer of high industrial importance owing to numerus unique properties including high purity, high crystallinity, biodegradability and enhanced mechanical strength (Hussain et al., 2019). Herein, a citrus processing waste-based biorefinery was developed employing CPI waste using ultrasound-assisted dilute acid hydrolysis (UADAH) targeting production of essential oils (EO), pectin and BC.

Materials and methods

CPI waste was characterized in terms of hemicellulose, cellulose, lignin and ash content using standard analytical methods, while the EO content was determined through Gas Chromatography. UADAH was employed for valorization of CPI waste aiming to produce pectin, EO and a sugar rich-hydrolysate. Optimization of the UADAH process was conducted identifying the experimental parameters maximizing the yield for EO, pectin and reducing sugars (RS), assessing different solid loadings, acid concentrations and reaction durations at constant temperature. Following UADAH, EO was isolated via liquid-liquid extraction, while pectin was recovered using ethanol precipitation. The resulting sugar-rich hydrolysate was employed in bacterial fermentations using *Komagataeibacter sucrofermentans* DSM 15973 as cellulose producer.

Results and discussion

CPI waste consisted of 23.1% cellulose, 4.8% hemicellulose, 0.5% lignin, 4.5% ash and 0.1% EO, while application of the UADAH process resulted in maximal production yields of EO (3.35 mg_{EO} $g_{dry\ basis\ (db)}^{-1}$), RS (0.31 g_{RS} g_{db}^{-1}) and pectin (0.41 g_{pectin} g_{db}^{-1}) at 1.21% H_2SO_4, 5.75% solid loading and 34.2 min process duration. The sugar-rich hydrolysate formed was employed in BC fermentations resulting in the production of 0.67 g L^{-1} BC and a corresponding yield of 5.82 g_{BC} per 100 g_{CPW}.

Conclusions

The present study demonstrated the application of UADAH as a valuable process for valorization of citrus processing waste towards manufacture of a range of commodities including EO, pectin and BC.

Acknowledgements: The work is part of the project BioTECPro (ENTERPRISES/0521/0185) funded by the Cyprus Research & Innovation Foundation.

References

Hussain, Z., Sajjad, W., Khan, T., Wahid, F. (2019). Production of bacterial cellulose from industrial wastes: A review. *Cellulose*, 26(5), 2895-2911.

Patsalou, M., Chrysargyris, A., Tzortzakis, N., Koutinas, M. (2020). A biorefinery for conversion of citrus peel waste into essential oils, pectin, fertilizer and succinic acid via different fermentation strategies. *Waste Management* 113, 469-477.

Enhancement of glucose yield from potato starch through hydrolysis via immobilization of *Aspergillus awamori* and *Aspergillus niger* on carbonaceous materials

M. Patsalou[1] and M. Koutinas[1]

[1]Department of Chemical Engineering, Cyprus University of Technology, Limassol, 30 Archbishop Kyprianou Str., Cyprus
Corresponding author email: michail.koutinas@cut.ac.cy

keywords: *starch; enzyme hydrolysis; char; immobilization.*

Introduction

Potato (*Solanum tuberosum*) consists the third largest food crop worldwide following cereal crops (rice, wheat), while its production accounts for 360 million t per year (FAO, 2022). The low requirements for its cultivation and the high starch content entailed renders potato a promising alternative raw material for saccharification and fermentation for the production of biofuels (Lareo and Ferrari, 2019). Saccharification of starchy substrates commonly requires application of acid and/or enzyme hydrolysis, where the enzymatic process can be performed under mild conditions, as compared to acid hydrolysis, resulting in high rate of biomass conversion to glucose (Bansal *et al* 2021).

Enzyme hydrolysis of starchy materials is performed in the presence of amylolytic enzymes, such as α-amylases and glucoamylases, which comprise the main highly efficient starch-degrading enzymes (Hua and Yang, 2016). Over the past decades, various researchers have assessed fungi such as *Aspergillus niger*, *Aspergillus awamori* or *Aspergillus oryzae* towards *in situ* production of amylolytic enzymes (Wang *et al* 2008, Haque *et al* 2016). Furthermore, *Aspergilli* hold the capacity to produce proteases enabling simultaneous hydrolysis of proteins, which constitutes an activity needed in a range of biotechnological applications (Silva-Lopez *et al* 2022).

Whole cell immobilization has attracted increasing interest for application in industrial biotechnology. Different carriers such as magnetic (Hermida and Agustian, 2022) and carbonaceous materials (Kyriakou *et al* 2019) have been assessed as cell immobilization matrices to improve biological processes including enzyme hydrolysis and ethanol fermentations. Specifically, carbonaceous materials (e.g. activated carbon, biochar) hold the capacity to assist interspecies electron transfer, buffering capacity and nutrient adsorption into their surface, improving cell activity and growth (Kyriakou *et al* 2019).

Herein, different types of carbonaceous materials were assessed as immobilization carriers to enhance starch hydrolysis. Specifically, *Aspergillus niger* and *Aspergillus awamori* were applied for amylolytic enzyme production, which was subsequently immobilized on the carriers selected to enhance the saccharification yield of the process.

Materials and methods

Potato (Spunta) was applied as starchy substrate, which was obtained from a local potato producer (Nicosia, Cyprus) and directly used in experiments upon collection. Characterization of potato was performed employing standard analytical methods including Kjeldahl nitrogen analysis, as well as ash, starch and fibre (cellulose, hemicellulose) content.

Aspergillus niger MUCL 28817 and *Aspergillus awamori* MUCL 28815 were employed in the enzyme hydrolysis process, while carbonaceous materials, char and biochar obtained via pyrolysis of recycled car tyres and pistachio shells respectively, were used as immobilization carriers.

Potato starch saccharification was determined during enzyme hydrolysis via analysis of reducing sugars' concentration through DNS method.

Results and discussion

Potato was initially characterized constituting 16.55% dry matter, 0.82% total nitrogen, 5.10% protein, 7.56% ash, 12.57% starch, 12.92% hemicellulose and 1.30% cellulose. The varying composition reported for potato (current study, Kita 2002, Sato *et al* 2017) could be attributed to a wide range of parameters associated to crop cultivation.

Potato infusion was used for *Aspergillus niger* and *Aspergillus awamori* cultivation, while 20% of potato solids was employed for saccharification. A preliminary study was conducted to determine the most efficient conditions for cultivation and enzyme production using each microorganism. Specifically, freely suspended and immobilized cells as well as free and immobilized enzymes were assessed for their capacity to hydrolyze potato starch using char as immobilization material. The release of reducing sugars in each trial indicated that immobilized *Aspergillus niger* cells and enzymes performed elevated saccharification rates as compared to the use of freely suspended cells and enzymes. Lower increase in reducing sugars yields were also observed in trials performed by immobilized *Aspergillus awamori* cells and enzymes as compared to the use of freely suspended cells and enzymes. Moreover, the two fungi strains were immobilized using different contents of char (1.6%, 3.2%, 6.4%, 12.8% and 25.6%) demonstrating that 3.2% of the material enhanced the release of glucose by both microorganisms applied. Char and biochar were additionally employed in different particle sizes as immobilization carriers for potato starch hydrolysis. Results demonstrated that the particles incorporating diameter between 0.3-0.5 cm enabled higher production of reducing sugars (20-25 g L^{-1} final concentration) as compared to the use of smaller particles (15 g L^{-1}) using char as material for immobilization of both fungi. Moreover, the co-cultures of the two strains assessed exhibited elevated glucose yields. The study will additionally include determination of enzyme activity during the process.

Conclusions

The current work constitutes a preliminary study demonstrating the potential for substantial enhancement of *Aspergillus niger* and *Aspergillus awamori* amylolytic activity using carbonaceous materials as immobilization carriers.

References

Bansal R., Katyal P., Jain D., 2022. Enzymatic and acidic hydrolysis of cull potatoes for production of fermentable sugars. *Starch* 74:1–2.

FAO, 2022, https://www.fao.org/3/cc0330en/cc0330en.pdf

Haque M.A., Kachrimanidou V., Koutinas A., Lin C.S.K., 2016. Valorization of bakery waste for biocolorant and enzyme production by *Monascus purpureus*. *Journal of Biotechnology* 231: 55–64.

Hermida L., Agustian J., 2022. The application of conventional or magnetic materials to support immobilization of amylolytic enzymes for batch and continuous operation of starch hydrolysis processes. *Reviews in Chemical Engineering*

Hua X., Yang R., 2015. Enzymes in starch processing In: Enzymes in food and beverage processing.

Kita A., 2002. The influence of potato chemical composition on crisp texture. *Food Chemistry* 76: 173–179.

Kyriakou M., Chatziiona V.K., Costa C.N., Kallis M., Koutsokera M., Constantinides G., Koutinas M., 2019. Biowaste-based biochar: a new strategy for fermentative bioethanol overproduction via whole-cell immobilization. *Applied Energy* 242: 480–491.

Lareo C., Ferrari M.D., 2019. Sweet potato as a bioenergy crop for fuel ethanol production: Perspectives and Challenges In: Bioethanol production from Food Crops.

Sato H., Koizumi R., Nakazawa Y., Yamazaki M., Itoyama R., Ichisawa M., Negichi J., Sakuma R., Furusho T., Sagane Y., Takano K., 2017. Data on the weights, specific gravities and chemical compositions of potato (*Solanum tuberosum*) tubers for food processing from different areas of Hokkaido, Japan. *Data in Brief* 11:601–605.

Silva-Lopez R.E., Araujo T.A.A., Monteiso H.J.J., Teixeira E.M.G.F, Tupi L., Silva Bon E.P., 2022. Study of protease activity from *Aspergillus awamori* INCQS2B.361U2/1 extracellular fraction and modification of culture medium composition to isolate a novel aspartic protease. *Brazilian Journal of Microbiology*

Wang Q., Wang X., Wang X., Ma H., 2008. Glucoamylase production from food waste by *Aspergillus niger* under submerged fermentation. *Process Biochemistry* 43: 280–286.

Evaluating the environmental benefits of utilizing hydrolyzed municipal biowaste for agricultural and biochemical value-added products

M.Christodoulou[1], M. Koutinas[1], M. Kallis[1], P. Photiou[1,2], E. Montoneri[3], I. Vyrides[1] and N. Tzortzakis[4]

[1] Department of Chemical Engineering, Cyprus University of Technology, 30 Archbishop Kyprianou Str., Limassol, Cyprus
[2] Sewerage Board of Limassol – Amathus (SBLA), 76 Franklin Rousvelt, Building A, Limassol, Cyprus
[3] Università di Torino, DISAFA, Via Leonardo da Vinci 44, Grugliasco, Torino, Italy
[4] Department of Agricultural Sciences, Biotechnology & Food Science, Cyprus University of Technology, 30 Archbishop Kyprianou Str., Limassol, Cyprus
Corresponding author: michail.koutinas@cut.ac.cy

keywords: *bioproducts; municipal biowaste; agriculture.*

Introduction

Municipal Biowaste (MBW) is a valuable feedstock utilized as a renewable substrate for obtaining a wide variety of bio-based products (BPs), which have shown promising applications as chemical auxiliary in the chemical industry and agriculture. Current examples comprise the use of BPs for textile dyeing, detergents manufacturing and hydrocarbons contaminated soil washing (Montoneri et al., 2011; Photiou et al. 2021). The present study was carried out within the LIFE EBP project funded under the LIFE programme of EU. The BPs employed incorporate the mixture of bioorganic molecules (containing aliphatic and aromatic C as well as several functional groups e.g. methoxyl, carboxylic acid, amide, ammine, etc) produced via chemical hydrolysis of MBW, aiming to evaluate at pilot-scale, in the sectors of MBW management and agriculture, i) replication of the BPs production process, ii) assessment of BPs quality and cost, iii) validation of BPs performance as fertilizers, plant biostimulants and anti-pathogen agents and iv) confirm BPs compliance with EU regulation for agriculture and environmental policy. The technology will be tested in 4 EU countries.

Materials and methods

Agricultural trials were conducted using tomato in an automate climate control greenhouse. Common agricultural practices for tomato were employed and 1-branch pruning based in vertical orientation/growth system. Pot size was at least 9 L and drip irrigation system was applied. Analyses included basic soil physicochemical analysis, plant growth, crop production, fruit quality and leaching. Treatments conducted with BPs application included addition of 150 kg/ha.

Experiments were conducted for food waste fermentation to produce biogas and digestate with low NH_3 content. The amount of BPs used in each treatment was between 0.05-0.2% (w/w) at 55 °C. Gas samples were analyzed for CH_4, CO_2, H_2, N_2, O_2 and N_2O using Gas Chromatography. Furthermore, the samples were analyzed for NO, NO_2 and NH_3.

Results and discussion

Depending upon MBW source, inoculum and BPs content in fermentation, up to 68% reduction of ammonium was monitored in the digestate as compared to control experiments without BPs addition. The microbial community and biogas production were not significantly affected by BPs addition. The data are consistent with biological and chemical processes occurring in BPs assisted fermentation. These comprise ammonia production by protein hydrolysis catalysed by proteolytic bacteria and ammonia oxidation to N_2 catalysed by BPs. Moreover, the study will include data assessing the environmental merits of BPs addition in agricultural trials.

Conclusions

Based on the findings obtained, the fermentation of FW coupled to BPs addition is capable of significantly reducing the ammonia content of the digestate. Moreover, no evidence occurred for potential presence of a biochemical reaction that involved changes in the abundance of bacteria correlated to changes in the content of organic and inorganic N species due to BPs addition. The replicability of BPs derived from MBW collected in various countries has been assessed in the different industrial environments existing in each area.

Acknowledgements: This study is supported by the LIFE EBP project funded under the LIFE project: Ecofriendly multipurpose Biobased Products from municipal biowaste (LIFEEBP), LIFE19 ENV/IT/000004

References

Montoneri, E., Boffa, V., Savarino, P., Perrone, D., Ghezzo, M., Montoneri, C. and Mendichi, R., 2011. Acid-soluble bio-organic substances isolated from urban bio-waste. Chemical composition and properties of products. *Waste Manag.*, 31, 10-17.

Photiou, P., Kallis, M., Samanides, C.G., Vyrides I., Padoan, E., Montoneri, E. and Koutinas, M., 2021. Integrated chemical biochemical technology to reduce ammonia emission from fermented municipal biowaste. *ACS Sustainable Chemistry and Engineering*, 9, 8402-8413.

Augmented Regression of Municipal Solid Waste Generation Rate Based on Economic and Social Data

M. Gavrilescu[1] and D. Gavrilescu[2]

[1]Faculty of Automatic Control and Computer Engineering,
[2] "Cristofor Simionescu" Faculty of Chemical Engineering and Environmental Protection,
"Gheorghe Asachi" Technical University of Iași, Romania
Corresponding author email: marius.gavrilescu@academic.tuiasi.ro

keywords: *municipal solid waste generation rate; augmented regression; non-linear model.*

Introduction

Municipal solid waste (MSW) management is a critical issue for modern societies, as it directly impacts public health, environmental sustainability, and economic development. The rapid increase in urbanization and population growth, as well as in consumption of materials and goods has led to a surge in MSW generation, and the improper disposal of waste has become a major global challenge. The improper management of MSW can lead to a host of environmental impacts, such as air and water pollution, soil contamination and human health risks. The effective management of MSW requires a deep understanding of the factors that influence the waste generation rates that would allow the most suitable treatment and disposal of waste. One way to gain this understanding is through the use of regression models, which are statistical tools that can identify the relationship between different variables that affect MSW generation. Regression models are particularly useful for analyzing complex MSW data because they can account for the many different factors that influence waste generation. It can be said that there are 2 main classes of factors affecting MSW generation: economic factors linked to consumption: i) the gross domestic product (GDP, Euro/capita/year), ii) domestic material consumption (DMC, tons/capita/year), and social factors, linked to demographics, out which population density (PD, inhabitants/km^2) and the level of education of the population (quantifiable via metrics such as the tertiary education attainment (TEA, % population) have been considered. To this extent, we propose a pipeline for deducing and fitting a regression model that learns the relationship between the aforementioned factors (GDP, DMC, PD, and TEA) and the MSW generation, with experimental data available over a period of 10 years (2010-2019). Considering the strongly non-linear nature of the data, our model fits well with low mean-squared error (MSE) and a high R^2 score, and is a good candidate for the analysis and prediction of the relationships between these factors and MSW generation thus supporting policymakers and waste management professionals in making informed decisions about waste management strategies.

Materials and methods

Our data consists in values for GPD, DMC, PD, TEA and MSW, determined within the territory of Romania, yearly, over the course of 10 years (2010-2019). We first search for the best fitting model for this data, considering the economic (2) and social (2)-related factors as inputs and the MSW generation rate as output. Using the 10 instances from our data set, we search through a wide range of possible regression model candidates, as shown in Table 1. We consider four main categories of models: linear models with regularization, polynomial models of different degrees, support vector machines, and k-nearest neighbors with different neighbor counts. Subsequently, we develop time-series models for both dependent and independent variables and use them to augment the data set so as to improve upon the original model.

Results and discussion

While searching for the best-fitting model, we use leave-one-out cross validation to assess the goodness-of-fit for each model, and we choose the model that minimizes the MSE over the desired and predicted outputs from the cross-validation steps. We use the same pipeline to deduce a time-series regression model that characterizes the MSW generation rates values over time. The best-fitting models found through cross validation are presented in Table 2, rows 5 and 6. Considering the MSE and R^2 values of these two models,

our initial finding is that the time-series model of the MSW fits better with the available data than the regression model that accounts for the four population-centric parameters (referred to as the "4-input model"). Therefore, a time-series model, on its own, constitutes a better predictor of such data. Consequently, we improve upon the initial 4-input model, so that it becomes a better predictor than the much simpler, time-based one. In order to achieve this, we first search for time-series regression models for the four input parameters, individually. In each case, we find the best-fitting time-series models through the same cross-validation strategy as for the 4-input model. The resulting best-fitting models are presented in Table 2, rows 1-4. We then use the corresponding model for each input parameter, as well as the time-series model previously obtained for MSW, to augment the original data set by adding additional instances obtained using each individual time-series model. The resulting data set therefore increases in the number of instances, with additional values generated using time-series predictions. The newly-augmented data set is used to generate a new 4-input augmented regression model. We find that the new model is an improved version over both the original one, and the time-series model fitted using the MSW values only (Table 2, row 6). Figure 1 shows a comparison between the original data points, the original 4-input and time-series MSW models, and the newly-augmented version.

Table 1. *The types of models and corresponding parameter ranges used to search for best-fitting models*

Regressor	Description	Parameter ranges
Ridge	regularized linear model with regularization parameter α	$\alpha \in [0, 1.0]$
Polynomial	polynomial of varying degrees	degree $\in \{2, \ldots, 7\}$
SVM	support vector machine with regularization parameter C and penalty tolerance margin ε	$C \in [0.1, 2.0]$ $\varepsilon \in [0.1, 0.5]$
kNN	nearest neighbors regressor with number of neighbors k	$k \in \{1, \ldots, 6\}$

Table 2. *Best-fitting time-series and 4-input regression models*

Row no	Model type	Best model found	R^2	Cross-validation MSE
1	GDP time-series	kNN, k = 2	0.967	0.00769
2	DMC time-series	Ridge, α = 0.0	0.819	0.02185
3	PD time-series	SVM, C = 1.3, ε = 0.1	0.900	0.02225
4	TEA time-series	kNN, k = 2	0.874	0.02186
5	MSW time-series	SVM, C = 2.0, ε = 0.11	0.914	0.04789
6	MSW 4-input	SVM, C = 0.8, ε = 0.1	0.891	0.05390
7	MSW 4-input augmented	SVM, C = 0.66, ε = 0.2	0.935	0.01468

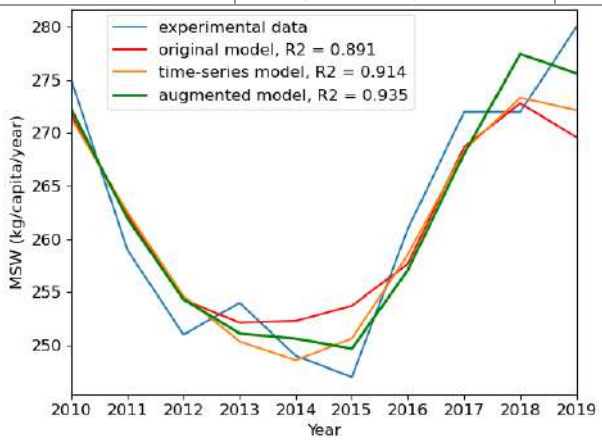

Figure 1. *Comparison between the initial, experimental data, the originally fitted 4-input model, the time-series model of the MSW and the augmented model.*

Conclusions

Our findings indicate that augmenting the initial data set using time-series models fitted for the independent parameters helped generate a better regression model for the dependent variable. In future work, we plan on experiment with various other data augmentation strategies and broaden our search to include other categories of regression models with expanded parameter domains.

The Sustainability of the Household Food Waste Management System in Romania

D. Gavrilescu[1], D. Oprisor[1,2] and C. Teodosiu[1]
[1]Department of Environmental Engineering and Management, "Cristofor Simionescu" Faculty of Chemical Engineering and Environmental Protection, "Gheorghe Asachi" Technical University of Iasi, Romania
[2]*ADI ECODOLJ, Craiova, Romania*
Corresponding author email: daniela.gavrilescu@academic.tuiasi.ro

keywords: *household food waste; sustainability; greenhouse gas emissions; impact.*

Introduction

Food loss (FL) and food waste (FW) are major concerns in our society, with striking values in both high income and low income countries. The implications of food loss and waste can be found on all aspects related to sustainability: inadequate nutrition and inefficient production and consumption of goods, economic losses, resources depletion and environmental pollution. Even though in European Union, food waste is not yet considered to be a major key waste stream, policies and legislation directed towards biodegradable waste are applicable. Legally binding per country food waste reduction targets are envisioned for 2023, but until then a food loss reduction commitment was set out in the European Union to halve the quantity of food losses per capita at retailer and consumer levels and to reduce it along the production and supply chains by 2030.

Food waste has become a more stringent issue with the European Decision 2019/1597 which is setting a common methodology for all European Member States and minimum quality requirements for the uniform measurement of food waste quantities. As a consequence, a first validated EU data set with food waste quantities was obtained for a reference year 2020, which states that on average 131 kg/capita of food waste is produced, out of which 53% comes from households. The methodology is based on both UNEP efforts with UNEP Food Waste Index and FAO Technical Platform on the Measurement and Reduction of Food Loss and Waste.

Regarding food loss, Romania has adopted a Food Loss Reduction Law in 2016 (Law 217/2016) and in 2019, the subsequent methodology on how to apply it. The European Decision 2019/1597 on Food Waste reporting was also adopted, however, up to this moment, there are no national reported data on Food Waste in Eurostat. However, there are few studies that state the Romanian food waste generations rates range between 165 kg/capita/year (Fusions, 2016; RO NWMP, 2018) over the entire food waste production supply and consumption cycle and 118 kg/capita/year (UNEP Food Waste Index, 2021) coming from households, whole sale and retail and food service, without production and processing stages.

The main objective of this study is to evaluate the sustainability of the Household Food Waste Management System at country level, by using a selected set of environmental, social and economic indicators.

Materials and methods

The Household Food Waste (HHFW) was selected for evaluation because it represents the largest proportion of the total Food Waste stream. The investigated period of time is 2016-2021, starting with the year in which food loss reduction targets were adopted by legislation in Romania and up to 2021, the last year with data available in literature for food waste generation rates.

For the sustainability framework, USEPA WARM method, version 15 was employed because it provides information on the selected set of indicators, namely: greenhouse gas emissions and energy impact correlated with the waste management operations for the environmental aspects, wages and taxes for the economic profile and number of working hours for the food waste treatment in the case of the social impact. USEPA WARM method, version 15 is designed to consider various food waste streams such as: food waste mix, food waste meat, bread products, fruits and vegetable and dairy products and specific waste options

like: composting, anaerobic digestion, landfilling. The quantification of waste prevention and reduction measures is also possible.

HHFW quantities (per each stream: meat, bread products, fruits and vegetables and dairy products and total) were modeled considering waste generation rates per capita from 4 sources: FUSIONS 2016, RO NWMP 2018, UNEP 2021 minimum and UNEP 2021 maximum, adjusted with population dynamics and food consumption patterns. It is considered that HHFW composition in Romania is 24% cooked food, 43% fruits and vegetables, 20% bread and pastry, 11% dairy products, 1% meat products and 1% other (www.foodwaste.ro). Currently, the only treatment option for HHFW is landfilling.

Results and discussion

The following results represent the case of a HHFW generation rate/capita of 79 kg/capita/year as suggested by UNEP, also named here as the UNEP 2021 minimum scenario. The environmental impact is quantified as greenhouse gas emissions resulted from the waste management stage and from production of goods and end of life practices and as the energy use in the waste management stage and energy use in the production and end of life management stage. The contribution of greenhouse gas emissions resulting from landfilling of HHFW is on average 20% of the emissions resulting from production plus end of life treatment.

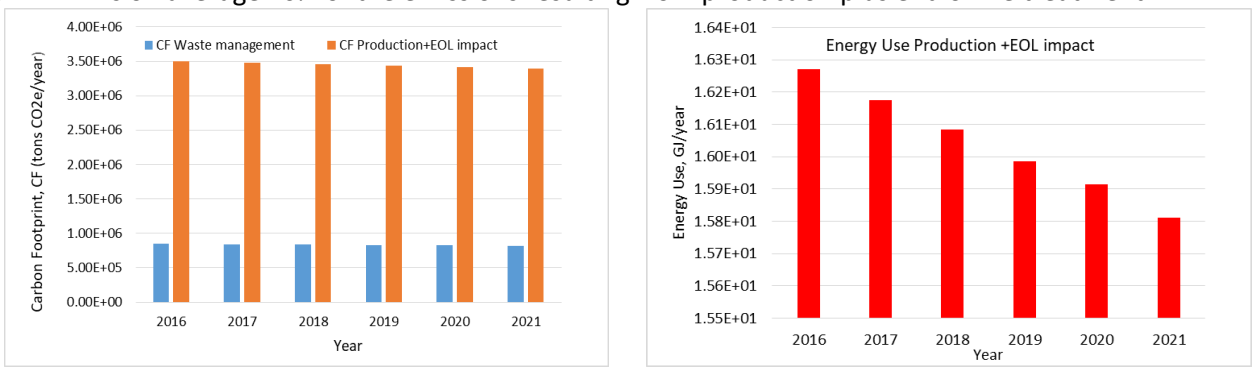

a) b)

Figure 1. Environmental impact of HHFW management, UNEP 2021 minimum scenario: a) total carbon footprint and b) energy use in production and end of life stages

As it may be observed in figures 1 a) and b), both greenhouse gas emissions and energy use display decreased values from 2016 to 2021. This pattern is mainly due to population decline and variations in consumption caused by the socio-economic context (purchase power, willingness to purchase, consumption habits etc.).

The social indicator, the amount of effort directed to HHFW management calculated as labour hours per year and economic indicators such as wages and taxes per year correlated to the waste management practices are summarized in Table 1. In all indicators presented in Table 1, a decrease of 3% is observed in 2021 as compared to 2016.

Table 1. Social and economic indicators of HHFW management, UNEP 2021 minimum scenario

Indicator	2016	2017	2018	2019	2020	2021
Labour Hours, h/year	2.33E+06	2.32E+06	2.31E+06	2.29E+06	2.28E+06	2.27E+06
Wages US $/year	7.85E+07	7.80E+07	7.76E+07	7.71E+07	7.67E+07	7.62E+07
Taxes US $/year	2.91E+07	2.89E+07	2.88E+07	2.86E+07	2.85E+07	2.83E+07

Conclusions

Currently, country official statistics on FW generation and composition in Romania are limited, while to the best of our knowledge, sustainability studies of food waste management options are not available.

In this study, the sustainability of the HHFW management system in Romania was evaluated by using a methodology based on a selected set of indicators. As within any study, the quality of primary data is very important because it significantly impacts the results obtained. The results show a decrease in all investigated indicators, even though HHFW management practices have remained unchanged. The trend is caused by population decline and consumption patterns.

Microplastic aging in freshwater and marine ecosystems

S.D. Martinho[1], V. Cruz Fernandes[1], S.A. Figueiredo[1], R. Vilarinho[2,3], J.A. Moreira[2,3] and C.D. Matos[1]

[1]REQUIMTE/LAQV, Instituto Superior de Engenharia do Porto, Instituto Politécnico do Porto, Rua Dr. António Bernardino de Almeida 431, 4249-015 Porto, Portugal
[2]Department of Physics and Astronomy, Faculty of Sciences of the University of Porto, Porto, Portugal
[3]IFIMUP—Institute of Physics for Advanced Materials, Nanotechnology and Photonics, Faculty of Sciences of the University of Porto, Porto, Portugal
Corresponding author email: vir@isep.ipp.pt/saf@isep.ipp.pt

keywords: *aquatic ecosystems; emerging contaminant; FTIR; microplastic; Raman.*

Introduction

Microplastics (MP) are defined as tiny plastic particles less than 5 mm in size. They can come directly from industries (primary source) or may result from the degradation and fragmentation of large plastics (secondary source). Their tiny size, low density and hydrophobicity give MP the ability to transport pollutants such as pesticides, heavy metals, pharmaceuticals, polychlorinated biphenyls (PCBs), and polycyclic aromatic hydrocarbons (PAHs) into various environments. The adsorption studies reported in the literature suggested several differences between the behavior of pristine and aged MP (Wang et al. 2023). The different environmental conditions concerning physical and chemical factors, such as ultraviolet radiation, thermal degradation, oxidation reactions and biodegradation, continuously change the properties of MP and lead to an aging process (Luo et al. 2020). Due to the lack of information about the effects of aging on the interaction of MP with other pollutants, this study aimed to explore the change of the properties of MP, aged in freshwater and marine aquatic ecosystems (simulated at laboratory scale), through evaluation by Raman spectroscopy and Fourier-transform infrared spectroscopy (FTIR).

Materials and methods

The microplastics (MP) polyamide 6 (PA6) (15 – 20 μm), low-density polyethylene (LDPE) (300 μm) and unplasticized polyvinylchloride (UPVC) (250 μm), were supplied by Goodfellow (Hamburg, Germany). The sandy soil was acquired from MIBAL – Minas de Barqueiros, S.A. (Apúlia, Portugal) and had a silica content of about 90%. The water of the Douro River (pH =7.63) from the Afurada marine (GPS 41.1412, -8.6519) and the seawater (pH = 8.06) from the beach of Canide Sul (GPS 41.1128, -8.6636), were collected in glass bottles and used for the aging process, simulated in the laboratory. The water samples were previously filtered (pore size 0.45 μm) to eliminate the suspended solids.

The aging procedure of MP was carried out by adding 100 mL of filtered water (river or sea) into pyrex graduated cylinders, with 25 g of sandy soil. A weighted amount of MP (around 300 mg) of each one was added to each cylinder. The assays were submitted to constant aeration and agitation using silicon tubes placed as close as possible to the bottom to ensure the constant movement of the MP particles. The experiments were carried out under continuous illumination, using cool white fluorescent lamps (84 lm/W) (PHILIPS, TL-D 36W/865, Warsaw, Poland) to simulate daylight irradiation. After 2 months, the MP were separated from the liquid phase by filtration (glass fiber filter 0.45 μm) and were analysed by Raman spectroscopy and FTIR spectroscopy.

Results and discussion

The results of the characterization by Raman and FTIR spectra are shown in Fig. 1 for pristine and aged PA6, as an example, both in freshwater and marine aquatic environments. Pristine and aged MP have the same functional groups, according to the Raman and FTIR analysis, showing that the aging process did not appear to cause chemical changes in their structures. Nevertheless, an increase in the background noise and changes in the intensities were observed in aged MP, both on sea and river water, which can be justified by the

presence of the sandy soil in the aging process. These interferences were more frequent in the MP submitted to freshwater aging due to the difficulty of pick analysis. The difficulty of obtaining a good analysis was evident in the freshwater samples, once the presence of sodium chloride (NaCl) in the seawater favored the flotation of MP, which helped the filtration and retention of MP in the filter. Both analyses, Raman and FTIR, confirmed the stability of the chemical structure of MP once no changes were observed between the results of the pristine and aged MP. However, PA6 was the most difficult MP to analyse by Raman in both aging methods, which could be due to its smaller particle size. Although there is no evidence of chemical alterations of the MP, the images collected by the Raman spectroscopy show significant changes in the surface of the MP. The next step was to explore the impact of these physical alterations on the MP surface on the adsorption behavior of MP.

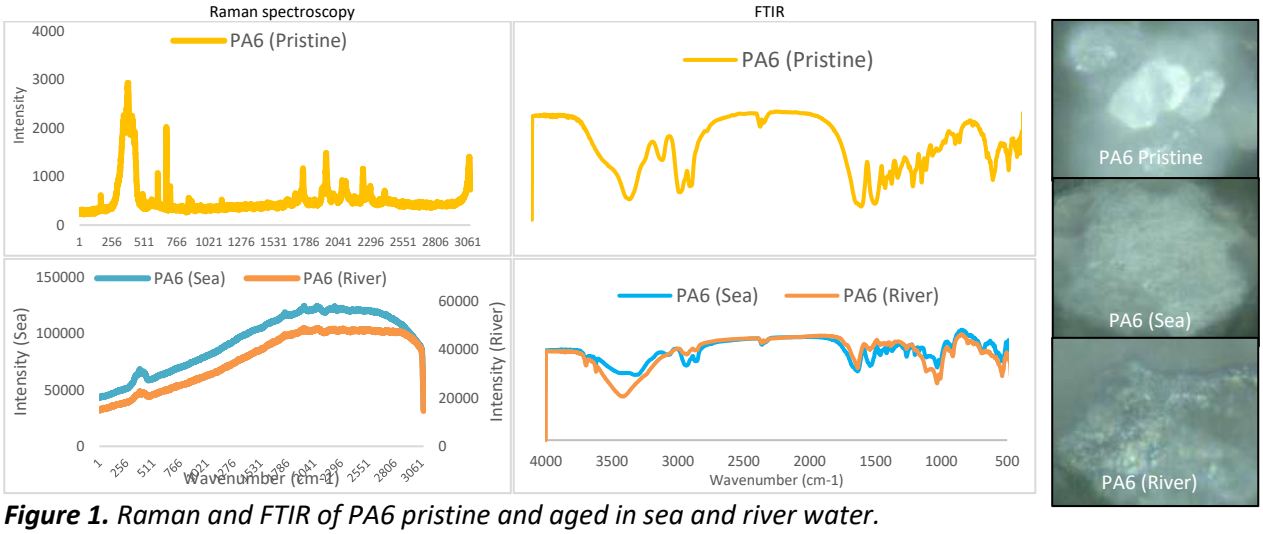

Figure 1. *Raman and FTIR of PA6 pristine and aged in sea and river water.*

Conclusions

In this study, the aging process of LDPE, PA6 and UPVC was conducted over 2 months, both in freshwater and marine aquatic environments (simulated in laboratory). Based on the Raman and FTIR spectra, the stability of the chemical structure of all MP was observed despite the noticed physical that could be related with the individual or combined effect of the soil abrasion, contact with water and irradiation. The Raman spectroscopy images show changes in the surface of all MP. Since the surface of MP is one of the properties that influence their behavior as a vector for the transport of other pollutants in the environment, the effect of the aging processes should be further explored to understand the real interactions in the environment.

Acknowledgements/Funding: This work received financial support from PT national funds (FCT/MCTES, Fundação para a Ciência e Tecnologia and Ministério da Ciência, Tecnologia e Ensino Superior) through the projects UIDB/50006/2020, UIDP/50006/2020, LA/P/0008/2020 and 2022.15094.CBM (under the Agreement between Portugal and France - 2023-2024 Person Program). This work was also financial support through the BiodivRestore Joint Call 2020–2021-European Union's Horizon 2020 research and innovation programme under grant agreement No 101003777-BiodivRestore-406/DivRestore/0002/2020-BioReset-"Biodiversity restoration and conservation of inland water ecosystems for environmental and human well-being". Sílvia Daniela Martinho thanks FCT for the financial support through a doctoral fellowship (SFRH/BD/13595/2022). The authors are greatly indebted to all financing sources.

References

Luo, H., Y. Zhao, Y. Li, Y. Xiang, D. He, and X. Pan. 2020. 'Aging of microplastics affects their surface properties, thermal decomposition, additives leaching and interactions in simulated fluids', *Sci Total Environ*, 714: 136862.

Wang, L., J. Zhang, W. Huang, and Y. He. 2023. 'Laboratory simulated aging methods, mechanisms and characteristic changes of microplastics: A review', *Chemosphere*, 315: 137744.

The backbones of an effective occupational health and safety program in nurseries

A. Eleftheriadou and E. Tzanakaki

Directory of Social Affairs, Municipality of Rethymno, Rethymno, Greece
Corresponding author email: eleftheriadou@rethymno.gr

keywords: *childcare; worker; safety; health.*

Introduction

Nursery workers are exposed to many safety and health risks. However, most of them are preventable and a precise and detailed recording and an early detection are of significant importance. The aim of the study was to explore the occupational health and safety risks in 9 regional Nurseries of the municipality of Rethymno.

Materials and methods

107 childcare workers were interviewed and their medical history was reviewed by a occupational health nurse. Data were analyzed and classified according to the most often described medical identities.

Results and discussion

- 3 childcare workers were excluded due to pregnancy
- 5 childcare workers denied to provide the additional information required.
- Among the rest of the staff:
- 27 reported occupational injuries because of the variety of physical tasks leading to high risk for musculoskeletal acute and chronic harm. The most common types of issues were shoulder pain, back discomfort and limitation of specific movements. Several visits to orthopedic specialists were mentioned as well as physiotherapy sessions accordingly.
- 31 reported stress issues related to work, and more specifically to staff poor communication and conflicts, and extremely high parent demands and supervisor demands.
- 5 reported total burn-out at particular period of time, after long period of emotional exhaustion.
- 19 reported very frequent viral and other, mainly respiratory and gastrointestinal infectious diseases.
- The small sample of participants is a limitation of the current study because results are preliminary, not suitable for statistical analysis, however the study is in progress.

The results of our study show that in order to reduce the risks of health issues in childcare staff, the development of workplace health promotion program is required. More specifically, ergonomic environment and equipment is mandatory in order to decrease physical remands and to reduce injuries. Furthermore, of high importance seems to be the positive and regular staff communication.
Finally, training the childcare staff to implement infection control and limit the risk of contamination and illness is important.

References

Calabro, K.S., Bright, K.A., Cole, F.L., Lindenberg, J. and Grimm, A. (2000) Child care work: Organizational culture and health safety. AAOHN Journal, 48(10), 480-486
Wortman, A.M. (2001) Preventing work related musculoskeletal injuries. Childcare Information Exchange, 7(1), 50-53

Coastline Protection & Management at Kythera Kapsali Bay through Summer School Project, the case of Island Kythera

E. Loupas[1] and M. Kalogeraki[2]

[1] PhDc, Professor on Environmental Education, Communication and Sustainability, Zakynthos, Ionian University
[2]BSc & Researcher on Computer Science, Heraklion, University of Crete
Corresponding author email: efsta9412@gmail.com

Keywords: *Coast Protection; & Management; Environmental Education; Summer School; Sustainable Development; Kythera Island.*

Abstract

Coastlines and beaches are continuously polluted by human activity and exploitation which leads to major issues regarding hygiene, marine and coast life. It is of high importance to secure the coastlines clean and nonpolluted by applying the guidelines of major institutions. Institutions and organizations like ... through agreements and laws are working together by setting guidelines that will address the major issues that we face with the environmental impact of human activity. Sea life and its natural habitats that is consisted of is the main victim of the human activity. Marine litter (ML) and overall rubbish and pollution with materials like plastic, paper, metal, glass etc. are the main litters of the coastal waters, seafronts and deep sea accordingly. The pollution affects not only sea life and the environment but the human health as well.

Most of the materials take hundreds of years to dissolve such as plastic and metal. Greek seas and coastlines suffer every year from the pollution caused from the industries of tourism, agriculture and heavy industry and fishing. On our case we are focusing on the pollution produced with solid waste in the beach of Kapsali in the island of Kythera. The conducted research addressed the litter found on the beach of Kapsali which is found in the southern part of the island of Kythera. Most of litter consisted of solid waste and was collected and recorded by the research team of the Environmental Summer School for five days two times a day morning and evening. For monitoring the amount of waste, a form was used and all the data were registered into the Microsoft Excel for making the boards and graphs.

Circular bioeconomy strategy in Greek livestock sector: The integration of bakery meal to pig diets

L.Melas[1], M. Batsioula[1], S. Skoutida[1], A. Malamakis[1],
C. Karkanias[1], D. Geroliolios[1], S.Patsios[2] and G. Banias[1]

[1] Centre for Research and Technology-Hellas, Institute for Bioeconomy and Agri-Technology, GR-57001 Thermi, Greece
[2] Centre for Research and Technology-Hellas, Chemical Process and Energy Resources Institute, GR-57001 Thermi, Greece
Corresponding author email: l.melas@certh.gr

keywords: *Pig Sector; Life Cycle Assessment; Bakery meal; Circular Bioeconomy.*

Introduction

The agri-food sector accounts for 34% of global GHG emissions while 15% of them are attributed to the livestock sector (Crippa et.al 2021). Pig meat represents 40% of all meat consumption and the pig sector is responsible for 9% of the livestock's emissions. Almost half of the GHG emissions attributed to the pig sector derive from feed production while almost a third of all cropland is reserved for feedstock production (Sejian et.al. 2016). A sustainable alternative of existing supply chains is to switch them towards a more circular approach(de Souza et al., 2022). Bakery meal is produced from bakery by-products and constitutes a sustainable alternative to corn with high potential. In this study, Life Cycle Assessment is used to environmentally evaluate the substitution of corn by bakery meal for pig feeding. The study was conducted within the scope of CPigFeed project and uses real time data for the analysis.

Materials and methods

To evaluate the environmental performance of bakery meal for pig meat production the following methodology is deployed:

1. Mapping of bakery by-product sources: The transport of bakery by-products and bakery meal is assumed as a significant impact contributor. Mapping the sources will help detect the distance that needs to be covered to provide the Bakery meal.
2. Set a baseline scenario: Within this study a certain pig farm is used as study case. To depict the influence of bakery meal in the Greek pig sector, the pig farm existing practices should be depicted accurately.
3. Comparative LCA: A sound method to compare two scenarios is LCA methodology as described in Handbook on Life Cycle Assessment. Moreover, the analysis takes place in SimaPro software, using the ReCiPe Midpoint method and Ecoinvent 3.9 database.

Results and discussion

Circular bioeconomy strategies are used in every sector to transform waste to valuable products. Food waste utilization can provide economic, environmental, and social benefits. The circular bioeconomy approach can help decrease dependency from fossil fuels, provide a sustainable option for waste management and mitigate the pressure on the ecosystem from human activities(Brandão et al., 2021). It has been reported that bakery waste can efficiently replace ingredients of pigs' feedstock(Kumar et al., 2014),(Tiwari, 2020), (Tiwari et al., 2020). Furthermore, bakery meal integration to feedstock provides security in the food supply chain(Ominski et al., 2021), while Bakery meal improved the environmental performance of pig farming systems in all impact categories(Mackenzie et al., 2016).

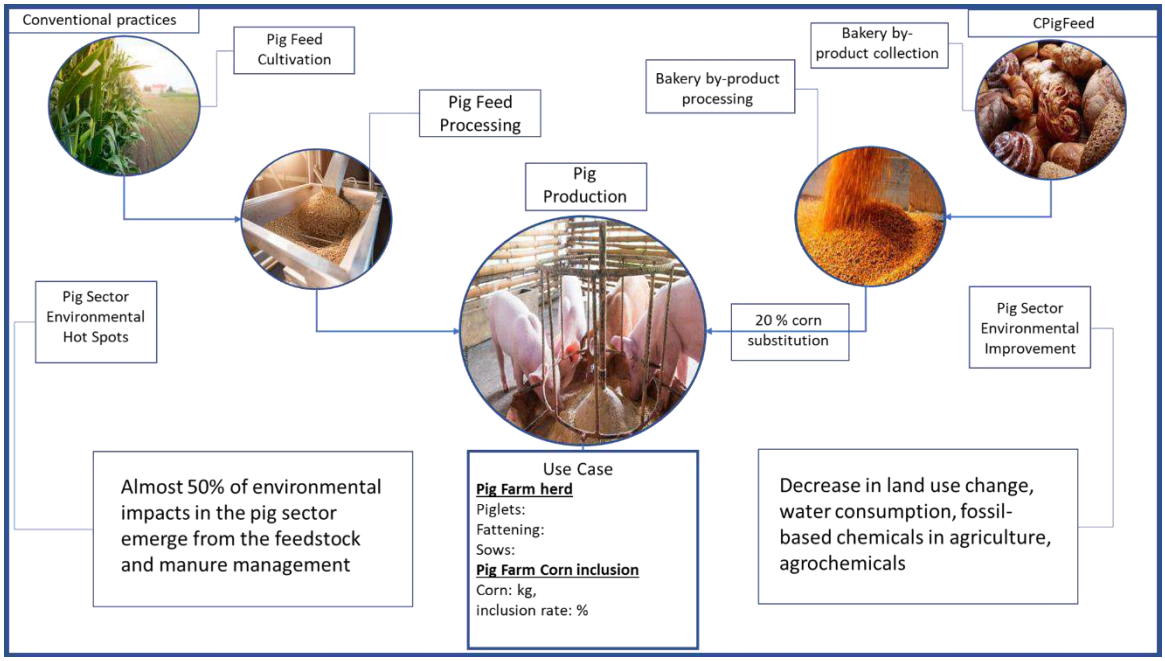

Figure 1. *Conventional vs CPigFeed feedstock production for pig meat production.*

Conclusions

Bakery meal can enhance the circularity of the Greek pig sector. Moreover, bakery meal can help pig farms increase their overall sustainability. Maize prices fluctuate throughout the year and decreasing the dependence of the sector can help at long-term management while it can evidently improve the environmental performance of the sector and reduce the amount of waste generated. As such, bakery meal integration in pig diets exhibits the potential of circular bioeconomy strategies to enhance resilience of the Greek pig sector and illuminate the path of a greener supply chain.

Acknowledgements: This study was co-financed by the European Regional Development Fund of the European Union and Greek national funds through the Operational Program Competitiveness, Entrepreneurship and Innovation, under the call RESEARCH – CREATE - INNOVATE (project code: T2EDK-04537).

References

Brandão, A. S., Gonçalves, A., & Santos, J. M. R. C. A. (2021). Circular bioeconomy strategies: From scientific research to commercially viable products. In *Journal of Cleaner Production* (Vol. 295). Elsevier Ltd. https://doi.org/10.1016/j.jclepro.2021.126407

de Souza, E. D., Kerber, J. C., Bouzon, M., & Rodriguez, C. M. T. (2022). Performance evaluation of green logistics: Paving the way towards circular economy. *Cleaner Logistics and Supply Chain*, *3*. https://doi.org/10.1016/j.clscn.2021.100019

Kumar, A., Roy, B., Lakhani, G. P., & Jain, A. (2014). Evaluation of dried bread waste as feedstuff for growing crossbred pigs. *Veterinary World*, *7*(9), 698–701. https://doi.org/10.14202/vetworld.2014.698-701

Mackenzie, S. G., Leinonen, I., Ferguson, N., & Kyriazakis, I. (2016). Can the environmental impact of pig systems be reduced by utilising co-products as feed? *Journal of Cleaner Production*, *115*, 172–181. https://doi.org/10.1016/j.jclepro.2015.12.074

Ominski, K., Mcallister, T., Stanford, K., Mengistu, G., Kebebe, E. G., Omonijo, F., Cordeiro, M., Legesse, G., & Wittenberg, K. (2021). Utilization of by-products and food waste in livestock production systems: A Canadian perspective. *Animal Frontiers*, *11*(2), 55–63. https://doi.org/10.1093/af/vfab004

Tiwari, M. R. (2020). Bakery Waste is an Alternative of Maize to Reduce the Cost of Pork Production. In *International Journal of Research in Agriculture and Forestry* (Vol. 7, Issue 5).

Tiwari, M. R., Dhakal, H. R., & Sudi, M. S. (2020). GROWTH COMPARISON OF PIGLETS FED WITH DIFFERENT LEVEL OF BAKERY WASTE IN BASAL DIET. In *Journal of Agriculture and Forestry University* (Vol. 4).

A Systematic Investigation of Pb^{2+} Removal from High-Salinity Wastewater by Electrocoagulation – Flocculation Process [ECF]

V. Chatzis[1], V. Korovesi[2], P. Petsi and K. Plakas[1]

[1] Chemical Process and Energy Resources Institute, Centre for Research and Technology-Hellas, 6th km Charilaou-Thermi road, Thermi, Thessaloniki, Greece
[2]Department of Chemical Engineering, Aristotle University of Thessaloniki, Thessaloniki, Greece
Corresponding author email: kplakas@certh.gr

keywords: *electrocoagulation; lead removal; brines; iron electrodes; optimization.*

Introduction

Electrocoagulation – Flocculation [ECF] process constitutes an innovative, promising and effective electrochemical approach for the treatment of a wide range of different contaminated water types, receiving significant attention on the removal of heavy metals from aqueous environments, as this category of pollution has emerged as a serious environmental issue the past decades. This study aims at optimizing the operational efficiency of electrocoagulation/flocculation for the in-situ production of Fe-based coagulating agents and the successful elimination of lead cations (Pb^{2+}) from high-salinity synthetic aqueous solutions by electrode reactions. For this purpose, an ECF pilot-scale unit was designed and built in house. Hence, pilot studies with a cell containing two pairs of iron electrodes of 10 cm^2 surface area each, in Monopolar-Parallel [MP-P] configuration, and effective volume of ~ 1.6 L, were performed. Aiming to optimize this ECF, Central Composite Design with Response Surface Methodology (RSM) was employed to assess the effects of three key process parameters and their interaction on Pb^{2+} removal and energy consumption.

Materials and methods

The experiments were performed in an ECF pilot-scale unit, with its components presented in Fig. 1a.

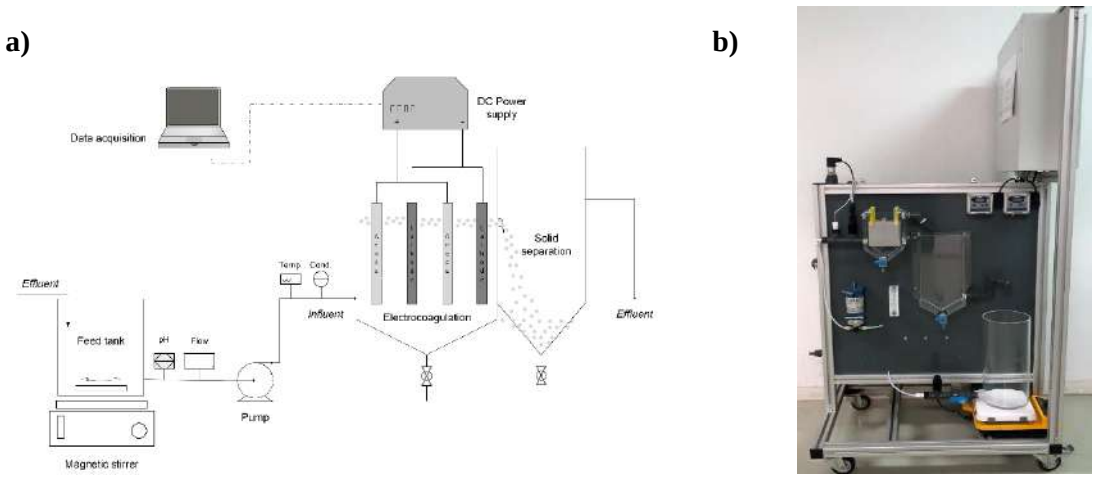

Figure 1. a) *Flow diagram,* ***b)*** *front view of the Electrocoagulation – Flocculation [ECF] pilot-scale unit.*

The pilot tests were initially focused on optimizing the performance of the ECF pilot plant in terms of maximizing Pb^{2+} cations removal (%Pb) and minimizing the respective energy consumption (EC in KWh/m^3). The experimental design and optimization of the process was carried out using the RSM. For this purpose, all those parameters related to the operation of the EC unit, namely the applied electric current density, the electrolysis time, and solution's pH, were altered. The pilot optimization were designed based on the Face-centered Central Composite design [FCC] with the help of the statistical package Design-Expert® v.7.0.0, using the three functional parameters (pH, j, E_t) at two levels. Based on the experimental design, a total of 16 pilot tests were performed, the operating conditions of which are summarized in Table 1, along with the

corresponding response results. The changes in Pb^{2+} cation concentrations were measured at the outlet of the ECF device, using Inductively Coupled Plasma – Optical Emission Spectrometry system (ICP-OES, Optima 4300 DV, Perkin Elmer).

Table 1. *Pilot test design & results of Pb^{2+} removal (2 Fe anode/cathode electrode pairs, distilled water).*

Run	Parameter 1 Current Density (mA/cm^2)	Parameter 2 Electrolysis Time (min)	Parameter 3 pH	Response Pb removal (%)	EC (kWh/m3)
1	10	9	10	97.47	0.875
2	50	66	5	92.36	79.560
3	10	66	10	100.00	8.077
4	50	66	10	98.81	87.707
5	50	37.5	7.5	92.61	47.402
6	30	9	7.5	98.40	5.191
7	30	37.5	10	94.66	24.752
8	30	37.5	7.5	88.18	23.741
9	10	9	5	84.52	0.846
10	50	9	5	94.00	11.938
11	50	9	10	99.10	15.515
12	10	37.5	7.5	80.82	3.154
13	30	66	7.5	100.00	38.688
14	30	37.5	5	89.35	19.754
15	30	37.5	7.5	88.18	23.741
16	10	66	5	100.00	6.205

Results and discussion

The statistical processing of the results helped to determine a combination of values for the three functional parameters, as a near optimum solution, setting as a criterion the maximization of Pb^{2+} removal and the minimization of EC in the cell arrangement (with Fe anode/cathode electrodes in MP-P configuration). 3D response surfaces and contour maps were developed by employing the Design Expert software. The response surface plots shown in Fig. 2 verify the results of the statistical analysis, since Pb ions can be effectively removed at low current densities and electrolysis times, at basic pH (10), with a rather minimum energy consumption. An almost complete removal of Pb^{2+} cations (~97.5 %) could be achieved under the following near optimal conditions: 10 mA/cm^2 of applied electric current density, 9 min of electrolysis, and pH 10.

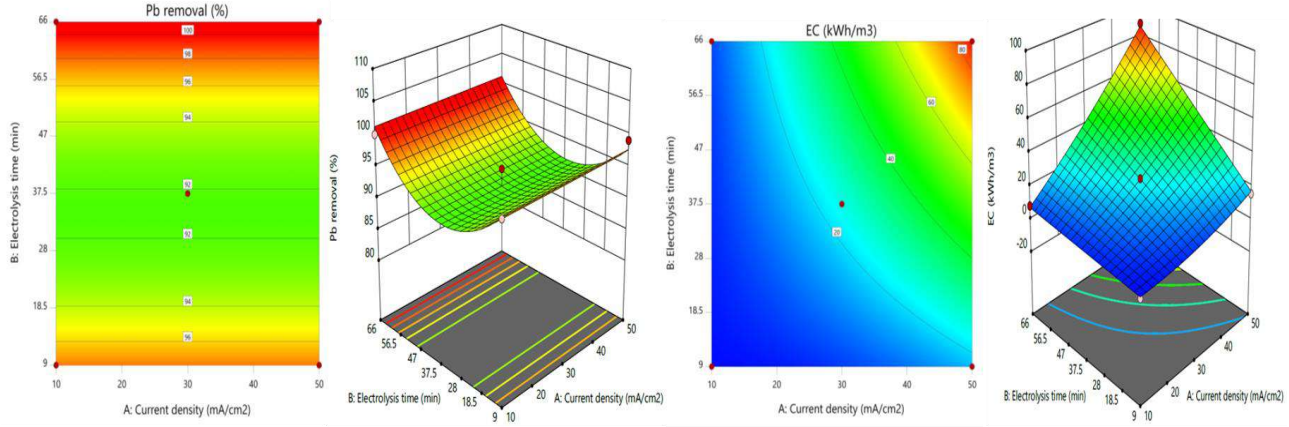

Figure 2. *Contour and 3D surface plots for the Pb^{2+} cations removal and energy consumption (EC) as function of electric current density (j) and electrolysis time (E_t), (at pH 10).*

Acknowledgements: The work has received financial support through the project CERESiS - ContaminatEd land remediation through energy crops for soil improvement to liquid biofuel strategies, funded through HORIZON2020 (GA No. 101006717).

References

Moussa, D. T., El-Naas, M. H., Nasser, M. and Al-Marri, M. J., 2017. A comprehensive review of electrocoagulation for water treatment: Potentials and challenges. *J. Environ. Manage.,* 186, 24–41.

Kobya, M., Omwene, P. I. and Ukundimana Z., 2020. Treatment and operating cost analysis of metalworking wastewaters by a continuous electrocoagulation reactor. *J. Environ. Chem. Eng.*, 8(2), 103526.

Magnisali, E., Yan, Q. and Vayenas, D. V., 2022. Electrocoagulation as a revived wastewater treatment method-practical approaches: a review. *J Chem. Technol. Biotechnol.,* 97, 9–25.

2nd International Conference on
Sustainable Chemical and
Environmental Engineering
14th – 18th June 2023, Limassol, Cyprus

Removal of benzotriazoles during municipal wastewater treatment in suspended-growth and attached-growth systems containing *Chlorella sorokiniana* and activated sludge

A. Koukoura, E. Gkalipidou, E. Zkeri, *G. Gatidou, M. Fountoulakis and A. Stasinakis

Water and Air Quality Laboratory, Department of Environment, University of the Aegean, Mytilene, Lesvos, Greece
Corresponding author email: ggatid@env.aegean.gr

Keywords: *Chlorella sorokiniana*; microalgae-bacteria consortia; emerging contaminants; wastewater treatment.

Introduction

Chlorella sorokiniana is a small (2-4.5 μm diameter), single celled sub species that can be grown both under mixotrophic and heterotrophic conditions (Lizzul et al., 2018). Various studies have shown that *Chlorella sorokiniana* is able to grow very fast under appropriate conditions. The combination of higher temperatures and mixotrophic conditions enhances its specific growth rate in municipal wastewater (Kotoula et al., 2020; Lee et al., 2017). Recent studies have tested the combination of microalgae and activated sludge for municipal wastewater treatment, presenting encouraging results (Gonçalves et al., 2017). Microalgae use CO_2 and produce O_2 through photosynthesis, which can be used by the bacteria for organic and nutrient removal (Mohsenpour et al., 2021). Moreover, through the oxidation of organic carbon, bacteria release CO_2 that could be used by algae during photosynthesis (Liu et al., 2019). In addition, microalgae release organic compounds, which are essential for the bacteria's growth (Gonçalves et al., 2017). Furthermore, through various methods, such as hydrolysis, photolysis, biodegradation, bioaccumulation, and bioadsorption, microalgae can eliminate microcontaminants (Gatidou et al., 2019). Benzotriazoles are classified as high production volume emerging contaminants due to their extensive industrial and domestic use and frequently detected in water and wastewater (Nika et al., 2017). The aim of the current study was to investigate the removal efficiency of benzotriazoles (BTRs) from municipal wastewater treatment in suspended and attached-growth systems containing *Chlorella sorokiniana* and activated sludge.

Materials and methods

Used Municipal wastewater

Pre-treated municipal wastewater was collected for a period of 6 months from a Wastewater Treatment Plant located in Antissa (Lesvos Island, Greece).

Operation of the lab-scale system

The experimental setup consisted of four Sequential Batch Reactors (SBRs) which were continuously stirred. The operating volume of the reactors was 1.2 L and contained *Chlorella sorokiniana* (SBR1*), Chlorella sorokiniana* and activated sludge (SBR2), *Chlorella sorokiniana* and biocarriers (SBR3), *Chlorella sorokiniana*, activated sludge and biocarriers (SBR4) (Figure 1). Each SBR was spiked with mixture of BTRs (200 $\mu g L^{-1}$). As biocarriers, sponge carriers were used (Nisshinbo Chemical Inc., Japan). The experiment was run for 6 months where reactors were exposed under mixotrophic conditions of 16 h light/8 h dark using four fluorescent lamps that had been placed around the reactors and operated at hydraulic residence times (HRT) of 3, 2 and 1 days. The samples of each SBR were analysed for COD, NH_4-N, NO_3-N, PO_4-P, TSS and optical density (OD). BTRs were analyzed by HPLC-DAD. The temperature, pH and dissolved oxygen were measured on a daily basis.

Results and discussion

According to the results, the operation of the systems at HRT of 2 and 3 days resulted to COD removals higher than 80% in all reactors, with the highest removal being observed in SBR4 (85%). The reduction of HRT to 1

d did not affect the performance of SBR1 and SBR2 whereas lower removal was observed in SBR3 (66%) and SBR4 (61%). A high efficiency in terms of NH_4-N removal was also observed for all SBRs at HRT values of 3 and 2 d reaching 98%. The reduction of HRT to 1 d did not affect the performance of SBR1 but decreased those of SBR2 (88%), SBR3 (51%) and SBR4 (40%). The dissolved oxygen concentration in each of the reactors was the reason for this decrease in efficiency. The removal of PO_4-P was partial (<55%) in all reactors regardless of the conditions and the HRT applied. According to the results, SBR2 caused the better removals (up to 89%) almost, for all the compounds tested. Dissolved oxygen found to be an important factor in the removal of BTRs, as in all SBRs the concentration was higher than 5 mgL^{-1}, except SBR4 (<2 mgL^{-1}) where the lowest removals were observed.

Figure 1. *Lac scale systems.*

Conclusions

Sufficient removal of COD and NH_4-N was observed on the current study under low HRT values, higher than 80%. The addition of activated sludge and the use of carriers did not affect the performance of the system. An important factor was the HRT value, as the efficiency of the system decreased significantly, especially for SBR3 and 4 for an HRT equal to 1 day. Combined use of *Chlorella sorokiniana* and activated sludge (SBR2) proved to be very promising in the elimination of target BTRS from municipal wastewater, as resulted in high removal percentages of the compounds.

Acknowledgements: This work has received funding from the European Union's Horizon 2020 research and innovation programme under grant agreement No 776643 within the framework of HYDROUSA project.

References

Gatidou, G., Anastopoulou, P., Aloupi, M., & Stasinakis, A. S. (2019). Growth inhibition and fate of benzotriazoles in Chlorella sorokiniana cultures. *Science of the Total Environment*, *663*, 580–586. https://doi.org/10.1016/j.scitotenv.2019.01.384

Gonçalves, A. L., Pires, J. C. M., & Simões, M. (2017). A review on the use of microalgal consortia for wastewater treatment. *Algal Research*, *24*, 403–415. https://doi.org/10.1016/j.algal.2016.11.008

Kotoula, D., Iliopoulou, A., Irakleous-Palaiologou, E., Gatidou, G., Aloupi, M., Antonopoulou, P., Fountoulakis, M. S., & Stasinakis, A. S. (2020). Municipal wastewater treatment by combining in series microalgae Chlorella sorokiniana and macrophyte Lemna minor: Preliminary results. *Journal of Cleaner Production*, *271*, 122704. https://doi.org/10.1016/j.jclepro.2020.122704

Lee, T. H., Jang, J. K., & Kim, H. W. (2017). Optimal temperature and light intensity for improved mixotrophic metabolism of Chlorella sorokiniana treating livestock wastewater. *Journal of Microbiology and Biotechnology*, *27*(11), 2010–2018. https://doi.org/10.4014/jmb.1707.07007

Liu, J., Pemberton, B., Lewis, J., Scales, P. J., & Martin, G. J. O. (2019). Wastewater treatment using filamentous algae – A review. *Bioresource Technology*, *298* (December 2019), 122556. https://doi.org/10.1016/j.biortech.2019.122556

Lizzul, A. M., Lekuona-Amundarain, A., Purton, S., & Campos, L. C. (2018). Characterization of chlorella sorokiniana, UTEX 1230. *Biology*, *7*(2), 1–12. https://doi.org/10.3390/biology7020025

Mohsenpour, S. F., Hennige, S., Willoughby, N., Adeloye, A., & Gutierrez, T. (2021). Integrating micro-algae into wastewater treatment: A review. *Science of the Total Environment*, *752*(September 2020), 142168. https://doi.org/10.1016/j.scitotenv.2020.142168.

Nika M.-Ch., Bletsou A.A., Koumaki E., Noutsopoulos C., Mamais D., Stasinakis A.S., Thomaidis N.S. (2017). Chlorination of benzothiazoles and benzotriazoles and transformation products identification by LC-HR-MS/MS. *Journal of Hazardous Materials*, 323 (February 2017), 400-413.

Experience of using IoT technologies and decision-support systems for smart-farming with real-time irrigation management and assessment of its impact on tree crops' economy in Greece.

T. Theodosiadis-Thomaidis and G. Panagopoulou[3]
[1] Pangaea R&D pc – E. Katsigra 1, Larisa, Greece
Corresponding author email: info@pan-gaea.gr

Keywords: *IoT Internet-of-Things; smart agriculture; smart irrigation; crop nutrition; crop economy, modelling; decision-support systems.*

Abstract

Semiarid Mediterranean environments suffer of water scarcity, where the unbalanced distribution of water resources, and the excessive consumption of water by agriculture dictate the adoption of integrated and innovative approaches towards the development of water-saving agricultural systems.

In this work are presented IoT systems and the associated decision support tools that forms interacting and integrated smart-farming decision-support systems, as developed by multidiscipline research teams.

They are employed to optimize the irrigation management of tree crops, by considering its impact on tree crop's economy considering nutrient content of irrigated water. They relies on integrated IoT ecosystems designed to foster and evaluate innovative, field-based solutions that aim to improve the efficiency and sustainability of agricultural resource management, featuring energy-autonomous, mesh Wireless Sensor Networks (WSN), Cloud Computing, and Decision-Support Systems to provide real-time Artificial Intelligence-based consultancy to farmers leveraging on distributed field data collection.

In that respect, this is accomplished by incorporating smart irrigation models (SIM) that are designed to lever0age key climatic, crop and soil parameters measured in-field as inputs.

A series of real cases were carried out during irrigation periods, in order to demonstrate how typical tree growers are benefited, to facilitate the irrigation decision-making process based on the comparison with the applied conventional irrigation treatment.

Therefore, conventional as well as model-based irrigation treatments were applied and compared to each other regarding their impact on irrigation & N-fertilization cost, as well as on crop nutrition. The results show that model-based irrigation treatments can generate significant water savings (up to 40%) and related cost-savings, along with N-fertilization cost-savings.

Concluding, integrated smart-farming decision-support systems based on smart irrigation models /treatments showed great results cost-environmental wise, compared to the conventional treatments.

References

"Development of an innovative smart-farming and decision-support service to improve clingstone peach cultivation", I Moutsinas, P Maletsika, A Apostolaras, J Mavridis, A Kalkanof, T Korakis, International Peach Symposium 1352, 583-592

"AgroNIT: Innovating Precision Agriculture", I Moutsinas, A Kalkanof, J Mavridis, V Zafeiris, F Oikonomou, G Tziokas, 2022 Global Information Infrastructure and Networking Symposium (GIIS), 6-12

"Development of computational tools for criticality analysis of process systems, utilizing Industrial IoTs", T. Theodosiadis-Thomaidis, G. Panagopoulou and E.N. Pistikopoulos.
Proceedings of the 1st International Conference on Sustainable Chemical and Environmental Engineering SUSTENG 2022, 31 Aug – 04 Sep 2022, Rethymno, Crete, ISBN: 978-618-86417-0-9

Fabrication, characterization and application of ternary magnetic recyclable Bi_2WO_6/BiOI@Fe_3O_4 composite for photodegradation of tetracycline in aqueous solutions

Z. Mengting[1]; T.A. Kurniawan[1,2]*; You Yanping[1]; Mohd Hafiz Dzarfan Othman[3], Ram Avtar[4]*, Dun Fu[5], Goh Hui Hwang[6]

[1] Key Laboratory of the Coastal and Wetland Ecosystems (Xiamen University), Ministry of Education, College of Ecology and Environment, Xiamen University, Xiamen 361102 Fujian, China.

[2] China-ASEAN College of Marine Sciences, Xiamen University Malaysia, Selangor Darul Ehsan, Sepang 43900, Malaysia.

[3] Advanced Membrane Technology Research Centre (AMTEC), School of Chemical and Energy Engineering, Universiti Teknologi Malaysia, 81310 Skudai, Johor, Malaysia

[4] Faculty of Environmental Earth Science, Hokkaido University, Sapporo 060-0810, Japan. Email: ram@ees.hokudai.ac.jp (co-corresponding author)

[5] Key Laboratory of Mine Water Resource Utilization of Anhui Higher Education Institute, School of Resources and Civil Engineering, Suzhou University, Suzhou 234000, PR China

[6] School of Electrical Engineering, Guangxi University, Nanning, Guangxi Province, China, 530004

*: the first and second authors equally contribute to this article and mutually share the first authorship

Corresponding author email: tonni@xmu.edu.cn

keywords: *Antibiotic resistance; Functional composite; ·OH; Magnetic separation, Water treatment.*

Abstract

We aim at fabricating a ternary magnetic recyclable Bi_2WO_6/BiOI@Fe_3O_4 composite that could be applied for photodegradation of tetracycline (TC) from synthetic wastewater. To identify any changes with respect to the composite's morphology and crystal structure properties, XRD, FTIR, FESEM-EDS, PL and VSM analyses are carried out. The effects of Fe_3O_4 loading ratio on the Bi_2WO_6/BiOI for TC photodegradation are evaluated, while operational parameters such as pH, reaction time, TC concentration, and photocatalyst's dose are optimized. Removal mechanisms of the TC by the composite and its photodegradation pathways are elaborated. With respect to its performance, under the same optimized conditions (1 g/L of dose; 5 mg/L of TC; pH 7; 3 h of reaction time), the Bi_2WO_6/ BiOI@5%Fe_3O_4 composite has the highest TC removal (97%), as compared to the Bi_2WO_6 (63%). After being saturated, the spent photocatalyst could be magnetically separated from solution for subsequent use. In spite of three consecutive cycles with 71% of efficiency, the spent composite still has reasonable photocatalytic activities for reuse. Overall, this suggests that the composite is a promising photocatalyst for TC removal from aqueous solutions.

2nd International Conference on
Sustainable Chemical and
Environmental Engineering
14th – 18th June 2023, Limassol, Cyprus

Improving prediction of bioethanol production through construction of a gene regulatory model in *Saccharomyces cerevisiae*

M. Christodoulou[1], M. Kyriakou[1], P.S. Stephanou[1] and M. Koutinas[1]

[1]Department of Chemical Engineering, Cyprus University of Technology, Limassol, Cyprus
Corresponding author email: michail.koutinas@cut.ac.cy

keywords: *Saccharomyces cerevisiae; Mathematical model; Genetic circuit; Bioethanol; Glycolysis.*

Introduction

The production of biofuels such as bioethanol from lignocellulosic biomass, constitutes a promising process holding numerous advantages including the reduction of fossil fuels and environmental pollution (Chen et al., 2021). Alcoholic fermentation is commonly performed by the industrial workhorse *Saccharomyces cerevisiae* (Nijland et al., 2021), utilizing glucose as the primary energy source via the pathway of glycolysis (Kim et al., 2021). The Rgt2 receptor, which is considered a glucose concentration sensor, is located on the plasma membrane of the cell detecting high glucose concentrations (>10 g/L) (Van Ende et al., 2019). Rgt2 is responsible for the expression of two glucose transporters within the cell, Hexose transporter 1 (HXT1) and Hexose transporter 3 (HXT3), which activate hexokinase 2 (HKX2), the first enzyme of glycolysis (Kim et al., 2021). Apart from the aforementioned intracellular components, pyruvate dehydrogenase (PDC5) and alcohol dehydrogenase (ADH1) also comprise crucial steps for bioethanol production (Patel et al. 2014). Previous research has shown that the development of experimentally validated models of key genetic circuits (comprising groups of cellular elements that interact) could improve prediction of the kinetic properties of a microorganism (Koutinas et al. 2011).

Materials and methods

Bioethanol fermentations were performed using *S. cerevisiae*, where the strain was pre-grown in a YPD medium consisting (g L^{-1}): glucose 20, peptone 20 and 10 yeast extract. Cultures were incubated at 30 °C in an orbital shaker stirred at 100 rpm for 20 h. The inoculum was centrifuged and 2g of wet biomass were transferred to a YPD fermentation medium consisting (g L^{-1}): glucose 20, peptone 20 and 10 yeast extract. Ethanol production was monitored through gas chromatography (GC) and to determine the glucose consumption rate, samples were collected at regular intervals and analyzed using high-performance liquid chromatography (HPLC). Quantitative PCR (qPCR) analysis was performed to determine the mRNA expression levels of *HXT1*, *HXK2*, *PDC5* and *ADH1* genes during *S. cerevisiae* fermentations.

Results and discussion

In order to predict the kinetics of the microorganism in relation to glucose uptake and consumption, a logic model was developed with the use of logic gates. In the logic model, the interacting molecular components were described as a combination of logic gates, producing an "electronic" representation following an analogy to electronic circuits [1]. The logic model implemented included glucose sensing processes, activation of glucose/hexose transporters (HXTs), glycolysis pathway and ethanol production. The presentation will include construction of a Boolean model combining logic gates to describe important regulatory loops, while Hill functions will be used as input functions to the relevant genes, aiming to produce a dynamic mathematical model using ordinary differential equations to describe mRNA production from the genes involved in glycolysis. Simulations of the developed model predicting the dynamic behavior of the molecular system will be presented.

References

J. Chen, B. Zhang, L. Luo, F. Zhang, Y. Yi, Y. Shan, B. Liu, Y. Zhou, X. Wang, X. Lü, 2021. A review on recycling

techniques for bioethanol production from lignocellulosic biomass. *Renew. Sustain. Energy Rev*., 149, 6, p. 111370.

J. G. Nijland, H. Y. Shin, E. Dore, D. Rudinatha, P. P. De Waal, and A. J. M. Driessen, 2021. D-glucose overflow metabolism in an evolutionary engineered high-performance D-xylose consuming Saccharomyces cerevisiae strain. *FEMS Yeast Res.*, 21, 1, 1–14.

J. H. Kim and R. Rodriguez, 2021. Glucose regulation of the paralogous glucose sensing receptors Rgt2 and Snf3 of the yeast Saccharomyces cerevisiae. *Biochim. Biophys*. Acta - Gen. Subj., 1865, 6.

M. Van Ende, S. Wijnants, and P. Van Dijck, 2019. Sugar sensing and signaling in Candida albicans and Candida glabrata. *Front. Microbiol.*, 10, 1, 1–16.

M. S. Patel, N. S. Nemeria, W. Furey, and F. Jordan, 2014. The pyruvate dehydrogenase complexes: Structure-based function and regulation. *J. Biol. Chem.*, 289, 24, 16615–16623.

M. Koutinas, A. Kiparissides, R. Silva-Rocha, M.C. Lam, V.A.P. Martins dos Santos, V. de Lorenzo, E.N. Pistikopoulos, A. Mantalaris, 2011. Linking genes to microbial growth kinetics-An integrated biochemical systems engineering approach. *Metab. Eng*., 13, 4, 401-413.

Seasonal shifts of soil microbiomes to conservation practices.

N. Paranychianakis[1], M. Frantzeskou[1] and S. Tul[1]

[1] School of Chemical and Environmental Engineering, Technical University of Crete, Chania, Greece
Corresponding author email: nparanychianakis@.tuc.gr

keywords: *soil health; soil restoration; microbiota.*

Introduction

In recent years there is a growing interest for ecological microbiome engineering as a potential way to address environmental challenges like, climate change mitigation, restoration of degraded ecosystems, and transition to sustainable agroecosystems. Adoption of appropriate agronomical practices may contribute towards this goal through their impacts on soil microbiome structure.
In this work we evaluate the effect of soil conservation practices (tillage, non-tillage, chemical pest control) on soil microbiome across different sites in olive orchards in the island of Crete, Crete.

Materials and methods

Seasonal soil samplings were performed during the 2022 in olive orchards differing subjected to soil restoration practices (non-tillage, intercroppinmg) and conventional management. DNA was extracted with the DNeasy PowerSoil Pro kit following the manufacturer's instructions. The universal prokaryotic primer set 515f/806r was used to amplify the V4 hypervariable region of the 16S rRNA gene. Amplicon sequencing was performed in a MiSeq Illumina platform at the NOVOGENE UK Facilities. Raw reads were processed with the DADA2 pipeline. Different metrics were used to estimate the α-diversity of microbial communities (Shannon, Pielou's J, Faith's PD) and β-diversity (Bray–Curtis dissimilarity, UniFrac distances). Network construction and analysis was performed with the Molecular Ecological Network Analysis Pipeline and differential abundance with the DESEQ2 package.

Results and discussion

Our findings reveal that soil restoration practices had a minor effect on the composition, α- and β-diversity of microbiomes in the bulk soil. However, local pedo-climatic conditions had a stronger effect in the composition of soil microbiomes and β-diversity. Finally, our analysis revealed strong links between soil properties and bulk soil microbiome.

Conclusions

Our findings provide important implications for soil management in the Mediterranean outlining the need for a better understanding of the effects of local pedo-climatic conditions to successfully engineer soil microbiome and improve the provisioning of ecosystem services.

Acknowledgements: This study is supported by the Horizon 2020 and the PRIMA program (EC): "RESilient to Climate CHange Extremes MeDiterranean AgricUltural Systems: LEveraging the Power of Soil Health and Associated Microbiota", RESCHEDULE.

Recovery of phosphate from wastewater using by-pass dust (BPD) from cement industry

P. Photiou[1], P. Christou[1] and I. Vyrides [1]

[1]Department of Chemical Engineering, Cyprus University of Technology, 30 Archbishop Kyprianou Str., Limassol, Cyprus

Corresponding author email: ioannis.vyrides@cut.ac.cy

Abstract

The increased waste generation and limited phosphorus reserves prompted the adoption of new industrial methods aimed at directing liquid waste towards phosphorus recovery processes for subsequent use as fertilizer in agriculture. To facilitate phosphorus recovery, a material known as by-pass dust (BPD), a by-product of the cement industry, was employed. The BPD underwent thermal treatment and was tested as a phosphate adsorbent for real wastewater. Various experiments were conducted, utilizing synthetic solutions (KH2PO4) with different concentrations of BPD to determine optimal adsorption conditions for phosphorus. Additionally, synthetic wastewater solutions were prepared to examine the impact of various ions on phosphorus adsorption. High concentrations of nitrate, sulfate, and ammonium ions did not exhibit significant phosphorus adsorption, while low concentrations of acetate and ammonium ions influenced adsorption. Phosphate ions were also sourced from dewatered sludge, and different concentrations of sulfuric acid (SA), citric acid (CA), and oxalic acid (OA) were employed as extraction agents. Results indicated that SA with a concentration of 0.5 M was the most effective acid, yielding the highest phosphorus concentration. Following extraction, BPD was utilized to adsorb (recover) phosphates, and the resulting solid residues were evaluated for their potential as fertilizer. The adsorption capacity of thermally treated BPD with rejected wastewater was assessed, confirming a high phosphate adsorption capacity (227.27 mg g−1) and an adsorption percentage of 82.95%. Synthetic wastewater demonstrated a 100% adsorption percentage. Phytotoxicity trials were conducted to evaluate BPD as a fertilizer substitute by monitoring the growth of two seed types (Lepidium sativum and Sinapis alba). The process revealed a positive effect on plant growth, with germination index (GI) values reaching up to 134.8% for both tested seeds. Conversely, the solid residue generated by leached DWAS solution adversely affected plant germination, likely due to harmful compounds present in DWAS. This study demonstrates the ability of thermally treated BPD to serve as a selective adsorbent material for phosphates in real wastewater, presenting a new opportunity for its utilization within the circular economy concept.

Treatment of municipal wastewater primary effluent by trickling filters

E. Gìka, E. Kypriotakis, I. Chourdakis and P. Gikas

School of Chemical and Environmental Engineering, Technical University of Crete, Chania, 73100, Greece
Corresponding author email: pgikas@tuc.gr

keywords: *trickling filter; wastewater; attached growth; support media; recirculation.*

Trickling filters have been employed for several decades for municipal wastewater treatment. They comprise of a permeable bed, filled with either rocks or especially designed plastic materials. Microorganisms are naturally attached on the surface of the filling media, while wastewater is sprinkled at the top of the bed using a rotating arm. During the conduct of wastewater with the attached microorganisms, BOD and ammonia are oxidized, while limited denitrification may also occur at the lower part of the filter (Ali *et al.*, 2017). Tickling filtration has high potential to replace the commonly used activated sludge process, especially if part of the suspended solids has been removed prior to trickling filtration (Gikas, 2017). The present study compares the performance of two types of support materials (a random flow high voidance one ("A") and a classical crossflow one ("B")) in trickling filters, at selected operational conditions (forced/natural aeration and recirculation rate varied from zero to 2.5) (Figure 1), for the treatment of primary clarified municipal wastewater. For this comparison two identical (apart of the support material) cylindrical filters have been used, with dimensions 2m × 0.2m (height × diameter).

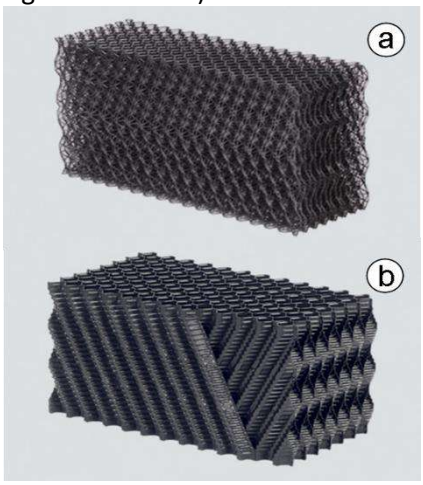

Figure 1. *Support materials used in trickling filters, manufactured by GEA 2H Water Technologies, GmbH. (a) PLASdekplash/Trickle fills, NET 150®, (b) BIOdek Cross-Fluted Fills with HX-factor, KZP 612®.*

A number of parameters have been determined (BOD5, COD, TSS, N-NH_4^+), at the inlet and outlet points. Inlet flowrate was set at 1 L/h, corresponding to hydraulic loading of 0.08 m/h). In all cases the trickling filter with support material type "A" proved superior compared with the performance of type "B". Forced aeration had a significant positive effect, in treatment efficiency of most of the monitored parameters, compared to natural ventilation Increase of the recirculation rate from zero up to 1 only marginally improved the treatment efficiency, while treatment efficiency reduced at recirculation rate 2.5.

References

Ali, I., Khan, Z.M., Peng, C., Naz, I., Sultan, M., Ali, M., Mahmood, M.H. and Niaz, Y., 2017. Identification and Elucidation of the Designing and Operational Issues of Trickling Filter Systems for Wastewater Treatment. Pol. J. Environ. Stud. 26(6), 2431-2444.

Gikas, P., 2017. Towards energy positive wastewater treatment plants. *J. Environ. Manage.*, 203, 621–629.

Soil enzymes activity in agroecosystems adopting conservation and conventional agronomical management practices.

M. Frantzeskou[1], S. Tul[1] and N. Paranychianakis[1]

[1] School of Chemical and Environmental Engineering, Technical University of Crete, Chania, Greece
Corresponding author email: nparanychianakis@.tuc.gr

keywords: *soil health; soil restoration; soil functioning.*

Introduction

Soils in the Mediterranean basin have been depleted in soil organic matter (SOM) by intensive conventional practices which in turn may adversely affect the resilience of agroecosystems to climate change with severely environmental, social, and economic impacts. To improve our understanding on the drivers regulating organic-C cycling in Mediterranean landscapes, we sampled soils for agroecosystems subjected to different agronomical practices and monitored soil enzyme activities involved in the C cycling, soil physico-chemical properties and greenhouse gasses (GHGs) emission patterns.

Materials and methods

Enzyme activities of β-glucopyranoside, β-D-xylopyranoside, N-acetyl-β-glucosaminide, and alkaline phosphatase were measured fluorometrically in autumn of 2022 and winter of 2023 in conventional fields and fields subjected to soil health restoration practices (no-tillage, pruning residual incorporation, and cover crops). In addition, SOM and nutrient content, pH, soil texture were also assessed using standard methods of soil analysis.

Results and discussion

Our findings revealed strong effects of the adopted management practices on SOM sequestration in the Mediterranean agroecosystems. These differences were linked to differences in enzyme activities and soil properties. In addition, our findings showed different patterns of soil respiration rates between the agroecosystems differing in the management practices but no emissions of N2O were detected independently of soil management regime. For instance, intercropping of olive orchards with legumes stimulated the accumulation of SOM and linked to lower soil respiration rates.

Conclusions

Our findings reveal strong effects of management practices on SOM sequestration and the functioning of soils in the Mediterranean that are context dependent.

Acknowledgements: This study is supported by the Horizon 2020 and the PRIMA program (EC): “RESilient to Climate CHange Extremes MeDiterranean AgricUltural Systems: LEveraging the Power of Soil Health and Associated Microbiota”, RESCHEDULE.

A generalized differential constitutive equation for polymer melts with a broad molecular weight distribution

P. C. Konstantinou[1] and P. S. Stephanou[1]

[1]Department of Chemical Engineering, Cyprus University of Technology, Limassol, Cyprus
Corresponding author email: pavlos.stefanou@cut.ac.cy

keywords: *rheological model; polymer melts; non-equilibrium thermodynamics; molecular weight distribution; normal stress coefficients.*

Introduction

Polymers are widely used in various industries due to their unique properties. High-molecular weight polymeric systems have a complex chain structure that results in an interesting rheological behavior, making them useful in a wide range of industries such as healthcare, electronics, and automotive ones. However, despite their usefulness, understanding their complex rheological behavior remains a challenging problem due to the complex interplay between the rheological properties and the molecular weight (MW) distribution (MWD) of the studied sample. The polydispersity index (PDI) is an important parameter used to characterize the distribution of molecular weight in a polymer sample and it is defined as the ratio of the weight-average molecular weight (M_w) to the number-average molecular weight (M_n) of the sample [Bird et al. (1987)]. A high PDI indicates a broad MWD.

The normal stress differences (N_1, N_2) or equivalently the normal stress coefficients (Ψ_1, Ψ_2) are important viscometric properties that, in addition to the shear viscosity η, are used to describe the behavior of large-molecular-weight polymers. They are affected by various factors such as the MW, chain architecture and deformation conditions. However, these are seldom measured in samples of industrial interest and usually the constitutive models used to predict them are not able to accurately predict the normal stress coefficients.

Stephanou et al. (2009) derived a generalized differential constitutive equation for polymer melts which self-consistently incorporates terms that account for anisotropic hydrodynamic drag, finite chain extensibility with nonlinear molecular stretching, nonaffine deformation, and variation of the longest chain relaxation time with chain conformation. Key elements in the new constitutive model were the functions describing the dependence of the nonequilibrium free energy and the relaxation matrix on the conformation tensor. With suitable choices of these two functions, the new equation reduces to several well-known viscoelastic models, such as the Phan-Thien Tanner (PTT), and Giesekus ones [Bird et al. (1987)]. It is, however, more general since it permits incorporating into a single constitutive differential equation more accurate expressions for the description of chain elasticity and relaxation. Since during the derivation Stephanou et al. (2009) used nonequilibrium thermodynamics, restrictions on the parameters entering the new model are obtained by analyzing the thermodynamic admissibility of the model. Although it was shown to accurately predict the rheological behavior of short monodisperse polyethylene melts obtained through direct nonequilibrium molecular dynamics simulations in shear and planar elongation, it has not been to date generalized to accommodate a MWD.

In the present work, we generalize the constitutive model of Stephanou et al. (2009) to handle a MWD, thus rendering it more appropriate for industrial polymeric systems. We further consider the use of a non-constant slip/nonaffine parameter ξ following Nikiforidis et al. (2022). To validate our model, we will compare its predictions against the rheological properties of high-molecular-weight high-density polyethylene (HDPE).

Results and discussion

The resulting constitutive model, i.e., the evolution equation for the dimensionless conformation tensor, $\tilde{\mathbf{c}}$, and the corresponding equation for the stress tensor, $\boldsymbol{\sigma}$, for polydisperse polymer melts, is given via,

$$\tilde{\dot{\mathbf{c}}}_{[JS]} = -\frac{1}{\tau(M)\tau^*(\mathrm{tr}\tilde{\mathbf{c}})}\left[\mathbf{I}+\alpha(1-\xi)B(\tilde{\mathbf{c}})\left(h_0(\mathrm{tr}\tilde{\mathbf{c}})\tilde{\mathbf{c}}-\mathbf{I}\right)\right]\cdot\left(h_0(\mathrm{tr}\tilde{\mathbf{c}})\tilde{\mathbf{c}}-\mathbf{I}\right), \quad (1a)$$

where,

$$\tilde{\dot{\mathbf{c}}}_{[JS]} \equiv \frac{\partial\tilde{\mathbf{c}}}{\partial t}+\mathbf{u}\cdot\nabla\tilde{\mathbf{c}}-(\nabla\mathbf{u})^T\cdot\tilde{\mathbf{c}}-\tilde{\mathbf{c}}\cdot\nabla\mathbf{u}+\frac{\xi}{2}(\dot{\boldsymbol{\gamma}}\cdot\tilde{\mathbf{c}}+\tilde{\mathbf{c}}\cdot\dot{\boldsymbol{\gamma}}), \quad (1b)$$

is the Johnson-Segalman derivative with $\nabla\mathbf{u}$ the velocity gradient tensor, $\dot{\boldsymbol{\gamma}}\equiv\left[\nabla\mathbf{u}+\nabla\mathbf{u}^T\right]$ the rate of deformation tensor ($\mathbf{A}^T$ is the transpose of $\mathbf{A}$), and,

$$\boldsymbol{\sigma} = G_N^0\int_0^\infty p(M)(1-\xi)\left(h_0(\mathrm{tr}\tilde{\mathbf{c}})\tilde{\mathbf{c}}-\mathbf{I}\right)dM\,, \quad (1c)$$

respectively. An example of a MWD customarily used is the log-normal MWD which is characterized by two parameters: the molecular weight $\bar{M}_m$ corresponding to the peak of the MWD, and the σ_D is the width of the MWD. Here, ξ denotes the slip/nonaffine parameter, α is the Giesekus anisotropic parameter, $\tau^*(\mathrm{tr}\tilde{\mathbf{c}}) = \exp\left[-\varepsilon(1-\xi)\left(h_0(\mathrm{tr}\tilde{\mathbf{c}})\mathrm{tr}\tilde{\mathbf{c}}-3\right)\right]$ with ε the PTT parameter, $h_0(\mathrm{tr}\tilde{\mathbf{c}}) = (b-3)/(b-\mathrm{tr}\tilde{\mathbf{c}})$ with b the extensibility parameter, $p(M)$ is the MWD, $\tau(M)=\tau_0\left(M/\bar{M}_m\right)^{2+\beta}$ is the polymer relaxation time, where $\tau_0\equiv\tau\left(\bar{M}_m\right)$ is the relaxation time of the polymer chains with a molecular weight corresponding to the peak of the MWD and β is an exponent with an expected value between 1-1.4, and G_N^0 is the plateau modulus (that is independent of molecular weight). In this work, we will use this model to predict the rheological properties of high-molecular-weight high-density polyethylene (HDPE), such as those reported by Konaganti et al. (2015).

Conclusions

The new constitutive model that we will present will allow for the more accurate prediction of the rheological response of polymeric systems used industrially, such as HDPE, that do possess an extensive spectrum of MW and not a very narrow distribution as it is customarily assumed when deriving a constitutive model. Only then would polymer engineers be able to accurately use the predictions of the revised constitutive model against the rheological response noted in actual industrial processes. Our findings provide a foundation for future research aimed at enhancing the properties of high molecular-weight polymers for diverse applications.

References

Bird, R. B., Curtiss, C. F., Armstrong, R.C. and Hassager, O., 1987. *Dynamics of Polymeric Liquids*; Vol. 2, Kinetic Theory, 2nd Ed. (John Wiley & Sons, New York).

Konaganti, V. K., Ansari, M., Mitsoulis, E. and Hatzikiriakos, S. G., 2015 Extrudate swell of a high-density polyethylene melt: II. Modeling using integral and differential constitutive equations. *J. Non-Newtonian Fluid Mech.* 225, 94-105.

Nikiforidis, V.-M., Tsalikis, D. G. and Stephanou, P. S., 2022 On the Use of a Non-Constant Non-Affine or Slip Parameter in Polymer Rheology Constitutive Modeling. *Dynamics*, 2, 380-398.

Stephanou, P.S., Baig, C., Mavrantzas, V.G., 2009. A generalized differential constitutive equation based on principles of non-equilibrium thermodynamics. *J. Rheol.*, 53, 309-337.

2nd International Conference on
Sustainable Chemical and
Environmental Engineering
14th – 18th June 2023, Limassol, Cyprus

Optimization of microalgae bio-products under industrial flue gas exposure

G. Makaroglou[1], D. Mitrogiannis[1] and P. Gikas[1]

[1]School of Chemical and Environmental Engineering, Technical University of Crete, Kounoupidiana, Greece
Corresponding author email: gmakaroglou@tuc.gr

keywords: *Stichococcus sp.; photo-bioreactors; flue gas; CO_2 fixation; high added value products.*

Introduction

Most microalgal species isolated from natural streams, lakes or oceans have been pre-adapted for the living environment through artificial domestication and have been successfully used for fixation of atmospheric CO_2. However, unlike atmospheric air which has low CO_2 content, post-combustion flu gas typically contains 4-14% or more v/v CO_2 concentration and possibly toxic compounds (SOx, NOx and trace elements) in a high flow rate, high temperature (80-120 °C or above). This means that the microalgal species need to be able to tolerate the harsh flue gas conditions in order to capture CO_2. Microalgal CO_2 bio-fixation is a complex physicochemical process. Apart from microalgal species, the process is also influenced by physicochemical and other culture parameters (such as CO_2 concentration, pollutants in the flue gas, initial inoculation density, culture temperature, light, nutrients and pH) and hydrodynamic parameters (for example, flow, mixing and mass transfer). Microalgal growth under coal combustion flue gas is usually more complex than that under atmospheric conditions (Zhang, 2015). Therefore, flue gas from natural gas could be used to lessen the negative effects on microalgae growth. The purpose of the current research is the reduction of CO_2 contained in flue gas of a natural gas-fired power plant, using microalgae biomass and its potential in producing high-value products.

Materials and methods

The present study took place in one of Greece's largest Public Power Corporation power plant. Two 15 L closed type photo-bioreactors were utilized for microalgae cultivation. Microalgae were grown attached on sandblasting glass, which covered the bottom of the bioreactors. Both photo-bioreactors were placed inside a small shed, providing protection from weather conditions and other limiting factors. *Stichococcus* sp. was used throughout the experiments. Carbon under the form of carbon dioxide contained in flue gas was provided into the photo-bioreactors at a rate of 0.6 L per minute. Cultures were illuminated by LED lamps (3,300 lux) and the temperature was controlled by an A/C unit (25 ± 1 °C). Samplings for pH measurement were taken every two days. Two lighting profiles were examined; constant and flashing lights (1,000 Hz), with a photoperiod of 16:8 hours day:night, to examine the effect of the flashing light on *Stichococcus* biomass and bioproducts. *Stichococcus* sp. was cultivated for 26 days in artificial seawater + Bold's Basal Medium with the composition of NaCl and $NaNO_3$ being 35 g L^{-1} and 0.75 g L^{-1}, respectively. Also, nitrogen starvation was being implemented 3 days prior to biomass harvesting in order to increase intracellular lipids production. At the end of cultivation period, the extracted biomass was separated from the sandblasted glass through scraping and then dried in order to quantify the dry cell weight. A portion of the extracted biomass was converted into high added value products (i.e., lipids, pigments, proteins and carbohydrates), to assess *Stichococcus* sp. potential for 3rd generation biorefineries.

Results and discussion

From the preliminary results of the study, it is found that *Stichococcus* sp. was able to withstand flue gas stream and convert the contained CO_2 into usable biomass. Dry cell weight was found to be 50.5 and 47.9 g m^{-2} with the implementation of constant and flashing light, respectively. Results are shown in Figure 1. Flashing lighting at 1,000 Hz, shows a decline in biomass productivity, while constant lights yield approximately 5% greater biomass. However, constant lighting consumed 33.1 kWh, while flashing lights

required 25.7 kWh during the 26 days of cultivation. To note that, pH showed an average value of 6.6 and 6.7, for constant and flashing lights, respectively.

With respect to bio-products production (Fig. 2), carbohydrates content was the highest amongst other bio-products, being 24.8 and 23.4 g m^{-2}, for the constant and flashing lights, respectively. Flashing lights increased lipids and chlorophyll content, by 4 and 20%. The total bioproducts content of *Stichococcus* sp. was equal to 39.8 and 38.2 g m^{-2}, which corresponds to approximately 79 and 80% of the produced biomass for each lighting profile.

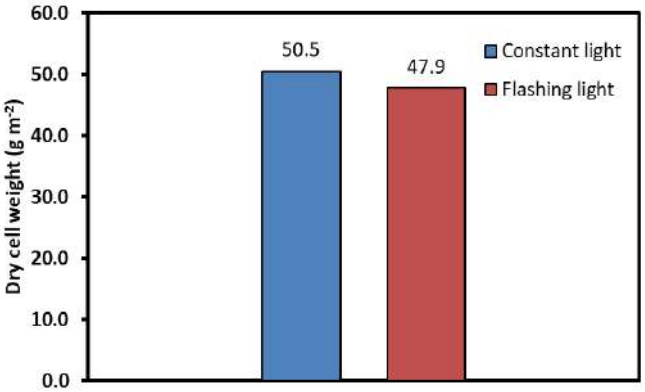

Figure 1. *Biomass productivity of Stichococcus sp. in lab scale photo-bioreactors, under constant and flashing lighting profiles.*

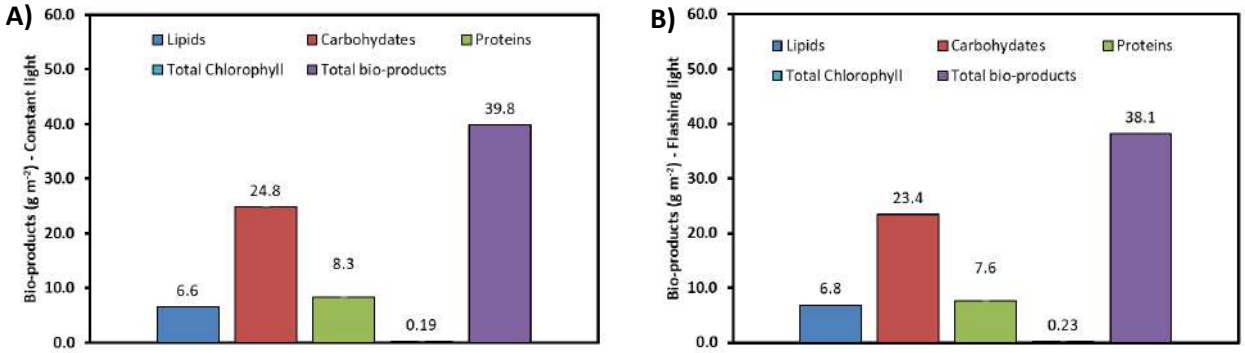

Figure 2. *Bio-products recovery from Stichococcus sp., under constant (A) and flashing (B) lighting profiles.*

Conclusions

According to the study, *Stichococcus* sp. was successfully grown under real-time industrial flue gas produced from a power plant consuming natural gas. Microalgae could be an efficient way to reduce CO_2 concentration from flue gases before they are released into the atmosphere, while the produced biomass could be harvested and processed for the production of high added value products. In conclusion, large scale microalgae photo-bioreactors could significantly reduce CO_2, therefore aiding in the mitigation of the greenhouse effect.

Acknowledgements: This research was co-financed by Greece and the European Union (European Social Fund-ESF) through the Operational Programme «Human Resources Development, Education and Lifelong Learning» in the context of the Act "Enhancing Human Resources Research Potential by undertaking a Doctoral Research" Sub-action 2: IKY Scholarship Programme for PhD candidates in the Greek Universities».

References

Zhang, X., 2015. Microalgae removal of CO_2 from flue gas. *IEA Clean Coal Centre*, London, United Kingdom.

SUST ENG 2023

FULL PAPERS

Artificial Neural Network for the Quantification of Cobalt Recovered from Li-ion Batteries

I.I. Pérez-Juárez[1]*, B.M. González-Contreras[2], M.A. Munive Rojas[2], J.A. Guevara-García[2] and E. Bonilla-Huerta[3]

[1]Postgrado de la Facultad de Ciencias Básicas, Ingeniería y Tecnología. Universidad Autónoma de Tlaxcala, Campus Apizaco, P.O. Box 140, 90300. Tlaxcala. México.
[2]Facultad de Ciencias Básicas, Ingeniería y Tecnología. Universidad Autónoma de Tlaxcala, Campus Apizaco, P.O. Box 140, 90300. Tlaxcala. México.
[3]Tecnológico Nacional de México/ Apizaco. Av. Instituto Tecnológico No. 418, San Andrés Ahuashuatepec, Tlaxcala, México. C.P. 90491.
Corresponding author email: 20224175@garzas.uatx.mx

keywords: *Artificial Neural Network; cobalt; Li-ion batteries; UV-visible spectroscopy.*

1. INTRODUCTION

In search for better chemical monitoring, optical detection methods are widely used because of its high efficiency and low laboriousness, among these, the ultraviolet–visible (UV-Vis) spectrophotometry have several advantages such as online analysis, simultaneous multi-parametric measurements, easily operated and inexpensive sample pretreatment, between others, making this analytical technique cheaper and faster than many others (Ríos-Reina & Azcarate, 2022). In recent years, UV-Vis radiation based methodologies have grown in applications and diversity hand in hand with deep learning algorithms, in particular of artificial neural networks (ANNs), for example, quality control analyses of food (Farag *et al*., 2022), rapid authentication of wine vinegars (Ríos-Reina *et al*., 2021), drinking water quality (Shi *et al*. 2022), pharmaceuticals (Huang *et al*., 2020), and environmental sciences (Ye *et al*., 2022).

In the case of heavy metal ions detection for management of environment pollution, it is of significance the use of UV-Vis detection in real-time (Cheng *et al*., 2020), even in presence of several species (Anni *et al*., 2018). But the development potential has not covered all areas, indeed, up to our knowledge there has been no report concerning the application of UV-Vis-ANN to the quantification of valuable metals from residues, i.e., urban mining, which is a remarkable area of both economic and environmental benefits.

Our research group has been working in the development of technologies for the recovery of metals from used batteries (Guevara-García & Montiel-Corona, 2012) and recently in ion-Li devices (Degante *et al*., 2022). In this last work, content of Li, Co, Mn, Ni, and Al of the initial cathodic material in leaching solutions of organic acids were recovered and analyzed by ICP, while the identification of the oxidation state of Co in the leachates was performed by UV-Vis.

In order to optimize our leaching method in terms of time, reactant concentration, temperature, etc., we should follow the extraction reaction kinetics, a technique that is not possible by ICP, but is handy using UV-Vis-ANN, once that UV-visible spectroscopy confirms that the oxidation state of the cobalt ion in the leachates is Co^{2+}, in the state of low spin and octahedral geometry, identified by means of by its charge transfer band in the region 470-200 nm, and the electronic transition, $^2E_g \rightarrow {}^2T_{1g}$, observed above 500 nm.

The objective of this work is to develop the analytical and computational bases for the construction of an Artificial Neural Network for the quantification of cobalt recovered from Li-ion batteries based on the UV-Vis spectrophotometry.

2. MATERIALS AND METHODS

Preparation of standard solutions of cobalt extracted by organic acids. Procedure of leaching experiments that were developed by our group (Degante *et al*., 2022), consist of a 500 mL three-neck round-bottom flask with an upright condenser and thermometer, on a temperature-controlled hot plate. A volume of 250 mL of a 6% hydrogen peroxide solution and one of three organic acids (acetic acid, 4.5 M, citric acid, 1 M, or lactic acid 1.5 M) was placed in each reactor. The solution was placed under constant stirring and 5 g of the cathode material recovered from the LIB's was added little by little. In order to obtain the high number of standard solutions needed to train the ANN model reproducing the spectral characteristics of the experimental leaching experiments, a mother solution was prepared using reactive-grade $Co(NO_3)_2$ salt (Baker, 99.8%) at 1M solution, 6% with respect to H_2O_2 and 1.5 M with respect lactic acid. Successive solutions of Co^{2+} known concentrations were prepared by taking the respective volume of the mother solution and diluting to 10 mL with bi-distilled water. Each prepared solution was subjected to the extraction procedure and measure with a UV-Vis spectrophotometer, VELAB brand, model VE-5000V, double beam, manufactured by Cientifica Vela Quin S.A. de C.V., Mexico.

Modeling of Cobalt Removal Using UV-Vis-ANN. According to the objective of this work, the following steps were considered: 1) determine the most appropriate type of data pretreatment to apply an ANN; 2) determine the most suitable ANN method for the quantification of the Co^{2+} concentration; 3) construction of the ANN prediction model.

To achieve the first goal three option were considering in this work: raw data as obtained in the spectrophotometer, without mathematical pretreatment; pretreatment of data taken a first derivative; pretreatment of data through deconvolution. The criteria to for chosen the methodology was literature survey.

For the second objective, a Backpropagation (BP) architecture is proposed in this article, configured in such a way that the training is performed without using additional resources such as a GPU, only CPU. This basic neural network model is proposed instead of sophisticated models that consume a high quantity of computational resources and are frequent options in the scientific community such due to the multiple virtues (Sornam & Devi, 2016).

The construction of the model, third objective, was accomplish taken the minimum topology possible while keeping a high accuracy to predict the level of Co^{2+} concentrations (mol/L) from the data set of absorbance levels. This was achieved with an architecture type 21x5x5x1. This means that 21 absorbance levels are taken as input to the neural network and a single hidden layer block of size 5x5 is defined, finally an output layer of 5x1 is defined. The function defined for each neuron in the BP model was the exponential function. The assignment of weights was randomized with a normal distribution. The number of epochs defined to achieve learning was 700.

3. RESULTS AND DISCUSSION

Obtaining the spectral series of feeding for the ANN. The series of UV-Vis spectra obtained with the procedure described in the methodology reproduce successfully the characteristics of original leaching experiments as can be seen in Figure 1b.

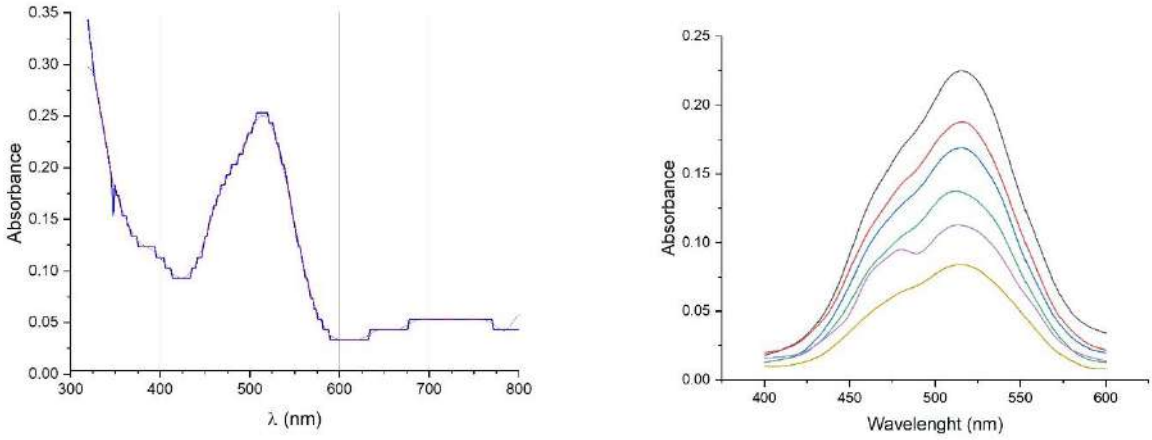

Figure 1. *(a) UV-Vis spectrum of a typical solution after the extraction of Co2+ with lactic acid from cathodic material of ion-Li battery, taken from Degante et al., 2022; (b) A reduced number of UV-Vis spectra obtained with the standard procedure of this work.*

Non-linear nature of UV-Vis spectroscopy. UV-Vis spectra usually contain only a few broad absorbance bands and are often quite broad and difficult to associate with individual chromophores. Because light is a form of energy, absorption of light by matter causes the energy content of the molecules (or atoms) in the matter to increase. The total potential energy of a molecule is represented as the sum of its electronic, vibrational, and rotational energies. These transitions result in very narrow absorbance bands at wavelengths highly characteristic of the difference in energy levels of the absorbing species. However, for molecules, vibrational and rotational energy levels are superimposed on the electronic energy levels. Because many transitions with different energies can occur, the bands are broadened. The broadening is even greater in solutions owing to solvent-solute interactions. Therefore, the resulting spectra is non-linear in nature. The presence of an absorbance band at a particular wavelength often is a good indicator of the presence of a chromophore. However, the wavelength position of the absorbance maximum is not fixed but depends partially on the molecular environment of the chromophore and on the solvent in which the sample is dissolved. Other parameters, such as pH and temperature, also may cause changes in both the intensity and the wavelength of the absorbance maxima (Skoog *et al*., 2013).

The Beer-Bouguer-Lambert law: $T = I/Io = e^{-kbc}$; where c is the concentration of the absorbing species (usually expressed in grams per liter or milligrams per liter) is used in analytical applications. This equation can be transformed into a linear expression by taking the logarithm and is usually expressed in the decadic form: $A = -\log T = -\log(I / Io) = \log(Io / I) = \sum bc$ Where A is the absorbance and ∑ is the molar absorption or extinction coefficient. This expression is commonly known as Beer's law (Skoog *et al*., 2013).

According to Beer's law, absorbance is proportional to the number of molecules that absorb radiation at the specified wavelength. This principle is true if more than one absorbing species is present. All multicomponent quantitative methods are based on the principle that the absorbance at any wavelength of a mixture is equal to the sum of the absorbance of each component in the mixture at that wavelength.

The effect of random noise can be reduced by using additional spectral information, that is, a series of data points can be used for quantification instead of only two. In this so-called overdetermined system, a least squares fit of the standard spectra to the spectrum of the measured sample yields quantitative results (Kisner *et al*., 1983). Other statistical approaches to multicomponent analysis include the partial least squares (PLS), principle component regression (PCR), and multiple least squares (MLS) methods. In theory, these methods offer some

advantages over those described above, however the calibration process can be much more complex (Zwart *et al*., 1984).

Where spectra are highly similar, derivative spectra may be used. As shown in Figure 2, the number of bands increases with higher orders of derivatives. These complex derivative spectra can be useful in qualitative analysis, either for characterizing materials or for identification purposes. For example, the absorbance spectrum of the steroid testosterone shows a single, broad, featureless band centered at around 330 nm, whereas the second derivative shows six distinct peaks (Kumar *et al*., 2012). The resolution enhancement effect may be of use as well in identifying an unknown.

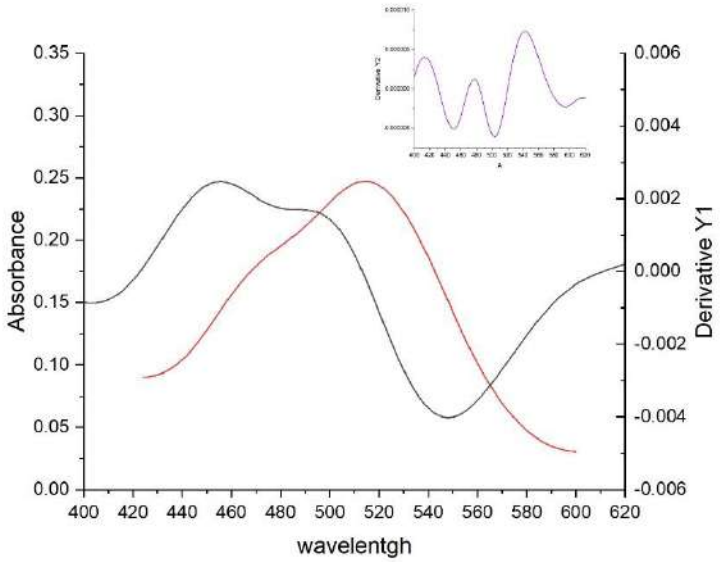

Figure 2. *UV-Vis spectrum original (red) and first (black) and second (purple, inset) for a typical solution after the extraction of* Co^{2+} *with lactic acid from cathodic material of ion-Li battery.*

A symmetrical spectral band is described by three parameters: position (wavelength or frequency corresponding to the absorption maximum), intensity (absorbance or molar absorptivity at the band maximum) and width (usually the bandwidth at half-height). UV-Vis spectra generally have a Gaussian band shape. The resolution of a complex absorption spectrum into individual absorption bands may be necessary if information about the position, height or width of individual bands is required. This technique has proven to be very powerful in various applications where various analytes are present in 2 or more phases, for example in drugs administered via bio-compatible aqueous surfactant-forming micelle (Calabrese *et al.,* 2015).

In the case of UV-Vis quantification of metals in solution, where more than one metal species is present, the overlapping of absorption bands with very close maximum wavelengths is very common, causing interference in the measurement. This effect can be minimized by using deconvolution to use only the absorption band of analytical interest, regardless of the interferences present. Figure 3 shows the deconvolution of the spectrum of a sample of cathode material extracted from Li-ion batteries.

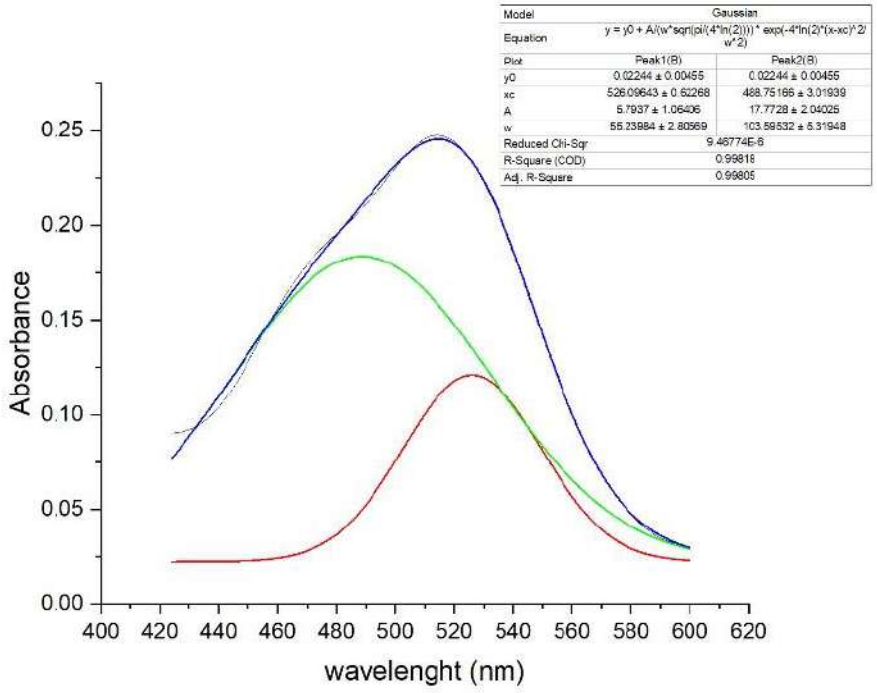

Figure 3. *UV-Vis spectrum deconvolution for its components using Gaussian functions in a typical solution after the extraction of Co^{2+} with lactic acid from cathodic material of ion-Li battery.*

Backpropagation architecture applied to cobalt recovery.
A shallow Backpropagation (BP) architecture is proposed in this article, configured in such a way that the training is performed without using additional resources such as a GPU, only CPU. The minimum topology suggested to predict the level of Co (II) concentrations (mol/L) from the data set of absorbance levels is: 21x5x5x1. This means that 21 absorbance levels are taken as input to the neural network and a single hidden layer block of size 5x5 is defined, finally an output layer of 5x1 is defined. The models are trained using Matlab 2017 and a macOS High Sierra, processor 2.9 GHz Intel Core i7.

The function defined for each neuron in the BP model is the exponential function. The assignment of weights is randomized with a normal distribution. The number of epochs defined to achieve learning is 700. This shallow neural network model is proposed instead of sophisticated models that consume a lot of computational resources and they are very popular in the scientific community such as convolutional networks.

The series of UV-Vis spectra obtained with the experimental procedure were treated with the BP model. The procedure BP reproduce successfully the concentration of the set of standard spectra with a R^2 maximum of 0.9978 for a Mean Squared Error (MSE) BP21X3X3X1 topology (Table 1).

Table 1. *Experimental results using BP with two topologies and without pre-processing technique*

Co (II) concentrations (mol/L)	MSE BP21X5X5X1 Prediction	MSE BP21X3X3X1 Prediction
Experiment 1	0.9964	0.9977
Experiment 2	0.9977	0.9962

Experiment 3	0.9979	0.9978
Experiment 4	0.9971	0.9973
Experiment 5	0.9974	0.9970
Experiment 6	0.9977	0.9964

Elapsed time 11.666960 seconds for first topology, 11.642327 seconds for second topology.

Figure 4 shows the number of bands related to the qualitative analysis for characterizing materials for the reduced number of UV-Vis spectra obtained with the standard procedure.

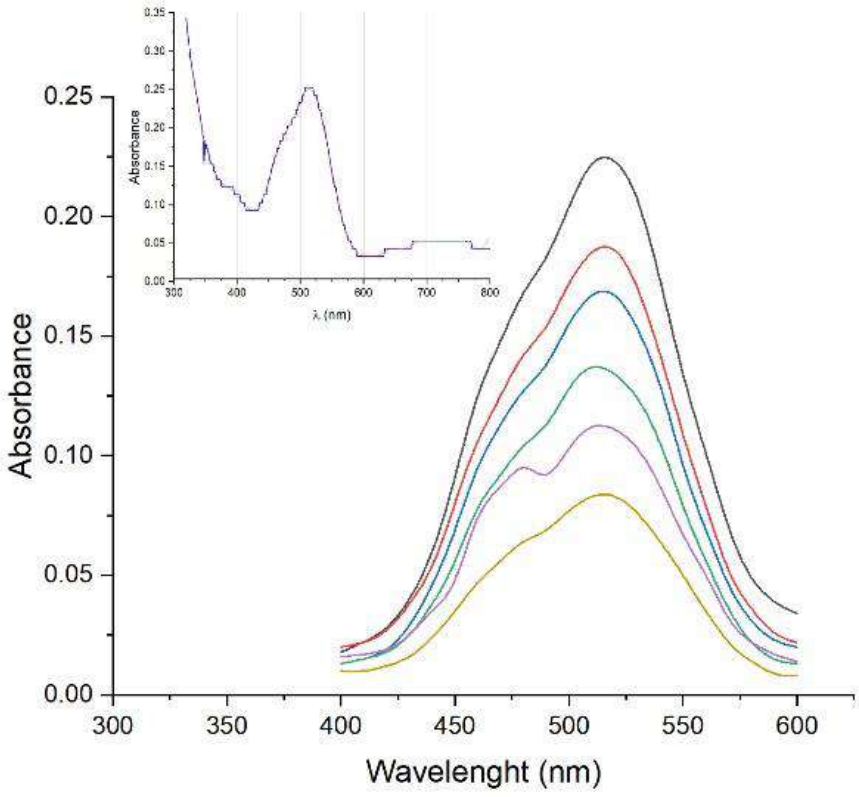

Figure 4. *(Left) A reduced number of UV-Vis spectra obtained with the standard procedure of this work, inset: UV-Vis spectrum of a typical solution after the extraction of Co^{2+} with lactic acid from cathodic material of ion-Li battery, taken from Degante et al., 2022.*

In Figure 5, it can be seen the level of error produced with the different BP procedures.

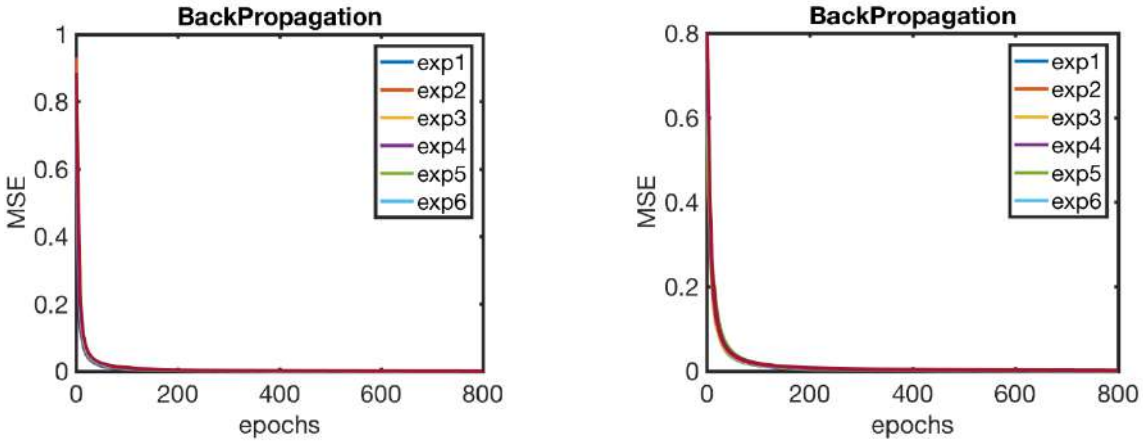

Figure 5. *(Left) MSE for Backpropagation with topology: 21x5x5x1 and 800 epochs. (Right) MSE for Backpropagation with topology: 21x3x3x1 and 800 epochs.*

In order to obtain better results in a shallow neural network it is needed to define a topology with a small number of neurons. However, BP offers better results in the learning process using at least 400 epochs and a learning rate of 0.3.

4. CONCLUSIONS

Up to our knowledge there has been no report concerning the application of UV-Vis-ANN to the quantification of valuable metals from residues, i.e., urban mining, which is a remarkable area of both economic and environmental benefits. While, a well-configured neural model can generalize concentration obtaining with higher performance rates than dense models such as convolutional networks. The Back propagation algorithm is the principal for training Feed Forward Neural Networks. It is proposed for reduce the mean square error (MSE) between the real outputs of a multilayer feed-forward neural network and the preferred outputs. Back Propagation network has a great advantage of simplicity of implementation and computation compared to other mathematically complicated techniques.

REFERENCES

Anni, A., Sepril, A. M., Andrew, P., & Abdul, M. 2018. Determination of Individual Spectra of Sm, Eu, Gd, Tb and Dy from the UV-Vis Spectrum of Mixture Solution. *Res. J. Chem. Environ*, 22, 342-346.

Calabrese, I., Merli, M., & Liveri, M. L. T. (2015). Deconvolution procedure of the UV–vis spectra. A powerful tool for the estimation of the binding of a model drug to specific solubilisation loci of bio-compatible aqueous surfactant-forming micelle. *Spectrochimica Acta Part A: Molecular and Biomolecular Spectroscopy*, 142, 150-158.

Cheng, F., Yang, C., Zhou, C., Lan, L., Zhu, H., & Li, Y. 2020. Simultaneous determination of metal ions in zinc sulfate solution using UV–Vis spectrometry and SPSE-XGBoost method. *Sensors*, 20(17), 4936.

Degante, J. P., Escobar, S. R., Quintero, L. J., Rojas, M. M., & Guevara-García, J. A. 2022. Novel economical method for recovering valuable metals from used Li-ion batteries. *Proceeding of 1st International Conference on Sustainable Chemical and Environmental Engineering*. SUSTENG 2022, 31 Aug-04 Sep, Rethymno, Crete, Greece. Page 265. ISBN: 978-618-86417-0-9.

Farag, M. A., Sheashea, M., Zhao, C., & Maamoun, A. A. 2022. UV fingerprinting approaches for quality control analyses of food and functional food coupled to chemometrics: A comprehensive analysis of novel trends and applications. *Foods*, 11(18), 2867.

Guevara-García, J. A., & Montiel-Corona, V. 2012. Used battery collection in central Mexico: Metal content, legislative/management situation and statistical analysis. *J. Environ. Manage*., 95, S154-S157.

Huang, L., Li, T., Zhang, Y., Sun, X., Wang, Y., & Nie, Z. 2020. Discrimination of narcotic drugs in human urine based on nanoplasmonics combined with chemometric method. *Journal of Pharmaceutical and Biomedical Analysis*, 186, 113174.

Kisner, H., Brown, W., Kavarnos, G. 1983. Multiple analytical frequencies and non-standards for the least-squares analysis of serum lipids. *Anal. Chem*. 1983, 55, 1703.

Kumar, S., Singh, P., & Chandra, H. (2012). UV Derivative Spectroscopic Studies to Characterize the Structure, Biotransformation, and Mechanism of Action of Testosterone. *Analytical letters*, 45(18), 2785-2806.

Ríos-Reina, R., & Azcarate, S. M. 2022. How Chemometrics Revives the UV-Vis Spectroscopy Applications as an Analytical Sensor for Spectralprint (Nontargeted) Analysis. *Chemosensors*, 11(1), 8.

Ríos-Reina, R., Caballero, D., Azcarate, S. M., García-González, D. L., Callejón, R. M., & Amigo, J. M. 2021. Vinegarscan: A computer tool based on ultraviolet spectroscopy for a rapid authentication of wine vinegars. *Chemosensors*, 9(11), 296.

Shi, Z., Chow, C. W., Fabris, R., Liu, J., & Jin, B. 2022. Applications of online UV-Vis spectrophotometer for drinking water quality monitoring and process control: a review. *Sensors*, 22(8), 2987.

Skoog, D. A., West, D. M., Holler, F. J., & Crouch, S. R. 2013. *Fundamentals of analytical chemistry*. Cengage learning. 4th ed.; McGraw Hill: New York, NY, USA.

Sornam, M., & Devi, M. P. (2016). A survey on back propagation neural network. *International Journal of Communication and Networking System*, *5*(1), 70-74.

Ye, B., Cao, X., Liu, H., Wang, Y., Tang, B., Chen, C., & Chen, Q. 2022. Water Chemical Oxygen Demand Prediction model Based on CNN and Ultraviolet-Visible Spectroscopy. *Frontiers in Environmental Science*, 2037.

Zwart, A., van Kampen, E., Zijlstra, W. 1984. Multicomponent analysis of hemoglobin derivatives with a reversed-optics instrument. *Clin. Chem*.,1984, 30, 373.

2nd International Conference on
Sustainable Chemical and
Environmental Engineering
14th – 18th June 2023, Limassol, Cyprus

Sustainable siting of offshore wind farms. Application in Crete (SusTainablE siting of offshore wind Parks. Application in Crete) Step – Ap

P. Gkeka Serpetsidaki [1] and T. Tsoutsos [2]

[1,2] Renewable and Sustainable Energy Systems Laboratory, School of Chemical and Environmental Engineering, Chania, Greece
Corresponding author email: ttsoutsos@tuc.gr

ABSTRACT

The European Union (EU) has already set targets for climate neutrality, with the main objective being the development of renewable energy sources (RES) for 2030 up to 40%. Climate change mitigation and decarbonisation can be achieved through the European Green Deal. In these terms, there is a priority to identify marine areas that are optimal for the sustainable installation of offshore wind farms. Land use conflicts may be alleviated by the development of offshore wind farms. Moreover, the under-construction electric interconnection between Crete and continental Greece may offer multiple opportunities for renewable energy penetration.

The STEP-AP project will provide alternative energy options for insular environments. It will take into account a large number of local opinions in parallel with ensuring a high spatial resolution for all available geographical information. It maintains a strict environmental framework for optimal site selection of OWFs, and analyzes a wide range of criteria. Following an evaluation of the optimal marine areas available, this work incorporates wide audience perspectives into the pre-assessment stage. This is to achieve a holistic approach that meets technical, environmental, economic, and political criteria.

The utilization of research results could be summarized below: (a) Mapping Crete's marine areas from a geological and environmental perspective; (b) insular marine spatial planning; (c) the development of new knowledge regarding the relationship between marine parks and the Cretan ecosystem.

Keywords: offshore wind farms; sustainable siting; islands; social acceptance;

1. INTRODUCTION

The European Union (EU) has already set targets for climate neutrality, with the main objective being the development of renewable energy sources (RES) for 2030 up to 40%. In this context, the development of offshore wind farms is now a political priority, as they can contribute the most to the achievement of the above goals and, in general, to the decarbonization of the planet. The European Parliament has already issued (2022) its strategy for increasing offshore wind farms, "A European strategy for offshore renewable energy (2021/2012(INI))"(2021/2012(INI), European Parliament), as well as our country, according to National energy and climate plan (NECP) has emphasized the importance of the development of offshore wind farms ("priority will be given, as well as marine wind farms with corresponding multiple combined benefits for the energy system, networks and the national economy" (National energy and climate plan (NECP), 2019). In this context, the Regional Plan for Adaptation to Climate Change of Crete refers, on the one hand, to the need to protect marine fauna and flora from man-made activities, as well as to the existing plan for sustainable siting of onshore wind farms (Regional Plan for Adaptation to Climate Change of Crete, 2022). It is based on the Special Study (Renewable and Sustainable Energy Systems Project, 2011), which evaluated necessary information for the siting of onshore wind turbines (areas of environmental interest and cultural heritage, residential activity areas, technical infrastructure networks and special uses and production activity zones or facilities), identified exclusion zones and optimal siting criteria, assessed available areas, and calculated the (ground) bearing capacity of wind farm sites to minimize local environmental impacts (Tsoutsos et al., 2015). They are, however, subject to several limitations (social, environmental, Techno-economic, etc.) and are,

therefore, a multifactorial "problem", which requires a holistic approach. At the same time, increasing land use conflicts, together with the increasing demand for green energy, combined with the untapped offshore wind potential, intensify the necessity to develop offshore wind farms. Therefore, their optimum placement based on marine spatial planning is a research field that needs to be further investigated, mainly for island environments due to: a) their need for long-distance energy security from the mainland and b) untapped offshore wind potential and land release needed. In conclusion, the optimal location of offshore wind farms for Crete should be further investigated for sustainable development and energy independence.

Finally, climate change mitigation and decarbonisation can be achieved through the European Green Deal. In these terms, the priority is the identification of marine areas that are optimal for the installation of offshore wind farms (based on a variety of criteria). There is an installed capacity of onshore wind energy in Greece, but no offshore wind energy capacity. Land use conflicts may be alleviated by the development of offshore wind farms. Moreover, the under-construction electric interconnection between the Cretan Island and continental Greece may offer multiple opportunities for the penetration of renewable energy systems.

OWFs have many advantages compared to the onshore ones, such as:

- As a result of the absence of physical restrictions such as mountains or high buildings, there is a more robust and consistent wind flow in marine areas.
- The size and capacity of offshore wind turbines could be higher and taller than onshore wind turbines, making their energy productivity higher.
- As compared to onshore farms, OWFs may reduce the likelihood of land-use conflicts.
- In nearby communities, OWFs could produce less noise than onshore generators.

There is a significant untapped asset that can be utilized by policymakers at the regional and national levels. A comparison of two types of offshore wind farm foundations is shown below, on the left are fixed, and on the right are the new emerging technology floating offshore wind farms (Tsarknias et al., 2022).

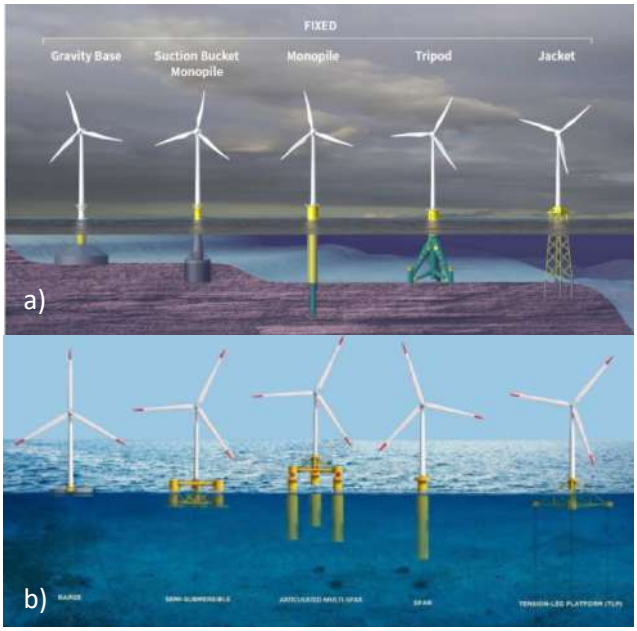

Figure 1. *Type of offshore wind turbines, a) Fixed (*Fixed Wind Foundations: An Independent Concept Screening Approach | 2H Offshore*, n.d.), b) Floating (*Excipio Energy Unveils New Hybrid Floating Offshore Wind Platform*, n.d.).*

Following is a summary of why this work is necessary:

- First of all, energy independence/electrification of islands is a high priority
- Also, it is necessary to shut down conventional fossil fuel plants over the next few years.
- The use of renewable energy sources is a unique solution for the supply of green energy on the islands.

Additionally, the following characteristics are specific to the islands as compared to continental lands:

- Land deficiency
- Land heterogeneity
- Fluctuations of energy needs, especially if they are touristic resorts, during peak season.
- Electric submarine interconnection is realised in some cases, but it is impossible to cover all islands.
- High unexploited offshore wind potential.

As a result, all the aforementioned reasons emphasize the necessity of developing offshore wind farms (OWFs) (Gkeka-Serpetsidaki & Tsoutsos, 2021).

The innovative nature of this work is also highlighted in the following paragraph. This work provides energy alternatives for insular environments. Also, it takes into account a large number of local opinions in parallel with a good spatial resolution is provided for all available geographic information. It maintains a strict environmental framework for the optimal site selection of OWFs, and it analyzes a wide range of criteria. Following an evaluation of the optimal marine areas that are available, this work incorporates the perspectives of a wide audience into the pre-assessment stage, so that a holistic approach can be achieved that will satisfy technical, environmental, economic, and political criteria.

2. METHODOLOGY

An overview of the methodological process is presented here, which includes the literature review, the creation of questionnaires, the implementation of the Analytic hierarchy process (AHP) method, the exclusion areas, and a final map showing the areas that are considered suitable. This paper provides additional details regarding the approach that was followed (Gkeka-Serpetsidaki & Tsoutsos, 2022).

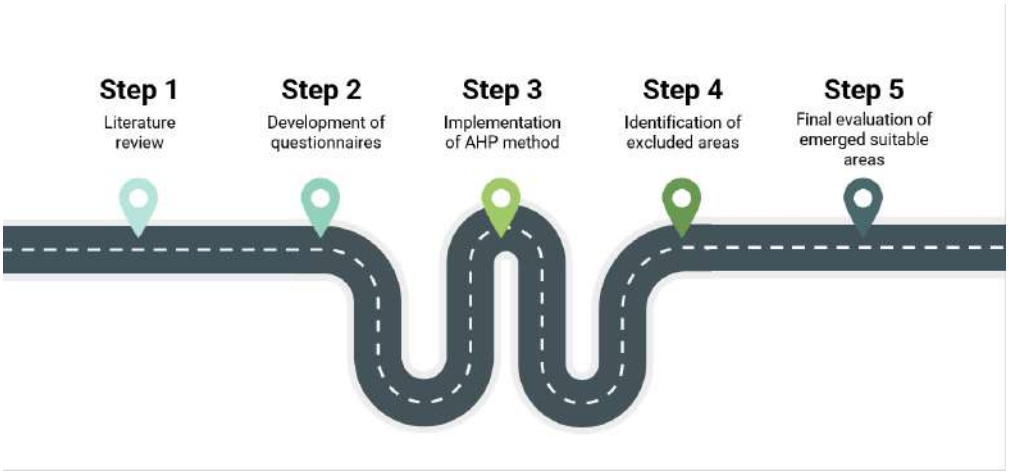

Figure 2. *Methodological framework of the sustainable OWP siting.*

The following are anticipated as part of the research:

- An examination of existing databases on a systematic basis
- Evaluation and ranking of the candidate areas in consultation with society and stakeholders, in addition to the existing legal and regulatory restrictions:
  Regional policymakers
  Academia
  Municipalities
  Transmission and Distribution of energy
  Port Authorities
  Non-Governmental Organizations
  Energy Production-Energy producers' associations
  Tourism -Tourist Associations
- Field surveys in five (5) candidate areas that meet the criteria.

- Emphasis on the effective protection of marine species and the avifauna of the region.
- Consultation and dissemination of results.

3. CONCLUSIONS

In summary, the project viability analysis can be summarized as follows:
Various relevant policies will be formulated based on the project's recommendations for sustainable RES siting and marine spatial planning. As a result:

- Stakeholders at the local and national level will be able to formulate new policies more effectively
- It will strengthen the attitude of the local bodies towards RES, especially considering the considerable increase in the penetration margin of RES as a result of the entire interconnection, which is expected to increase the RES penetration by at least double in 2021 (29.5% already).
- critical decisions will be made regarding the future exploitation of sustainable sites on the island. On the basis of past experience gained from other sustainable siting studies conducted by the Renewable & Sustainable Energy Systems Laboratory (2011, 2014), this methodology will be adopted by other island and coastal regions as well.
- A comprehensive database of geographical and other data will be delivered, allowing the database to be updated in the future with all available information regarding the island of Crete.
- TUC will continue to support the results of the research project, both for the Region of Crete and interested municipalities and social groups after the end of the chartered period. The use of tools and scientific information is predicted to continue to be of interest beyond 2030, either as a result of the decisions made by the licensing authorities or as a result of scientific publications and results announcements.

Finally, the utilization of research results could be summarized below:

1. Mapping the marine areas of Crete from a geological and environmental perspective,
2. An island's marine spatial planning, including the locations of marine RES.
3. The completion of a PhD in "Sustainable siting of offshore wind farms" and at least three (3) diploma theses at the Technical University of Crete.
4. The adoption of the methodology by other islands, both Greek and with similar conditions (for example, in the Mediterranean).
5. The development of new knowledge regarding the relationship between marine parks and the Cretan ecosystem.

4. ACKNOWLEDGEMENTS

This study entitled "Sustainable siting of offshore wind farms. Application in Crete (SusTainablE siting of offshore wind Parks. Application in Crete) Step – Ap" is supported by the Green Fund. ("RESEARCH AND IMPLEMENTATION" of the "PHYSICAL ENVIRONMENT & INNOVATIVE ACTIONS 2022").

REFERENCES

European Parliament, 2021, (2021/2012(INI)), https://oeil.secure.europarl.europa.eu/oeil/popups/ficheprocedure.do?lang=en&reference=2021/2012(INI), *(accessed* 5 June 2023).

Excipio Energy unveils new hybrid floating offshore wind platform, https://www.windpowerengineering.com/excipio-energy-unveils-new-hybrid-floating-offshore-wind-platform/, *(accessed* 3 June 2023).

Fixed Wind Foundations: An Independent Concept Screening Approach, https://2hoffshore.com/knowledge/fixed-wind-foundations-an-independent-concept-screening-approach, *(accessed* 3 June 2023).

Gkeka-Serpetsidaki, P., and Tsoutsos, T., 2021. Sustainable site selection of offshore wind farms using GIS-based multi-criteria decision analysis and analytical hierarchy process. Case study: Island of Crete (Greece). In *Low Carbon Energy Technologies in Sustainable Energy Systems* (pp. 329–342). Elsevier. https://doi.org/10.1016/b978-0-12-822897-5.00013-4.

Gkeka-Serpetsidaki, P., and Tsoutsos, T., 2022. A methodological framework for optimal siting of offshore wind farms: A case study on the island of Crete. *Energy*, *239*. https://doi.org/10.1016/j.energy.2021.122296.

National energy and climate plan (NECP), 2019, https://ypen.gov.gr/energeia/esek/, *(accessed* 22 June 2023).

Regional Plan for Adaptation to Climate Change of Crete, 2022, https://www.crete.gov.gr/perifereiako-schedio-prosarmogis-stin-klimatiki-allagi-stin-kriti/, *(accessed* 10 June 2023).

Tsarknias, N., Gkeka-Serpetsidaki, P., and Tsoutsos, T., 2022. Exploring the sustainable siting of floating wind farms in the Cretan coastline. *Sustainable Energy Technologies and Assessments*, *54*, 102841. https://doi.org/10.1016/J.SETA.2022.102841.

Tsoutsos, T., Tsitoura, I., Kokologos, D., and Kalaitzakis, K., 2015. Sustainable siting process in large wind farms case study in Crete. *Renewable Energy*, *75*, 474–480. https://doi.org/10.1016/j.renene.2014.10.020.

2nd International Conference on
Sustainable Chemical and
Environmental Engineering
14th – 18th June 2023, Limassol, Cyprus

Valorization of spent coffee grounds for removal of chromium from wastewater

R. Campbell and C. Mangwandi[1]

[1]School of Chemistry and Chemical Engineering, Queen's University Belfast, Belfast, United Kingdom
Corresponding author email: c.mangwandi@qub.ac.uk

ABSTRACT

In this work, spent coffee grounds are converted to a valuable porous adsorbent for the removal of chromium (VI) from wastewater. Eight samples of activated spent coffee ground adsorbents were synthesized under varying conditions of pyrolysis temperature, pyrolysis duration and impregnation ratio of activating agent, KOH. Characterization of the samples was made by using SEM, XRD, FTIR, TGA, BET and adsorption studies varying temperature and dosage were conducted. The results show that the spent coffee grounds were successfully synthesized with yields up to 34%. Furthermore, the adsorbents successfully removed chromium (VI) from water with removal efficiencies ranging from 100% - 75% for chromium (VI). The adsorbent also demonstrates the ability to reduce hexavalent chromium (Cr (VI)) to trivalent chromium (Cr (III)). Various adsorption isotherms were analyzed, and it was found Langmuir was most suitable. Furthermore, thermodynamics studies reveal the endothermic nature of chromium (VI) adsorption process.

keywords: *Chromium; Spent coffee grounds, Chemical Activation, Pyrolysis, Adsorption, Porous adsorbent*

1. INTRODUCTION

Heavy metal exposure has been on the increase due to modern industrialization. Contamination of water by toxic metals is an environmental concern and hundreds of millions of people are being affected around the world. Chromium is one of the most toxic heavy metals. Though naturally found in rocks, plants, and volcanic dust, several industrial activities such as chrome plating, leather tanning, metal fabrication and textile dyeing have been sources of chromium in drinking water. The most common forms of chromium are trivalent chromium (Cr^{3+}) and hexavalent chromium (Cr^{6+}) with hexavalent chromium being more toxic as it is a known carcinogen and a reproductive toxicant for males and females. Persons who have consumed chromium in drinking water over the years have faced several health problems such as kidney problems, liver damage and allergic dermatitis [1].

The goals of this study were to produce a porous adsorbent material from spent coffee grounds by activating it with potassium hydroxide (KOH) at different mass ratios, pyrolysis temperatures and activation durations to find the optimum adsorbent for chromium removal. From this material produced, the capacity of the adsorbent to remove Cr^{6+} from wastewater was found and evaluated in different adsorption conditions such as temperature and dosage.

2. METHODOLOGY

2.1 Preparation of the adsorbents

Based on the chemical activation method in literature, dried spent coffee grounds (SCG) and potassium hydroxide (KOH) are weighed in two mass ratios – 1:1 and 2:1 (KOH g: SCG g). Potassium hydroxide is the activating agent used and its role is to increase the porosity of the coffee grounds [2]. The mixture was then placed in a blender along with 20 grams of distilled water to increase the particle size (granulation). The mixture was weighed in crucibles and placed in the tubular furnace with nitrogen gas flow connections set up. Nitrogen gas flowed through the system for a minimum of 5 minutes and then the furnace was switched on and the temperature set to 400°C and 600°C. The mixture is heated for a constant heating rate of 5°C per minute and the pyrolysis duration varied for 1 and 2 hours. After pyrolysis, the material was cooled down with N_2 gas still flowing for 1 hour and then the gas flow ceased. The sample was collected from the furnace and the weight recorded. The activated coffee grounds are then washed with distilled water in a packed

column until a neutral pH was achieved. The adsorbent was then placed in the oven to be dried for ~12 hours at 105 °C. Once completely dried, the final product is weighed and stored in a sealed, labelled vial. Overall, eight adsorbent samples were made by varying pyrolysis temperature, pyrolysis duration and mass ratio of potassium hydroxide to spent coffee grounds.

Each of the 8 samples made were contacted with chromium (VI) solution with concentrations ranging from 5.2 – 52 ppm over a 3-hour period. The residual concentration of the solution was determined using UV–Visible spectrophotometry. The chromium concentration in solid phases was calculated from the equation:

$$Q_e = \frac{(C_i - C_e)\,V}{m}$$

Where C_i and C_e are the liquid-phase concentrations of chromium initially and at equilibrium respectfully and both measured in mg/L. V is the volume of solution (L) and m is the mass of dry adsorbent used for the experiment in grams.

2.2 Characterization of the adsorbent

2.2.1 FTIR Analysis

The functional groups of spent coffee ground adsorbents were determined by Fourier Transform Infrared (FTIR) Spectroscopy within the range 4000–600 cm^{-1} for before and after adsorption. This gives information on the functional groups active in the adsorption process and the type of adsorption taking place.

2.2.2 Surface Area Analysis

The specific areas of the samples were measured using the Brunauer – Emmette – Teller (BET) method wih a Micrometrics Tristar 3020 instrument at temperature of 77K using nitrogen as the adsorbent. The pore volumes of the samples were determined using BJH (Barret, Joyner and Halenda) method.

3. RESULT AND DISCUSSION

3.1 Characterisation

According to Figure 1, when comparing the before and after adsorption spectra, there is a reduction of the peak at 3300-2500 cm^{-1} which pertains to the stretching and bending vibrations of surface –OH, indicating that chromate is adsorbed onto the surface via hydrogen bond formation involving the surface functional group, –OH. Furthermore, the peaks at around 2100 cm^{-1} pertaining to C≡C stretching group (alkyne) disappears after adsorption, and this also indicate the adsorption of Cr (VI). Overall, the FTIR spectra before and after is quite similar however, which also indicates that physical adsorption is occurring rather than chemical adsorption.

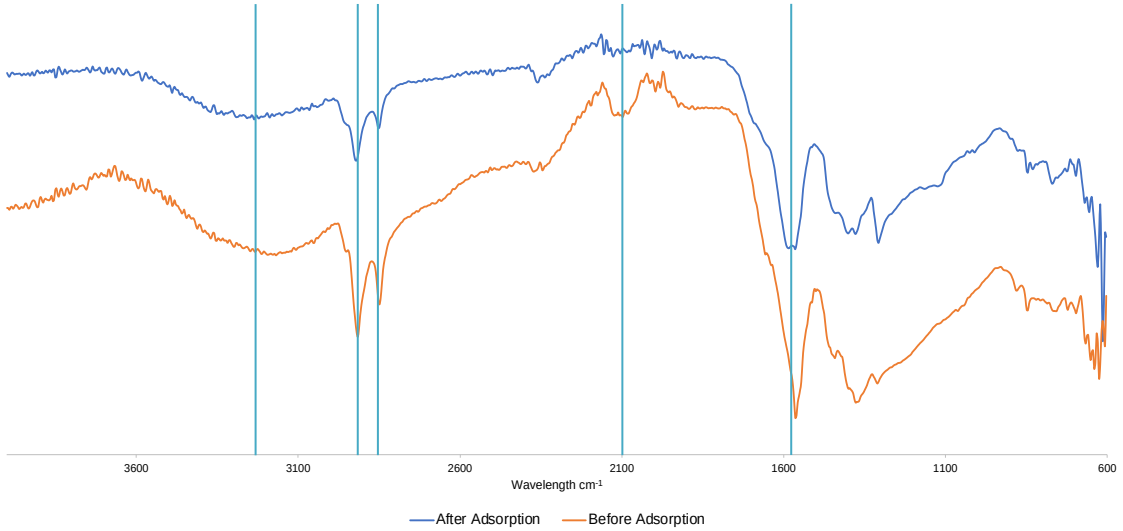

Figure 1 Comparison of the FTIR spectra of the AC1R sample before and after adsorption of Cr^{6+}.

3.2 Chromium Removal Results

Figure 2 shows the removal % of Cr^{6+} for each sample made (see sample conditions in Table 1). The highest removal was obtained with AC1R adsorbent which is produced with a duration of thermal activation of 2 hours, pyrolysis temperature of 400 °C and with a mass ratio of 1:1 (KOH: SCG). Furthermore, this adsorbent sample has the highest Q_{max} value of 207 mg/g as shown in Table 1. The worst percentage removal over the 3-hour duration of the adsorption experiment was 75% for AC4R under the conditions of 600°C for 2 hours with 2:1 mass ratio.

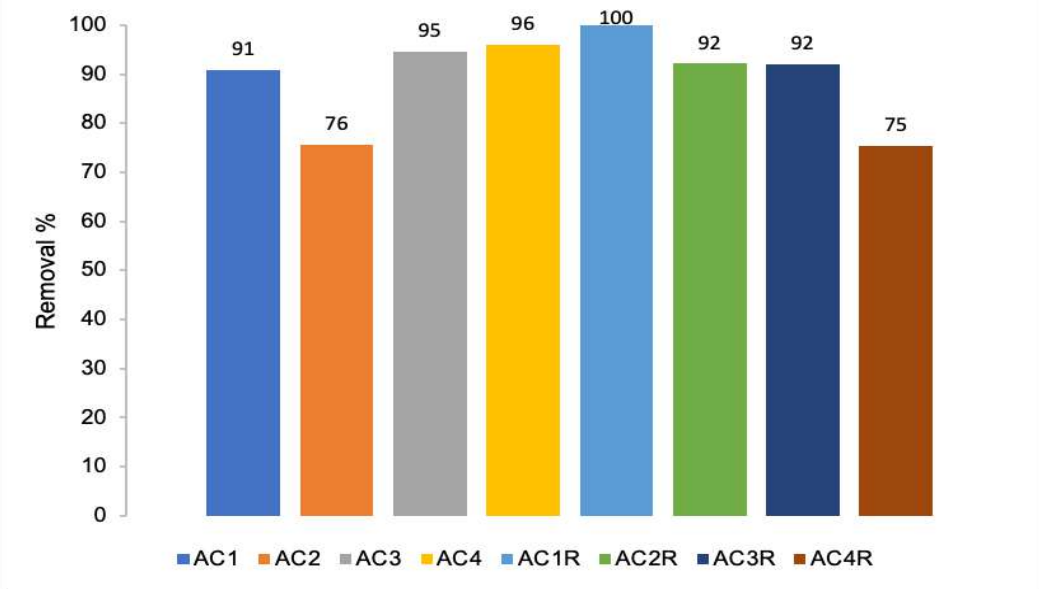

Figure 2 Cr^{6+}Removal % for each sample produced

According to the Q_{max} values in Table 1, for the 1-hour pyrolysis samples, as the pyrolysis temperature and the impregnation ratio increase, greater removal of Cr^{6+} is seen. However, for the 2-hour pyrolysis samples, there is an opposite effect where, as the activation temperature and ratio increase, the removal performance decreases. There is a strong correlation between removal % and surface area as shown in the Table 1, where

the worst adsorbent sample (AC4R) has the lowest surface area of 1.07 m^2/g, and the best adsorbent sample (AC1R) has one of the highest surface areas of 11.26 m^2/g.

Table 1 Adsorbent samples produced under varying process conditions

Sample	Pyrolysis Temp (°C)	Mass Ratio	Pyrolysis Duration (hrs)	Q_{max} (mg/g)	Surface Area (m^2/g)
AC1	400	1:1	1	57.94	1.07
AC2	600	1:1	1	75.08	1.97
AC3	400	2:1	1	114.10	5.80
AC4	600	2:1	1	145.00	827.91
AC1R	400	1:1	2	207.21	11.26
AC2R	600	1:1	2	194.71	2.55
AC3R	400	2:1	2	125.99	2.98
AC4R	600	2:1	2	98.03	1.07

3.3 Comparison with literature

Table 2 compares the performance of different adsorbents for the removal Cr (VI). The performance data shows that the best adsorbent (AC1R) outperforms other low-cost adsorbent materials reported in literature. However, differences in adsorption conditions such as dosage, pH, temperature and contact time need to be taken into consideration.

Table 2 Comparison of the performance of different adsorbent materials found in literature based on Q_{max} values.

Adsorbent Material	Isotherm Model	Q_{max} (mg/g)	Reference
Coffee dusts	Langmuir	39	[3]
Bio-waste granules	Langmuir	64-73	[4]
Banana peel	Langmuir	90	[5]
Tea waste	Langmuir	107.8	[6]
Magnetic Bleached Teawaste (MBTW2)	Langmuir	80	[7]
Spent Coffee Grounds	Langmuir	207	Current Study

4. CONCLUSION

According to Figure 2, the worst percentage removal over the 3-hour duration of the adsorption experiment was 75% for AC4R under the conditions of 600°C, 2 hours and 2:1 mass ratio. The optimum adsorbent was 1:1 ratio, 400°C for pyrolysis temperature and the time of pyrolysis was 2 hours. The detailed adsorption study showed that the best coffee ground adsorbent had a Cr^{6+} removal capacity (207 mg/g) which is competitively high when compared to other adsorbent materials reported in literature. The new adsorbent developed in this work show great potential for heavy metal removal. Future studies will focus on optimizing adsorption conditions through kinetic, thermodynamic and dosage studies.

5. REFERENCES

[1] Chakraborty, R., Renu, K., Eladl, M.A., El-Sherbiny, M., Elsherbini, D.M.A., Mirza, A.K., Vellingiri, B., Iyer, M., Dey, A. and Valsala Gopalakrishnan, A. (2022). Mechanism of chromium-induced toxicity in lungs, liver, and kidney and their ameliorative agents. Biomedicine & Pharmacotherapy, [online] 151, p.113119. doi:https://doi.org/10.1016/j.biopha.2022.113119.

[2] Yang, H.M., Zhang, D.H., Chen, Y., Ran, M.J. and Gu, J.C. (2017). Study on the application of KOH to produce activated carbon to realize the utilization of distiller's grains. IOP Conference Series: Earth and Environmental Science, 69, p.012051. doi:https://doi.org/10.1088/1755-1315/69/1/012051.

[3] Prabhakaran, S.K., Vijayaraghavan, K. and Balasubramanian, R. (2009). Removal of Cr(VI) Ions by Spent Tea and Coffee Dusts: Reduction to Cr(III) and Biosorption. *Industrial & Engineering Chemistry Research*, 48(4), pp.2113–2117. doi:https://doi.org/10.1021/ie801380h.

[4] Jaiyeola, O.O., Chen, H., Albadarin, A.B. and Mangwandi, C. (2020). Production of bio- waste granules and their evaluation as adsorbent for removal of hexavalent chromium and methylene blue dye. *Chemical Engineering Research and Design*, 164, pp.59–67. doi:https://doi.org/10.1016/j.cherd.2020.09.020.

[5] Chen, H., Huang, Z., Wu, J. and Chirangano Mangwandi (2022). Enhancing the Chromium Removal Capacity of Banana Peel Wastes by Acid Treatment. *Advances in science, technology & innovation*, pp.317–320. doi:https://doi.org/10.1007/978-3-030-72543- 3_71.

[6] Albadarin, A.B., Chirangano Mangwandi, Walker, G., Allen, S.J., Mohammad Nazir Ahmad and Majeda Khraisheh (2013). Influence of solution chemistry on Cr(VI) reduction and complexation onto date-pits/tea-waste biomaterials. *Journal of Environmental Management*, 114, pp.190–201. doi:https://doi.org/10.1016/j.jenvman.2012.09.017.

[7] Jiahong W., Hamza A., Haili, Mangwandi, C. (2023) Upcycling teawaste particles into magnetic adsorbent particles for removal of Cr(VI) from aqueous solutions. Particuology, 80, pp. 115-126. Doi: https://doi.org/10.1016/j.partic.2022.11.017

2nd International Conference on
Sustainable Chemical and
Environmental Engineering
14th – 18th June 2023, Limassol, Cyprus

Removal of chromium from aqueous solution using CeO2@starch nanocomposite material and olive stone in a continuous system

O. Jaiyeola and C. Mangwandi[1]

[1]School of Chemistry and Chemical Engineering, Queen's University Belfast, Belfast, United Kingdom
Corresponding author email: c.mangwandi@qub.ac.uk

ABSTRACT

This project aims to assess the potential of CeO_2/Starch nanocomposite with olive stone as adsorbent materials in micro-columns for continuous removal of Cr (VI)/Cr (III) from synthetic chromium wastewater solutions. The nanocomposite material is synthesized in the lab using starch and cerium (III) nitrate hexahydrate. Micro-columns are designed to simulate the continuous treatment process. The micro-columns produce "breakthrough curves" under various conditions, allowing for the evaluation of total chromium removal. The project explores the effects of initial Cr (VI) flow rate, initial Cr (VI) concentration, and adsorbent dosage on these breakthrough curves.

keywords: *Chromium; Starch, adsorption; Starch cerium oxide*

1. INTRODUCTION

The study focuses on evaluating the potential of two low-cost adsorbents, namely starch/cerium oxide nanocomposite and olive stone, in a continuous system for the complete removal of hexavalent and trivalent chromium from synthetic aqueous solutions. Apart from their adsorption capabilities, the nanocomposite also demonstrates the ability to reduce hexavalent chromium (Cr (VI)) to trivalent chromium (Cr (III)), which is advantageous for removal. A principal concern of many environmentalists is hexavalent and trivalent chromium due to its toxicity and impact on human health/the environment (Malik, A et al. 2004).

To simulate large-scale processes and assess the adsorbents' performance, column techniques were employed. By using small-scale columns, the researchers were able to observe and analyze "breakthrough curves" under different conditions. Breakthrough curves provide valuable information about the adsorbents' efficiency and their capacity to remove chromium from the solution over time (Sarin, V et al. 2006).

The results of the study demonstrate that both the starch/cerium oxide nanocomposite and olive stone exhibit promising potential as adsorbents for chromium removal. The nanocomposite effectively adsorbs chromium from the solution, and its ability to convert Cr (VI) to Cr (III) further enhances the removal efficiency. On the other hand, olive stone proves to be particularly effective in removing Cr (III) from the solution.

One of the key advantages of the adsorbents used in this study is their low cost. The starch/cerium oxide nanocomposite and olive stone are affordable and readily available materials, making them suitable for large-scale applications. Moreover, these adsorbents can be reused, adding to their economic feasibility.

While adsorption is considered a promising method for heavy metal removal, it should be noted that adsorbents generally have lower capacity compared to other commonly used methods. This limitation implies that the adsorption process may require more frequent regeneration or replacement of the adsorbents, depending on the specific conditions and demands of the application. In conclusion, this study investigates the potential of starch/cerium oxide nanocomposite and olive stone as low-cost adsorbents for the removal of hexavalent and trivalent chromium from aqueous solutions. The results demonstrate their effectiveness in a continuous system, with the nanocomposite offering adsorption and conversion capabilities and olive stone exhibiting strong removal performance. These findings contribute to the development of environmentally friendly and economically viable approaches for heavy metal removal in industrial wastewater treatment.

2. METHODOLOGY

The process of starch preparation involved dissolving 3.0g of starch in 100ml of deionized water. To facilitate cross-linking, 3.0g of citric acid and 1.5g of sodium hypophosphite monohydrate catalyst were added to the starch solution. The resulting starch suspension was stirred at 60°C for 2 hours and then cooled to room temperature.

For the synthesis of hydrous cerium oxide nanoparticles, 0.02 moles of sodium hydroxide powder were dissolved in 100ml of absolute ethanol to create a 0.2 M sodium hydroxide/ethanol solution. Additionally, 0.005 moles of cerium (III) nitrate hexahydrate were dissolved in 100ml of absolute ethanol to form a 0.05 M Ce $(NO_{3)3}$/ethanol solution. The sodium hydroxide/ethanol solution was added to the Ce $(NO_3)_3$/ethanol solution under vigorous stirring at room temperature.

The combination of the two solutions resulted in the formation of a dark brown precipitate, which gradually changed colour to grey yellow and eventually bright yellow over a 20-minute stirring period. The precipitates were collected by centrifugation, washed with deionized water and absolute ethanol multiple times, and then dried at 60°C for 12 hours. The dried product was subsequently crushed into fine particles of uniform size and shape using a mortar and pestle, resulting in starch/cerium oxide nanoparticles.

In the case of the secondary material, olive stones were crushed to a size range of 0-500μm and used in the second column. The olive stones were not subjected to any pre-treatment before the absorption experiments. Prior to each experiment, the olive stone was washed within the column with deionized water for 4 hours to remove any adhering dirt. The maximum adsorption capacity of the olive stone for chromium (VI) was found to be 3.1 mg/g, while for chromium (III), it was 5.19 mg/g (G. Blazquez et al. 2011)

2.1 BREAKTHROUGH CURVES

Breakthrough curves are used to assess the performance of fixed bed columns and provide valuable information about the behaviour and loading capacity of the starch/cerium oxide nanocomposite and olive stone in column 2 for chromium (VI) and chromium (III) removal. A typical breakthrough curve is depicted in Figure 1 below (G. Blazquez et al. 2011) These curves illustrate the response time of the materials in removing the respective ions. The breakthrough point is reached when the outlet concentration of the column (C_t) reaches 5% of the inlet concentration (C_o). This point indicates the onset of breakthrough. The shape of the breakthrough curve changes from 0% to 100% of the initial concentration as the fluid passes through the column. The point of exhaustion is reached when the outlet concentration approaches ≈95% of the inlet concentration. The breakthrough curve is typically represented as C_t/C_o plotted against the outlet volume at a specific column height. The outlet volume (V_{out}) can be calculated using the flow rate (Q) in mL/min and time (t) in minutes, according to the equation.

$$V_{out} = Q.t$$

By analysing the breakthrough curves, valuable insights can be obtained regarding the performance and efficiency of the adsorption process for chromium removal.

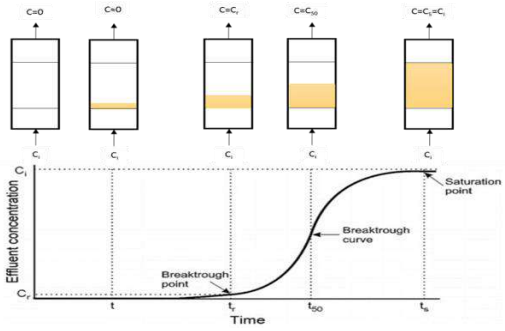

Figure 1 - Typical Breakthrough Curve at a Specific Bed-Depth (G. Blazquez et al. 2011)

2.2 ADSORPTION STUDIES

In adsorption studies, calculations are performed after reaching equilibrium to evaluate the efficacy of the starch/cerium oxide nanocomposite and olive stone in removing chromium (VI) and chromium (III) from synthetic wastewater. The effectiveness and capacity of the adsorbent materials are determined by integrating the areas under their respective breakthrough curves with respect to time, considering the feed concentration and flow rate.

$$q_{total} = \frac{Q}{1000} \int_{t=0}^{t=t_{total}} C_R dt \quad (1)$$

where C_R is the concentration of metal removal in mg/L

2.3 CHROMIUM PREPARATION

To prepare chromium solutions for analysis, a stock solution is created by dissolving 2.847g of potassium dichromate in 1 dm^3 of de-ionized water. Dilutions are then made to obtain desired concentrations, with a dilution factor considered for accurate readings on the spectrophotometer. Samples were extracted from the columns at pre-determined times and concentration of Cr (VI) was determined spectrophotometrically using procedure descried by (Mangwandi et al. 2020). The concentration of chromium (III) in the effluent of the columns can be calculated by subtracting the chromium (VI) concentration from the total chromium content obtained from ICP results.
Equation 2 calculates the total amount of metal ions sent to the column.

$$m_{tot} = \frac{C_i V_{out}}{1000} \quad (2)$$

Where C_i is the concentration at the inlet of the column (mg/L)

For more precise elemental determinations, Inductively Coupled Plasma Mass Spectrometry (ICP-MS) is utilized. This technique utilizes a high-temperature ICP source coupled with a mass spectrometer to convert elements into ions for separation and detection. ICP-MS is capable of handling complex matrices with minimal interference due to the higher temperature of the ICP source.

2.4 EFFECT OF INITIAL CR(VI) CONCENTRATION

The effect of initial Cr (VI) concentration on Cr (VI)/Cr (III) adsorption was investigated in this experiment to determine its impact on the adsorption process and verify its consistency with existing literature. Synthetic solutions with pH 2 containing Cr (VI) concentrations of 20, 40, 60, and 80 ppm were prepared. These concentrations were chosen based on the maximum absorbance capacity of the starch/cerium oxide nanocomposite, which was previously determined to be 48.54 mg/g 1 at 22℃ in a previous study.

$$q_{Total} = m \ q_e \quad (3)$$

The equation was used to calculate the maximum loading capacity of the nanocomposite, where m represents the mass of the adsorbent in the column and qe is the maximum loading capacity.

2.5 EFFECT OF INITIAL CR(VI) FLOW RATE

The effect of initial Cr (VI) flow rate on absorption was also examined in this study. The system tested the adsorption of chromium (VI)/(III) at different flow rates of 5.5 mL/min, 7 mL/min, 8.5 mL/min, and 10 mL/min,

all at a concentration of 40 ppm and pH 2. The aim was to understand the influence of the initial flow rate on the interaction between the adsorbent and the solute in continuous systems.

2.6 EFFECT OF BED DEPTH

Furthermore, the effect of bed depth was investigated to assess how the mass of the nanocomposite affects absorption in a continuous system. Four 500 mL solutions of Cr (VI) with an 80ppm concentration and pH 2 were prepared and passed through the system at four different nanocomposite bed depths of 1 cm, 1.5 cm, 2 cm, and 2.5 cm. Samples were collected at regular intervals to analyse the presence of chromium (VI) and (III) in the effluent of both columns, providing insights into the impact of bed depth on the absorption process.

2.7 THOMAS MODEL

The Thomas model is a commonly used approach to describe the behaviour in a fixed-bed column. However, it has a key limitation as it is derived from Langmuir adsorption/desorption theory, assuming that adsorption is not restricted by chemical reactions but rather controlled by mass transfer at the solute/adsorbent interface. Additionally, it assumes second-order reversible reaction kinetics. These assumptions can introduce inaccuracies when applied to absorption processes under specific conditions. The Thomas model can be expressed by the following equation (4):

$$\frac{C_t}{C_o} = \frac{1}{1+\exp\left[\frac{K_t}{F}(q_o m - C_o V)\right]} \quad (4)$$

Here, K_t represents the Thomas rate constant (mL/min.mg), q_o is the maximum concentration of the solute in the solid phase (mg/g), F denotes the flow rate (mL/min), m signifies the mass of the adsorbent (g), and V represents the cumulative throughput volume (mL). To simplify the equation, it can be linearized as follows (equation 5):

$$ln\left(\frac{1-C_t}{C_t}\right) = \frac{K_t}{F}(q_o m - C_o V) \quad (5)$$

3. RESULT AND DISCUSSION

3.1 PARAMETERS OF BREAKTHROUGH CURVES FOR ALL THREE DYNAMIC EXPERIMENT STUDIES

As stated in the project objectives, the main aim of this study is to determine the volume of breakthrough (V_{bt}) i.e., when the outlet concentration reaches 5% of the inlet concentration. The volume of saturation (V_s). i.e., when the outlet concentration reaches 95% of the inlet concentration along with many other variables in both columns, for each condition studied. From the results obtained from all breakthrough curves, the most significant parameters have been tabulated as can be seen in Tables 1 and 2 for columns 1 and 2 respectively: q_e is the absorption capacity of the column, q_{tot} is the total amount of metal removal, m_{tot} is the amount of metal passing through the column and %R is the percentage of metal removal.

3.2 EFFECT OF INITIAL CR(VI) CONCENTRATION

The effect of initial concentration of Cr (VI) on breakthrough curves was examined in this study. Figures 2 illustrate the results of experiments conducted with bed depths of 0.646g and 0.91g of nanocomposite/olive stone, respectively, at a flow rate of 5.5mL/min. Higher initial concentrations led to lower breakthrough points and decreased wastewater treatment capacity in both columns. The increase in initial Cr (VI) concentration from 20-80ppm resulted in an increase in the amount of Cr (VI) taken up by the

Parameter (pH2)	V_{bt} (mL)	V_s (mL)	q_e (mg/g)	q_{tot} (mg)	m_{tot} (mg)	%R
Initial Concentration (ppm)						
20.0	38.0	96.0	11.5	7.4	9.9	74.7
40.0	34.0	91.0	20.4	13.2	19.8	66.7
60.0	23.0	82.0	23.8	15.4	29.7	51.9
80.0	- [1]	60.0	29.3	18.9	39.6	47.7
Initial Flow Rate (mL/min)						
5.5	14.0	156.0	20.4	13.2	19.8	66.7
7.0	6.0	129.0	17.6	11.4	19.8	57.6
8.5	-	112.0	11.5	7.4	19.8	37.4
10.0	-	109.0	9.1	5.9	19.8	29.8
Bed Depth CeO2/Starch Nanocomposite (cm)						
1 (0.3473g)	14.0	128.0	35.7	12.4	39.2	31.6
1.5 (0.6461g)	28.0	269.0	29.3	18.9	39.2	48.2
2 (0.8617g)	29.0	322.0	25.0	21.5	39.2	54.8
2.25 (1.077g)	34.0	361.0	31.7	34.1	39.2	87.0

nanocomposite, rising from 11.5 mg/g to 29.3 mg (Cr (VI)/g. This suggests that the diffusion of the adsorbate in the adsorbent is influenced by the initial concentration (Malkoc, E et al. 2006).

In column 2, the presence of olive stone further enhanced Cr (VI) removal compared to the nanocomposite. When measuring Cr (III) concentrations, it was found that at an initial concentration of 40ppm, the breakthrough point occurred after 6mL of wastewater passed through column 1. At this concentration, the highest equilibrium concentration of Cr (III) was observed (75mg). However, column 2, with olive stone, exhibited the highest removal of Cr (III) with a q_e value of 81.3 mg (Cr (III)/g. The removal percentage of Cr (III) was 97.6% for an initial Cr (VI) concentration of 40ppm.

Table 1 :Parameters of Cr (VI) absorption by CeO_2/Starch Nanocomposite

Table 2 - Parameters of Cr (III) absorption by Olive Stone

Parameter (pH2)	Vbt (mL)	Vs (mL)	qe (mg/g)	qtot (mg)	mtot (mg)	%R
Initial Concentration (ppm)						
20.0	16.0	208.0	11.1	10.1	38.0	26.6
40.0	6.0	151.0	81.3	74.0	75.8	97.6
60.0	-	149.0	6.3	5.8	8.9	65.0
80.0	-	132.0	4.4	4.0	10.6	37.8
Initial Flow Rate (mL/min)						
5.5	32.0	229.0	13.2	12.00	17.15	70.0
7.0	-	224.0	11.5	10.50	17.65	59.5
8.5	-	145.0	16.5	15.00	17.15	87.5
10.0	-	111.0	18.1	16.51	17.68	93.4
Bed Depth CeO2/Starch Nanocomposite (cm)						
1 (0.3473g)	-	226.0	-	-	23.3	-
1.5 (0.6461g)	59	204.0	-	-	20.3	-
2 (0.8617g)	61	239.0	47.0	42.8	59.3	72.2
2.25 (1.077g)	74	262.0	48.7	44.3	56.3	78.7

1. (–) signifying data not available.

For initial Cr (VI) concentrations of 60 and 80 ppm, the results for Cr (III) removal were not satisfactory. This could be attributed to either excessively high initial concentrations or insufficient adsorbent mass, leading to quick saturation of active sites within the nanocomposite and reduced production of Cr (III) through the reduction of Cr (VI) (Chu, K.H.,2004). Equilibrium Cr (III) concentrations at the outlet of column 1 for initial concentrations of 60 and 80ppm were 8.88mg and 10.6mg, respectively. Some Cr (III) was removed by olive stone, as evidenced by Cr (III) concentrations of 3.1mg and 6.6mg at the outlet of column 2, with removal percentages of 65% and 37.78% for Cr (III) at these initial concentrations. Small fluctuations observed in the trend lines on the plotted graphs were likely caused by back pressure issues within the system or potential human error. This study confirms that as the initial concentration of Cr (VI) increases, the breakthrough time decreases for a fixed flow rate (5.5mL/min). This observation aligns with previous research on the biosorption of heavy metals using different adsorbents (G. Blázquez et al. 2009, K. Vijayaraghavan et al. 2005, J.M. Brady et al. 1999). In column 2, the adsorption of Cr (III) is attributed to ionic attraction between the ion and functional groups present in olive stone, particularly the carboxyl functional group as indicated by IR spectra of loaded olive stone (Chu, K.H.,2004).

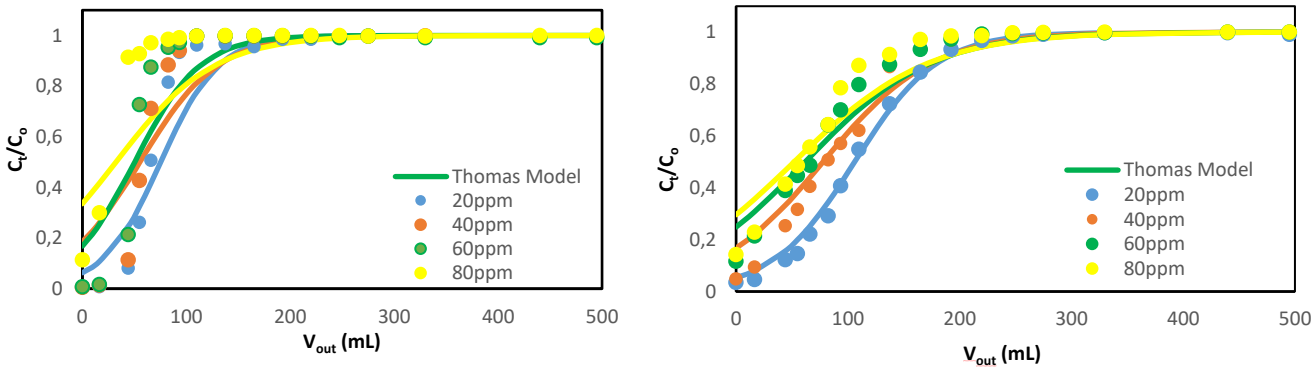

Figure 2 – (a) Cr (VI) Breakthrough Curve + Thomas Model, Nanocomposite (b) Cr (VI) Breakthrough Curve + Thomas model, Olive Stone

4. CONCLUSION

The most favourable results for continuous total chromium removal are observed under the following conditions: effect of initial Cr(VI) flow rate (continuous): 5.5 mL/min, effect of initial Cr(VI) concentration (continuous): 40ppm, effect of CeO2/starch nanocomposite adsorbent dosage (continuous): 2.25cm (1.077g) These findings suggest that achieving the highest removal of Cr(VI) and Cr(III) requires a higher bed depth and a lower flow rate. This configuration enables the system to effectively handle varying concentration levels of chromium in industrial wastewater, within a reasonable range, while maintaining a pH of 2. It is apparent, after conducting experiments and analysing the results, starch/CeO_2 nanocomposite can reduce and remove Cr (VI)/Cr (III). In addition to this, a second column packed with olive stone to remove any Cr (III) generated proved to be quite useful. This made the system quite promising, to continuously remove both hexavalent and trivalent chromium from aqueous wastewater solution.

5. REFERENCES

Chu, K.H. (2004). Improved fixed bed models for metal biosorption. Chemical Engineering Journal, 97(2), pp.233–239.

G.Blázquez, Martín-Lara, M.A., Tenorio, G. and Calero, M. (2011). Batch biosorption of lead (II) from aqueous solutions by olive tree pruning waste: Equilibrium, kinetics and thermodynamic study. Chemical Engineering Journal,168(1), pp.170–177.

G. Blázquez, Martín-Lara, M.A., Dionisio-Ruiz, E., Tenorio, G. and Calero, M. (2011). Evaluation and comparison of the biosorption process of copper ions onto olive stone and pine bark. Journal of Industrial and Engineering Chemistry, 17(5), pp.824–833.

G. Blázquez, F. Hernáinz, M. Calero, M.A. Martín-Lara, G. Tenorio,2009. The effect of pH on the biosorption of Cr (III) and Cr (VI) with olive stone, Chem. Eng. J. 148, 473–479.

J.M. Brady, J.M. Tobin, J.-C. Roux, 1999. Continuous fixed bed biosorption of Cu_{2+} ions: application of a simple two parameters mathematical model, J. Chem. Technol. Biotechnol. 74,71–77.

K. Vijayaraghavan, J. Jegan, K. Palanivelu, M. Velan, 2005. Batch and column removal of copper from aqueous solution using a brown marine alga Turbinaria ornata, Chem. Eng. J. 106, 177–184.

Malik, A., 2004. Metal bioremediation through growing cells. environment international 30, 261–278.

Malkoc, E., Nuhoglu, Y., Dundar, M.,*2006* Adsorption of chromium (VI) on pomace-An olive oil industry waste: Batch and column studies, J. Hazard. Mater*., B138, 142 151*.

Sarin, V., Singh, T.S., Pant, K.K., 2006. Thermodynamic and breakthrough column studies for the selective sorption of chromium from industrial effluent on activated eucalyptus bark, Bioresource. Technol., 97, 1986-1993.

2nd International Conference on
Sustainable Chemical and
Environmental Engineering
14th – 18th June 2023, Limassol, Cyprus

Can biodiesel become a determinant Bioeconomy factor towards sustainability: Mixture physicochemical composition and Input-Output (I-O) indicators of biodiesel sector

M.E. Kyriklidis[1], C. Kyriklidis[2], V. Vasileiadis[3], E. Loizou[4] and C. Tsanaktsidis[5]

[1]*Department of Regional Development and Cross Border Studies, University of Western Macedonia, Kila, Kozani, Greece*
[2]*Department of Chemical Engineering, University of Western Macedonia, Kila, Kozani, Greece*
[3]*Department of Chemical Engineering, University of Western Macedonia, Kila, Kozani, Greece*
[4]*Department of Regional Development and Cross Border Studies, University of Western Macedonia, Kila, Kozani, Greece,*
[5]*Department of Chemical Engineering, University of Western Macedonia, Kila, Kozani, Greece*
Corresponding author email: er.kiriklidis@gmail.com

ABSTRACT

Energy deployment owns an important role by introducing dynamic strategies, in order to achieve the long-term purpose of sustainability. The challenge of climate change and a potential increase in the energy demand, following the expected society development rebound after COVID-19 and war in Ukraine, could ideally lead central decision-making policies to produce technological, economic, social, environmental viable solutions. The goal of Bioeconomy, through sustainable production and the rational use of biological resources (including waste), is to produce more from less. The purpose of this paper is to point out the beneficial effects of using biodiesel or mixtures of biodiesel, both as in the physicochemical composition of the mixture, and also as an indicator employed to reveal the potential of biodiesel to induce knock-on effects in the national economy of Greece. In order to analyze the composition of the mixture, extensive experimentation (about 3500) has been executed under normal conditions (as it is defined by government protocols), providing significant information about the two mixture ingredients (diesel and biodiesel). Moreover, in order to assess the significance of biodiesel at national level, in terms of output, employment and income creation, an Input-Output (I-O) model and I-O multipliers were used.

keywords: *Sustainability; Biodiesel mixtures; Input-Output (I-O) Multipliers; Bioeconomy; Physicochemical composition.*

1. INTRODUCTION

Energy markets became overburdened in 2021 because of a variety of factors, including the rapid economic revival after the pandemic. The above situation intensified into an absolute global energy crisis following Russia's invasion of Ukraine in February 2022. At the same time, the price of natural gas reached record highs, and as a result so did electricity in many markets, while Oil prices hit their highest level since 2008. Therefore, energy prices led to very high inflation, forcing factories to reduce production or even shut down, slowing economic growth to the point that some countries are heading towards severe recession and pushing in general, many people into poverty. In this context Biofuels and as a result Bioeconomy, have the chance to prove themselves as an alternative solution to the above powerful reminder of the world's dependence on fossil fuels.

According to the EU, Bioeconomy involves the above decision-making policies, so as to produce renewable biological resources and convert them and their waste streams into value-added products, such as food, feed, organic-based products and bioenergy. The goal of Bioeconomy, through sustainable production and the rational use of biological resources (including waste), is to produce

more from less. By 2030, the EU aims to increase the share of renewable energy in transport to at least 14%, including a minimum share of 3.5% of advanced biofuels. EU countries are required to set out an obligation on fuel suppliers that ensures the achievement of this target.

The purpose of this paper is to point out the beneficial effects of using Biodiesel or mixtures of Biodiesel, both as in the physicochemical composition of the mixture, and also as an indicator employed to reveal the potential of Biodiesel to induce knock-on effects in the national economy of Greece. In order to analyze the composition of the mixture, extensive experimentation (about 3500) has been executed in the Laboratory of Chemical Engineering Department in the University of Western Macedonia under normal conditions (as it is defined by government protocols), providing significant information about the two mixture ingredients (Diesel and Biodiesel). Moreover, in order to assess the significance of Biodiesel at national level, in terms of output, employment and income creation, an Input-Output (I-O) model and I-O multipliers were used.

2. Biodiesel: A Bioeconomy index in the National I-O table of Greece.

The huge demand for energy, mostly based on fossil fuels, has caused serious environmental effects, including greenhouse gas (GHG) emissions and global warming. While energy can be supplied from different renewable sources, such as solar, wind and water, the aforementioned are hard to manage, difficult to predict and depend more and more on climate changes. In this context, biodiesel has emerged as one of the potential solutions provided by Bioeconomy, to add to the renewable energy mix.

Bioeconomy offers opportunities at national, regional and multi-regional level in countries, such as Poland (Loizou et al., 2019), Japan (Wen et al., 2019), Germany (Budzinski et al., 2017), China (Song et al., 2015), the Baltic region (Brizga et al., 2019), and many other countries in Asia, Europe and USA (Asada et al., 2020). Usually, biological resources, either on land or at sea, are widely distributed in rural and remote areas, where alternative ways to acquire a livelihood are usually scarce.

In order to implement the bioeconomy oriented I-O model, the latest published National I-O table, published by the Hellenic Statistical Service for the year 2015 (ELSTAT, 2015), was used. After the initial manipulations to the national I-O table; aggregating the non-important sectors and disaggregating those of special interest, the initial scheme of 65 sectors resulted in a table of 74. The most important manipulations to the 74 sectors national I-O table were concerning the creation of the biobased sectors. A total of 17 sectors of economic activity consists of the fully biobased (BIO) and mixed biobased (BIO-PART) sectors (table 1).

Table 1. Bioeconomy sectors (mixed and fully bio-based) in the I-O table

	Sector	BIO Type (% of the original sector)		Sector	BIO Type (% of the original sector)
1	Agriculture	BIO (100%)	**10**	Bioethanol	BIO-PART (15%)
2	Forestry	BIO (100%)	**11**	Biodiesel	BIO-PART (22%)
3	Fishing	BIO (100%)	**12**	Chemicals and products	BIO-PART (19%)
4	Food products	BIO (100%)	**13**	Pharmaceutical products	BIO-PART (21%)
5	Leather products	BIO (100%)	**14**	Rubber and plastic	BIO-PART (22%)
6	Wood industry (except furniture)	BIO (100%)	**15**	Furniture	BIO-PART (31%)
7	Paper	BIO (100%)	**16**	Biogas	BIO-PART (14%)
8	Biobased Textiles	BIO-PART (13%)	**17**	Biomass	BIO-PART (18%)
9	Biobased Wearing apparel	BIO-PART (14%)			

For the disaggregation procedure and the creation of the mixed biobased sectors, external data and information were used, from the Hellenic Statistical Service and the JRC (Joint Research Center) that reports specific data for bioeconomy for all EU countries.

After constructing the I-O model, the significance of Biodiesel sector had to be assessed at national level. The indicators employed to reveal the potential of the sector and its ability to induce knock-on effects in an economy, in terms of output, employment and income creation are the I-O multipliers.

Interesting results emerged regarding the potential of the Biodiesel sector. Particularly, in terms of output, employment and income, the sector ranks exceptionally high among the 74 sectors of the national economy, indicating that through any final demand change (e.g. external fund inflows), there will be high positive effects. This means that policies aimed at strengthening the Biodiesel sector in Greece, will indirectly support the whole national economy, while it appears that the sector has the potential to induce indirect impacts, due to sector's interconnections. Biodiesel sector's multipliers (employment, output and income) and their ranking, for the national economy of Greece, can be seen in table 2.

Table 2. Employment, Output, and Income Multipliers of Bioeconomy sectors for the regional economy

Sector	OM	R	EM	R	IM	R
Biodiesel	1.8081	10	7.6017	4	4.8561	3

Output Multiplier (OM), Employment Multiplier (EM), Income Multiplier (IM), National Ranking (R)

3. Experimental production analysis of Biodiesel

Fossil fuel consumption has increased significantly over the past half-century, around eight-fold since 1950, and roughly doubling since 1980. The impetuous environmental problems and the Greenhouse effect reduced fossil fuels' contribution value in humanity development. Thus, the researchers are working intensively to introduce good alternative solutions to fossil fuels with almost the same properties. Biodiesel has been projected as a clean renewable fuel with competitive prices (Kalogirou 2001; Gerpen et al. 2004; Bezergianni 2011). Besides from being low cost, Biodiesel has other advantages such as being biodegradable and nontoxic compared to conventional diesel fuel (Burton 2008; Gomez 2008; Balat M and Balat H 2010; Pérez-Cisnerosa et al. 2016; Deya et al. 2021). This environmentally friendly solution leads to an increasing Biodiesel demand, a fuel of high quality and in large availability.

Strategies that improve biodiesel sustainability were presented by Ramos et al. in 2019. Europe is the main Biodiesel producer all over the world, because of the applied environmental policy. The emissions reduction of greenhouse gases (GHG), in combination with the energy supply security, are the basic goals of EU.

At the same time, experimental process for the mixtures production in laboratories is time consuming and costs a lot, when researchers carry out extensive analysis to produce as much as possible the optimum fuel quality and price (Tsanaktsidis et al. 2018). Intelligent techniques, nature inspired intelligence, machine learning and evolutionary computation approaches provide high quality near-optimal results to complicated optimization problems (Kyriklidis and Dounias 2016). Nature inspired approaches are implemented in many sectors providing high quality results (Kyriklidis et al. 2022).

For the new Biodiesel production of our analysis, an extensive experimentation (about 3500) has been executed in the Laboratory of Chemical Engineering Department in University Western Macedonia, providing significant information about the two mixture ingredients (diesel and biodiesel). Biodiesel as second ingredient came from 50% animal fat sources and 50% vegetable sources.

The experiments performed were classified into 5 different temperatures 5°, 10°, 15°, 20° and 25°. Given the temperature in each set of experiments, changes in the physicochemical properties were

recorded in 1) Density, 2) Conductivity, 3) API (American Petroleum Institute), while the percentages of participation of the new biodiesel elements were changed. The change rate was chosen at 5%, with a total of 20 new mixture categories. In addition, regarding the components of the new biodiesel, Diesel was the first component of the new mixture and as a second component of the blend, three alternatives were available: 1) 50% vegetable and 50% animal biodiesel, 2) 100% animal biodiesel, and 3) 100% vegetable biodiesel.

As it can be observed in Figures 1,2,3, while the participation of biodiesel in the mixture increases, so does the value of the density in the mixture increase (almost proportionally). A remarkable observation regarding the density value for the mixtures at 5° can be spotted. While in the initial measurements (proportions (100-0) % and (95-5) % the density values recorded at 5° are lower than the corresponding mixtures at the other temperatures (10°, 15°, 20° and 25°), when the mixture is made in proportions (90-10) % (diesel-biodiesel) then the value of the density becomes higher than the corresponding mixtures at the remaining temperatures. This behavior is confirmed in all 3 types of mixtures (1) 50% vegetable and 50% animal biodiesel, 2) 100% animal biodiesel and 3) 100% vegetable biodiesel), while in the mixture of 100% animal biodiesel we observe interesting fluctuations in the mixture of temperatures at 20° which, however, still follow the increasing trend of density as the biodiesel increases.

The above experimental measurements are displayed analytically in table 3 below for temperatures 5°, 10°, 15°, 20° and 25°. The new mixtures are 20 in total, and for each new mixture the changes their physicochemical properties are presented. In the specific table it is observed that, as the participation of 50% vegetable and 50% animal biodiesel increases, the index of density, conductivity increases, on the contrary, the index of API decreases.

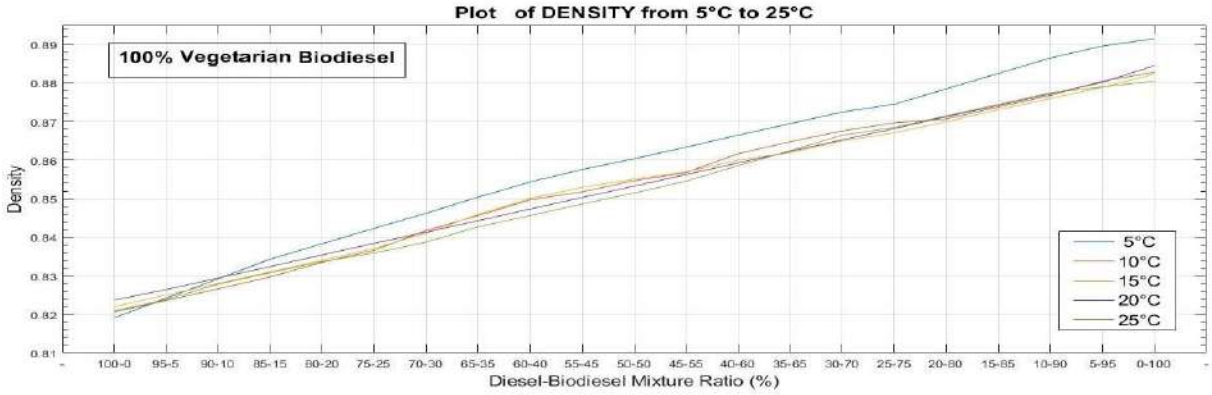

***Figure 1**. Plot of Density from 5° to 25° for all Diesel-Biodiesel (100% Vegetarian) mixtures*

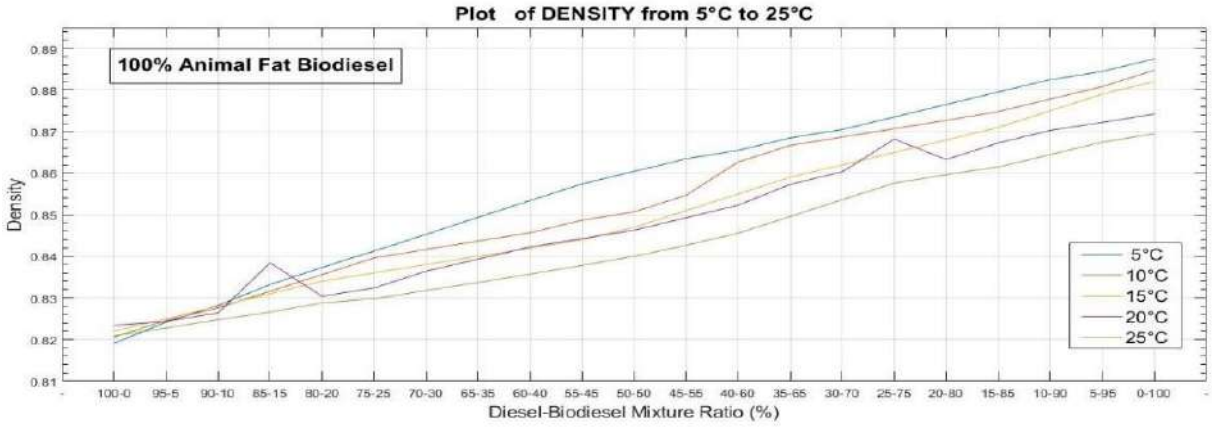

***Figure 2.** Plot of Density from 5° to 25° for all Diesel-Biodiesel (100% Animal Fat) mixtures*

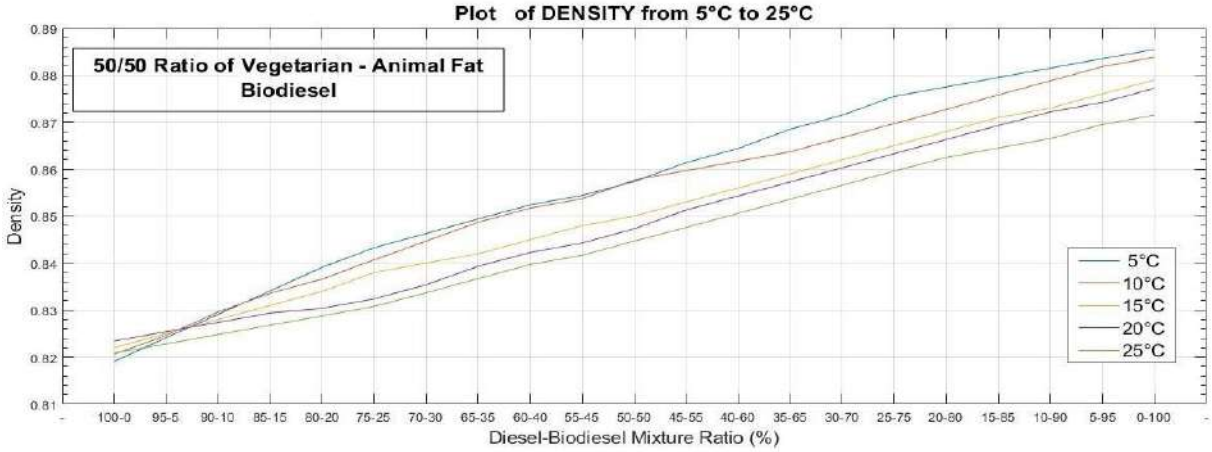

***Figure 3**. Plot of Density from 5° to 25° for all Diesel-Biodiesel (50%Vegetarian -50% Animal Fat) mixtures*

Table 3. Density of all Diesel-Biodiesel (100% Vegetarian, 100% Animal Fat, 50% Vegetarian-50% Animal Fat) mixtures in temperatures of 5°, 10°, 15°, 20° and 25°.

RATIO (D-B) %	100% Vegetarian Biodiesel					100% Animal Fat Biodiesel					50% Vegetarian Biodiesel - 50% Animal Fat Biodiesel				
	Density					Density					Density				
Temperatures	5°	10°	15°	20°	25°	5°	10°	15°	20°	25°	5°	10°	15°	20°	25°
100-0	0.8191	0.8206	0.8220	0.8237	0.8209	0.8191	0.8206	0.8220	0.8237	0.8209	0.8191	0.8206	0.8220	0.8234	0.8209
95 -5	0.8242	0.8236	0.8250	0.8264	0.8238	0.8242	0.8246	0.8250	0.8244	0.8228	0.8241	0.8246	0.8250	0.8254	0.8228
90 -10	0.8292	0.8266	0.8280	0.8294	0.8278	0.8282	0.8276	0.8280	0.8264	0.8248	0.8291	0.8296	0.8280	0.8274	0.8248
85 -15	0.8343	0.8297	0.8310	0.8324	0.8308	0.8332	0.8316	0.8310	0.8384	0.8266	0.8341	0.8336	0.8310	0.8294	0.8268
80 -20	0.8383	0.8335	0.8340	0.8354	0.8337	0.8373	0.8356	0.8340	0.8304	0.8288	0.8391	0.8366	0.8340	0.8304	0.8288
75 -25	0.8423	0.8366	0.8371	0.8384	0.8359	0.8413	0.8396	0.8360	0.8324	0.8298	0.8433	0.8407	0.8380	0.8324	0.8308
70 -30	0.8462	0.8417	0.8410	0.8413	0.8387	0.8453	0.8417	0.8380	0.8364	0.8318	0.8463	0.8447	0.8400	0.8354	0.8337
65 -35	0.8504	0.8456	0.8459	0.8443	0.8427	0.8494	0.8437	0.8400	0.8393	0.8337	0.8494	0.8487	0.8420	0.8393	0.8367
60 -40	0.8544	0.8497	0.8500	0.8473	0.8456	0.8534	0.8457	0.8420	0.8423	0.8357	0.8524	0.8517	0.8450	0.8423	0.8397
55 -45	0.8576	0.8518	0.8530	0.8503	0.8486	0.8574	0.8487	0.8440	0.8443	0.8378	0.8544	0.8537	0.8480	0.8443	0.8417
50 -50	0.8604	0.8547	0.8551	0.8533	0.8515	0.8604	0.8507	0.8470	0.8463	0.8400	0.8574	0.8577	0.8500	0.8473	0.8447
45 -55	0.8634	0.8568	0.8570	0.8563	0.8546	0.8635	0.8547	0.8510	0.8493	0.8427	0.8614	0.8597	0.8530	0.8513	0.8476
40 -60	0.8665	0.8617	0.8600	0.8593	0.8586	0.8655	0.8627	0.8550	0.8523	0.8456	0.8644	0.8617	0.8560	0.8543	0.8506
35 -65	0.8695	0.8648	0.8620	0.8623	0.8625	0.8685	0.8667	0.8590	0.8573	0.8496	0.8685	0.8637	0.8590	0.8573	0.8536
30 -70	0.8725	0.8676	0.8650	0.8653	0.8665	0.8705	0.8687	0.8620	0.8603	0.8536	0.8715	0.8667	0.8620	0.8603	0.8566
25 -75	0.8745	0.8697	0.8671	0.8682	0.8685	0.8735	0.8707	0.8650	0.8682	0.8576	0.8755	0.8697	0.8650	0.8633	0.8596
20 -80	0.8785	0.8707	0.8700	0.8713	0.8715	0.8765	0.8727	0.8680	0.8633	0.8596	0.8775	0.8727	0.8680	0.8663	0.8625
15 -85	0.8825	0.8738	0.8731	0.8742	0.8745	0.8795	0.8748	0.8710	0.8673	0.8615	0.8795	0.8758	0.8710	0.8693	0.8645
10 -90	0.8865	0.8768	0.8760	0.8772	0.8775	0.8825	0.8778	0.8750	0.8703	0.8645	0.8815	0.8788	0.8730	0.8722	0.8665
5 -95	0.8896	0.8805	0.8789	0.8802	0.8790	0.8845	0.8808	0.8790	0.8722	0.8675	0.8835	0.8818	0.8760	0.8742	0.8695
0 -100	0.8915	0.8828	0.8823	0.8815	0.8805	0.8875	0.8848	0.8820	0.8742	0.8695	0.8855	0.8838	0.8790	0.8772	0.8715

The density increase is desirable up to the limits resulting from ASTM D1298-99 limits: 0.8200 g/ml - 0.8450 g/ml, as the calorific value of the new fuel increases. Density greater than 0.8450 g/ml implies additional fuel storage costs, due to which the fuel is more flammable.

From the diagrams uploaded to Mendeley Data (1*,2**), it is also observed that as the participation of biodiesel in the mixture increases, the degree of API decreases (almost proportionally). Same as the density value, the observation regarding the API value in the 5° mixture is noteworthy. While initially at 5°, the API value is higher than the values of other mixtures at different temperatures, after the ratio (90-10) % the API value of the mixture becomes lower.

Finally, it is observed that the more the participation of biodiesel in the mixture increases, the more (almost proportionally) the value of the conductivity in the mixtures increases.

All tables and related diagrams are available at the following link: Mendeley Data.

1* KIRIKLIDIS, MARIOS-ERRIKOS; Kyriklidis, Christos; KYRIKLIDIS, MARIOS-ERRIKOS; Vasileiadis, Vasileios; Loizou, Efstratios; Tsanaktsidis, Constantinos (2023), "Can biodiesel become a determinant Bioeconomy factor towards sustainability: Mixture physicochemical composition and Input-Output (I-O) indicators of biodiesel sector.", Mendeley Data, V1, doi: 10.17632/cz6cz3tf3z.1

2** Dataset is in moderation (It will become public as soon as it will be approved)

4. CONCLUSIONS

The energy crisis of 2021-2022, caused by COVID-19 and the war in Ukraine, revealed that the transition to renewable energy was abrupt and not sufficiently gradual. Biodiesel can be proposed as the factor that will close the gap between fossil fuels and the energy of the future. The above relies on both the beneficial effects of using biodiesel or mixtures of biodiesel, and also as an indicator employed to reveal the potential of biodiesel, to induce knock-on effects in the national economy of Greece. Specifically, changes in the physicochemical properties (Density, Conductivity, API) improve the quality and the desired properties of the fuel (Tsanaktsidis et al. 2018), and at the same time it appears that biodiesel sector has the potentials to induce indirect impacts, due to interconnections in the Greek economy. For example, as can be seen in table 2, biodiesel sector is one of those with the largest Output multipliers (1.8081) (R=10). This means that for every unitary euro increase in the final demand of this sector, the total output of the national economy will increase by 1.8081 euros due to the direct and indirect linkages of the specific sector with the other in the economy of Greece.

REFERENCES

Balat, M. and Balat, H., 2010. Progress in biodiesel processing. Applied Energy, 87, 1815–1835.

Bezergianni, S., Kalogeras, K. and Pilavachi, PA., 2011. On maximizing biodiesel mixing ratio based on final product specifications. Computers and Chemical Engineering, 35, 936–942.

Brizga, J., Miceikienė, A., Liobikienė, G., 2019. Environmental aspects of the implementation of bioeconomy in the Baltic Sea Region: An input-output approach. J. Clean. Prod. 240.

Budzinski, M., Bezama, A., Thrän, D., 2017. Monitoring the progress towards bioeconomy using multi-regional input-output analysis: The example of wood use in Germany. J. Clean. Prod. 161, 1–11.

Burton, R., 2008. Biodiesel Standards and Testing Methods. Alternative Fuels Consortium, Central Carolina Community College, USA.

Deya, P., Raya, S. and Newarb, A., 2021. Defining a waste vegetable oil-biodiesel based diesel substitute blend fuel by response surface optimization of density and calorific value. Fuel, 283, 118978.

Gerpen, JV., Shanks, B., Pruszko, R., Clements, D. and Knothe, G., 2004. Biodiesel production technology NREL/SR-510-36244. National Renewable Energy Laboratory, Colorado, USA.

Gomez, LD., Steele-King, CG. and McQueen-Mason, SJ., 2008. Sustainable liquid biofuels from biomass: the writing's on the walls. New Phytologist, 178, 473–85.

Kalogirou, SA., 2001. Artificial neural networks in renewable energy systems applications: A review. Renewable and Sustainable Energy Reviews. 5(4), 373–401.

Kyriklidis, C. and Dounias, G., 2016. Evolutionary computation for resource leveling optimization in project management. Integrated Computer-Aided Engineering, IOS Press, 23(2), 173-184.

Kyriklidis, C., Kyriklidis, ME., Loizou, E., Stimoniaris, A. and Tsanaktsidis, CG., 2022. Optimal Bio Marine Fuel production evolutionary Computation: Genetic algorithm approach for raw materials mixtures. Fuel, 323, 124232.

Loizou, E., Jurga, P., Rozakis, S., Faber, A., 2019. Assessing the potentials of bioeconomy sectors in Poland employing input-output modeling. Sustain. 11, 1–12.

Pérez-Cisnerosa, ES., Mena-Espinoa, X., Rodríguez-Lópezc, V., Sales-Cruzb, M., Viveros-Garcíaa, T. and Lobo-Oehmichen, R., 2016. An integrated reactive distillation process for biodiesel production. Computers and Chemical Engineering, 35(5), 936-942.

Ramos, M., Dias, APS., Puna, JF., Gomes. J. and Bordado, JC., 2019. Review on biodiesel production processes and sustainable raw materials. Energies, 12(23), 4408.

Wen, X., Quacoe, Daniel, Quacoe, Dinah, Appiah, K., Danso, B., 2019. Analysis on bioeconomy's contribution to GDP: Evidence from Japan. Sustain. 11, 1–17.

Song, J., Yang, W., Higano, Y., Wang, X., 2015. Modeling the development and utilization of bioenergy and exploring the environmental economic benefits. Energy Convers. Manag. 103, 836–846.

Tsanaktsidis, CG., Stimoniaris, AZ., Spinthiropoulos, KG., Papadimitriou, A., Tzilantonis, GT., Smaragdis IN. and Vasiliadis, B., 2018. Creation of Environmentally Friendly Fuel High in Energy by Mixing Marine Fuel Oil and Biodiesel. J. of Marine Env. Eng, 10, 149–162.

2nd International Conference on
Sustainable Chemical and
Environmental Engineering
14th – 18th June 2023, Limassol, Cyprus

Optimal Biodiesel Mixtures: Cost and Density Evaluation Function Application by Genetic Algorithm

V. Vasileiadis [1], M.E. Kyriklidis[2], C. Kyriklidis[1], E. Terzopoulou[1] and C. Tsanaktsidis[1]

[1]*Department of Chemical Engineering, University of Western Macedonia, Kila, GR-50100, Kozani, Greece*
[2]*Department of Regional Development and Cross Border Studies, University of Western Macedonia, Kila, Kozani, Greece*
Corresponding author email: vvasiliadis@uowm.gr

ABSTRACT

The present paper proposes a new approach for solving fuel mixtures optimization problems in Biodiesel production. Diesel emissions in combination with the high cost converge to the searching of alternative fuels. Its desulphurization consumes time and requires significant investments. On the other hand, Biodiesel as an alternative solution, has become more attractive because it is produced from renewable and environmentally friendly materials. In this work, an adjusted genetic algorithm is improved, which investigates initially the ingredients percentages in the fuel mixtures, to optimally create their combinations as Biodiesel fuel. The main ingredients of the proposed biodiesel are diesel and biodiesel (50% animal fat sources and 50% vegetable sources) and the evaluation of the new Biodiesel was implemented from a fitness function, which estimate the fuel cost and density. Except cost, density as a physicochemical characteristic of fuels, determine the suitability on a new fuel for general use and sale. Detailed experiments produced highly accurate Biodiesel mixtures, proposing an optimal fuel solution per set. Fuel Mixture in Set 1 produced from 75.031% diesel and 24.969% biodiesel with mixture cost: 1.6975 €/l and mixture density: 0.8355 g/ml. In Set 2, the Fuel Mixture came from 75.016% diesel and 24.984% biodiesel with mixture cost: 1.6977 €/l and mixture density: 0.8366 g/ml. The new Biodiesel fuels cost less 15.13% (Set 1) and 15.12% (Set 2) than the diesel cost (2.0000 €/l), provide competitive fuel prices, have lower sulfur content and their consumption reducing the pollutant emissions.

Keywords: Optimal Biodiesel Mixtures; Optimization Problems; Genetic Algorithms; Evolutionary Computation.

1. INTRODUCTION

In the last decades, due to the society development, energy requirements are constantly increasing. The combination of the not inexhaustible diesel reserves, the diesel consumption environmental harmful emissions as well as the global crises, led many researchers to evaluate the use and development of alternative fuels (Semwal et al. 2011). Biodiesel constitutes a renewable energy product, with environmentally friendly advantages: non-toxic, biodegradable and clean, contains no aromatic compounds and pollutants sulfur oxides emissions, carbon monoxide, unburned hydrocarbons and soot from the burning of the diesel engines are very low (Lotero et al. 2005; Huber et al. 2006; Marchetti et al. 2007; Georgogianni et al. 2009; Semwal et al. 2011; Deya et al. 2021).

On the contrary, the diesel use implies sulfur presence, which is responsible for the main pollutant oxides. While diesel desulphurization consumes time and requires significant investments, the only

effective approach for the emission reduction is the fuel improvement in mixtures of diesel and biodiesel. The fuel quality is maintained as sulfur content is significantly reduced.

Another important issue of fuel physicochemical properties constitutes density. The fuel density defines the fuel economy in CI engines to a great extent (Lee et al. 2012; Roschat et al. 2012; Deya et al. 2021). The experimental process for the mixtures production in laboratories is time consuming and costs a lot, when researchers carry out extensive analysis to produce as much as possible the optimum fuel quality and price (Tsanaktsidis et al. 2018).

Intelligent techniques, nature inspired intelligence, machine learning and evolutionary computation approaches provide high quality near-optimal results to complicated optimization problems. Thus, operational research (OR) application bases on their implementation and evolution (Chenga et al. 2016; Kyriklidis and Dounias 2016; Mohadesi and Rezaei 2018).

The approach effectiveness concerns: a) the problem innovative modelling, with specific function evaluation modelling improvements and b) the way genetic algorithm is defined and tuned. Furthermore, significant results are provided from the experimental simulations of the current approach, as follows: 1) Experiments Cost Minimization, 2) Experiments Duration Minimization, 3) Cost and Density Improvement through Evaluation Function Minimization and 4) Environmentally Friendly Fuel.

This new decision-making tool is available for the Laboratory researchers and advances optimal fuels. The genetic algorithm in short time, after solution evaluation, proposes the optimal mixture for experimentation in Laboratory, between 750*106 alternative mixtures per experiment set. The profits of the proposed approach contribute to mixture production process, when the new Biodiesel becomes more attractive than the competitive fuels.

The rest of the paper is organized as follows: In Section 2, the mathematical formulation of the Fuel Mixture Problem is given, and the problem restrictions based on ingredients availability. Section 3 presents the main methodological issues of the proposed approach, in order to perceive a better understanding of the underlying mechanism of the used algorithm. Finally, the last Section summarizes concluding remarks and interesting points.

2. FUEL MIXTURE PROBLEM

The Fuel Mixture Problem concerns a study sector, that many researchers investigate intensively. As dynamic-complicated real-world problem, it is not possible, to produce all feasible mixtures on Laboratory experimentation. The large experiment numbers imply excessive costs as well as a long execution time. The present approach provides flexible management of the mixture production under simulation process.

A function evaluation of each mixture, through the present GA, provides targeted and quality mixtures and proposes the best solution in a short experimental time. The function for mixture's value minimization results from the following mathematical function as multiple objectives.

Minimization of the *Total Mixture Function Value* (*min TMFV*)

The ***Total Mixture Function Value*** of the ingredients *i* is expressed as the weighted sum (w_1) of the multiplication between ingredient normalized cost per *l* and the ingredient percentage on mixture minus the weighted sum (w_2) of the multiplication between ingredient normalized density per *l* and the

ingredient percentage on mixture: $\boldsymbol{TMFV} = w_1 * \sum_{i\in\{1,..,n\}} (\frac{c_i}{c_{max}}) * p_i - w_2 * \sum_{i\in\{1,..,n\}} (\frac{d_i}{d_{max}})\text{^}4 * p_i$ (1)

The goal of the raw materials optimization problem is to minimize the new biodiesel mixture function value: $\mathbf{min}\,\boldsymbol{TMFV}$ (2)

Problem **Restrictions: 1)** *Min Ingredient Percentage % ≤ p_i ≤ Max Ingredient Percentage %,* **2)** *c_i, where c_1: diesel cost and c_2: biodiesel cost,* **3)** *di where d_1: diesel density and c_2: biodiesel density and* **4)** *Weights: w_1+w_2 =100%.*

3. ALGORITHMIC FRAMEWORK

Nature inspired approaches, are implemented on many sectors providing high quality results. As concerns Genetic algorithms, whose main properties based on evolutionary computation, they were first introduced by Holland (1992). The present study introduces a Genetic Algorithm (GA) evolutionary method for biodiesel mixture problem. The relative algorithms utilize the operators of selection, crossover, and mutation to evolve the population chromosomes, through generations progress (Kyriklidis and Dounias 2016, Kyriklidis et al. 2022).

3.1 GA - Chromosome Representation

Chromosome Example: A mixture example consisting of two ingredients. The ingredients percentages summarize always 100%. Example: Diesel 78.22% and Biodiesel 21.78%.

3.2 Construction of the Next Generation

The generations' production is separated to two phases. In the first phase, the first generation formed by randomly creating feasible mixtures. In the second phase and for the following generations, the chromosomes production consists of three parts:

a) **Part 1**: The 10% of the generation chromosomes, which will evaluate as best chromosomes (TOP Mixtures), is transferred directly to the next generation.

b) **Part 2**: The following 70% of solutions, consists of chromosomes, which are produced from the Crossover operator.

c) **Part 3**: Mutation provides the last 20% chromosomes, generated in the same way by which the initial population was formed.

Fuel mixtures are generated by taking diesel and biodiesel percentages contained in each chromosome. Then, the fitness function is used to evaluate each mixture - chromosome (criterions: cost and density) and ranking all the mixtures.

The solutions that are produced from crossover and mutation operators, consist of ingredients percentages between specific ingredient percentages (minimum % - maximum %), when the mixture ingredient summarizes always to 100%. The proposed approach produces only feasible solutions, and no feasible solution is excluded by the assessment process.

After the initial population creation, a frame $\pm$ IPLS from the best chromosome percentages has been implemented. This frame was introduced by (Kyriklidis et al. 2022), supporting the optimal solution process around the previous generation best chromosome. A specific range (e.g., 5% - 10%) for IPLS values is defined and for every generation is randomly selected a new IPLS value (e.g., Generation 1, IPLS: 6%; Generation 2, IPLS: 9%; ... Generation 100, IPLS: 10%). In conclusion, after extensive

experimentation, more than 100,000 simulations, have been selected all GA parameters (Kyriklidis and Dounias 2016). Their effectiveness is comparable until nowadays with competitive approaches, providing better results.

3.3 Benchmark experiments

The performance of the proposed GA-approach has been tested for 2 different versions of experiments classified based on mixtures' temperature: 5C°, 10C°, 15C°, 20C° and 25C° (called sets further on):
(a) Set 1 - Emphasis on Cost: The weight value w_1 from Evaluation Function ***TMFV*** ranges equal and more than 50%, $w_1 \geq 50\%$.
(b) Set 2 - Emphasis on Density: The weight value w_2 from Evaluation Function ***TMFV*** ranges equal and more than 50%, $w_2 \geq 50\%$.
(c) Set 1 and Set 2: The size of population was set to 100, the number of generations was set to 300 and the ingredients costs were diesel 2.0000 €/l and biodiesel 0.7901 €/l and the ingredients densities were diesel 0.8191 g/ml and biodiesel 0.8855 g/ml at 5C° Ingredients density is differentiated depending on temperatures between 5C° - 25C°.
(d) To the next generation were transferred directly the 10% best chromosomes of the last evaluated generation.
(e) Crossover operator produced 70% of the population, subjected to IPLS value, which was randomly per generation defined between $\pm\ 5\%\ until\ 10\%$.
(f) In the remaining 20% of chromosomes, the Mutation operator was applied.
(g) Each experiment was set to 1000 independent simulations made per Set and temperature (Set1 - 5C° - 1000 iterations, Set 1 – 10C° – 1000 iterations, …, Set 2 – 25C° - 1000 iterations).

Biodiesel as second ingredient came from 50% animal fat sources and 50% vegetable sources.

The vegetable sources prices (rap oil and sun oil) are available worldwide from the Food and Agriculture Organization of the United Nations (FAOSTAT: https://www.fao.org/faostat/en/#data/PP) and at Hellenic Statistical Authority (HSA: https://www.statistics.gr/) in Greece.

In the case of Greece 15 companies carry out the collection of animal fat acid and cooked olive oil. The ingredients prices are directly dependent on the demand from the refineries which determine the final price of Biodiesel.

The classification of the experimental sets based on the parameter of temperature from 5Co - 25Co, experiments with Emphasis on Cost (Set 1: w1 ≥ 50%) and experiments with Emphasis on Density (Set 2: w2 ≥ 50%). For example, w1 = 70% and w2 = 30% as settings, provide Emphasis on Cost, because cost criterion is weighted more than the density criterion.

- **Set 1**: 50% **/** 50%, 60% **/** 40%, 70% **/** 30%, 80% **/** 20%, 90% **/** 10%.
- **Set 2**: 50% **/** 50%, 40% **/** 60%, 30% **/** 70%, 20% **/** 80%, 10% **/** 90%.

Additional experimental information follows. Diesel and biodiesel cost 2.000 €/l and 0.7901 €/l respectively and density amounts from 0.8191 g/ml – 0.8855 g/ml depending on temperature. Also, the ingredients percentages in mixtures are available, diesel percentage between 1% - 99% and biodiesel percentage between 1% - 30%. The present values concern the availabilities and the actual prices during the period of the laboratory experimentations.

3.4 Experiments Results

Firstly, an implementation of the proposed GA performance on Set 1 was made, where the 25,000 independent simulations per temperature (5Co - 25Co) and weights (w1 and w2) combination took place for 3,506,25 sec (or 58.44 min ≈ 1h).

Optimal Mixture in Set 1 (temperature 5C0, w1 = 50%, w2 = 50%): Diesel percentage: 75.031%, Biodiesel percentage: 24.969%, TMFV: -0.0727, Mixture Cost: 1.6975 €/l and Mixture Density: 0.8355 g/ml (Fig. 2)

Set 2 contains the information of the optimal mixture between 1000 independent simulations (or 25 optimal mixtures in total). The assessment is based on minimum Total Mixture Function Value (or TMFV). As the value of w2 increases, so does the value of TMFV. In this way, the density criterion is emphasized than the cost criterion. Ingredients percentages in optimal mixtures, optimal mixtures cost, and density differ to small degree as presented above.

Optimal Mixture in Set 2 (temperature 20C0, w1 = 10%, w2 = 90%): Diesel percentage: 75.016%, Biodiesel percentage: 24.984%, TMFV: -0.8146, Mixture Cost: 1.6977 €/l, Mixture Density: 0.8366 g/ml (Fig. 3).

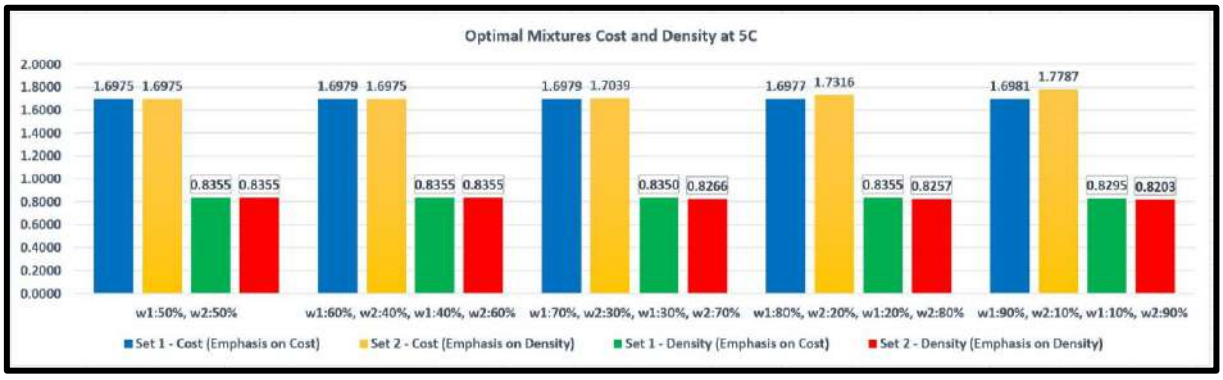

Fig. 2 Optimal Mixtures Cost and Density at 5C°.

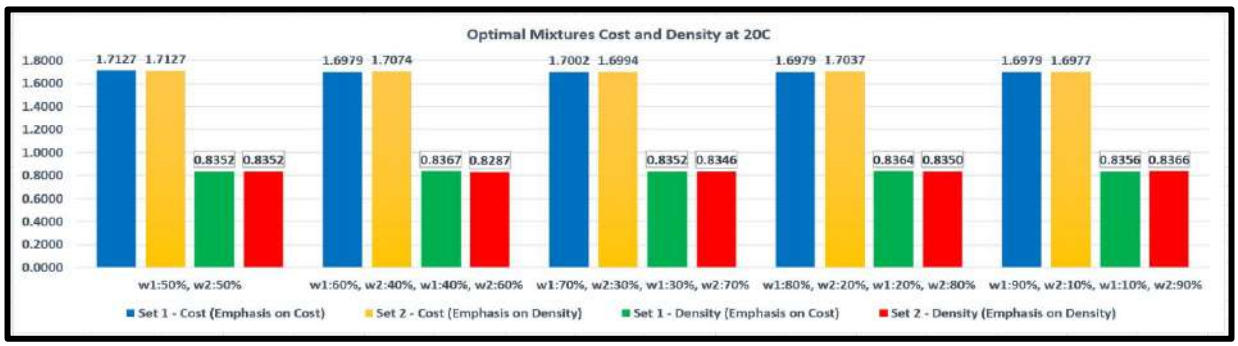

Fig. 3 Optimal Mixtures Cost and Density at 20C°.

4. CONCLUDING REMARKS

This paper presents a genetic algorithm approach, providing optimal solutions of the fuel mixture problem. The basic contribution of the approach relates to the way that the diesel and biodiesel (50% fat sources -50% vegetable sources), as mixture ingredients, obtain feasible percentage, thus leading to new fuel

improvement. When the decision maker can search the area surrounding of the optimal ingredient's percentage, by using the efficient IPLS mechanism.

Furthermore, the Total Mixture Function Value (or TMFV) is applied on the new Biodiesel mixtures assessment, reflecting the production of competitive fuel, based on the ingredient's availability. The two function's parts providing emphasis in two fuel parameters the cost and the density. The weights w1, w2 determine this emphasis, when w1 contributes "Emphasis on Cost", while w2 provides "Emphasis on Density" under experimental fuel evaluation.

The new optimal Biodiesel mixtures were investigated through repeated experimentation (150*107 mixtures). Two sets have been determined with experiments temperature between 5Co - 25Co: a) Set 1 – "Emphasis on Cost" and b) Set 2 – "Emphasis on Density". Optimal Mixture in Set 1 (temperature 5C0, w1 = 50%, w2 = 50%) had the following parameter values: Diesel percentage: 75.031%, Biodiesel percentage: 24.969%, TMFV: -0.0727, Mixture Cost: 1.6975 €/l and Mixture Density: 0.8355 g/ml. Optimal Mixture in Set 2 (temperature 20C0, w1 = 10%, w2 = 90%) had the following parameter values: Diesel percentage: 75.016%, Biodiesel percentage: 24.984%, TMFV: -0.8146, Mixture Cost: 1.6977 €/l and Mixture Density: 0.8366 g/ml. The new Biodiesel mixtures cost less 15.13% (Set 1) and 15.12% (Set 2) than the diesel cost (2.0000 €/l), provide competitive fuel prices, have lower sulfur content and their consumption is reducing the pollutant emissions.

REFERENCES

Chenga, M-Y., Prayogo, D., Juc, Y-H., Wua Y-W. and Sutantoc, S., 2016. Optimizing mixture properties of biodiesel production using genetic algorithm-based evolutionary support vector machine. International Journal of Green Energy, 13(15), 1599–1607.

Deya, P., Raya, S. and Newarb, A., 2021 Defining a waste vegetable oil-biodiesel based diesel substitute blend fuel by response surface optimization of density and calorific value. Fuel, 283,118978

Georgogianni, K., Katsoulidis, A., Pomonis, P. and Kontominas, M., 2009. Transesterification of soybean frying oil to biodiesel using heterogeneous catalysts. Fuel Processing Technology, 90, 671–676.

Holland, J. H., 1992. Genetic Algorithms. Scientific American, 267(1), 66-72.

Huber, GW., Iborra, S. and Corma, A., 2006. Synthesis of transportation fuels from biomass: chemistry, catalysts, and engineering. Chemical Reviews, 106, 4044–4098.

Kyriklidis, C. and Dounias, G., 2016. Evolutionary computation for resource leveling optimization in project management. Integrated Computer-Aided Engineering, IOS Press, 23(2), 173-184.

Kyriklidis, C., Kyriklidis, ME., Loizou, E., Stimoniaris, A. and Tsanaktsidis, CG., 2022. Optimal Bio Marine Fuel production evolutionary Computation: Genetic algorithm approach for raw materials mixtures. Fuel, 323,124232.

Lee, S., Posarac, D. and Ellis, N., 2012. An experimental investigation of biodiesel synthesis from waste canola oil using supercritical methanol. Fuel, 91, 229–237.

Lotero, E., Liu, Y., Lopez, DE., Suwannakarn, K., Bruce. DA. And Goodwin, JG., 2005. Synthesis of biodiesel via acid catalysis. Industrial & Engineering Chemistry Research, 44(14), 5353–5363.

Marchetti., J., Miguel, V. and Errazu, A., 2007. Possible methods for biodiesel production. Renewable and Sustainable Energy Reviews, 11, 1300–1311.

Mohadesi, M. and Rezaei, A., 2018. Biodiesel Conversion Modeling under Several Conditions Using Computational Intelligence Methods. Environmental Progress & Sustainable Energy, 37(1), 562-568.

Roschat, W., Kacha, M., Yoosuk, B., Sudyoadsuk, T. and Promarak, V. 2012. Biodiesel production based on heterogeneous process catalyzed by solid waste coral fragment. Fuel, 98, 194–202.

Semwal, S., Arora, AK., Badoni, RP. and Tuli, DK., 2011. Biodiesel production using heterogeneous catalysts. Bioresource Technology, 102, 2151–2161.

Tsanaktsidis, CG., Stimoniaris, AZ., Spinthiropoulos, KG., Papadimitriou, A., Tzilantonis, GT., Smaragdis IN. and Vasiliadis, B., 2018. Creation of Environmentally Friendly Fuel High in Energy by Mixing Marine Fuel Oil and Biodiesel. J. of Marine Env. Eng, 10, 149–162.

2nd International Conference on
Sustainable Chemical and
Environmental Engineering
14th – 18th June 2023, Limassol, Cyprus

Fabrication of Ceramic Composite Films for Solid Oxide Electrochemical Cells(SOEC) by Solution Spray Pyrolysis(SSP)

C. Ziazias[1], C. Matsouka[2], C. Tsanaktsidis[1] and N. Kiratzis[3]

[1] Department of Chemical Engineering /School of Engineering, University of Western Macedonia, ZEP, Kozani 50100, Greece
[2] Chemical Process and Energy Resources Institute-CPERI / Centre for Research and Technology Hellas-CERTH, 57001 Thermi, Thessaloniki, Greece
[3] Department of Mineral Resources Engineering /School of Engineering, University of Western Macedonia, Kila, Kozani 50100, Greece
Corresponding author email: nkiratzis@uowm.gr

ABSTRACT

Electrodic polarization resistances in Solid Oxide Cell (SOC) devices (that include both Solid Oxide Fuel i.e. (SOFC) and Electrolyzer Cells i.e. SOEC) should always remain low for high performance cell operation and low degradation rates. Major research efforts are still required not only in terms of materials but also within the realm of the adoption of the appropriate fabrication technologies that will ensure the required morphologies at large scale production rates. The technique of solution spray pyrolysis (SSP) offers an attractive method of producing thin films of electrodes and electrolytes due to its simplicity, low cost and potential for industrial large scale application. In the present communication, we use this technique to fabricate composites of LSM- YSZ on dense YSZ substrates and CGO-$La_xSr_{1-x}FeO_3$(CGO-LSF) on dense LSF substrates with focus on morphology, crystal structure and thermal characteristics of the precursor salts.

Keywords: Solid Oxide Electrochemical Cell; Spray Pyrolysis; Ceramic Films; Ceramic Composites; Electrodes.

1. INTRODUCTION

Low electrodic polarization resistances in Solid Oxide Cells (SOC) operating either as Fuel (SOFC) or Electrolyzer Cells i.e. SOEC) are always desirable in order to assure high performance and low degradation rates. This is also important in the case of operation of a reversible solid oxide cell (RSOC) (i.e. the same device operating either in a Fuel Cell or Electrolyzer mode) (Mogensen et al., 2019).

With respect to the oxygen or air electrode based on a typical $Zr_{0.84}Y_{0.16}O_{1.92}$ (YSZ16) electrolyte, composites of $La_{0.75}Sr_{0.25}MnO_3$ (LSM)-YSZ are ubiquitously used due to the thermodynamic stability of LSM. Alternatively, Sr substituted $LaFeO_{3-\delta}$ (LSF) constitutes an interesting material for a cathodic electrode in a SOFC due to its mixed conductivity mode (i.e. electronic and ionic) and good electrocatalytic activity for oxygen reduction. In the case of LSF (Matsouka et al., 2018), interfaces with the electrolyte $Ce_{0.9}Gd_{0.1}O_{1.95}$ (CGO10) instead of direct contact with YSZ due to the accompanying reactions with YSZ at high sintering temperatures.

The technique of solution spray pyrolysis (SSP) (Kiratzis et al., 2022) offers an attractive method of producing thin films of electrodes and electrolytes due to its simplicity, low cost and potential for industrial large scale application (Irvine et al., 2016, Tsimekas, 2019). In the present communication, we focus on the cathodic interface by fabricating composites of LSM- $Zr_{0.92}Y_{0.08}O_{1.96}$(YSZ8) on dense YSZ (i.e. $Zr_{0.84}Y_{0.16}O_{1.92}$) substrates by SSP. Alternatively, films of composites of $La_{1-x}Sr_xFeO_{3-\delta}$–CGO10 on dense $La_{1-x}Sr_xFeO_{3-\delta}$ (LSF) (x=0.3 or 0.5) substrates were fabricated and compared.

2. EXPERIMENTAL

The experimental setup (Figure1) consists of a syringe pump, to provide the solution at the desired flow rate control during spraying, an air compressor (vol.50L) with a manometer and a flow controller for adjusting the air flow rate. Solution and air were mixed in a spray nozzle that produced a spray consisting of 10-100 μm

diameter droplets. Aqueous solutions of the precursor salts were prepared using distilled water at total ion concentrations of either 0.025M or 0.1M. Depositions of LSM or YSZ films were made on dense YSZ pellets and CGO10 and LSF films on dense LSF pellets. Optimized values for the air flow rate and pressure were 18.36 L/min and 250 kPa respectively. The liquid flow rate was set at 30 ml/h and the total volume was 50ml. This yielded a constant deposition time of all experimental runs at 100 min. Actual coated area ranged between 0.9 to 1.0 cm^2. The substrates of yttria stabilized zirconia (YSZ) were prepared by uniaxially pressing in a hydraulic press at ≈187 MPa and subsequently sintering at 1300°C for 5 hours. In some cases, fragments of YSZ thin dense substrates produced by tape casting at U. of St. Andrews (thick.0.200 mm) (Savaniu and Irvine, 2009) were used. Dense $La_{1-x}Sr_xFeO_{3-\delta}$ (LSF) (x=0.3 or 0.5) substrates were synthesized by a co-precipitation method using the nitrate salts of the metallic anions as described in detail by Matsouka et al.(2018). Characterization was performed by XRD and SEM in addition to TGA of the precursor salts and obtained post deposition films.

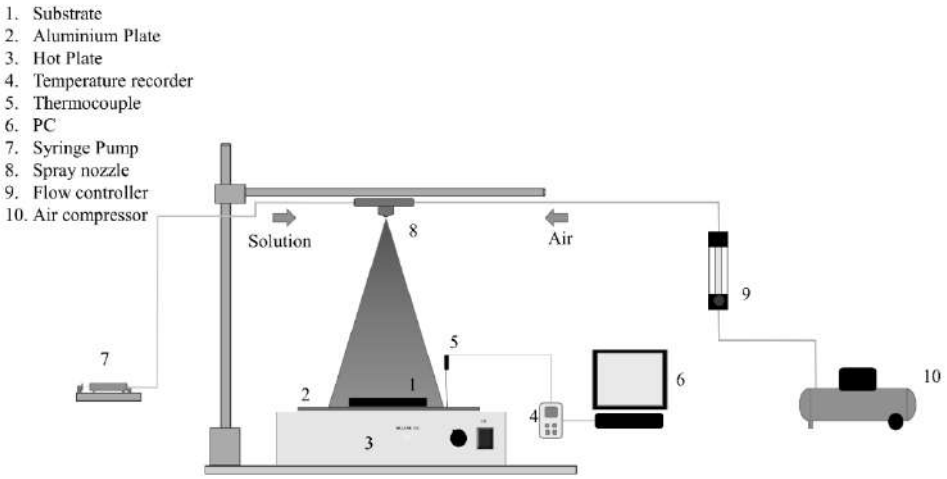

Figure 1. *Schematic of the experimental apparatus.*

3. Results and Discussion

The procedure for film deposition is shown in Table 1.

Table 1. *Type of films, experiments and characterization.*

Sample#	Film (Total Precursor Ion Concentrations, M)	Substrate	Sintering scheme*	Tdep	Characterization
1	YSZ(0.1)/LSM(0.025)	YSZ16	A2	339±28/219±16	-
2	YSZ(0.025)/LSM(0.025)	YSZ16	A2	141±13/220±28	XRD,SEM-EDS
3	YSZ(0.025)/LSM(0.025)	YSZ16	B2	142±3/98±38	-
4	YSZ(0.1)/LSM(0.025)	YSZ16	B2	168±13/208±23	XRD,SEM-EDS
5	LSF30(0.025)/CGO10(0.1)	LSF30	A2	229±6/195±8	XRD,SEM-EDS
6	CGO10(0.025)	LSF50	A1	232±9	XRD,SEM-EDS

Key: A=Whole composite sintered (700°C/4hr), B=Intermediate sintering of first deposited layer followed by additional sintering of the composite (1,2 denote single or double layered film).

3.1. XRD results

Figure 2 shows XRD typical outputs of an YSZ(0.1)/LSM(0.025) composite on YSZ16 substrate (a) and a CGO10 film on LSF30 substrate. It can be seen that 700°C is an adequate sintering temperature to form the desired phases while being relatively low to prevent formation of detrimental additional phases. This is expected, as this technique allows for the generation of very active germinal particles that should eventually yield agglomerates requiring lower sintering times than conventional particulate based ceramic fabrication schemes.

3.2. Film morphology

Figure 3 compares two structures of YSZ/LSM composites fabricated with different sintering profiles (Table 1). The LSM film at the top of the figure exhibits a smoother surface with less cracks though some roughness is evident at certain possibly uncoated spots. Although, the average temperature is within the range observed in our previous report (Krestou et al., 2018) for smooth films, temperature variation in this case as given by standard deviation is larger by about a factor of 4 and this could be the cause for the observed cracking. In contrast, more extensive cracking is observed at the bottom picture of the same Figure which corresponds to a similar composite (i.e. YSZ/LSM) but after firstly sintering the first YSZ layer followed by deposition of LSM and again re-sintering the whole structure. This film, besides cracking, it also exhibits a surface feature not evident in the first film which is probably due to the surface roughness characteristics of the underlying and sintered YSZ layer. Temperature standard deviation is also relatively large in this case which could be conducive to the more extensive cracking observed as well as to some uncoated spots on the surface verified by EDS. Generally, it can be concluded that a two step sintering scheme is not preferable to a one step sintering of the whole structure for composites made of YSZ/LSM by solution spray pyrolysis.

However, no cracks are observed throughout the whole thickness (Figure 4) of the film at the interface which is consisted of a mixture of YSZ and LSM particulates as verified by cross section EDS with LSM enriched at the outer surface. Adhesion seems excellent within a relatively thick composite film of about 20-30μm. Thus, it is concluded that a better temperature control could yield smoother surfaces with minimal cracking.

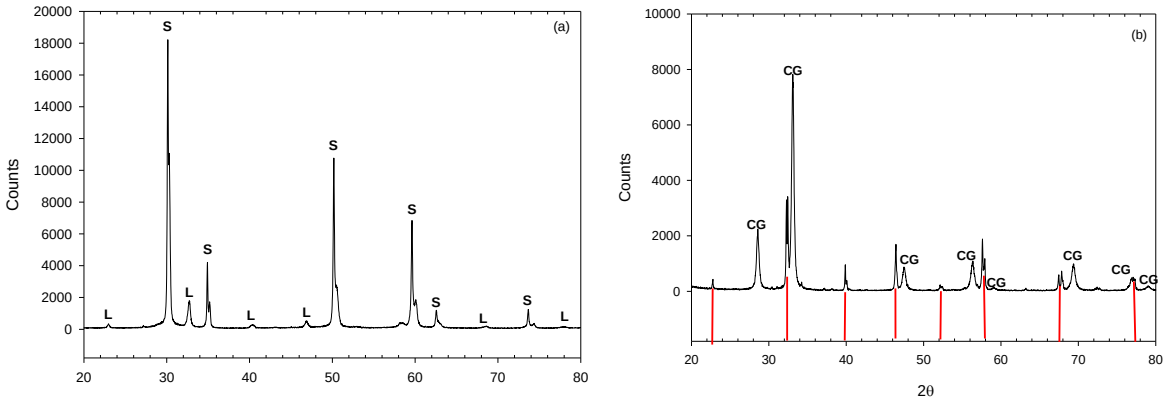

Figure 2. *XRD results for a) YSZ(0.1)/LSM(0.025) composite on YSZ16 substrate and b) CGO10 film on LSF30 substrate(Key: S=YSZ16, CG=CGO10, L=LSM. Red lines indicates reference peaks for LSF).*

Figure 5 shows surface and cross section of an LSF30/CGO10 composite coated on an LSF30 substrate. Here, a better temperature control was achieved (i.e. standard deviation of ±7°C) and a better quality film was fabricated in terms of fully coating the substrate and thickness uniformity. Nevertheless, cracking is also shown on the surface which is most probably due to the lower temperature employed in this case for the top CGO10 layer from a staring solution of total ion precursor concentration of 0.1 M (Krestou et al., 2018).

These cracks, however, seem to be constrained only on the surface as shown at the bottom picture of the same Figure in which a uniform CGO layer of thickness of about 1.2 μm is depicted. This has been verified by the respective EDS. Interestingly, no intermediate film of LSF30 is discernible but only the CGO10 film. It

should also be noticed that the substrate temperature during the first deposition was significantly higher than the second (i.e. by about 35-40°C) which could promote the appearance of the Leidenfrost effect resulting in partial or lack of coating on the substrate surface.

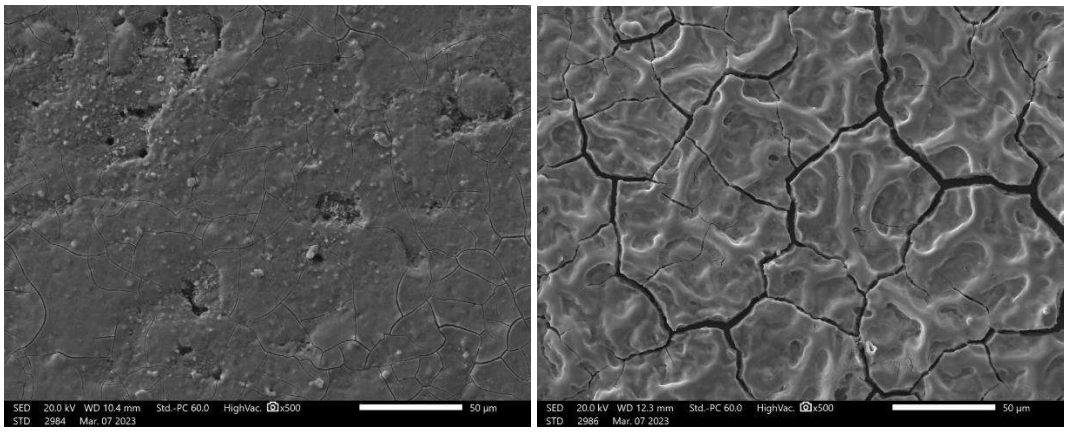

Figure 3. *Top surface SEM for YSZ/LSM composite after (left) one sintering step (sample 2 of Table 1) and (right) after two sintering steps (sample 4 of Table1).*

In fact, this could be the case for the film of sample #6 of Table I, for which no film of CGO10 was detected after spraying for 100 min on the LSF50 dense substrate as verified by EDS. In this sample, the temperature was also kept relatively high at about 232°C. It should be emphasized, that the Leidenfrost point for a specific precursor that dictates the maximum possible coating temperature, is a function of the solvent boiling point, the metal salt concentration and the type of the salt and the thermal properties of the specific substrate expressed as the product of density, thermal conductivity and heat capacity (Muecke et al., 2009).

3.3. TGA characterization of precursor salts and films

Figure 6 shows the TGA characteristics of the YSZ and CGO10 precursor salts. Notice that, in both cases the applied sintering temperature of 700°C is adequate to decompose the precursor salts to their respective oxides. It can also be observed the major portion of weight loss is occurring at 350°C resembling rather the behavior of the $Ce(NO_3)_3 \cdot 6H_2O$ salt than the $Gd(NO_3)_3 \bullet 6H_2O$ salt.

La and Mn precursor salts (Figure 7) seem to totally decompose above 678 and 350°C while that of the Sr salt requires a temperature of 800°C which should direct to a higher sintering temperature for LSM films. The LSM film itself seems to follow a decomposition pattern similar to that of the $La(NO_3)_3 \cdot 6H_2O$ precursor with somehow more abrupt drop after 260°C. These trends, seem to agree with Weber et al. (2013), that the suitable deposition temperature for a film is given by the penultimate decomposition step of the precursors. A more detailed analysis of the precursor decomposition steps for the CGO10 and the LSM films has been given by Krestou et al. (2021). Finally, TGA results for both the Fe precursor nitrate salt as well as an LSG30 film is shown at the bottom diagram in Fig.7. $Fe(NO_3)_3$ decomposes in two steps that terminate at 164 and 360°C respectively, with the LSF30 film resembling mostly the behavior of the La nitrate precursor salt.

4. CONCLUSIONS

The technique of solution spray pyrolysis was used to fabricate composites of YSZ/LSM films on dense YSZ substrates as well as CGO10 or LSF30/CGO10 composite films on LSF substrates. For the YSZ/LSM composite films it was concluded that one sintering step of both sequentially deposited films is preferable to applying two separate sintering steps for each film in terms of thickness uniformity and extent of cracking. In the case of the double sintering step, surface features of the top LSM film appear following the features of the sintered

YSZ film substrate. Temperature standard deviation gives a rough indication of the quality of the film and should be kept below 10°C.

For the LSF/CGO10 film, it was found that a good interface is formed with the LSF substrate at a deposition temperature of the CGO10 film of about 195°C though to avoid surface cracks a lower concentration than 0.1 M should be used. On this particular substrate, it was found that lower concentration of either CGO10 or LSF30 of the order of 0.025 M do not result in coating at temperatures of or above 230°C most probably due to the appearance of the Leidenfrost effect that cause droplets to levitate above the substrate surface and subsequently to be removed by the air stream.

Finally the thermal characteristics of the precursor salts and deposited mixed oxide films as revealed by TGA showed that a temperature of 700°C is adequate for decomposition of all salts except that of $Sr(NO_3)_2$ which requires a temperature of 800°C for complete decomposition. The thermal degradation characteristics of the respective mixed oxide films resemble mostly that of the precursor salt that exhibits a penultimate decomposition step among all steps exhibited by all the precursors. Definitely more work is required in assessing the quality of these composites electrochemically in terms of performance and degradation characteristics.

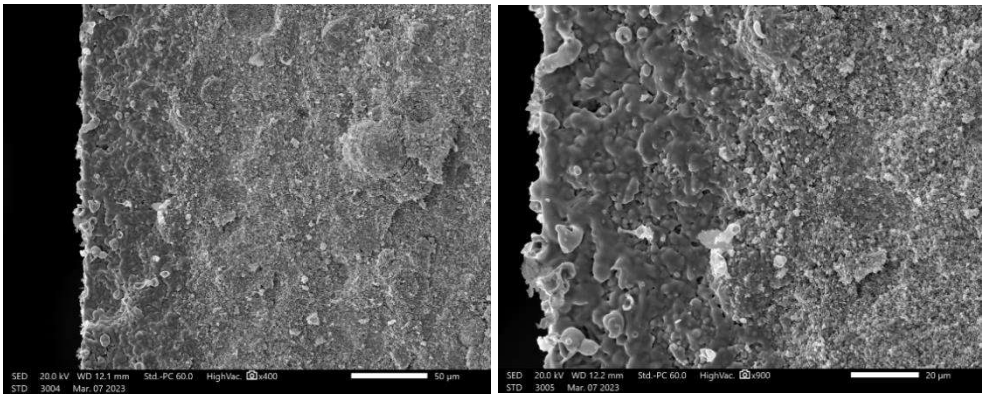

Figure 4. *Cross section SEM for YSZ/LSM composite after two sintering steps (sample 4 of Table1).*

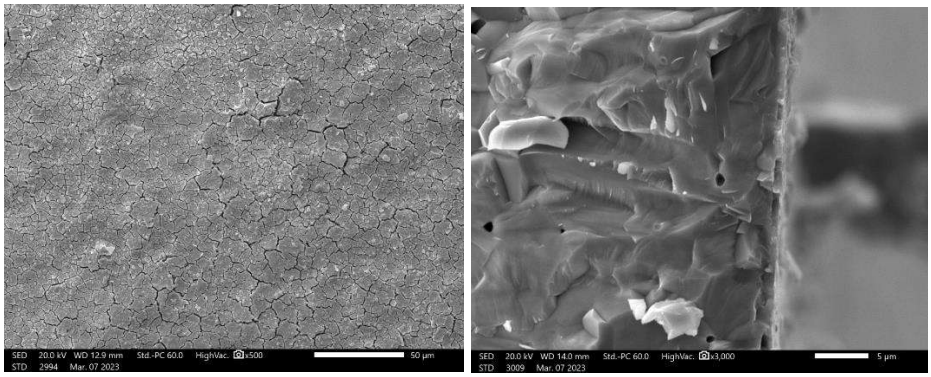

Figure 5. *Surface (left) and cross section SEM of LSF30/CGO10 film on a LSF30 substrate (for deposition conditions see Table 1, sample#5).*

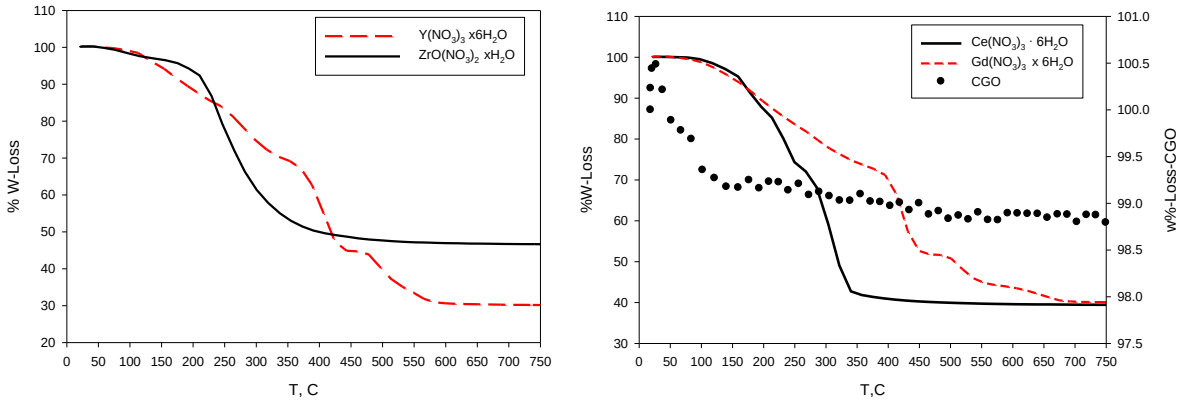

Figure 6. *TGA results for Y, Zr (left) and Ce anf Gd precursor salts and a CGO10 film directly after spray deposition..*

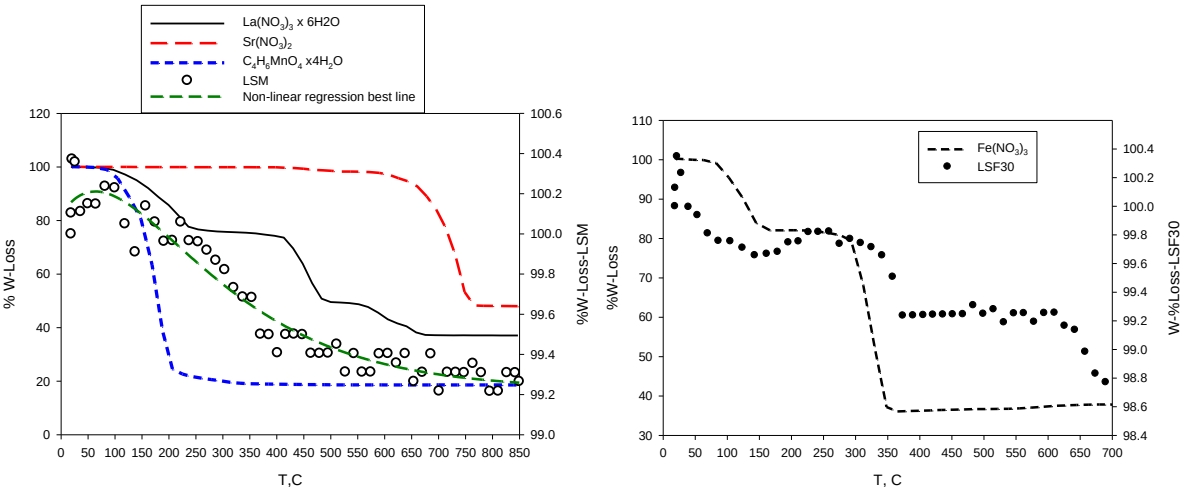

Figure 7. *TGA results for La, Sr, Mn, LSM film (left) and Fe precursor salts along and LSF30 film directly after spray deposition..*

5. ACKNOWLEDGEMENTS

We acknowledge the University of Western Macedonia for partially supporting financially this research through the postgraduate program (MSc) in Energy Investments and Environment.

REFERENCES

Irvine J.T.S., Neagua D., Verbraeken M. C., Chatzichristodoulou C., Graves C., Mogensen M. B., 2016. Evolution of the electrochemical interface in high-temperature fuel cells and electrolyzers. *Nat Energy,* 1, 15014.

Kiratzis N. E., Barbatsis A., Kosmarikos N., Bisbas A., Matsouka C. and Nalbandian L., 2022. Fabrication of Fluorite and Perovskite Functional Films by Solution Spray Pyrolysis. *Nano Hybrids and Composites,* 34, 47–52.

Krestou A., Barmpatsis A., Tsanaktsidis C., Matsouka C., Nalbandian L., and Kiratzis N., 2021. Fabrication and Characterization of Functional Ceramic Films By Solution Spray Pyrolysis: Correlations with the Thermal Decomposition Characteristics of the Constituent Salts. *ECS Transactions*, 103(1), 123-138.

Krestou A., Giozis I., Maroulis G., Barbatsis A., Tsanaktsidis C., Kyriakou V. and Kiratzis N. E., 2018. Fabrication of Thin Functional Films by Solution Aerosol Thermolysis (SAT). *ECS Journal of Solid State Science and Technology,* 7, P660– P670.

Matsouka C., Zaspalis V., Nalbandian L., 2018. Perovskites as oxygen carriers in chemical looping reforming process–Preparation of dense perovskite membranes and ionic conductivity measurement. *Materials Today: Proceedings*, 5, 27543–27552.

Mogensen M.B., Chen M., Frandsen H.L., Graves C., Hansen J.B., Hansen K.V., Hauch A., Jacobsen T., Jensen S.H., Skafte T.L. and Sun X., 2019. Reversible solid-oxide cells for clean and sustainable energy. *Clean Energy*, 3 (No. 3), 175–201.

Muecke U. P., Messing G. L., Gauckler L. J., 2009. The Leidenfrost effect during spray pyrolysis of nickel oxide-gadolinia doped ceria composite thin films. *Thin Solid Films,* 517, 1515– 1521.

Savaniu C-D and Irvine J. T. S. 2009. Reduction studies and evaluation of surface modified A-site deficient La-doped SrTiO3 as anode material for IT-SOFCs. *J. Mater. Chem.,* 19, 8119-8128.

Tsimekas 2019. Optimization of Spray Pyrolysis for Cathode-Supported Solid Oxide Fuel Cells. *PhD Thesis*, University of St Andrews, UK.

Weber S.B., Lein H.L., Grande T., Einarsrud M.-A., 2013. Influence of the precursor solution chemistry on the deposition of thick coatings by spray pyrolysis. *Surface & Coatings Technology,* 221, 53–58.

2nd International Conference on
Sustainable Chemical and
Environmental Engineering
14th – 18th June 2023, Limassol, Cyprus

The energetic potential of surgical masks: a possible approach as solid recovered fuels

S. Pinho

[1]*LEPABE, Department of Metallurgical and Materials Engineering Faculty of Engineering, University of Porto, Portugal*
Corresponding author email: scpinho@fe.up.pt

ABSTRACT
Using waste as a substitute for traditional fuels is a highly effective means of recovering energy, and the cement industry has already implemented it in numerous countries worldwide. Nevertheless, current laws only recognize nonhazardous wastes as potential solid recovered fuels (SRF), which does not include hazardous medical wastes, namely surgical masks. In the current pandemic context, the surgical mask used by the population has been managed as urban solid waste. However, the utilization of wastes as surgical masks that have the potential of being used to recover energy and consequently its reduction in landfills it could be an option to consider. The aim of this study was to evaluate the energetic potential of using surgical mask wastes as SRF. The calorific value demonstrated the ability of the masks to be used as an alternative fuel efficiently. This capacity is also evidenced by its classification according to ISO 21640:2021, the net calorific value, chlorine, and mercury content are in class 1, which demonstrates the best values predicted by the standard.

Keywords: Surgical mask, energetic potencial, incineration

1. INTRODUCTION

Until the novel coronavirus (SARS-CoV-2) arose, the surgical mask was essentially used to protect healthcare professionals from preventing the risk of infections. These wastes generated within healthcare facilities are treated as medical waste. Autoclaving and incineration are the main processes used for treating medical waste. Since the appearance of SARS-CoV-2, the use of face masks was recommended by the World Health Organization (WHO) and different countries' governments to the population to prevent the risk of coronavirus transmission. This recommendation has a phenomenal demand for surgical masks. China has been the major producer of global face masks since March 1, 2020 (Chowdhury et al, 2021). According to customs statistics, China has exported 504.8 million surgical masks (Marine Pollution Bulletin, 2020). The surgical mask to single-use was used by millions of persons worldwide, causing a colossal increase in the number of masks discarded in unsorted waste, being more worrying when their discarded is in the environment. If only a small fraction of the produced masks, 1%, are disposed of improperly in the environment, this will result in about 30,000-40,000 kg of plastic waste per day (Haque et al, 2021). The disposal of face masks in public places, natural environments and beaches has been observed in several countries (Ammendolia et al., 2021; Ardusso et al., 2021; Cordova et al., 2021). The density of disposable face masks on beaches seems to be considerably greater than in any other location (Silva et al, 2021). According to a recent report, about 1.56 billion face masks entered the oceans in 2020 (Mghili et al, 2022). The surgical mask to single-use can be produced from different polymeric materials such as polypropylene, polystyrene, polyurethane, polycarbonate, polyester, polyethylene and polyacrylonitrile. Under environmental conditions, these materials break down into smaller sizes, particles (under 5 mm) being a significant source of microplastics in the ocean, freshwater and marine environment (Fadare and Okoffo, 2020). As a result of indiscriminately disposed of surgical masks into the environment, a new source of microplastics has been emerging. Mask reuse is an option to increase your usage time; therefore, some attention has been turned to decontaminating face masks. Researchers have studied decontamination by

ultraviolet germicidal irradiation, chemical disinfection, micro-waves, and heat-based methods. However, there is limited evidence on the safety or efficacy of decontamination and reuse of surgical masks (Zorko et al. 2020). In this context, the utilization of wastes, as surgical masks, that have a potential to be used to recover energy and reduce this disposal of landfills could be an option to consider. In the last years, the use of alternative fuel (as refuse derived fuel, tire derived fuel, sewage sludge, municipal solid wastes) has shown to be ecologically and economically profitable (Chatziaras and Psomopoulos, 2016). However, current laws only recognize nonhazardous wastes as potential refused derived fuel (RDF), which does not include the hazardous medical wastes. Nevertheless, in the current pandemic context, the surgical mask used by the population is considered urban solid waste. The objective of this study was to evaluate the possibility of using surgical mask wastes as SRF, analyzing the parameters set as mandatory by European standards.

2. MATERIALS AND METHODS

2.1. Materials

Surgical masks used in this work consist of three layers; an inner layer made of polyester (PE) and pressed polypropylene (PP) (fibrous material), middle layer constituted by PP (melt-blown filter), and an outer layer made of PP (nonwoven, which are water-resistant and coloured), and tapes made of polyurethane.

2.2. Methods

TG, DSC and FTIR analyses

Thermogravimetric and differential scanning calorimetric analyses were performed using two equipment's (Setaram, model 92-16.18 and model Lab- sys, respectively). Samples were placed in a platinum crucible (TG), or aluminium crucible (DSC), heated at a rate of 10 °C/min up to 200 °C and held 3600 s at that temperature in order to reach the end of melting peaks of both materials (data not shown). Blank tests were carried out for TG and DSC analyses with unloaded crucibles using the same conditions. The surgical mask was characterized by Fourier transform infrared spectrometer (JASCO FT/IR-4100 assembled with an ATR (ATR PRO410-M) accessory, 64 scans, resolution of 4 cm^{-1}).

Chemical and physical analyses

The gross calorific value was performed at 25 °C in a bomb calorimeter model Parr 1672 according to EN 15400:2011. The chloride was absorbed or dissolved in an aqueous solution after combustion in the oxygen atmosphere, according to CEN/TS 15408:2011, and determined in solutions according to 4500 B Argentometric Method (APHA, 1998). Total carbon was determined with a Shimadzu TC analyzer model TOC-VCSH, according to EN 13137 (2001). The ash content and moisture content were determined according to CEN/TS 15403:2011 and CEN/TS 15414-1: 2011, respectively. All determinations were performed at least in triplicate. For metal quantification, the samples were subjected to chemical attack with aqua regia, according to the ISO 11466:1995 standard. The digestions were carried out in *Kjeldahl* tubes, with approximately 1 g of each sample and 10 mL of aqua regia for 3 h at 90 °C. At least 3 samples of each material were digested. After cooling, the solutions were filtered and diluted with deionized water until obtaining a volume of 100 mL. The metals were determined in the solutions by Atomic Absorption Spectrometry (AAS) using a UNICAM 969 AA spectrometer. Elemental analysis was carried out on a vario MICRO cube analyzer from Elemental GmbH in CHNS mode. Each element (CHNS) was determined by combustion of the sample at 1050 °C and calculated by the mean of three independent measurements, using a per-day calibration with a standard compound.

3. RESULTS AND DISCUSSION

TG, DSC and FTIR analyses

The surgical mask TG profile presented slight weight losses (approximately 0,6 %), as shown in Figure 1. This insignificant weight loss is characteristic of components with excellent chemical and thermal resistance in the range of conditions tested. The DSC profile, Figure 1, shows well defined patterns of endothermic transformations with 2 peaks whose temperatures are 130 °C and 160 °C, indicating that the surgical mask is

composed by PP polymers. The weight and heat flow changes detected in the blank tests of TG and DSC analyses were negligible. The weight loss values at a given temperature by the replicates in the three TG tests showed very low scatter with coefficients of variation of less than 0.7 %.

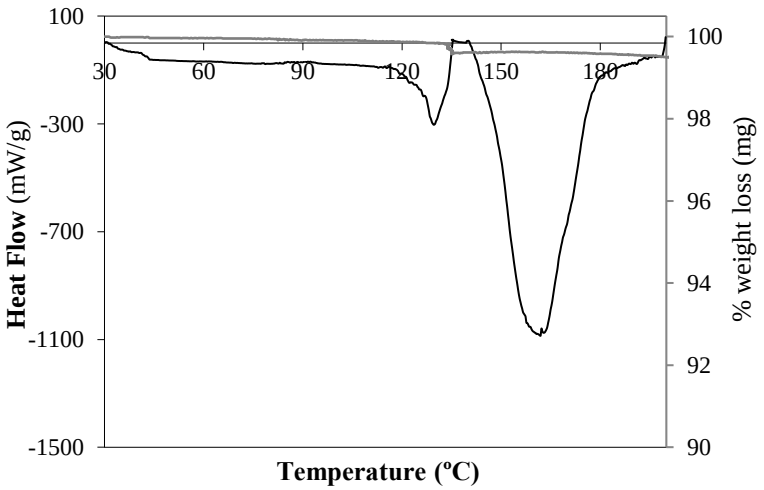

***Figure 1**. TG and DSC profiles of surgical mask*

The FTIR spectra of outer and middle layers exhibit two significant peaks of 1376 and 1456 cm^{-1} characteristic of symmetry deformation of methyl groups ($–CH_3–$ and $–CH_2–$), a peak at 1653 cm^{-1} attributed to the C=C stretching vibration and two peaks at 2920 and 2953 cm^{-1} are the assignments of CH_3 stretching. The inner layer FTIR spectra show a small peak at 647 and 668 cm^{-1} correspondents at symmetry deformation of -CH- group, a peak at 725 cm^{-1} characteristics of $-CH_2-$ rocking, the peaks around 1101 to 1247 cm^{-1} are assigned to the C–O stretching, a peak at 1750 cm^{-1} is attributes to the C=C stretching vibration and two peaks at 2850 and 2918 cm^{-1} are the assignments of CH_3 stretching. Other studies presented similar polypropylene infrared spectral analysis (Aragaw, 2020). The functional groups in the FTIR spectra corroborate with manufacturers' information on surgical masks that have been produced from polymeric materials, namely polypropylene and polyester.

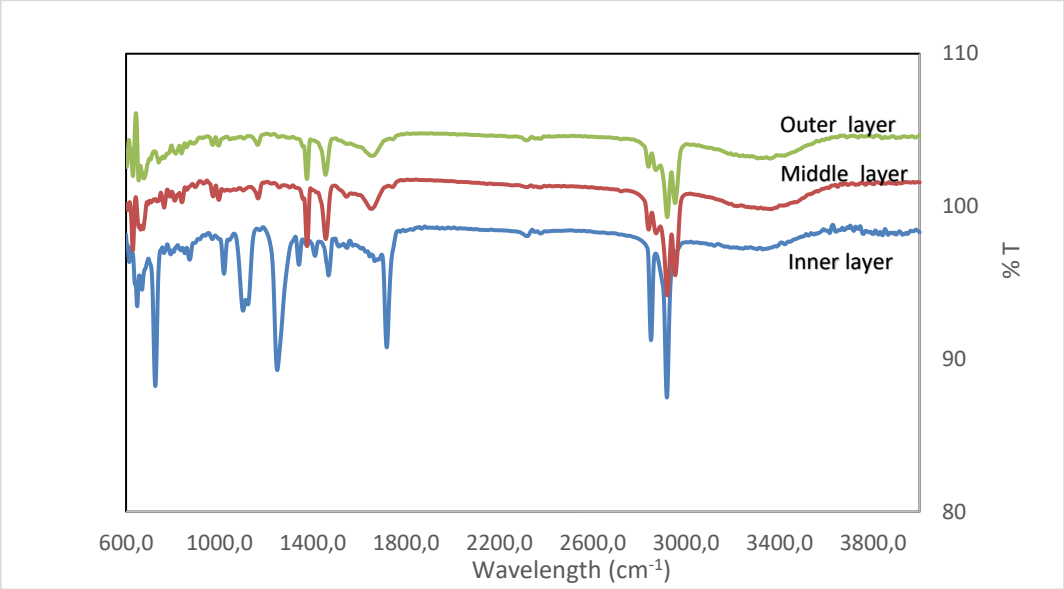

Figure 2. *FTIR spectra of surgical mask.*

Chemical and physical analyses

The mask's elemental analysis showed a high total carbon content of 84.5 %, with a hydrogen content of 12.8 %, as expected due to its composition, mainly polymeric materials. The polymeric part presents a low ash content, about 0.36%, corroborated by elemental analysis and chemical composition. Table 1 reports the values of the mandatory specification physical parameters defined by the ISO 21640:2021 standard. The results obtained on the masks show a high net calorific value of dry (d) and as received (ar) samples, nearly the heating value of diesel and fuel oil which is about 40 - 50 MJ/kg. Concerning ash and moisture content, these wastes have low values.

Table 1. *Mandatory specification physical parameters*

Parameter	Value
Ash content, %	5.4 ± 0.05
Moisture content, %	0.66 ± 0.02
Net calorific value, MJ/kg (d)	43.64 ± 0.003
Net calorific value, MJ/kg (ar)	40.85 ± 0.003

Table 2 shows the values of the mandatory specification chemical parameters in samples; the mercury content and chlorine content were significantly low.

Table 2. *Mandatory specification chemical parameters*

Parameter	Value

Antimony, mg/kg (b.s.)	< 15.3
Arsenic, mg/kg (b.s.)	<0.1
Cadmium, mg/kg (b.s.)	<1.5
Lead, mg/kg (b.s.)	<5.6
Chlorine, % (b.s.)	<0.05
Cobalt, mg/kg (b.s.)	<2.0
Copper, mg/kg (b.s.)	3.5
Chromium, mg/kg (b.s.)	6.8
Manganese, mg/kg (b.s.)	8.7
Mercury, mg/kg (b.s.)	<0.5
Nickel, mg/kg (b.s.)	3.4
Thallium, mg/kg (b.s.)	2.2
Vanadium, mg/kg (b.s.)	<10.8
∑ **Heavy metals,** mg/kg	< 72.9

The ISO 21640:2021 standard uses a classification system for SRF based on three parameters: an economic parameter (net calorific value), a technical parameter (chlorine content), and an environmental parameter (mercury content). Each parameter is divided into five classes (described in table 2 of the standard), and the class code combines these three classifications.

The net calorific value of the surgical mask obtained was greater than 25 MJ/kg; therefore, it is in class 1; the chlorine content was lower than 0.2 %, corresponding to class 1. The median mercury content and the 80th percentile were ≤ 0,02 ≤ 0,04 mg/MJ, respectively, thus corresponding to class 1, as reported in Table 3. Therefore, the surgical mask with these determined characteristics is coded as PCI 1; Cl 1; Hg 1, according to ISO 21640:2021.

Table 3. *Classification of surgical mask according ISO 21640:2021 standard*

Parameter	Value	Classes
Net calorific value, MJ/kg (ar)	40.85	1
Chlorine, % (d)	<0.05	1
Mercury [mg/MJ], (ar) Median 80th percentile	0.0082 0.0092	1

4. CONCLUSIONS

Although it is slightly lower than diesel and fuel oil, the calorific value of the masks is above coal, so it can say that the capacity of these residues can be used as an alternative fuel. This capacity is also ensured by its classification according to ISO 21640:2021 since, in terms of economic, technical, and environmental parameters, they are class 1, which is the best value provided for in the standard. Indeed, based on the analyzed surgical mask`s characteristics, energy production can be an asset in its management both from an environmental and economic point of view.

5. ACKNOWLEDGEMENTS

This work was financially supported by LA/P/0045/2020 (ALiCE), UIDB/00511/2020 and UIDP/00511/2020 (LEPABE), funded by national funds through FCT/MCTES (PIDDAC).

REFERENCES

Ammendolia, J., Saturno, J., Brooks, A., Jacobs, S., Jambeck, J. R., 2021. An emerging source of plastic pollution: environmental presence of plastic personal protective equipment (PPE) debris related to COVID-19 in a metropolitan city. *Environ. Pollut.,* 269, 116160.

Aragaw,T., A., 2020. Surgical face masks as a potential source for microplastic pollution in the COVID-19 scenario. *Marine Pollution Bulletin*. 159, 111517.

Ardusso, M., Forero-López, A. D., Buzzi, N. S., Spetter, C. V., Fernández-Severini, M. D., 2012. COVID-!9 pandemic repercussions on plastic and antiviral polymeric textile causing pollution on beaches and coasts of South America. Sci.*Total Environ.* 763, 144365.

Chatziaras, N., Psomopoulos, C. S., 2016. Use of waste derived fuels in cement industry: a review. *Management of Environmental Quality: An International Journal*, 27, 178–193

Chowdhury, H., Chowdhury, T., Sait, S. M., 2021. Estimating marine plastic pollution from COVID-19 face masks in coastal regions. *Marine Pollution Bulletin*, 168, 112419.

Cordova, M. R., Nurhati, I. S., Riani, E., Nurhasanah, Iswari, M.Y., 2021. Unprecedented plastic made personal protective equipment (PPE) debris in river outlets into Jakarta Bay during COVID-19 pandemic. *Chemosphere*. 268, 129360.

EN 15400:2011. Solid recovered fuels - Determination of calorific value.

EN 13137:2001. Characterisation of waste – Determination of total organic carbon (TOC) in wastes, sludges and sediments.

EN 15403:2011**.** Solid recovered fuels - Determination of ash content.

EN 15414-1: 2011. Solid recovered fuels - Determination of moisture content using the oven dry method - Part 3: Moisture in general analysis sample.

Fadare, O., O., Okoffo, E. D., 2020. Covid-19 face masks: A potential source of microplastic fibers in the environment. *Science of the Total Environment*. 737, 140279.

Haque, S., Sharif, S., Masnoon A., 2021. SARS-CoV-2 pandemic-induced PPE and single-use plastic waste generation scenario. *Waste Management & Research*. 39 (1), 3-17.

ISO 11466:1995. Soil quality—Extraction of trace elements soluble in aqua regia.

ISO 21640:2021. Solid recovered fuels — Specifications and classes.

Mghili, B., Analla, M., Aksissou, M., 2022. Face masks related to COVID-19 in the beaches of the Moroccan Mediterranean: An emerging source of plastic pollution. *Marine Pollution Bulletin*. 174, 1131181.

Zorko, DJ., Gertsman, S., O´Hearn, K., et al, 2020. Decontamination interventions for the reuse of surgical mask personal protective equipment: a systematic review. *Journal of Hospital Infection*, 106, 283-294

2nd International Conference on
Sustainable Chemical and
Environmental Engineering
14th – 18th June 2023, Limassol, Cyprus

Experimental and Mathematical study on CO_2 separation performance of biogas using commercial polyimide hollow membrane in a 2-stage process.

C. Koutsiantzi[*1], P. Gkotsis[2], A. Zouboulis[2], M. Mitrakas[1] and E.S. Kikkinides[1]

[1] Department of Chemical Engineering, Aristotle University of Thessaloniki
[2] Department of Chemistry, Aristotle University of Thessaloniki
** Corresponding author email: koutsiac@cheng.auth.gr*

ABSTRACT

In the current work, a 2-stage membrane separation process is examined. The membrane modules that are used are 2 identical Polyimide hollow fiber membranes (UBE Industries, Ltd., Japan). This is accomplished with the addition of two identical membranes, through which the permeate stream from the 1st membrane passes into the 2nd and the CO_2 recovery was tested both in experimental and mathematical approach. The result of the addition of the 2nd stage is the achievement of a degree of CO_2 stream purity that reaches 95%, for effective CO_2 capture and reuse.

Keywords: Biogas Upgrade, Membranes, Gas Separation, CO_2 removal, 2 stage Separation, Mathematical Modeling

1. INTRODUCTION

Biogas is considered a renewable energy source, which is expected to play an important role in the future of meeting energy needs worldwide (Nguyen et al., 2020). The production of biogas is achieved by the decomposition of organic matter, in the absence of oxygen. Specifically, biogas is the product of the anaerobic digestion of microorganisms in a closed system, such as in an anaerobic digester (or bioreactor). Methane (CH_4) and carbon dioxide (CO_2) are the main components of biogas, while traces of moisture and hydrogen sulfide (H2S) are also contained. After biogas upgrading, the process which leads to the production of biomethane, it can be used as a fuel. The capture and use of the CO_2, which is separated in the permeate stream either directly or after treatment (cleaning) is a promising approach, which in the context of a circular economy reuses an environmentally harmful gas by converting it into a useful product for future applications (Khosroabadi et al., 2021). Previous studies and tests on membrane biogas upgrading have shown that the production of high purity biomethane (>95%) is feasible for 1-stage processes, but the capture of a CO2-rich permeate stream (>95%) is not easily achieved employing 1-stage processes (Koutsiantzi et al., 2022).

By conducting experiments on a laboratory scale of biogas upgrading using a polyimide membrane and applying different experimental operating conditions (pressure, total volumetric gas supply, feed composition), conclusions were reached on the separation behavior of CH_4/CO_2 mixtures that simulate the different biogas compositions. The main and most important results that emerged from the above study are that the application of a polyimide membrane in biogas mixtures, regardless of the initial composition, combined with the application of high pressures (9 bar) lead to the production of methane current with a purity higher than 95%. At the same time, regarding the production of CO_2-rich stream, a second identical membrane was added through which the permeate stream from the first membrane passes. The result of the addition of this second stage is the achievement of a purity degree of CO_2 current that reaches 95%.

2. MATERIAL AND METHODS

2.3. Membrane module

The membrane module that is used for the gas separation process is a commercial membrane module consisting of polyimide hollow fibers (Fig. 1). The membrane module was purchased be UBE Industries Ltd., Japan. Not every geometrical characteristic was known from the construction company, so a theoretical model helped for the better visualization of the inside of the membrane. Microscopy and SEM Spectroscopy were used to make sure that the fibers are non- porous so there is no hypothetical gas diffusion in the inner wall of the membranes. The main membrane characteristics are presented on the Table 1 below.

Table 1 *PI membrane characteristics.*

Material	**Polyimide**
Inner diameter of HF (μm)	267
Outer diameter of HF (μm)	415
Module length, L (cm)	30
Outer Diameter, OD (cm)	3
Number of Fibers, N	1000

On previous part of the study, the simulation of the mass flow of the gas mixture in the membrane has been developped, for 1- stage separation process where both cocurrent flow and crossflow were tested theoritically . The theoretical resuls were compared with the experimental gas separation results of the 1 stage process, and the crossflow model was selected as the closest to the actual results.

The cross-flow model was in accordance with the experimental results for selectivity $\alpha^* = 48$ for an initial gas mixture of CH_4/CO_2 55/45 (%vol) and ΔP=7 bar. Through the selectivity, the permeance values of each gas was calculated and showed that $Perm_{CO2}$ = 97.5 GPU and $Perm_{CH4}$= 1.53 GPU.

Figure 1 *Polyimide HF membrane module (UBE Industries, Japan)*

2.4. Experimental Setup

For the 2 stage experiments, the addition of a 2nd identical membrane module is considered right after the 1st module for the enrichment of the permeate stream in CO_2. Consequently, the initial 1 stage set up which was presented in previous publication of our study (Koutsiantzi et al., 2022) is modified and presented at Fig. 2. As the permeate stream exits the 1st module with atmospheric pressure, it needs to be compressed at 3 bars to enter the 2nd stage of separation.

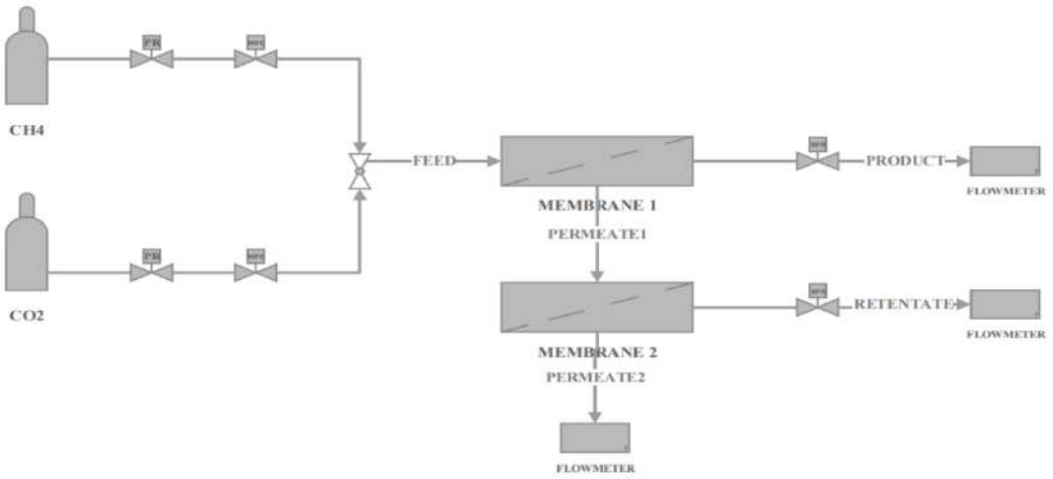

Figure 2 *2-stage separation flow chart (PC: Pressure Controller, MFC: Mass Flow Controller, BPR: Back Pressure Regulator)*

2.5. Experimental Conditions

As described above, the initial conditions have been selected after evaluation of the polyimide membrane for the single stage separation and are presented at Table 2. The initial biogas samples for separation were selected to be 2 usually found CH_4/ CO_2 concentrations after biogas pretreatment: 55/45 %vol and 70/30 %vol to examine conditions of higher and lower initial CO_2 composition and its recovery.

Before the 2nd stage a compressor should be used, in order to compress the gas stream at 3 bars. The reason for the operation in lower pressures during the 2nd stage, is the high CO_2 percentage which in combination with the lower mass flow conditions (500 – 1000 mL/min) is not capable of achieving higher pressure values. After the 2nd separation, the permeate and retentate are in atmospheric pressure.

Table 2 *Experimental conditions during 2 stage experiments*

Experimental conditions		
	1st stage	2nd stage
Feed gas composition, (CH_4/CO_2 %vol)	55/45, 70/30	Depends on the 1st stage permeate stream
Feed pressure, (bar)	6 -10	3

Permeate pressure (bar)	1	1
Retentate pressure (bar)	1	1
Feed Flow L/min	1-3	Is the 1st stage permeate stream
Feed Temperature (ºC)	20	20

2.6. Crossflow model for membrane separation

The membrane separation process is regarded as a combination of countercurrent flow and crossflow according to the existing bibliography (Geankoplis, 2003). In the certain study, as the crossflow model was close to the actual achieved results for the 1 stage separation, the 2nd stage simulation was also selected to work on the crossflow model.

The flow during separation is presented on Fig. 3. In this case, the longitudinal velocity of the high pressure (p_h) stream is so large that the gas stream is considered in plug flow and flows parallel to the membrane. On the low pressure (p_l) side, the permeate stream is considered to be pulled into vacuum and the flow is essentially perpendicular to the membrane. The model assumes no mixing on each side. The permeate composition at each point along the membrane is determined by the relative rates of permeation of the feed components at that point. Weller and Steiner have developed an analytical model with equations that can calculate the total membrane area. Stage cut θ can be obtained from the membrane area equation which is presented below (Eq. 1) (Geankoplis, 2003; Weller & Steiner, 1950):

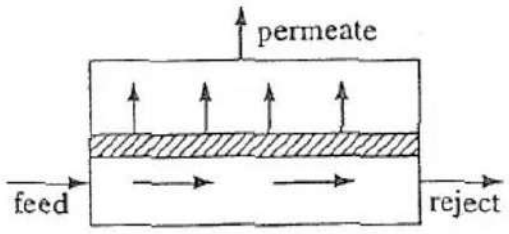

Figure 3 *Crossflow model representation for membrane separation.*

$$A_m = \frac{tL_f}{p_h P'_B} \int_{i_0}^{i_f} \frac{(1-\theta*)(1-x)di}{(f_i - i)\left[\frac{1}{1+i} - \frac{p_l}{p_h}\left(\frac{1}{1+f_i}\right)\right]} \quad Eq.\ 1$$

3. RESULTS AND DISCUSSION

The results of the CO_2 purity and recovery are presented on Fig. 4 and Fig. 5 for the different conditions that were discussed, where the CO_2 purities between 1 and 2 stage processes can be compared. In general, the CO_2 purity is increased by 20-30% for each condition.

It is observed that for the 2-stage separation process of the CH_4/CO_2 mixtures, the CO_2 % content that is achieved exceeds 90% for all cases, meaning that the further gas stream treatment is essential and effective for further carbon capture and reuse.

In terms of recovery, the application of a second stage, leads to recoveries between 60-90%. The reason for the decreased recovery in comparison with the 1st stage is due to the influence of the initial and the permeate mass flow on the recovery calculation.

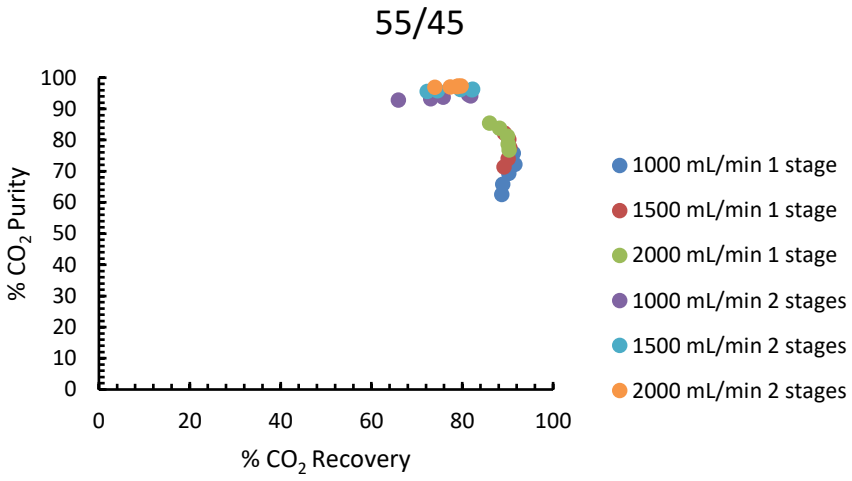

Figure 4 *Comparison of CO_2 recovery and purity in permeate stream for 1- and 2-stage processes. (55/45% CH_4/CO_2, P=6-10 bar for the 1st stage, and P= 2 bar for the 2nd stage (first exit))*

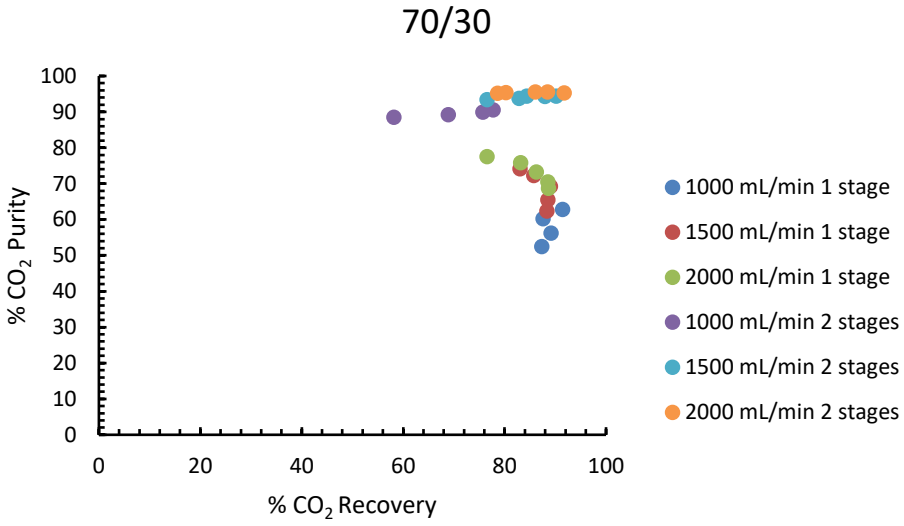

Figure 5 *Comparison of CO_2 recovery and purity in permeate stream for 1- and 2-stage processes. (70/30% CH_4/CO_2, P=6-10 bar for the 1st stage, and P= 3 bar for the 2nd stage (first exit))*

4. CONCLUSIONS

In the certain work, the evaluation of a 2-stage separation membrane module for CO_2 capture of biogas is examined, both theoretically with the development of a crossflow model in Matlab and experimentally

with the operation of a laboratory membrane setup. Pre-work has been done for the 1 stage separation with the same polyimide hollow fiber membrane (UBE Industries, Japan), where the CO_2 on the permeate stream showed limited purity values, around 60-80 %, a fact that does not allow its direct capture and reuse.

To further enrich the CO_2 stream, the permeate stream was fed to a second identical polyimide membrane in series with the permeate stream exiting the first separation stage. From the 2nd stage, a permeate stream of CO_2 with purity greater than 95% exits, a percentage that makes it suitable for its direct use in various uses, supporting a circular economy model.

5. ACKNOWLEDGEMENTS

This research has been co-financed by the European Union and Greek national funds through the Operational Program Competitiveness, Entrepreneurship, and Innovation, under the call RESEARCH-CREATE-INNOVATE (project code: T2EDK-01293).

REFERENCES

Geankoplis, Christie. J. (2003). *Transport Processes and Separation Process Principles: (includes Unit Operations)* (4th ed.). Prentice Hall Professional Technical Reference.

Khosroabadi, F., Aslani, A., Bekhrad, K., & Zolfaghari, Z. (2021). Analysis of Carbon Dioxide Capturing Technologies and their technology developments. *Cleaner Engineering and Technology*, *5*, 100279. https://doi.org/https://doi.org/10.1016/j.clet.2021.100279

Koutsiantzi, C., Mitrakas, M., Zouboulis, A., Kellartzis, I., Stavropoulos, G., & Kikkinides, E. S. (2022). Evaluation of polymeric membranes' performance during laboratory-scale experiments, regarding the CO2 separation from CH4. *Chemosphere*, *299*, 134224. https://doi.org/https://doi.org/10.1016/j.chemosphere.2022.134224

Nguyen, L. N., Kumar, J., Vu, M. T., Mohammed, J. A. H., Pathak, N., Commault, A. S., Sutherland, D., Zdarta, J., Tyagi, V. K., & Nghiem, L. D. (2020). Biomethane production from anaerobic co-digestion at wastewater treatment plants: A critical review on development and innovations in biogas upgrading techniques. *Science of The Total Environment*, 142753. https://doi.org/https://doi.org/10.1016/j.scitotenv.2020.142753

Weller, S., & Steiner, W. A. (1950). Separation of Gases by Fractional Permeation through Membranes. *Journal of Applied Physics*, *21*(4), 279–283. https://doi.org/10.1063/1.1699653

Contact

Professor Petros Gikas
Design of Environmental Processes Laboratory
School of Chemical and Environmental Engineering Technical University of Crete, Greece
T: +30 28210 37836
E: pgikas@tuc.gr, secretariat.susteng@tuc.gr
W: www.deplab.tuc.gr

The Interreg V-A "Greece – Cyprus 2014-2020" Cooperation Program is co-funded by the European Union and by the National Funds of Greece and Cyprus.

Sponsors

Gold sponsor

Gold sponsor

Sponsor

Sponsor